FENTON'S OXIDATION OF HERBICIDES IN WATER

Thesis

Submitted in partial fulfilment of the requirements for the degree of

DOCTOR OF PHILOSOPHY

by

SANJEEV SANGAMI

Reg.No.145016CV14F09

DEPARTMENT OF CIVIL ENGINEERING

NATIONAL INSTITUTE OF TECHNOLOGY KARNATAKA

SURATHKAL, MANGALORE – 575025

JULY, 2018

D E C L A R A T I O N

by the Ph.D. Research Scholar

I hereby declare that the Research Thesis entitled "**FENTON'S OXIDATION OF HERBICIDES IN WATER**" which is being submitted to the **National Institute of Technology Karnataka, Surathkal** in partial fulfilment of the requirements for the award of the Degree of   **Doctor of Philosophy** in **Civil Engineering**, is a bonafide report of the research work carried out by me. The material contained in this Research Thesis has not been submitted to any University or Institution for the award of any degree.

145016CV14F09, SANJEEV SANGAMI

Department of Civil Engineering

Place: NITK-Surathkal

Date: 03-07-2018

C E R T I F I C A T E

This is to certify that the Research Thesis entitled "**Fenton's Oxidation of Herbicides in Water"** submitted by **Mr. SANJEEV SANGAMI,** (Register Number: **145016CV14F09**), as the record of the research work carried out by him, is accepted as the Research Thesis submission in partial fulfilment of the requirements for the   award of degree of **Doctor of Philosophy**.

(Dr. Basavaraju Manu)
Assoc. Professor and Research Guide
Department of Civil Engineering

Chairman - DRPC
Department of Civil Engineering

DEDICATED

TO

MY PARENTS, WIFE, DAUGHTER,

FAMILY MEMBERS, TEACHERS

AND

FRIENDS

ACKNOWLEDGEMENT

NITK, Surathkal   (SANJEEV SANGMI)

Date: 03-07 -2018

ABSTRACT

The present   study attempts the conventional Fenton's process (CFP) and advance Fenton's process (AFP) for the oxidation of herbicides (2,4-D, dicamba and ametryn) in actual agriculture runoff water and   in aqueous medium. The degradation experiments were initiated with CFPs ($FeSO_4.7H_2O$ as a precursor) and later the AFP (FeNPs synthesized from laterite and sustainable plant extract) was performed. Both RSM (response surface methodology) and Taguchi methods were applied for the design of experiments. The influence of H_2O_2/COD, H_2O_2/Fe $^{2+}$ pH and reaction time were   studied on four responses (ametryn, 2,4-D, dicamba and COD removal efficiency). Agriculture runoff water and aqueous solution   were successfully treated by CFPs with the removal efficiencies of 71-100% and 84.01-100% respectively. The whole oxidation process was monitored by LC/MS and COD. It was found that compounds were mineralized to oxalic acid, thiocynate ion and maleic acid for dicamba, ametryn and 2,4-D respectively with the release of chloride ion. The regression analysis was performed, in which coefficient of variation (<8), and adequate precision (>12) were in good agreement with model values. Finally, the treatment process was validated by performing the additional experiments.

In AFPs the Fe nanoparticles were synthesized using Eucalyptus Globulus (EG)(Nilgiri) and Tactona Grandis (TG)(Teak) extracts. The low cost and locally available laterite was used as a source of iron rather than using iron salts. The raw laterite particles (RLPs) and synthesized green iron nanoparticles (GLFeNPs) were characterized using FESEM-EDX, XRD, FTIR, and BET techniques. The obtained results confirmed that 20-70 nm (EG) and 50-100nm (TG) of spherical FeNPs were formed (surface area of 31- 36.62 m^2/g and pore volume of 0.038-0.0394cm^3/g) for TG and EG respectively. The XRD analysis shows that GLFeNPs consists of mainly Fe^0, Fe_2O_3, Fe_3O_4 and polyphenols. Later, the GLFeNPs were applied as a Fenton-like catalyst and 100% removal of all herbicides was observed. The EG extract is   showing higher polyphenols and antioxidant power than TG extract and the 1st order kinetic model was best fitted to the experimental data than the 2nd order   (R^2 >0.85). The AFP is working near to the neutral pH than CFP and more degradation efficiency was observed in AFP. Finally, the cost analysis for the synthesis of FeNPs was performed, which is less than the commercial grades and hence it can be recommended for the alternative novel catalyst for the oxidation studies.

Keywords: 2,4-D, Dicamba, Ametryn, Laterite , Green synthesis, Advance Fenton Process

CONTENTS

LIST OF FIGURES

LIST OF TABLES

NOMENCLATURE

Name	Full form
2,4-DB	4-(2,4-Dichlorophenoxy)Butyric Acid
2-4 D_0	2,4-Dichlorophenoxyacetic Acid at 0 time
2,4,5-T	2,4,5-Trichlorophenoxyacetic Acid
24DR	24D Removal
4-CPA	4-Chlorophenoxy-Acetic Acid
2,4-DCP	2,4- Dichlorophenol
1,4-D	1,4-Dioxane
AR17	Acid Red 17
AG25	Acid Green 25
AM_0	Ametryn at 0 time
AWWA	American Water Works Association
AR	Ametryn Removal
APHA	American Public Health Association
AFT	Advanced Fenton's Oxidation
AOPs	Advanced Oxidation Process
BBD.	Box-Behnken Design
BB3	Basic Blue 3
BDD	Boron-Doped Diamond Thin-Film Electrode
CCD	Central Composite Design
CFP	Conventional Fenton's Process
CCC	Central Composite Circumscribed
CCI	Central Composite Inscribed
CCF	Central Composite Face Centered

COD	Chemical Oxygen Demand
COD R	Chemical Oxygen Demand Removal
DR	Dicamba Removal
D_0	Dicamba at 0 time
DR28	Congo Red 28
DNA	Deoxyribonucleic Acid,
DOE	Design Of Experiments
DNBP	Di-N-Butyl Phthalate
EDC	Endocrine Disrupting Chemical
E^0	Oxidation Potential
EOP	Electrochemical Oxidation Potential
EDS or EDX	Energy-Dispersive X-Ray Spectroscopy
EZVI	Emulsified Nano-Zero-Valent Iron
FTIR	Fourier Transform Infrared Spectroscopy
FAO	Food And Agriculture Organization
FeNPs	Iron nanoparticles
GAC	Granular Activated Carbon
GC-ECD	Gas Chromatography – Electron Capture Detector
GCMS	Gas Chromatography Mass Spectrometry
GE	Green Extract
HCH	Hexachlorocyclohexane
HPLC	High Performance Liquid Chromatography
HRT	Hydraulic Retention Time
K_d	Solid–Water Distribution Coefficient
K_{oc}	Organic Carbon Partition Coefficient

K_{ow}	Octanol-Water Partition Coefficient
LCMS	Liquid Chromatography—Mass Spectrometry
LE	Laterite Extract
LMWOAs	Low-Molecular-Weight Organic Acids
M P and B P	Melting Point and Boiling Point
M W	Molecular Weight
MAC	Mesoporous Activated Carbon
MBBR	Moving-Bed Biofilm Reactor
MCPA	2-Methyl-4-Chlorophenoxyacetic Acid
MIEX	Magnetic Ion Exchange
NAPL	Non Aqueous Phase Liquid
NMR	Nuclear Magnetic Resonance
OC	Organochlorine
PCBs	Polychlorinated Biphenyls
POME	Palm Oil Mill Effluent
PPCPs	Pharmaceutical And Personal Care Products
PSD	Particle Size Distribution
R^2	Coefficient of Determination
RNIP	Reactive Nanoscale Iron Particles
RSM	Response Surface Methodology.
SEM	Scanning Electron Microscopy
SSA	Specific Surface Area
TBA	Tertiary Butyl Alcohol
TCE	Trichloroethene
TCP	Trichloropropane

TEM	Transmission Electron Microscopy
TiO$_2$	Titanium Oxide
TMT	Thousand Metric Tons
TOC	Total Organic Carbon
TOP	TEMPO-Oxidized Pulp
TPs	Transformation Products
USEPA	United Nations Environment Protection Agency
WEF	Water Environment Federation
WHO	World Health Organization
XPS	X-Ray Photoelectron Spectroscopy
XRD	X-Ray Diffraction

CHAPTER 1

INTRODUCTION

1.1 BACKGROUND AND MOTIVATION

Water is a very important for all living beings for their metabolic activities. In recent day's water pollution due to the bad agricultural practice showed considerable attention along with industrial and domestic sources. In the world, every day 14000 people are losing their lives and it is more in developing countries like India (60% of the population is farmers, FAO 2011). Now a day's there is a great challenge for the farmers to kill several varieties of insects and weeds that are present in the field crops and for this, many pesticides like fungicides, herbicides, and insecticides have been practiced. Herbicides are mainly used to kill unwanted plants (weed) from farmlands, industrial sites, and forestry. During rainfall, after the application of herbicides, it leads to agricultural runoff and moves towards downstream along with the pollutants (natural and man-made) and thereby contributing the pollutant load on the surface water body (Conte et al. 2016). The major source of water pollution includes overdose, improper application, air spraying, container washing, and unintentional leakage from pesticide containers.

Mixture of herbicides is more popular due to their synergic effect on the different types of weeds (broad leaf, grass and sedges) and are mainly applied to agricultural crops such as maize, sugar cane and rice (Sandoval-Carrasco et al. 2013, Cserhati and Forgacs 1998). Among all the herbicides 2, 4-D (2,4-dichlorophenoxy acetic acid), dicamba(3,6-dichloro-2-methoxybenzoic acid) and ametryn ((2-ethylamino)-4-(isopropylamino)-6-(methylthio)-s-triazine) are most commonly used around the world with different formulations(Ghoshdastidar and Tong 2013, Sandoval-Carrasco et al. 2013). When these herbicides are applied to the affected plants, the major portion is (99%) retained in the top soil surface and during heavy rainfall, finally it reaches the water body (Jiang et al., 2008, Kolpin et al. 1998, Laabs et al. 2002). Sometimes traces of these herbicides are detected in food chain also exa: sugarcane juice (Zuin et al. 2006). The extent of contamination

depends on the properties of the herbicides (leaching potential and solubility) and the soil (adsorption capacity and permeability). These herbicides have high water solubility (dicamba=4500 mg/L, 2,4-D=890 mg/L, ametryn= 209mg/L at 25 ^{0}C), with less adsorption by any of the soil (Kasozi et al. 2012). These are considered as an endocrine disrupting chemicals (EDC) and affect the animals, human beings, non-targeted plants, and useful microbes present in the soil (USEPA 2005). Also, these herbicides undergo some chemical reactions and thereby forming some intermediate products (chloro anilines and phenols), which are more toxic than the parent compounds (Chu et al. 2004, Farran and Ruiz 2004). Hence, in drinking water the maximum permissible limit is recommended (2,4-D=29 $\mu g \cdot L^{-1}$, WHO 2003; ametryn = 1.4 (ground water) -14 $\mu g \cdot L^{-1}$ (surface water), USEPA 2010; dicamba=200 $\mu g \cdot L^{-1}$ (Hamilton 2003)).

In India, about 6000 tons of herbicides were applied to crop land and from last few years market raised from 34.8% in 1970 to 51.9% in 2001. Arora and Gopal (2004) studied the residual herbicides in Indian agricultural research institute, Delhi and showed that, there is an existence significant level of concentration in soil and water. Weed management in sugar cane field is quite different from other field crops and it is estimated that weeds reduces the crop yield from 12-72%. The reasons are i) sugar cane is cultivated with wider row spacing ii) growth is very slow at the beginning iii) 30-45 days are required for complete germination and another 2 months for developing full canopy cover. In Karnataka, Belgaum is the maximum sugar cane cultivation district (more than 2000 ha in 2014, 80% of the Karnataka state), there is a lot of demand for the herbicide and the usage increased 10 times from the last 4 years (Rao et al., 2015). It is unavoidable due to lack of labourers availability to remove the weeds from the field. To monitor the concentration of these herbicides in cropland, there are no such rules and regulations provided by the regulatory authority. And also, still knowledge about residual concentration, degradation mechanism and the interaction between these herbicides with insecticides, fungicides and fertilizers in the farmland is more essential

than the ultimate receiving water body (Heppell and Chapman 2006). Therefore, it is very important to monitor these herbicides in this region.

Many physico- chemical   and biological treatment methods were adopted such as aqueous Cl_2 (Xu et al. 2009, Lopez et al. 1997) and reverse osmosis for ametryn degradation (Shurvel et al. 2014) and biodegradation process   for 2,4-D and dicamba (Ghoshdastidar and Tong 2013, Sandoval-Carrasco et al. 2013). However, all these compounds having a stable carbon –chlorine bond in their structure lead to lesser degradation (more toxic to the microbes) with slow reaction kinetics and filtration processes are more expensive due to their continuous replacement of the filter members (Davis 2007).

Therefore, in recent years   Fenton's types of advanced oxidation processes (AOPs) have become more popular, which are simple, effective, and economical. Fenton process is the combination of oxidant (H_2O_2) and catalyst (iron), which generates highly reactive $^\bullet OH$ radical (oxidation potential=2.8 V) and has the capacity to degrade all types of organic pollutants present in water (Khataee et al., 2014) (Eq.1.1-1.3). In this process the iron(II) is oxidized to iron(III) in the first stage, forming OH radical and hydroxide ion and later the iron (III) is reduced to iron (II) by forming hydroperoxyl radical. The homogeneous Fenton process (conventional Fenton process) works at narrow pH range(around 3) with iron salts ($FeSO_4.7H_2O$, $FeCl_3$) as   catalysts, where the particles distributes uniformly and creates a lot of iron hydroxide sludge containing extra sulfates and chlorides   and also it limits the recycling of iron for further use. This can be overcome by adding the H_2O_2 and Fe by stages or by sludge recirculation (Manu and Mahamood 2011) and reduction in sludge was observed from 7% to 17.

$$H_2O_2 + Fe^{2+} \rightarrow\ ^\bullet OH + OH^- + Fe^{3+}$$ (1.1)

$$H_2O_2 + Fe^{3+} \rightarrow\ ^\bullet OOH + H^+ + Fe^{2+}$$ (1.2)

$$^\bullet OH + Organics\ \rightarrow\ Degraded\ \ products$$ (1.3)

The conventional process can be improved by using different heterogeneous catalysts such as magnetite (Kong et al. 1998), goethite (ά-FeOOH) (Ortiz et al. 2010), pyrite

(Khataee et al. 2016), iron supported clays (Hassan and Hameed 2011), copper modified bentonite supported ferrioxalate (ayodele et al. 2014), Al-pillared Fe–smectite (Li et al. 2015) and ZnAlFe layered double hydroxides (Mantilla et al. 2009). It is said that, the heterogeneous catalyst is having less active sites and reduces the mass transfer rate(Zhang et al. 2015). This can be overcome by the application of heterogeneous catalyst in nano-size (Zhang et al. 2015), which possesses a high surface area and reactivity.

Many synthetic methods like $NaBH_4$ (Xu and Wang 2011) and co-precipitated iron (Fe^{2+} and Fe^{3+}) (Xu and Wang 2012) were applied to produce FeNPs, however, these are having the limitations like complexity, toxic nature of $NaBH_4$ and methanol, rapid agglomeration and expensive towards industrial application (Huang et al. 2014). Hence, recently many researchers produced the iron nano particles from different plant extracts and successfully applied in Fenton process to degrade many organic pollutants (Shahwan et al. 2011, Kuang et al. 2013). These extracts contain polyphenols/caffeine, which limits the rapid agglomeration of particles (capping agent) and acts as reducing agents in the synthesis process. However, all these processes involve the use of ferrous sulfate/ferric chloride salts as precursors, which add extra sulfates and chlorides to the treatment system. Hence, locally available laterite was applied as a iron source and sustainable plant extract was considered for the synthesis of heterogeneous catalyst in nano scale.

The laterite has many advantages such as temperature susceptibility, non-toxic, economical and available at all the places and hence many researchers have preferred (Khataee and Pakdehi 2014, Khataee et al. 2015, Manu and Mahamood 2011). And also it is said that iron extracted from laterite shows lesser degradation than conventional iron source ($FeSO_4$) (Amrutha and Manu 2016) and this can be overcome by the production of nano particles from laterite. Here, Eucalyptus Globulus(EG)(Nilgiri) and Tectona grandis(TG) (Teak leaves) leaves are used, which are having high content of bioactive contents such as polyphenols and Quinones. (Kore et al. 2011) and moreover the leaves are waste products in wood and paper mill industry (King et al. 2006). In

some cases, the leaves are used for the extraction of oils (medicinal value) (Chen et al., 2014).

Recently, a few researchers have successfully produced the FeNPs from EG extracts and are applied for the removal of many of the contaminants like nitrate (Wang et al. 2014a), Cr (VI) (Madhavi et al. 2013) and eutrophic wastewater (Wang et al. 2014b) and silver NPs from TG extracts (Nalvothula et al. 2014). According to the best of the author knowledge, no research work has been reported on Fenton's treatment of a mixture of 2, 4- D, dicamba and ametryn in agriculture runoff water and synthesis of laterite based FeNPs and their application as a Fenton-like catalyst for the degradation of these herbicides in water. Therefore, in this research work, the Fenton's treatment was performed by applying proper DOE (Design of Experiments) tool than conventional methods (one –variable - at a -time (OVAT)). This OVAT is expensive, consumes more time and chemicals, and does not give any significant interactions between the factors (Mason et al. 2003). The DOE consists of factorial design, response surface design (RSM), mixture of design, and Taguchi design. Here, Taguchi and RSM methods were preferred, which involve the systematic way of designing the experiments and ANOVA is a tool for the analysis of the results. The Taguchi design is cost effective, flexible, and provides a better knowledge with the help of standard statistical analysis (S/N ratio: signal to noise ratio). However, it gives comparatively less quality of information at each point, and (Ali et al. 2004) it preferred where the sample size is less and to optimize the process with a very less number of experiments.

The RSM also involves only a few sets of experiments with a wide range of values and gives the best-fit model, where the optimal response occurs. It also provides significant interactive effects between the variables with the help of surface and contour plots (Ahmadi et al. 2005, Myers et al. 2002). Here, the CCD (central composite design) type of RSM was considered, which is flexible, efficient and measures experimental errors accurately and it works under both region of interest and operatability (Ahmad et al. 2005). Hence, this method has been successfully applied in many degradation studies

(Yirsaw et al. 2016, Masomboon et al. 2010, Colombo et al. 2013, Ahmadi et al. 2005, Myers et al. 2002, Tiwari et al 2008).

1.2 OBJECTIVES

The main objective

To assess the feasibility of Fenton's oxidation of herbicides in water.

Specific Objectives

- To study the effect of various factors such as initial concentration, H_2O_2/Fe^{2+}, P^H and reaction time for the effective degradation of herbicides in agricultural runoff water.
- To study the effect of various factors such as initial concentration, H_2O_2/Fe^{2+}, P^H and reaction time for the effective degradation of each selected herbicides and mixture of herbicides in aqueous medium.
- Plant based synthesis of iron nanoparticles using laterite and their application as Fenton-like catalyst for the degradation of each selected herbicides and mixture of herbicides in aqueous medium.

1.3 ORGANIZATION OF THE THESIS

Chapter 1

This chapter provides the introduction to the herbicides, their effects on the environment and the treatment techniques such as conventional and advanced Fenton process, need, significance, and objective of the research.

Chapter 2

It gathers the information about research work carried out so far on various herbicides (2.4-D, ametryn and dicamba) degradation techniques such as physic-chemical, biological and AOPs. Both conventional ($FeSO_4$. $7H_2O$ as a precursor) and advanced Fenton process with FeNPs (Laterite as a precursor) are discussed in detail. The Taguchi and RSM (response surface methodology) type of DOE (design of experiment) are also presented.

Chapter 3

It gives the details about the sampling, materials, experimental methodology, analytical techniques, and the tools used for the optimization process.

Chapter 4

This chapter deals with the results and discussion on the conventional Fenton treatment for the treatment of agriculture runoff water and aqueous solution containing herbicides.

Chapter 5

It presents the results and detailed discussion on the synthesis of FeNPs from laterite using sustainable plant extracts and its application as a Fenton like catalyst for the effective degradation of herbicides.

Chapter 6

It gives the information about the conclusions drawn, based on the experimental results. The recommendations and scope for the future work were also presented.

CHAPTER 2

LITERATURE REVIEW

This chapter focuses on the literature related to the herbicides namely 2,4-D, dicamba and ametryn, their toxic effects on human, plants, and animals. The treatment technologies such as physico- chemical, biological and advanced oxidation process (AOPs) for the degradation of these herbicides are discussed.

2. 1 GENERAL

Water is a very essential component of our life. Due to the industrialization (industrial effluents), urbanization (domestic wastewater) and agriculture bad practices (pesticide contamination, fertilizers) leads to the contamination of water bodies (Rajkumar and Palanivelu 2004, USEPA 1999). The major sources of herbicide contamination include agriculture runoff, cleaning of irrigation equipments and empty containers. During pesticide application on the farm land, it undergoes biotic and abiotic transformation, resulting in intermediate products (Transformation products -TPs) (Roberts 1998). All these pesticides move vertically in the soil profile to underlying groundwater (Broholm et al. 2001). The TPs can also move laterally through surface runoff and enters agricultural ditches and streams, then carried to major rivers, and ocean systems (Aga et al. 2001, Shin et al. 2011) (Figure.2.1).

These herbicides have an adverse affect on cells (both white and red blood cells), DNA, genes, hormones, which lead to the cancer with suppression of human immune system (Jones and Kerswell 2003, Mantilla et al. 2009, Derylo-Marczewska et al. 2010). Human beings are mainly exposed through i) skin contact ii) inhalation 3) ingestion during preparation and spraying of herbicides. Some people are affected due to i) consumption of fish exposed to pesticides ii) consumption of pesticide-contaminated water and food (WHO 1993).

The triazine (atrazine), chlorinated herbicides (2,4-D,), nitrogenous herbicides have been found to the greatest extent in surface water sources near agricultural areas, because of their extensive use in farming (Barbash et al. 2001, Jacomini et al. 2009). These

herbicides undergo different transformations such as chloroanilines, which are found in rivers, reservoirs, and groundwater (Mills et al. 2005, Hallberg 1989, Coupe and Blomquist 2004) and are more toxic than the parent compounds. Among all the chlorinated herbicides, the 2,4-dichlorophenoxyacetic acid (2,4-D) and dicamba were widely used for controlling broad leaf weeds and noxious weeds. 2,4-D is an ionizable herbicide and is weakly retained in soil components (Mantilla et al. 2009) and has higher tendency towards surface water(through surface runoff) and groundwater (seepage) aquifer. It is available in the form of the salts (sodium, the dimethylamine and diethylamine) and esters (butyl, ethylhexyl, octyl). Both forms are considered as a priority herbicides and need to be monitored in the aquatic environment. Ametryn is a selective type of herbicide used to kill unwanted plants (broad leaf and grass weeds) and traces are detected in sugarcane juice in Brazil (Zuin et al., 2006).
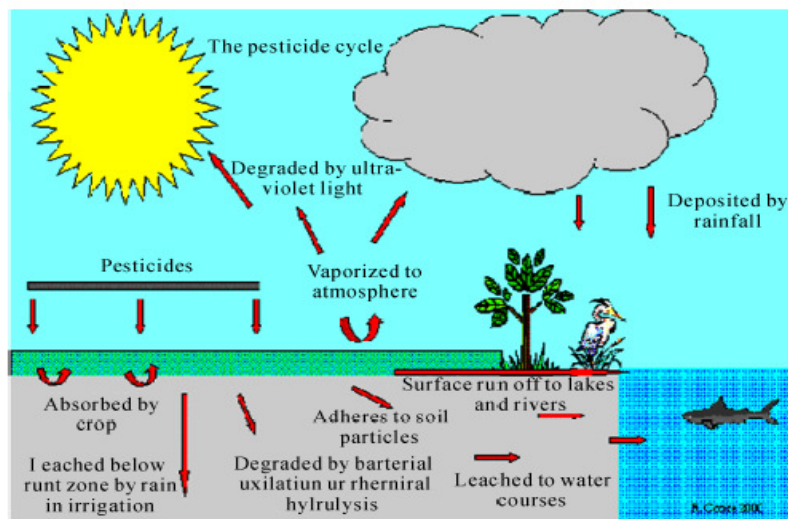
Figure 2.1 Different stages pesticide cycle (Web: Ecifm, accessed on 10-10-2014)

The herbicide residues in soil can be minimized by crop rotation and extent of retention depends on mainly environmental factors such as soil composition, microbial activity and organic matter. The problem of herbicidal residual toxicity in the soil can be overcome by i)the use of optimum dose ii) addition of organic matter iii) the use of herbicide tolerant crops iv) the use of surfactants with herbicides can lower the dose of

herbicides and reduces the overall toxicity v) use of less residue persistent herbicides. Due to the technology improvement, the farmers have started applying the mixture of herbicides to control different types of weeds. The mixture of herbicides have synergic effect on different kind of weeds, that are present in field   ex: 2, 4-D (1kg/ha) + Dicamba (2kg/ha).

2.2. PHYSICO– CHEMICAL TREATMENT OF HERBICIDES

The physico-chemical treatment involves the physical process or chemical process or sometimes a combination of both processes (chemical coagulation, sedimentation, filtration, adsorption, ion exchange etc.). In these processes, the   partial degradation of herbicides is achieved and it depends on indicator parameter of behavior of pesticides in soil and water environment   (Malato et al. 1997) such as K_{ow}(octanol-water partition coefficient), K_{oc} (organic carbon partition coefficient) and K_d (solid–water distribution coefficient).

The ametryn and chlorinated herbicides are considered as endocrine disrupting chemicals (EDCs) and therefore more resistant towards physic-chemical treatment process. The limitations include i) EDCs toxicity levels are too high and that can't be removed with the required efficiency in any of the physico -chemical process. Therefore, these processes are not so effective for the removal of EDCs. The literatures on some physico- chemical processes are shown in Table 2.1 and the results showed that, less removal was observed in both GAC (granular activated carbon), PAC (powded activated carbon) adsorption. A significant increase in the removal efficiency occurred   with the use of imprinted amino-functionalized silica gel sorbent and MIEX resin.

Table 2.1 Physico-chemical treatment of herbicides

Author, Year, Journal	Treatment Method and compound Name	Experimental conditions	Results and Inference
Ding et al. 2012, Ind. Eng. Chem. Res.	Adsorption on MIEX Resin, 2,4-D	$2,4 D_0 = 5,10,20$ mg/L HPLC: C_{18} column, $\lambda_{max} = 284$ nm, pH of 5–9, ACN/ultrapure water (70/30, 1 mL of formic acid), 40 °C.	293 mg of 24D /g resin is adsorbed with pH =8 as optimum, Temperature was not affected the adsorption.
Dehghani et al. 2014, J. of Env. Health Sci. and Engg.	Adsorption on GAC, 2,4-D	$2,4 D_0 = 0.5$ -3 mg/L pH (3–9), contact time (3–90 min), amount of adsorbent (0.1-0.4 g), HPLC: C_{18} column	63% removal at pH 6 in 60 min(optimum values) Langmuir and Freundlich models($R^2 = 0.999$.
Navaratna et al. 2012, Bioresource Technology	Adsorption and Biodegradation, Ametryn	$AM_0 = 0$-5 mg/L, amount of adsorbent (0.0-0.5 g); temp 20-28 ^{0}C, Time: 1-90 hr, HPLC: C_{18}, $\lambda_{max} = 222$ nm and 254 nm; ACN/ultrapure water (70/30, V/V).	Only 20–40% removal in MBR and remaining in GAC adsorption.
Derylo-Marczewska et al. 2010, J. Therm. Anal. Calorim	Adsorption with PAC, 2,4-D	$2,4 D_0 = 0.4$–2.2mM, $\lambda_{max} = 278$ nm, Temperature =15-45 ^{0}C, pH-6-8.	50-60% removal at 25 ^{0}C.
Han et al. 2010, J. Environ. Sci.-China	-Imprinted Amino-Functionalized Silica Gel Sorbent, 2,4-D	$2,4 D_0 = 50$-800 mg/L HPLC: C_{18}, $\lambda_{max} = 280$ nm, ACN/ultrapure water (70/30), 1 ml/min flow rate, pH = 1–7, 5-120 min of Reaction Time	70-90% removal in 120 min.

2.3. BIOLOGICAL TREATMENT OF HERBICIDES

Bioremediation is the use of microorganisms to degrade environmental contaminants. It has numerous applications like clean-up of surface water, ground water, soil and sludge. Bioremediation operates in multiphase, heterogeneous environments and hence, it is important to know the microbiology, engineering, ecology, geology, and chemistry for the success and full remediation. It involves both in- situ and ex situ methods. They are land farming, composting, bioreactors, bioventing, biofilters, bioaugmentation, biostimulation, pump and treat. The main aim in bioremediation is to stimulate microorganisms with nutrients and other chemicals that will enable them to destroy the contaminants. The bioremediation systems in operation today depends on microorganisms native to the contaminated sites, encouraging them to work by nutrient supplements for their metabolism. Thus, today's bioremediation systems are limited by the capabilities of the native microbes. However, researchers are currently investigating ways to augment contaminated sites with non-native microbes—including genetically engineered microorganisms—specially suited to degrading the contaminants of concern at particular sites. Furthermore, the byproducts of microbial processes can provide indicators that the bioremediation is successful. These biological treatment methods have their own limitations like slow degradation, inability to break the bonds involved in the choloro aromatic compounds, operation and maintenance of biological systems etc. (Farre et al. 2002). With all limitations, still many researchers have applied biological systems for the degradation of herbicides (Table 2.2) and results showed that, 96-100% removal was observed in > 70 days of reaction time.

Table 2.2 Bioremediation of herbicides

Author, Year, Journal Name	Treatment Method and compound Name	Experimental conditions	Results and Inference
Celis et al. 2008, Water Research	Biodegradation with SBRs, 2,4-D	2 ,4 D_0=120,500,700 mg/L, HRT of 48 h, 3:1 mixture (by weight) of fresh sludge and biomass, 2 L capacity	Complete removal occurred at 30 d (aerobic SBR) and 70 d (anaerobic SBR).
Goshdastidar and Tong 2013, J Environ. Sci. Pollut. Res	MBR, 2,4-D and Dicamba	D_0 and 2,4 D_0 = 300 µg/L to 3.5 mg/L, Bioreactor=10 L, HPLC: Water :methanol (65:35), 0.5 mL/min, λ_{max} =210 nm.	2,4-D =99.0 % removal in 12 days and dicamba removal of 75.4 % in 112 days.
Navaratna et al. 2012, Bioresource Technology	Biodegradation , Ametryn	$AM_0^=$ 0.1 mM, Temp=15-25 °C, HPLC: ACN-water-glacial acetic acid in 60:39.5:0.5(v/v), 1.0 mL/min, Column Temp= 30℃; λ_{max} =271 nm.	100 % degradation in 145 days at 25 °C.
Sandoval-Carrasco et al. 2013, Bioresource Technology	Biodegradation, ,4-D and Ametryn	$AM_0^=$ 31.5-50mg/L, 2-4D_0 =23-50mg/L,HPLC :ACN-water (30:70), 1.0 mL/min, λ_{max} =222 nm(Both).	The removal efficiencies upto 97% for both herbicides in 76 days

2.4 Advance Oxidation Process

To overcome the limitations of physico-chemical and biological process, the advanced oxidation processes (AOPs) were recommended to treat the herbicides in water and wastewater. These processes involve the generation of powerful oxidant species like hydroxyl radical (OH•) with rate constants of 10^6–$10^9 M^{-1}$ s^{-1} (Hoigné and Bader 1983). The OH radicals degrade or mineralize (CO_2, H_2O and inorganic acids) even at very high or low concentration. The AOPs involve UV/H_2O_2, UV/TiO_2, H_2O_2/Fe^{2+}, O_3/H_2O_2 etc (Figure. 2.2). Among all, conventional Fenton reagent (H_2O_2/Fe^{2+}) proved to be the best treatment technique for the remediation of many of the pollutants (Mendoza-Marin et al. 2010, Garcia et al. 2013).
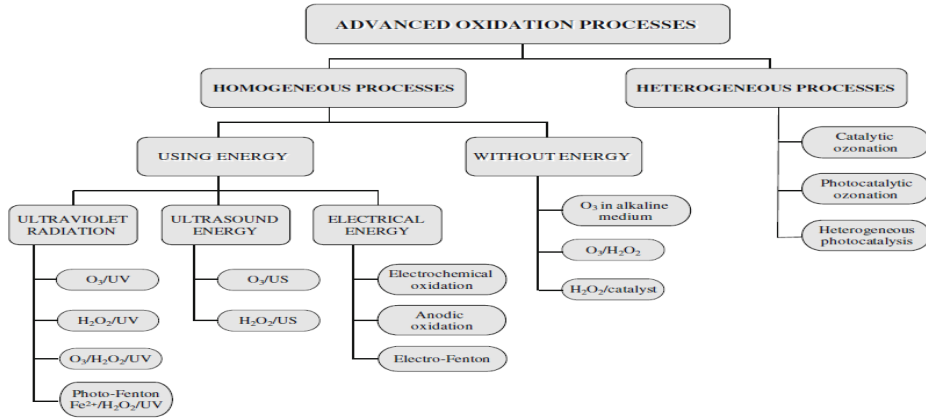
Figure 2. 2: Advanced oxidation processes (AOPs) classification (Poyatos et al. 2010).

2.5 CONVENTIONAL FENTON'S PROCESS

Introduction

Fenton's reagent was used for destroying toxic organics from water as redox process. The Fenton's process involves the reaction between Fe^{2+} / Fe^{3+} (catalyst) and H_2O_2, where the OH• radicals are produced (oxidation potential 2.8V) and thereby promoting the oxidation of organic compounds by various mechanisms like hydroxylation of benzenes, oxygen atom transfer etc (Riviere et al. 2004). H_2O_2 has wide application for the treatment of inorganics such as sulphites, hypochlorites and pharmaceuticals . (Venkatadri and Peters 1993, Beltrán and Rey 2018) and this can be sometimes directly injected into the subsurface to enhance the biodegradation process (Calabrese and Kostecki 1989, Wang et al., 2015, Tawabini, 2014).

Oxidation by H_2O_2 alone is not effective for many of the aromatic compounds and hence iron, ozone and UV-light are used to enhance the activity of H_2O_2 by forming OH radicals(E^0= 2.8V) are shown in Eqs 2.1, 2.2, 2.3.

$$O_3 + H_2O_2 \rightarrow OH^{\bullet} + O_2 + HO_2^{\bullet} \qquad \text{(Ozone and Hydrogen peroxide)} \qquad (2.1)$$

$$Fe^{2+} + H_2O_2 \rightarrow Fe^{3+} + OH^{\bullet} + OH^{-} \text{ (Iron salts and hydrogen peroxide)} \qquad (2.2)$$

$$H_2O_2 + UV \rightarrow 2OH^{\bullet} \qquad \text{(UV light and hydrogen peroxide)} \qquad (2.3)$$
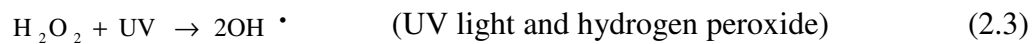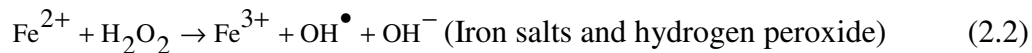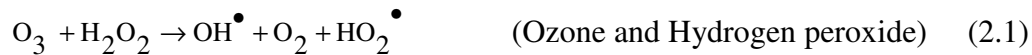
The main important operating conditions of the Fenton process are catalyst/ H_2O_2 ratio, (Yoon et al. 2000; Bigda 1995) pH, temperature and pollutant concentration. Iron usually

exists as Fe^{2+} or Fe^{3+} or sometimes Fe^{6+} (ferrate). Under acidic conditions ferrate is a powerful oxidant (E^0 = 2.2 V in acidic and 0.7 in basic condition) and the details are shown in Table 2.3 and Eqs. (2.4–2.6).

$$FeO_4{}^{2-} + 8H^+ + 3e^- \rightarrow Fe^{3+} + 4H_2O \text{ (Acidic)} \tag{2.4}$$

$$FeO_4{}^{2-} + 2H_2O + 3e^- \rightarrow FeO_2{}^- + 4OH^- \text{ (Alkaline)} \tag{2.5}$$

$$FeO_4{}^{2-} + 4H^+ + 3e^- \rightarrow Fe(OH)_3 + OH^- \text{ (For weak, neutral and alkali solutions)} \tag{2.6}$$
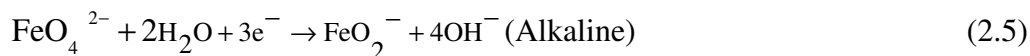
Table 2.3 Comparison of E^0 for selected oxidizing agents (Source :Sharma, 2002)

Oxidizing agent	Electrode Oxidation Potential (V)
OH (Acidic environment)	2.80
Ferrate (acidic and basic)	2.20 and 0.7
O_3	2.08
H_2O_2	1.78
Cl_2	1.36
Chlorine dioxide	1.27

The conventional Fenton process works in the acidic range of pH around 3 where more OH• radicals are produced and that radicals react with most of the organics to form low-molecular-weight organic acids (LMWOAs), such as oxalic and acetic acids or sometimes carbon dioxide and water (Sun and Pignatello. 1993). At higher pH levels, the oxidizing species precipitate as ferric hydroxide, so that it is not possible to regenerate the active species (Fe^{2+}). Some of the literatures related to AOPs are tabulated below (Table 2.4). The results showed that, all the treatment processes (solar photo-Fenton-biological system, anodic Fenton, UV/H_2O_2/micro-aeration, solar photocatalysis, Fenton-like process, photoelectro-Fenton process, radiolytic degradation) are able yield 75-100% of degradation (2,4-D) and these processes are less effective in mineralization of 2,4-D (69-90% TOC removal). Very few literatures are available related to degradation of ametryn and dicamba (UV:H_2O_2:TiO_2 and UV:H_2O_2), where >95 % of degradation was observed and as per the authers knowledge, no studies were reported on Fenton oxidation of ametryn and dicamba in agriculture runoff water.

Table 2.4 AOPs for herbicides

Author, Year, Journal	Treatment Method and compound Name	Experimental conditions	Results and Inference
Mendoza-Marín, et al. 2010, J. of Haz. Mat.	Solar photo-Fenton-biological system, 2,4-D and Diuron	Real w/w : 2,4- D_0 (860–930 mg/L) and Diuron (21–600 mg/L), Synthetic w/w: 2,4-D (300mg/L) and Diuron (29mg/L), HPLC : C-18, methanol-water (45:55), flow rate: 1ml/min, UV power of $30Wm^{-2}$, H_2O_2/Fe^{2+}: 5-35, P^H=3.	Mineralization of 79.8% in synthetic wastewater and 82.5% in real industrial wastewater
Wang et al. 2001, Env. Sci. & Tech.	Anodic Fenton, 2,4-D	2 ,4-D_0=200 µM, HPLC: C-18, ACN-water (45:55), flow rate: 1ml/min, UV power of $30Wm^{-2}$, H_2O_2/Fe^{2+}: 1:1- 100:1, P^H=3, λ_{max} =280nm, current = 0.010 A	90% removal in 10 min and optimum H_2O_2/Fe^2:10:1
Conte et al. 2012 and 2016, Ind. Eng. Chem. Res.	Photo-Fenton Degradation, 2,4-D	2 ,4-D_0 =0.13 mM and pH= 3, HPLC: C-18, ACN-water (50:50), flow rate: 1mL/min, UV power of $30Wm^{-2}$; H_2O_2/Fe^{2+}: 5:50, λ_{max} =280nm and 236 nm; T (°C) = 20- 50, pH=6-6.5.	100 % degradation of 2,4-D after 60 min.
Kamble, et al. 2004, Ind. Eng. Chem. Res.	Solar Photocatalytic Degradation, 2,4-D	2 ,4 D_0 =100 -400 mg/L,UV power of 9.3 W m^{-2}, HPLC: C-18 column, ACN-water: acetic acid (50:50:0.2 %v/v), flow rate: 0.5mL/min, λ_{max} =280nm, P^H=2-4.	TOC removal = 88.6- 69.9% and 2,4-D removal= 99.5- 99% within 4 h.
Chu et al. 2009, Sci. China. Ser B-Chem.	$UV/H_2O_2/$ micro-aeration, 2,4-D	2 ,4 -D_0 =59.2 to 300.0 µg·L^{-1}, UV= 183.6 to 1048.7 µW·cm^{-2}, Temp 15 to 30°C, H_2O_2 and pH ranged from 0 to 50 mg·L^{-1} and 5 to 9, HPLC: C-18, ACN-water (70:30), flow rate: 0.8 mL/min, λ_{max} =284nm.	95.6 % removal under optimum conditions of UV intensity 843.9 µW·cm^{-2},H_2O_2 =20 mgL^{-1} and pH =7.

Table 2.4 AOPs for herbicides (Continued….)

Author, Year, Journal	Treatment Method and compound Name	Experimental conditions	Results and Inference
Chen et al.2015, Chemical Engineering Journal	Fenton-like process 2,4-D	2 ,4 -D_0 =10 mg/L, Temp 20- 50°C; H_2O_2 and pH ranged from 3 -10mM and 2 to 6.5, Fe : 0.5 -1 g/L, Time 0-350 min, HPLC: C-18, methanol –water:acetic acid (75:23:2% v/v), flow rate: 1.0 mL/min, λ_{max} =285nm.	Optimum values are pH = 4.5, H_2O_2= 10 mM, Temperature =30 ^{0}C, Fe=0.5 g/L ,Time =300 min, 2, 4- D removal=100 % and TOC removal=70.4% .
García et al. 2013, Electrocatalysis	Electro-oxidation and Electro-Fenton Processes, 2,4-D	2 ,4-D_0 =60 mg/L, Temp 20- 22°C, H_2O_2 and pH ranged from 54-64mg/L and 2 -5, Fe^{2+} =0.3-0.7mM, Time=0-180min, HPLC: C-18, ACN :water (75:25); flow rate: 0.9 mL/min, Column Temp= 30°C; 3-L pilot plant, 64 cm^2 of electrode area; pH 3.0, current densities : 7.8-31 mA cm^{-2} and liquid flow 4 -10 L min $^{-1}$, Boron diamond electrodes .	The electro-oxidation=70 % mineralization (160 min). In electro-Fenton /BDD=81–83 % of mineralization in 120 min with lowest energy cost of 95 kWh kg^{-1} TOC with of pH=3.
Brillas et al. 2007, Chemosphere	Electro oxidation, electro-Fenton and photoelectro-Fenton , 2,4-D	2 ,4- D_0 = 217 mg/L; Temp 35°C, H_2O_2 and pH were 20mM and 3, Fe^{2+} = 0.5 - 2.0 mM, Time 0-420 min, HPLC=C-18, 50:45:5% (v/v) methanol/water phosphate buffer (pH 2.5), 1.0 mL/min, λ_{max} =280 nm; 76 cm^2 of electrode area, current densities = 100-450 mA cm^{-2} and Pt or Boron diamond electrodes.	100 % degradation of 2, 4-D in 180 min. Other intermediates and acids were degraded in 360 min. Photo electro-Fenton proved to be the better process.
Brillas et al. 2004, Chemosphere	Electro oxidation, electro-Fenton Process, 2,4-D	2 ,4 D_0 = 230 mg/L; Temp 35°C; H_2O_2 and pH were 20mM and 3, Fe^{2+} = 0.5 - 2.0 mM ; Time 0-420 min, HPLC: C-18,50:45:5% (v/v) methanol/water phosphate buffer (pH 2.5), 1.0 mL/min, Column Temp= 35°C, λ_{max} =280 nm, 76 cm^2 of electrode area,0.05M Na_2SO_4, current densities = 100-450 mA cm^{-2} and Boron diamond electrodes.	100 % degradation and 82 % mineralization of 2,4-D in less than 60 min with 1 mM of Fe^{2+}.

Table 2.4 AOPs for herbicides (Continued….)

Author, Year, Journal	Treatment Method and compound Name	Experimental conditions	Results and Inference
Kwan and Chu 2003, Wat. Res.	Photo degradation, 2,4-D	2,4- D_0 = 2.26mM, 2 UV lamps at 254 nm,H_2O_2 and pH were 1mM and 2.8, Fe^{2+} = 0.1 mM,Time 0-120 min, HPLC: C-18 column, 50:50 ACN /water(0.5 % of acetic acid), 1.5 ml/min, sample volume= 20 μL, Column Temp= 35℃, λ_{max} =283 nm.	100 % degradation by UV with ferrous oxalate
Brillas et al. 2000, Wat. Res.	Electro-Fenton and photoelectro-Fenton, 2,4-D	2 ,4 D_0 = 230 mg/L, Temp 35℃, H_2O_2 and pH were 17-73 mM and 3.1, Fe^{2+} = 0.5 - 2.0 mM,Time 0-420 min, HPLC: C-18, 60:40: ACN /phosphate buffer (pH 2.5), λ_{max} =280 nm, 76 cm^2 of electrode area, C.D = 100-450 mA cm^{-2} and Boron diamond electrodes.	99% TOC removal was observed after 4hr with 400 mA cm^{-2} in photo electro-Fenton process.
Drzewicz et al. 2005, Arch. Env. Contam. Toxicol	Radiolytic Degradation, 2,4-D	D_0=110 mg/L (0.5 mM), γ-irradiation=0-10 kGy, HPLC: C-18, Water :methanol: Acetonitrile : (65:35:5) v/v, 1.0 mL/min, Column Temp= 30℃, λ_{max} =210 nm.	The 100 % decomposition at 2.7 kGy of irradiation.
Fabbri et al. 2007, Res. Chem. Intermed.	Photo-degradation, Dicamba	D_0=25 mg/L, UV =120 W, TiO_2 (150–500 mg/L), H_2O_2 (4.7 × 10^{-4} – 4.7 × 10^{-2} M), Time =0-400 min, HPLC: C-18, ACN : ammonium acetate of P^H=6.8 (4:96 v/v) ; 1.0 mL/min, Column Temp= 30℃, λ_{max} =274 nm or 220 nm.	The mixed UV:H_2O_2:TiO_2 treatment was able to remove 94% at 80 min
Gao et al. 2009, J. of Haz. Mat.	UV/H_2O_2, Ametryn	AM_0= 1-5 mg/L, UV lamp (30W, 253.7 nm), pH=4 -8, H_2O_2 =0 – 150mg/L, HPLC: C-18, ACN : Water (60:40); 0.8 mL/min, λ_{max} = 240 nm	>95% of ametryn removed in 50 min

2.6 ADVANCE FENTON PROCESS

The conventional Fenton process involves the use of iron salts such as ferrous sulfate, ferric chloride, adds extra sulfate to the treatment system and also generates a lot of iron sludge. To overcome these limitations, many researchers have applied heterogeneous Fenton-like processes e.g. nano scale zero valent iron (nZVI) (Xu and

Wang 2011), iron supported clay (Hassan and Hameed, 2011), goethite (ά-FeOOH) (de la Plata et al., 2010) and Fe_3O_4 (Zhang et al. 2009).

Nano size particles have higher specific surface area and reactivity, which helps in degradation of contaminates (Shahwan et al. 2011). Hence, FeNPs are synthesized by using $NaBH_4$ as reducing agent (Xu and Wang, 2011) and co-precipitation of Fe^{2+} and Fe^{3+} (Xu and Wang 2012). However, these methods have the limitations like stability, toxic nature of sodium borohydrate, corrosive, agglomeration of particles, the use of organic solvents like methanol and are more expensive towards large scale field applications (Chen et al. 2013, Huang et al. 2014). Therefore, green synthesis of iron nano particles (GFeNPs) using plant extracts have been developed and later synthesized FeNPs were applied as a Fenton's like catalyst to degrade various pollutants (Shahwan et al. 2011, Kuang et al. 2013). The leaf extract contains polyphenols/caffeine, which acts as both reducing and capping agent, provides the best platform for the synthesis. The efforts are made to synthesize iron nanoparticles from locally available laterite from sustainable leaf extracts such as Tactona Glandis (Teak) (TG) and Eucalyptus Globulus leaf extracts (Nilgiri)(EG).

2.7 LATERITE AS A FENTON'S CATALYST

The term laterite includes a variety of minerals in oxide forms and can be found in several parts of the world including India. It is essentially a mixture of ferric hydroxide, aluminum hydroxide, silica, titanium and manganese in varying proportions (Maiti et al., 2010). The laterite has the advantages like abundance, low cost, thermally stable, no toxicity in the environment and a proper alternative to the traditional iron. Hence, it is applied as Fenton's catalyst for the removal of sodium azide (Khataee and Pakdehi 2014), azo dye (Khataee et al. 2015), dye (Aleksica et al. 2010) and pharmaceuticals (Manu and Mahamood 2011; Karale et al. 2013). The removal efficiency of pharmaceuticals with iron extracted from a laterite is less, compared to ferrous sulfate and this can be improved by producing the GFeNPs from natural laterite. Laterite belongs to the natural mesoporous structure (Khataee and Pakdehi 2014) and degradation process that takes place on the surface of a solid catalyst. Also, in comparison with other

solid catalysts such as natural clays, resin supports and zeolites, laterite possesses higher content of Fe ions and is used for the preparation of inorganic polymers (Gualtieri et al. 2015). The typical laterite soil consists of SiO_2 (38–43%), Al_2O_3 (25–28%), Fe_2O_3 (26–30%), TiO_2 (3–4%), K_2O (1–2%). CaO (0.5%), C (0.2%) (Khataee and Pakdehi 2014). The degradation of pollutants with laterite is accomplished in ambient temperature compared with clays and zeolites (requires 60^0C) (Navalon et al. 2010). Hence, it is a proper alternative to the traditional ferrous salts.

Khataee and Pakdehi (2014) investigated the   treatment of sodium azide in aqueous solution by a heterogeneous Fenton process in the presence of natural laterite as   a catalyst. The effect of initial pH, dosage of laterite, H_2O_2, sodium azide concentration and reaction time on removal efficiency was investigated. Optimized experimental conditions were pH = 3, laterite= 1 g/L, 3 mM H_2O_2 with removal efficiency of 97% in 60 min. The XRD pattern shows the existence of two   Fe phases such as goethite(FeO(OH)) and hematite (Fe_2O_3). Goethite contains –OH group and de-hydroxylation of goethite produce hematite. Also, experimental results demonstrated that laterite is a suitable alternative for typical ferrous salts. Khataee et al. (2015)) studied the treatment of C.I. Acid Red 17 (AR17) by heterogeneous photo-Fenton-like process using calcined laterite soil as an iron source. The calcined laterite is of Type IV, according to the IUPAC classification and the complete characterization was performed. Comparing with the heterogeneous Fenton-like and photo- Fenton-like, the photo-Fenton process led to the highest decolorization efficiency (94.71% at 120 min).

 As discussed earlier several methods were used for the production of iron nanoparticles, namely i) top-down methods (Li et al. 2006) such as vacuum sputtering or the decomposition of iron pentacarbonyl ($Fe(CO)_5$) in organic solvents. ii)Bottom-up methods that promote the 'growth' of the nanostructures via chemical synthesis(exa. the reaction of iron(II) or iron(III) salts with sodium borohydride) (Wang and Zhang 1997). However, the top-down methods are generally expensive and require specific and costly equipment and the bottom-up approaches relate to the safety issues due to the toxicity of

sodium borohydrate and the production of flammable hydrogen gas during the process (Li et al. 2006). In addition, these methods are having the tendency to form large agglomerates at a faster rate with lesser reactivity. These disadvantages are overcome by the green synthesis by selecting the 'greener' solvents and reducing agents or the utilization of appropriate capping agents (Hoag et al. 2009). In this approach, extracts of natural leaf (Chrysochoou et al. 2012, Valle-Orta et al. 2008) with high antioxidant capacities are used. The compounds present in these extracts react with iron in solution to form FeNPs (Nadagouda et al. 2010). The main advantages of this method include i) No use of toxic chemical like borohydrate ii) rich in polyphenols enhancing their reactivity iii) leaves are considered as wastes except some medicinal benefits. iv) extract having high water solubility v) acts as a nutrient source and enhance the degradation (Hoag et al. 2009, Nadagouda et al. 2010). In addition, the leaf extracts have other benefits such as antimicrobial, antiviral, and anti-inflammatory properties along with their antioxidant activity (Ignat et al. 2011). Machado et al. (2013) synthesized FeNPs from many leaf extracts such as apple, passion fruit, apricot , peach avocado, pear, cherry, eucalyptus, pomegranate, kiwi, plum, lemon, quince, mandarin, raspberry, medlar, strawberry, mulberry, tea-black, oak, tea-green, olive, vine, orange, walnut and the oak, pomegranate, green tea leaves producing extracts with maximum removal efficiency. The eucalyptus and tactona glandis leaf extracts are non-toxic, biodegradable and are byproducts of timber and paper mill industry and sometime these are used for the extraction of oils (medicinal value) (Chen et al., 2014). Hence, FeNPs were produced from eucalyptus leaves and are applied for the degradation of many contaminants like nitrate (Wang et al. 2014a), Cr (VI) (Madhavi et al. 2013) and eutrophic wastewater (Wang et al. 2014b).

Madhavi et al. (2013) applied eucalyptus globulus leaf extract as a bioreducing agent to synthesize FeNPs and synthesized particles were found to be stable for about 2 months. The Cr^{6+} (400 mg/L) was degraded up to 98.1% with 0.8 g/L of FeNPs in 30 minutes. Wang et al. 2014 applied EG leaf extract and green tea extract for the remediation of nitrate in water and highest removal efficiency of 59.7% was observed. The 2nd order

degradation kinetics was best fitted and the removal mechanism was dominated by adsorption followed by co-precipitation.

King et al, 2006 studied the adsorption of copper with teak leaves powder by maintaining the operating conditions such as initial concentration, pH, adsorbent dosage and particle size. The removal efficiency was 71.66% with 0.1 g of Teak powder (20 mg/L of copper, time 180 min and pH=5.5). Both Langmuir and Freundlich models were adopted and best model was finally determined. Both 1st and 2nd order models were studied and 2nd order kinetics proved to be the best model.

2.8 DESIGN OF EXPERIMENTS (DOEs)

Selecting a good set of points in a given space for carrying out experiments is known as (DOEs) design of experiments. The DOE involve many levels for the variables (factors) based on the type of application. They are 2 (each control factor has only two levels), 3,4, 5 levels and mixed level designs (control factor have many levels). The DOE consist of four types and they are Factorial, RSM (response surface methodology), mixture and Taguchi design. In our present study, the Taguchi and RSM are preferred.

RSM and TAGUCHI method

Taguchi design can be applied, where the less number of samples are available and to optimize the variables involved in the treatment system with minimum noise. The response surface methodology (RSM) is a statistical technique for the design of experiments, which involves modeling and analysis of problems where response of interest is influenced by several factors and the objective is to optimize this response or to refine the models. The RSM was introduced by Box and Wilson in 1951 with first-degree polynomial. Later, Mead and Pike improved the RSM to form response curves (Myers et al. 1989) with orthogonal design and after that Box and Behnken (1960) suggested the central composite designs (CCDs) with second-order models. The main objective of studying RSM is to understand the response surface details (maximum and minimum along with ridge lines) and the optimal region on the surface. Basically the RSM is classified as i) CCD ii) Box-Behnken design(BBD).

The CCD is most commonly used, which models the curvature by adding center and axial points(star points). Central composite design is created from a 2-level factorial design and can easily fit to a full quadratic model. It efficiently estimates the first- and second-order terms. The CCD consists of 3 and 5 levels for each factor. BBD has few design points than CCD with the same number of factors and it is less expensive and it also provides first- and second-order equations, however it has always 3 levels per factor. BBD is weak at the corners of the cube in design space and strong near the center and has fixed positioning in design space. It is not recommended if the experiment is ended with missing runs, or bad runs, then the whole design process has to be repeated. The RSM was illustrated by following example: The growth of a plant(y: dependent variable) is affected by water x_1 and sunshine x_2 factors (independent variables)(Eq. 2.7).

$$y = f(x_1, x_2) + e \tag{2.7}$$

Where e is experimental error and the first-order polynomial equation(2.8).

$$y = \beta_0 + \beta_1 x_1 + \beta_2 x_2 + \varepsilon \tag{2.8}$$

If the curvature is more, then higher degree model equations are preferred and with 2 variables second-order model is written in Eq. 2.9. The multiple-regression model equations is shown in Eqs. 2.10 and 2.11, where β_0, β_1, β_2, β_{11}, β_{22}, β_{12} are coefficients, q=independent variables, where $N > q$. The parameter β_j defines the predicted change in dependent factors per unit increase in independent factors and i denotes observation with j level. The RSM can be clearly defined by graphically with surface and contour plots and these plots consists of hills, valleys, and ridge lines, which helps in understanding the interactive effect on the responses.

$$y = \beta_0 + \beta_1 x_1 + \beta_2 x_2 + \beta_{11} x_{11}^2 + \beta_{22} x_{22}^2 + \beta_{12} x_1 x_2 + \varepsilon \tag{2.9}$$

$$y = \beta_0 + \beta_1 x_{i1} + \beta_2 x_{i2} + \ldots + \beta_q x_{iq} + \varepsilon_i \ldots \ldots where(i = 1,2...N) \tag{2.10}$$

$$y = \beta_0 + \sum_{i-1}^{q} \beta_j x_{ij} + \varepsilon_i \ldots \ldots where(j = 1,2....q) \tag{2.11}$$

CCD Points and Types of CCD

Based on the location of the points in the design space the CCD can be classified as i) Circumscribed (CCC) ii) Inscribed (CCI) iii) Face Centered (CCF) shown in Figure.

2.3(b) and has three types of design points they are (a) fractional factorial design points (factorial points) (b) axial points (star points) (c) center points. The CCD points are explained in Figure. **2.3**(a).
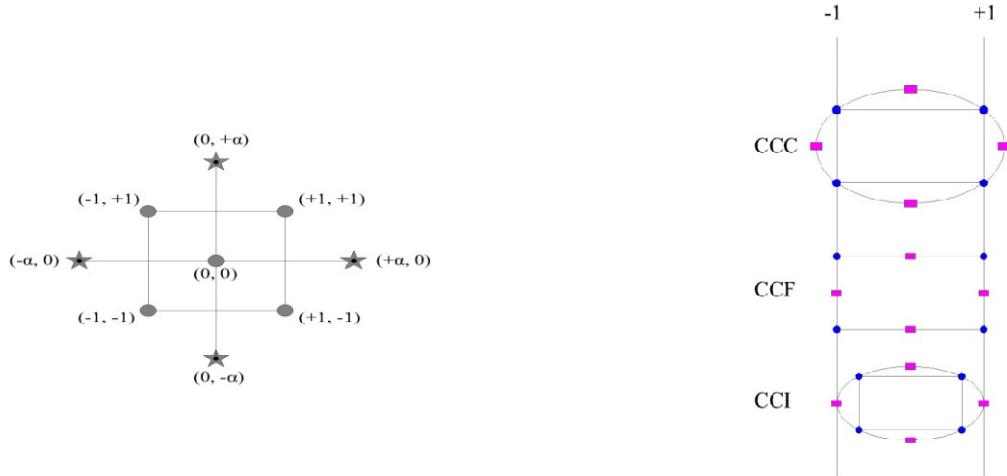
Figure 2.3 a) Typical sketches showing the points of CCDs b) Types of CCDs

Factorial Points: For two-factor with two levels (-1 and +1), the points are (-1, -1) (+1, -1) (-1, +1) (+1, +1)

Star or Axial Points: These points always have the middle point (0) followed by +/- Alpha. The points are (-Alpha, 0) (+Alpha, 0) (0, -Alpha) (0, +Alpha) for 2 factor design matrix. The value of Alpha is calculated as $2^{2/4} = 1.414$ (factors= 2 and runs= 2^2) (Eq.2.12).

α= [number of factorial runs] $^{1/4}$ (2.12)

 Center Points: Center points are written as (0, 0) and are usually repeated 3-4 times for best results.

Hermosilla et al. (2012) studied the RSM based optimization of Fenton and photo-Fenton oxidation processes for retentate (reverse osmosis) in a paper mill industry. The Fenton process achieved about 80% reduction in COD at pH = 2.8, and <60% without adjusting the initial pH and the efficiency was increased with TiO_2-photocatalysis. Saeeda et al. (2014) studied the post treatment palm oil mill effluent (POME) using a Fenton oxidation process with CCD. Important parameters such as reaction time, H_2O_2,

Fe^{2+}and pH were varied. The maximum removal efficiencies of 97.36% (color removal) and 91.11% (COD removal) was achieved at pH 3.5 with the reaction time of 30 min. Kasiri and Khataee (2011) studied the decolorization of (Basic Blue 3 (BB3) and Acid Green 25 (AG25)) dyes by UV/H$_2$O$_2$ process. The process was optimized by CCD by studying the effects of operational parameters like the time, pollutant concentration, H$_2$O$_2$ and distance of UV lamp from the dye. The predicted values of the removal efficiency were in good agreement with experimental values. Li et al. (2010) applied CCD in Fenton process for the oxidation of biologically treated landfill leachate. The effect of pH, Fe(II), H$_2$O$_2$/Fe(II) and reaction time, were considered with two responses such as COD and color and the optimal conditions were found to be pH =5.9, Fe^{2+} = 9.60 mM, H$_2$O$_2$/Fe(II)= 2.38, reaction time = 5.52 h with the removal efficiency of 70-85%. Schenone et al. (2015) studied the degradation and optimization of 2,4-D by photo-Fenton with the 3 level factorial design. The several influencing parameters were varied (temperature and H$_2$O$_2$/ 2,4-D) and the removal efficiency was observed to be >95%.

2.9 SUMMARY OF THE LITERATURE REVIEW

It consists of introduction of the three herbicides such as 2, 4-D, dicamba, ametryn and their effect on the human beings, animals, aquatic life, beneficiary plants and worms present in soil. Many treatment options like physico-chemical, biological, conventional Fenton's process(CFP) and advanced Fenton's process(AFP) using green synthesized laterite as a catalyst were discussed in detail along with the optimization process.

Chlorinated herbicides are quick, easy, and inexpensive in controlling weeds in agriculture field. During the production, handling, spraying or applying herbicides to weeds, the residue remains in soil and during heavy rainfall, it reaches the water body. The extent of pollution depends on the properties of both soil and water. Human beings are exposed to these herbicides thorough skin contact, inhalation, and ingestion. These toxic compounds have many adverse health impacts like xenotoxicity, changes in the body immunity and reproductive system, cellular and DNA damage leading to cancer, affects the non-target organisms in soil (insects), useful plants(sugar cane, maize, rice

etc.), fish, and birds. Therefore, many treatment methods (physico- chemical and biological) were discussed to remove these herbicides (2,4-D, dicamba, amtryn). The chlorinated herbicides are popularly known as EDCs and are having the limitations towards both physico-chemical and biological processes. The limitations are i) high toxicity levels and are not readily biodegradable ii) time required for complete removal is more (difficult to grow cultures (up to one year)) iii) the herbicides containing halogen bonds in their structure. These difficulties were overcome by AOPs (advanced oxidation process). In AOPs, UV–H_2O_2 and ozone is reliable and efficient compared to Fenton's treatment, however costly due to the high energy consumption of UV-lamps. The homogeneous Fenton's process proved that, it can degrade or mineralize the contaminants to harmless compounds, e.g.CO_2 and water, mineral acids. However, it works at narrow pH range(around 3) with iron salts ($FeSO_4.7H_2O$, $FeCl_3$) as a catalyst and creates a lot of iron hydroxide sludge containing extra sulfates and chlorides and limits the recycling of iron for further use. This can be overcome by the use of heterogeneous Fenton's catalyst in nano scale. Hence, FeNPs are synthesized by green extracts (Eucalyptus Globulus and Tactona Grandis), which are waste products in timber and paper mill industry with natural laterite as precursor rather than chemical synthesis. The chemical synthesis involves the limitations like complexity, toxic nature of $NaBH_4$ and methanol and rapid agglomeration.

The laterite has many benefits such as temperature registivity, non-toxic, economical and available at all the places and hence this has been preferred for the synthesis of FeNPs and these NPs are applied as Fenton catalyst in degradation of herbicides. Now a day's statistical design of experiments (DOE) is an essential part of the any process or research, which helps in differentiating experimental variables and the responses with minimal number of experiments (both continuous or batch processes). Here, taguchi and central composite design (CCD) type RSM were successfully applied in Fenton's process than BBD and other factorial designs, which are cost effective and more reliable.

CHAPTER 3
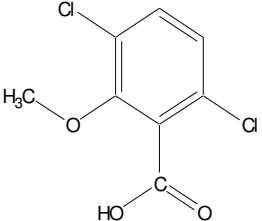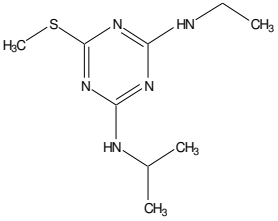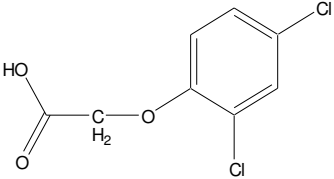
MATERIALS AND METHODS

3.1 GENERAL

The detail properties (both physical and chemical) of herbicides (ametryn, 2,4-D and dicamba) are shown in Table 3.1. The chemicals used for the determination of COD, residual iron, residual hydrogen peroxide, polyphenol and antioxidant property are listed below. The detailed experimental methodology (RSM and Taguchi) and analytical procedures are explained below.

3.2 PHYSICAL AND CHEMICAL PROPERTIES HERBICIDES

Table. 3.1 Physical and chemical properties of dicamba, ametryn and 2,4-D

Properties	Dicamba	Ametryn	2,4 -D
Structure			
Synonym	3,6-dichloro-2-methoxybenzoic acid	(2-ethylamino)-4-(isopropylamino)-6-(methylthio)-s-triazine	2,4-Dichlorophenyloxy acetic acid
Appearance	White crystalline solid	White crystalline solid	white to yellow powder
M. W	221 g/mol	227.35 g/mol	221 g/mol
Chemical Formula	C_6H_2 $Cl_2(OCH_3)CO_2H$	$C_9H_{17}N_5S$	$C_8H_6Cl_2O_3$
Water solubility (mg/L)	4500 at 25 ^{0}C	209 at 25°C	890 at 20 ^{0}C
M. P and B P	115 and 200 °C	84-85°C and 337 °C	140.5 °C and 160 °C
Density (g/cc)	1.57	1.18	1.416

3.3. MATERIALS

The 2, 4-D, ametryn and dicamba were purchased from Sigma Aldrich. The reagents hydrogen peroxide (H_2O_2, 50%w/w), 2,4,6-tripyridyl-s-traizine(TPTZ), ferric chloride, methyl red indicator, gallic acid, Folin- ciocalteu's phenol, sodium carbonate, hydrochloric acid (HCl, 35%), sulfuric acid (H_2SO_4, 98%), iron (II) sulfate heptahydrate ($FeSO_4.7H_2O$), sodium hydroxide (NaOH, 98%), potassium iodide (KI), mercuric sulfate ($HgSO_4$), potassium dichromate, silver sulfate (Ag_2SO_4), FAS (ferrous ammonium sulfate), ferroin indicator, starch, sodium thiosulfate ($Na_2S_2O_3$) and ultra pure water were procured from Merck manufactured in India.

3.4 SAMPLING LOCATION
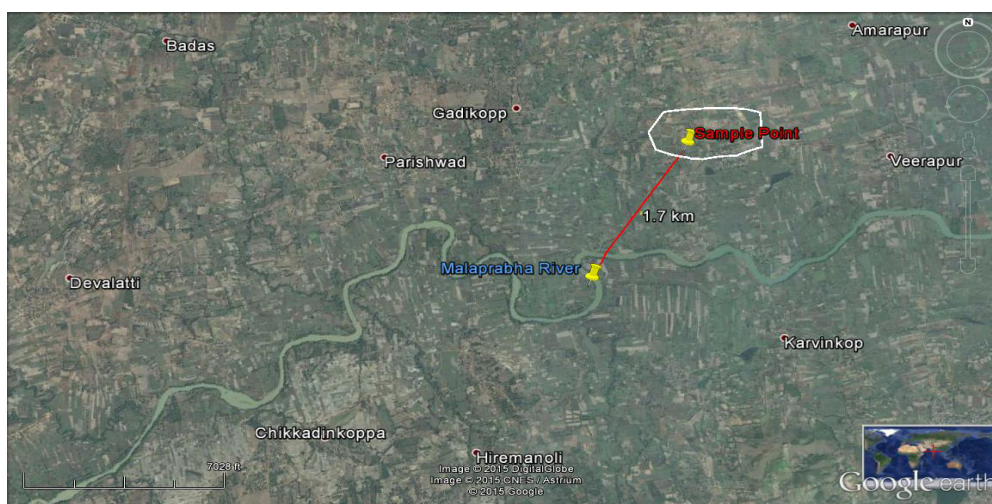
Figure 3.1 Agriculture runoff water sampling point

The agriculture runoff water was collected from Veerapur village, Belgaum district, Karnataka state, India (Latitude: 15°41'27.64"N; Longitude: 74°39'9.11"E) shown in Figure 3.1. This district produces more than 82 lakh tons per year of sugarcane in 2000 ha area (80% of the total district) and from last 5 years, farmers have started using three herbicides 2,4-D, ametryn and dicamba with different formulations based on the type of weeds (broad leaf weeds) and the quantity of weeds that are present in the field. The usage of these herbicides has increased 10 times from the last 4 years and the farmers are spraying 6-9 times in a year. Nearby the sampling site, the river Malaprabha is flowing (Latitude: 15°40'32.73"N; Longitude: 74°38'33.43"E) and there are chances

30

that, the runoff water may reach the river and contaminate it. The runoff water was collected from 0.5 acres of land and water was preserved below 4 ^{0}C according to the standard methods (APHA 2005) for further analysis.

3.5 EXPERIMENTAL METHODOLOGY

The stock solution (3 mM of 2, 4-D, dicamba and 0.4 mM of ametryn) and standard solution (0.13-0.65 mM 2,4-D, dicamba and 0.02-0.1 mM of ametryn) was prepared in HPLC(high performance liquid chromatography) grade water. Then, the HPLC methods were developed by applying proper experimental conditions (Table 3.2) and calibration curves for all standards were prepared (AI:1-9). The runoff water was filtered with 0.2µm filter paper and the herbicide concentrations were quantified with the help of HPLC and they were 25.5 mg/L, 93.7 mg/L and 3.4 mg/L of 2, 4-D, dicamba and ametryn respectively (AI:10-12)**.** The Taguchi experimental design was applied for treatment of real samples (sample size is less) and RSM (response surface methodology) was used for treatment of aqueous solution containing herbicides.

Initially preliminary experiments were performed to know the range of values for all independent variable (H_2O_2/COD, H_2O_2/Fe, pH, and reaction time). Then, the actual experiments were started by considering the initial herbicide concentration (0.13- 0.39 mM for 2,4-D and dicamba, 0.02-0.06 mM for ametryn) based on the actual values observed in the field. In the starting phase, the conventional Fenton process (CFP) using ferrous sulfate as precursor was initiated and in the later stage, preceded by an advanced Fenton process (AFP). In AFP, initially the FeNPs were synthesized with laterite using sustainable plant extracts and then FeNPs were used as a Fenton-like catalyst for the degradation of herbicides. Total 26 experiments were performed in a conical flask (250 ml sample volume) according to the CCD (Central composite design) matrix at room temperature with shaking speed of 200 rpm and the pH was adjusted 0.1 N H_2SO_4. Without adding oxidant and catalyst, the experiment was conducted (24 hrs) and no degradation of any of the herbicide was observed. Each set of experiment was conducted three times and the average of the values was finally considered.

Table. 3.2 HPLC Conditions of dicamba, ametryn, and 2, 4-D

Parameter	Dicamba	Ametryn	2,4-D
Ratio of Mobile Phases	50: 50	58: 42	80 :20
Temperature of the column	35 ^{0}C	25^{0}C	30 ^{0}C
Retention Time (min)	1.382	8.882	1.7
Wavelength λ_{max}	274 nm	223 nm	230 nm
Flow Rate	0.75ml/min	1 ml/min	0.5 ml/min

Sample volume=20 µL; Total run time=20 min; column name and size = RP- C18, 100*4.6 mm, 3.5µ pore size; mobile phase= methanol: water.

After the completion of each set of experiments, the sample was filtered (0.2 μm) and absorption intensity was measured with HPLC calibration curves. The mineralization of all the three compounds was measured in terms of COD (chemical oxygen demand) and are confirmed by LCMS(liquid chromatography/Mass spectrometry) analysis and interference of H_2O_2 was corrected (Wu and Englehardt 2012). The results were analyzed with the help of Minitab software.

3.6 ANALYTICAL METHODS

The final concentration of all three herbicides at different reaction time was measured by HPLC (Agilent 1260) equipped with UV and diode array detector (DAD) and the conditions are listed in Table 3.2. The mineralized products were analyzed by LC/MS-2020(Shimadzu) with single quadrapole having a C-18 column. The closed reflux titration technique (APHA 2005) was used to determine the COD (Eq.3.1) and λ_{max} value was determined by ultra –violet, visible (UV-Vis) double beam spectrophotometer (systronics, AU-2701). TOC (Total organic carbon) was measured with TOC analyser (Shimadzu). The pH was measured using a pH meter (systronics). The concentration of residual hydrogen peroxide was detected by iodometric titration. The standard methods (APHA 2005) were used to determine the nitrates, sulfates, and chlorides in runoff water. The residual iron as Fe^{3+} was measured with a potassium thiocynate method and as Fe^{2+}

with phenanthroline method using UV-visible -spectrophotometer (systronics). The total iron was measured by the method developed by Henna instruments.

$$COD\,removal\,efficiency = (COD_i - COD_f)/COD_i \tag{3.1}$$

Where COD_i is the initial COD (mg/L) of all the three herbicides and COD_f (mg/L) is its final COD after reaction time.

3.7 PREPARATION OF THE NANO CATALYST

The iron nano particles were synthesized using laterite (sampled from Surathkal, Karnataka, India). The laterite was crushed to a finer material and removed the lighter particles with water. The remaining particles were dried, sieved (105 micron) (PLPs-powdered laterite particles) and preserved in dark bottles for further use. Typically, 3 g of sieved soil was mixed with 15 ml concentrated HCl (35%) and the total mixture was heated till all acid was fully evaporated. Further, once again 15 ml of acid was added and heated till dryness. Then, 20 ml of hot distilled water was transferred to a reaction mixture and vacuum filtered (Whatman 42). The filter paper containing mixture was ignited in a muffle furnace (650^0C) and final residue was considered as silicon dioxide. The filtrate is the mixture of aluminium and iron oxides and other traces of elements. The reaction mixture is diluted to 250 ml and 50% of the liquid was used to obtain Al_2O_3 and Fe_2O_3 and the remaining sample was used for the extraction of iron (IS-2720 (Part- XXV)-1982).
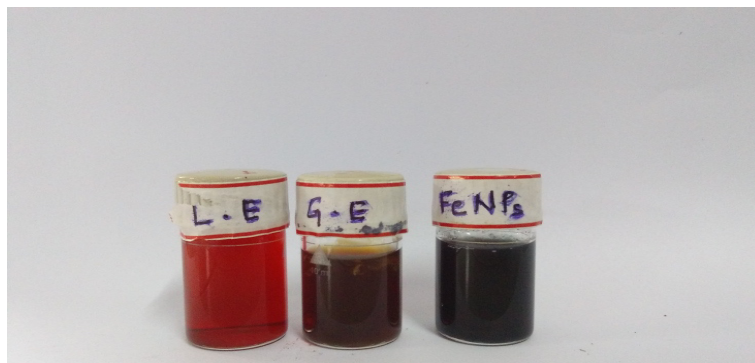
Figure.3.2 Formation of Green iron FeNPs(L.E=Laterite Extract, G.E=Green Extract, FeNPs=iron nanoparticles)

Around 100 g of (Tectona Grandis) TG and (Eucalyptus Globulus) EG leaves were collected from NITK campus, washed with water, and dried at room temperature. 60g of dried TG Leaves were dissolved in 1 liter of boiling water (Temp 80 ^{0}C, 1h) and the whole solution was filtered and stored in grey bottles (Koffi et al. 2015, Setiawan et al. 2013). Nanoparticles were synthesized by mixing 5.5 g/L of extracted iron with plant extract in different volume proportions (1:1, 2:1, 3:1 and 4:1) at room temperature in magnetic stirrer, for 60 min and finally vacuum filtered. The formation of black color liquid confirms the production of nanoparticles (LFeNPs-laterite based iron nanoparticles) (Figure. 3.2) and liquid was dried at 50 ^{0}C and preserved in grey bottles.

3.8 TOTAL PHENOLIC CONTENT AND ANTIOXIDANT PROPERTIES

The antioxidant property of the TG (Tactona Grandis) and EG (Eucalyptus Globulus) leaves was analyzed by FRAP (Ferric reducing antioxidant power) method (AI-16) (Pulido et al. 2000). The calibration curve (λ_{max}=593 nm) of Fe^{2+} standards (0 -3mM) was prepared using ferrous sulfate. Later, 1ml of extracted sample and 15 ml of FRAP reagent was mixed in a conical flask (vortex mixer, 10 min). Final antioxidant power was measured using calibration curve and expressed as mM of Fe^{2+}. Blank sample was also prepared by adding 1 ml of distilled water instead of extracted sample. The leaf mass to volume of the water, extraction time was optimized.

Total phenolic content of EG and TG leaves was measured using standard method (ISO, 2005). Here, also calibration curve was prepared using gallic acid standards (0-50 mM, λ_{max}=765 nm) [AI-17]. To measure the phenolic content of the extract, the sample was prepared by adding 1.6 ml extract, 8 ml Folin-ciocalteau reagent and 6.4 ml of 7.5% $Na_2S_2O_3$(Total 16 ml) and the final concentration was measured using calibration curve and expressed as mM of gallic acid.

3.9 CHARACTERIZATION OF NANOPARTICLES

The morphology and elemental composition of powdered laterite particles(PLPs) and laterite based iron nano particles (LFeNPs) was obtained using FESEM- EDX (Field emission scanning electron microscopy- X-ray energy-dispersive spectrophotometer)

34

(Carl Zeiss, Oxford instruments with sputtering, 5.kV voltage). The structural properties were studied by XRD (X-ray diffraction) (Cu K_α radiation ($\lambda = 1.54A^0$), voltage=40kV, current =15mA, scanning speed and range = 1^0 per min and $10\text{-}90^0$). Bruker (Alpha) FTIR (Fourier transform infrared spectroscopy) was used to study the functional groups (wave number range = 375–4000 cm^{-1}, KBr: sample=5:1). The surface area and pore volume were measured using BET and BJH (Brunauer–Emmett–Teller, Barrett–Joiner–Halenda) method (Smart sorb 92 instrument).

3.10 TAGUCHI EXPERIMENTAL DESIGN

 In Taguchi method, the output of the design is transformed as signal to noise ratio(S/N) instead of the results itself. The S/N ratio is the mean value of standard deviation, which tells about the deviation from the desired value of the each response with actual experimental values. There are mainly three types of S/N ratios in Taguchi design depending upon the type of process: smaller the better, larger-the-best, and nominal-the-better. In Fenton's process, the larger S/N ratio was selected   to optimize the variables involved and it was calculated for each factor level according to the Eq 3.2. In the present study   four independent variables (H_2O_2/COD (A), H_2O_2/ Fe^{2+} (B), pH (C) and reaction time (D)) and   four responses (%COD(Y_1), % ametryn(Y_2), % dicamba(Y_3) and % 2,4-D removal(Y_4)) were considered.

$$S/N = -10\log(\sum (1/Y^2)/n$$

(3.2)

where Y = responses at the given factor level and n = number of responses at the factory level.

3.11 RESPONSE SURFACE METHODOLOGY

The RSM was used to design the experiments, which provides interactive effects between the variables and optimize the responses. Here, CCD (central composite design) was preferred, which is better than the box- behnken design (BBD) (Zolgharnein et al. 2013). The CCD was designed in three levels (-1, 0, +1) for each variable and the variables are (A-D)   with four responses (Y_1- Y_4). The second order polynomial equation was used to study the interactions between the two types of variables (Eqs. 3.3-3.5).

$$Y=b_0+\sum_{i=1}^{k}b_iX_i+\sum_{i=1}^{k}b_{ii}X_i^{2}+\sum_{i=1}^{k}\ \sum_{j=1}^{k}b_{ij}X_iX_j \qquad (3.3)$$

% COD R = F_0 + F_1 A + F_2 B + F_3 C + F_4D + F_5A*A + F_6B*B + F_7C*C + F_8D*D +F_9A*B + F_{10}A*C + F_{11}A*D + F_{12}B*C + F_{13}B*D + F_{14}C*D   (3.4

% 24D R or % DR or % AR = F_0 + F_1 A + F_2 B + F_3 C + F_4D + F_5A*A + F_6B*B + F_7C*C + F_8D*D +F_9A*B + F_{10}A*C + F_{11}A*D + F_{12}B*C + F_{13}B*D + F_{14}C*D

(3.5)

Where Y is the response and X_i, X_j are independent variables (k=4) (X_1, X_2, X_3, X_4) which are assigned as A, B, C and D respectively. The b_0, F_0 (constant or intercept), b_i (linear term), b_{ii} (quadratic term)and b_{ij} (second order terms) are the coefficients(F_1,F_2,F_3,F_4,F_5,F_6,F_7,F_8,F_9,F_{10},F_{11},F_{12},F_{13},F_{14}) and k is the number of control variables (Bashir et al. 2009). Total 26 runs were considered, in which two runs are repeated for consistency in the responses (Eq.3.6).

N = factorial Points (2^k) + axial points (2*k) + center points   (3.6)

$= 2^4$+ (2 * 4)+2=26

In Fenton process (both heterogeneous and homogeneous), selection of the proper H_2O_2 dosage depends on the combined COD of all the three herbicides and hence, a H_2O_2/COD ratio of 2-2.5 was selected as center value, in which more $^\bullet$OH radicals are generated and this value is near to 2.125 (Kim et al. 1997), 2.15 (Kavitha and Palanivelu 2004). In many of the literatures, the ratio of H_2O_2/Fe^{2+} was reported as 9.5 (Torrades et al. 2011), 50 (Martins et al. 2010) and 165 (Manu and Mahamood 2011, Manu et al. 2011). It was also evident that, this ratio depends on the   nature and type of the compound (Mater et al. 2007). Hence, in this present study the H_2O_2/Fe^{2+} ratios are selected as 5- 37(dicamba), 5-59(2, 4-D) and 5-50(ametryn). Here, the ratios are based on mass (molar) and many of the researchers reported it (Bach et al. 2010; Aziz et al. 2012). The nano catalyst dosage was decided, based on the recent literatures 11.2-28mg/L (Wang et al., 2016), 10-1000mg/L (Zhang et al., 2017) and 10 mg/L (Ambika et al. 2016). Hence, the degradation study started with   lower doses of catalyst (5.38-344mg/L). The pH was varied from acidic –neutral (2-7)   based on the type of process

(homogeneous (2-5) and heterogeneous (3-7)). The reaction time was varied from 30-240 min. The supporting literatures are pH 2-5 and a reaction time of 30-240 min (Wang et al. 2016, Kuang et al. 2013), pH 3-6 and reaction time 0-240 min (Ambika et al. 2016, Zhang et al. 2017), pH 2-5 and reaction time 0-240 min (Xu et al. 2004) and pH 3-4 and reaction time 30-240 min (Lucas et al. 2007, Manu and Mahamood 2011). The ANOVA (analysis of variance) was carried out to study the performance of polynomial equations. The coefficient of determination (R^2), Fisher's test (F-test) and the probability (P) value at its 95% confidence level were studied (Garcia-Gomez et al. 2016). The 3D surface and contour plots were used to know the significant interactions between the responses and control factors.

CHAPTER 4

FENTON PROCESS

4.1 GENERAL

This chapter deals with Fenton's treatment of agriculture runoff water and aqueous solution containing three herbicides namely ametryn, 2,4-D and dicamba. The Taguchi and response surface methodology were used for the design of experiments (DOEs). The ANOVA (analysis of variance) was used to interpret the results with probability (P) value of 95%. The 2nd order polynomial equation and 3D surface plots were studied to know the significant interactions between the responses and control factors. Finally, the LC/MS analysis was performed to know the degradation products after Fenton's treatment process.

4.2 TREATMENT OF AGRICULTURE RUNOFF WATER

Taguchi method was applied to study the effect of variables (H_2O_2/COD (A), H_2O_2/Fe^{2+} (B), pH (C) and reaction time (D)) on responses (%COD, % ametryn, % dicamba and % 2,4-D removal). All four independent variables with their levels are listed in Table 4.1 and design matrix was shown in Table 4.2. The initial characteristics of agriculture runoff water were shown in Table 4.3.

Table 4.1 Factors and levels of orthogonal array

Parameter	Level 1	Level 2	Level 3
A (H_2O_2/COD)	1	2.125	3.25
B (H_2O_2/Fe^{2+})	5	27.5	50
C (pH)	2	3.5	5
D (Reaction Time in min)	30	130	240

Table 4.2 Taguchi design matrix

Independent variables					Dosage of H_2O_2 and Fe^{2+} (mM)		Dependent variables (%)				S/N ratio			
Run No	A	B	C	D	H_2O_2	Fe^{2+}	COD R	AR	D R	2,4-D R	COD R	AR	D R	2,4-D R
1	1	5	2	30	5.44	0.67	37	85	45.35	64.94	31.36	38.59	33.13	36.25
2	1	27.5	3.5	135	5.44	0.12	75	100	95.42	88.02	37.50	40.00	39.59	38.89
3	1	50	5	240	5.44	0.07	50	75	81.19	68.09	33.98	37.50	38.19	36.66
4	2.125	5	3.5	240	11.56	1.42	58	80	83.47	77.81	35.27	38.06	38.43	37.82
5	2.125	27.5	5	30	11.56	0.26	71.3	95.93	86.27	82.4	37.06	39.64	38.72	38.32
6	2.125	50	2	135	11.56	0.14	64	95.43	78.49	80.19	36.12	39.59	37.90	38.08
7	3.25	5	5	135	17.68	2.16	45	62	53.71	61.74	33.06	35.85	34.60	35.81
8	3.25	27.5	2	240	17.68	0.39	47.6	65	58.31	60.93	33.55	36.26	35.31	35.70
9	3.25	50	3.5	30	17.68	0.22	46	70	47	70	33.25	36.90	33.44	36.90

Note:CODR=COD removal, AR=ametryn removal,DR=dicamba removal, 2,4-DR=2,4-D removal

4.2.1 Interactions between independent factors and % COD removal

The experimental results generated by performing experiments with the help of the Taguchi orthogonal array and S/N ratios are almost close to each other and these values were listed in Tables 4.2 and 4.4. It is seen that the delta value of A is higher than other three parameters and the values were 3.74 2.81, 1.02 and 2.54 for A, B, C and D respectively. Therefore, the A, B, C and D parameters were ranked as 1, 2, 4 and 3 respectively and it can be concluded that the parameter A is having more influence on the COD removal. Furthermore, the ANOVA analysis was carried out in Table 4.5 to confirm the results obtained in Table 4.4. The Fisher's Test (F-test) value were 2.37, 1.51, 0.14 and 66 with PC (Percentage contribution) of 44.16, 33.54, 4.31 and 17.99 for A, B, C and D respectively. Therefore, it can be seen that, the higher the F value, higher contribution for the response. The main effects plots for S/N ratios for % COD removal was shown in Figure.4.1 and it was observed that the optimum values were found to be 2.125, 27.5, 3.5 and 135 min for A, B, C and D respectively.

The Fenton's reagent is the reaction between H_2O_2 and Fe^{2+}, forms $^\bullet OH$ radicals and thus produced radicals react with herbicides according to the equations 4.1, 4.2 and 4.3. The dosage of H_2O_2 varied from 5.44-17.68 mM and these values were calculated from

H_2O_2/COD (A) and H_2O_2/ Fe^{2+} (B). Usually, by increasing the H_2O_2 concentration, increases the COD removal by producing the more $^•OH$ radicals (Pignatello 1992).

Table 4.3 Initial characteristics of agriculture runoff water

Parameter	Value	Unit
Nitrate Nitrogen as NO_3-N	57±3	mg/L
pH	5.9±1	-
Chlorides as Cl^-	88±2	mg/L
Conductivity	0.8±0.01	mS/cm
Turbidity	52±2	NTU
Iron as Fe^{3+}	1.6±0.01	mg/L
COD	185±4	mg/L
Ametryn	3.4	mg/L
2,4-D	25.5	mg/L
Dicamba	93.7	mg/L
Sulfates as SO_4^{2-}	78±2	mg/L

However, from the Table 4.2, it is seen that, the dosage of (17.68mM) H_2O_2 was able to yield lesser % COD removal (34-45%). This is due to the fact that, adding the excess amount of H_2O_2, the Fenton's process was inhibited by decreasing the $^•OH$ radical production and increasing the O_2 production (Masomboon et al. 2009). When the dosage of H_2O_2 was decreased from 17.68 -11.5mM, 71.3% COD removal was achieved. Decreasing the H_2O_2 dosage from 11.5-5.44mM, maximum removal of 75% was achieved with 0.12mM of Fe^{2+} in 135 min. The removal was faster at 30 min and then it was slowly increased from 71.3-75% irrespective of pH 5(Run 5). After that, no COD removal was observed. Hence, the pH has less contribution in the Fenton's process. This is probably because, initially there was a reaction between ferrous ion (Fe^{2+}) and H_2O_2, after that there is a reaction between ferric (Fe^{3+}) and H_2O_2 (Masomboon et al. 2009). Therefore, the ratio of H_2O_2 / Fe^{2+} helps in higher COD removal efficiency.

$$H_2O_2 + Fe^{2+} \rightarrow {^•OH} + OH^- + Fe^{3+}$$

(4.1)

$$H_2O_2 + Fe^{3+} \rightarrow {^•OOH} + H^+ + Fe^{2+}$$

(4.2)

$$^•OH + Organics \rightarrow Products$$

(4.3)

The role of ferrous iron is very important and it varied from 0.07-2.16mM, which promotes the hydrogen peroxide to produce more $^\bullet$OH radicals by increasing the rate of reaction. However, when the iron dosage was at 2.16 mM, only 45% COD removal was achieved and this may be due to, the excess iron that reacts with $^\bullet$OH radicals and stops further production of radicals shown in Eq 4.4 (Pignatello 1992). Therefore, the optimum values of H_2O_2, Fe^{2+} were taken as 5.44 and 0.12 mM with reaction time of 135 minutes at pH 3.5. The residual H_2O_2 of 0.35mM (93.57% consumption) and residual iron of 0.02mM (97% iron as Fe^{3+}) were observed at optimum conditions. The yield of Fe^{3+} (residual iron) was almost similar to the research work (Colombo et al. 2013).

$$Fe^{2+} + {}^\bullet OH \rightarrow Fe^{3+} + OH^-$$

(4.4)

Table 4.4 Taguchi analysis of % COD removal (%COD R) versus A, B, C and D as S/N ratio

Level	A(H_2O_2/COD)	B(H_2O_2/Fe^{2+})	C(pH)	D(Reaction time)
1	34.28	33.23	33.68	33.02
2	36.15	36.04	34.47	35.56
3	32.42	33.58	34.70	34.27
Delta	3.74	2.81	1.02	2.54
Rank	1	2	4	3

Table 4.5 ANOVA analysis of % COD removal (% COD R) versus A, B, C and D

Source	DF[a]	Adj SS [b]	Adj MS [c]	F-Value [d]	PC [e]
A	2	742.4	371.2	2.37	44.16
B	2	564.0	282.0	1.51	33.54
C	2	72.48	36.24	0.14	4.31
D	2	302.5	151.2	0.66	17.99

[a] DF=degrees of freedom; [b]Adj SS=adjacent sum square; [c]Adj MS= Adjacent mean square; [d] F-value (Fishers test); [e] PC=percent contribution
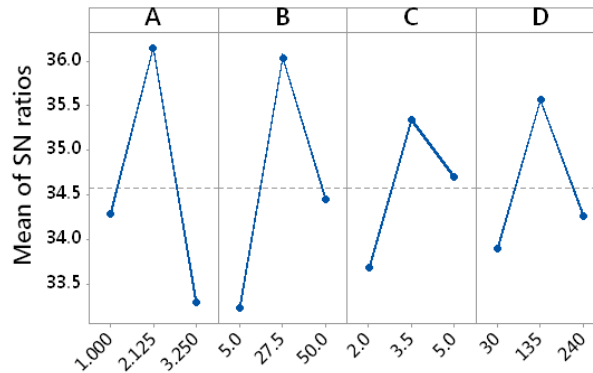
Figure. 4.1. Main effects plot for SN ratios for % COD removal

4.2.2 Interactions between independent factors (A, B, C and D) and % ametryn removal (%A R)

Table 4.2 shows that, 100% removal was achieved at 5.44 mM of H_2O_2 and 0.12mM of Fe^{2+} with reaction time of 135 minutes at pH 3.5. However, the Table 4.6 shows the values of the Taguchi analysis of % ametryn removal (%AR) versus A, B, C and D. The delta values are 2.76, 1.13, 0.66 and 1.21 and they are ranked as 1, 3, 4 and 2 for A, B, C and D respectively. Therefore, it can be concluded that the parameter A is having more influence on the ametryn removal efficiency and factor D (reaction time) is having 2nd priority than B (H_2O_2/Fe^{2+}). Furthermore, the ANOVA for % ametryn removal versus A, B, C and D were carried out in Table 4.7 to confirm the results obtained in Table 4.6. The F (Fishers Test) values were 6.25, 0.42, 0.10 and 0.61 with PC (Percentage contribution) of 67.57, 12.30, 3.29 and 16.84 for A, B, C and D respectively. The main effects plot for S/N ratios for % ametryn removal was shown in Figure.4.2 and the optimum values were found to be 2.125, 27.5, 3.5 and 135 min for A, B, C and D respectively.
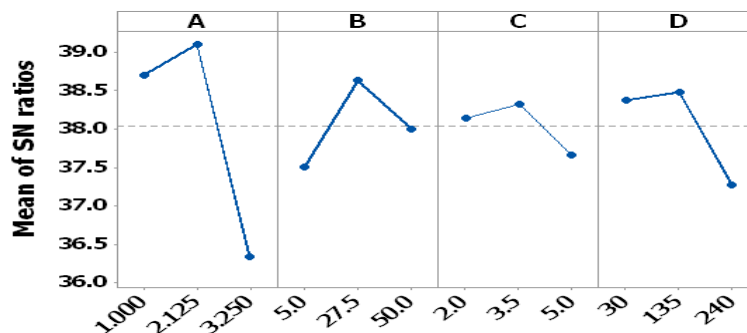
Figure 4. 2. Main effects plot for S/N ratios for % ametryn removal

43

Table 4.6 Taguchi analysis of % ametryn removal (%AR) versus A, B, C and D as S/N

Level	A(H₂O₂/COD)	B(H₂O₂/Fe²⁺)	C(pH)	D(Reaction time)
1	38.70	37.50	38.15	38.38
2	39.10	38.63	38.32	38.48
3	36.34	38.00	37.66	37.27
Delta	2.76	1.13	0.66	1.21
Rank	1	3	4	2

Table 4.7 ANOVA analysis of % ametryn removal versus A, B, C and D

Source	DF	Adj SS	Adj MS	F-Value	PC
A	2	1069.7	534.86	6.25	67.57
B	2	194.7	97.33	0.42	12.30
C	2	52.06	26.03	0.10	3.29
D	2	266.7	133.3	0.61	16.84

As presented in Table 4.4 and 4.6, it was observed that pH is having fourth influencing parameter in both responses (% ametryn and COD removal) and also it was found that the ametryn removal was decreased when the pH was lesser than 3.5 and more than 3.5 (Table 4.2). In case of higher pH (>3.5), the decomposition of H_2O_2 was observed by losing its oxidation potential and also there might be deactivation of Fe^{2+} that was observed by forming ferric hydroxide complexes, which reduces the $^\bullet$OH radical production (Lucas and Peres, 2006; Lucas et al., 2007; Wang, 2008). Hence, ametryn removal efficiency was reduced. At lower pH (<3.5), may be the scavenging effect of $^\bullet$OH radicals by H^+ ions was observed, leading to the lesser degradation of ametryn (Eq. 4.5) (Martins et al. 2010). Therefore, the optimum pH was selected as 3.5. This acidic pH (3.5) can be overcome by the use of heterogeneous catalyst (FeOOH) (Yaping and Jiangyong 2008), in which the % removal efficiency of the pollutant was relatively better at pH at 7.47 (86.4%) compared to pH 3.07 (98.2%).

$$Fe^{3+} + H_2O_2 \rightarrow Fe^{2+} + H^+ + HO_2^\bullet$$

(4.5)

From the Table 4.6, it is seen that the reaction time (D) is also showing significant effect on ametryn removal efficiency along with H_2O_2/COD (A). Based on the experimental results presented in Table 4.2 it was observed that, at 30 min(run 5), the reaction was faster and 95.9 % of ametryn removal was achieved, after that 100% removal efficiency was achieved at 135 min (Run 2). It clearly shows that, within 30 min, a large number of hydroxyl radicals are produced (Eq 4.1) and after 30 min the hydroperoxyl radicals ($HO_2^{\bullet}$) were produced (Eqs 4.6 and 4.7), which are having lesser oxidation capacity than $\bullet$OH radical.

$$H_2O_2 + Fe^{3+} \rightarrow H^+ + FeOOH^{2+}$$

(4.6)

$$FeOOH^{2+} \rightarrow HO_2^{\bullet} + Fe^{2+}$$

(4.7)

4.2.3 Interactions between independent factors (A, B, C and D) and % dicamba removal

It can be seen from the Figure.4.3, the optimum values of A, B, C and D were found to be 2.125, 27.5, 3.5 and 135 min respectively. The same trend was observed in COD and ametryn removal efficiencies. From the Table 4.2, the maximum dicamba removal efficiency was observed to be 95.42 % with 5.44mM and 0.12mM of H_2O_2 and Fe^{2+} respectively. From Table 4.8, the delta values are 4.44, 2.49, 1.72 and 2.81 and they are ranked as 1, 3, 4, and 2 for A, B, C and D respectively. The ANOVA analysis was performed in Table 4.9 and the percentage contribution (PC) values were achieved as 51.85, 18.01, 9.60 and 20.54 for A, B, C and D respectively. The same trend followed in both % ametryn and dicamba removal, however the variation in the percentage contribution (PC) was observed. The Fishers test (F-test) value are 3.23, 0.66, 0.32, and 0.78 for A, B, C and D respectively. Comparing with PC values of B and D, only 2% difference was observed and it clearly says that, these two parameters contributed equally in the degradation process.

45
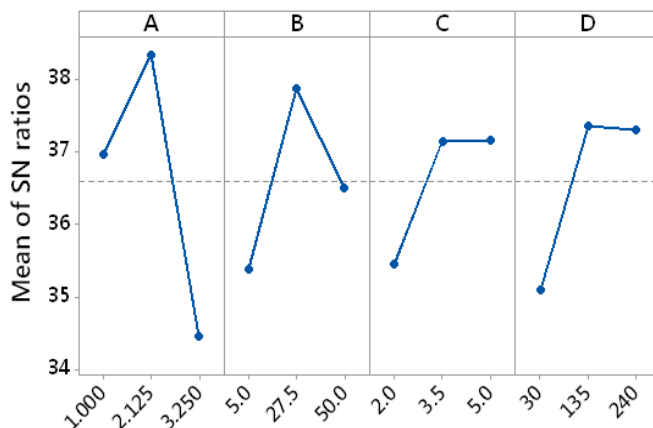
Figure. 4.3. Main effects plot for S/N ratios for % Dicamba removal

Table 4.8 Taguchi analysis of % dicamba removal versus A, B, C and D as S/N ratio

Level	A(H_2O_2/COD)	B(H_2O_2/Fe^{2+})	C(pH)	D(Reaction time)
1	36.97	35.39	35.45	34.56
2	38.35	37.87	36.61	37.36
3	33.91	35.97	37.17	37.31
Delta	4.44	2.49	1.72	2.81
Rank	1	3	4	2

Table 4.9 ANOVA analysis of % dicamba removal versus A, B, C and   D

Source	DF	Adj SS	Adj MS	F-Value	PC
A	2	1686	843.1	3.23	51.85
B	2	585.7	292.9	0.66	18.01
C	2	312.2	156.1	0.32	9.60
D	2	668.1	334.1	0.78	20.54

The results indicate that increasing initial concentration of H_2O_2 to 17.68mM could degrade only 60 -70% (Run 7, 8, 9) of dicamba. Decreasing the H_2O_2 values from 17.68-11.56mM enhanced the dicamba removal from 70-86%. However, 95% of removal was achieved at 5.44mM of H_2O_2. It clearly says that increase in the H_2O_2 concentration, the

oxidation process might be inhabited by deactivating the $^\bullet$OH radical by producing the $\bullet$OOH radical (Eq.4.8) (Duesterberg and Waite 2006).

$$H_2O_2 + {}^\bullet OH \rightarrow H_2O + OOH^\bullet$$

(4.8)

The dicamba removal was increased from 81-95% by increasing the Fe^{2+} dosage of 0.07-0.26mM (Run 2, 3). However, the removal efficiency was decreased at iron concentration >0.26mM. May be at higher a concentration of iron the Fe^{2+} enhances self-scavenging of $\bullet$OH radicals given in Eq. 4.9 (Hameed and Lee 2009).

$$Fe^{2+} + {}^\bullet OH \rightarrow Fe^{3+} + OH^-$$

(4.9)

4.2.4 Interactions between independent factors (A, B, C and D) and % 2, 4-D removal

Figure.4.4 displays the main effects plot of % 2, 4-D removal versus A, B, C and D. The optimum values were achieved to be 2.125, 27.5, 3.5 and 135 min for A, B, C and D respectively. From the Table 4.10 the delta values are observed as 1.94, 1.01, 1.20 and 0.87 and they are ranked as 1, 3, 2 and 4 for A, B, C and D respectively. The ANOVA results show that, the percentage contribution (PC) values were 50.66, 15.86, 21.70 and 11.78 with F values of 3.08, 0.57, 0.83 and 0.40 for A, B, C and D respectively, which are listed in Table 4.11. It was also observed that, the factor A (H_2O_2/COD) is contributing more in all the responses. This is mainly due to the fact that, the H_2O_2 is directly taking part in the removal of COD and also the optimum value 2.125(A) is following the standard relation(1 g of COD=2.125 g of H_2O_2). Since, the pH variable was ranked as 2, which has a significant effect on the 2, 4-D removal efficiency than reaction time (D) and H_2O_2/Fe^{2+} (B). At pH 2, the 2, 4-D degradation efficiency of 60-80% (Run 1, 6, 8) and at pH 5, 61.74-68.09 % removal was observed (Run 3 and 7). However, in case of run 5 the removal efficiency was observed to be 82.4 %. This increase in 2, 4-D removal is due to the proper selection H_2O_2/Fe^{2+} ratio (27.5). The highest removal efficiency of 88% was found to be at pH 3.5. At pH values below 3, may be the oxidation process was inhibited by the production of oxonium ions and makes the H_2O_2 less

reactive towards ferrous ion and thus decreasing the $^\bullet$OH radical production (Oliveira et al. 2006).
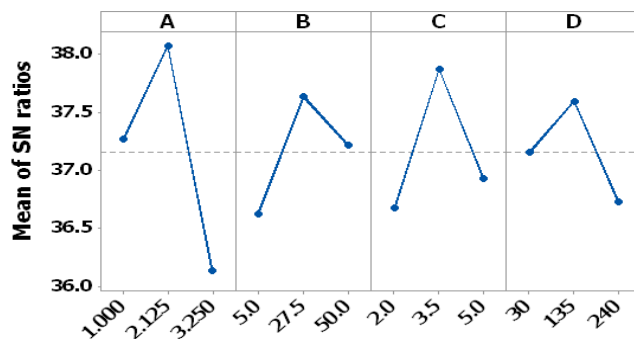
Figure. 4.4. Main effects plot for S/N ratios for % 2,4-D removal

Table 4.10 Taguchi analysis of % 2, 4-D Removal (% 2, 4-D R) versus A, B, C and D as S/N ratio

Level	A(H_2O_2/COD)	B(H_2O_2/Fe^{2+})	C(pH)	D(Reaction time)
1	37.27	36.63	36.68	37.16
2	38.07	37.64	37.87	37.60
3	36.14	37.22	36.93	36.73
Delta	1.94	1.01	1.20	0.87
Rank	1	3	2	4

Table 4.11 ANOVA analysis of % 2, 4-D removal versus A, B, C and D

Source	DF	Adj SS	Adj MS	F-Value	PC
A	2	384.2	192.11	3.08	50.66
B	2	120.3	60.14	0.57	15.86
C	2	164.6	82.29	0.83	21.70
D	2	89.33	44.67	0.40	11.78

It was also said that at low pH of 2, the less soluble species of Fe^{3+} are available to enhance the $^\bullet$OH radical production and at higher pH(>3.5) the formation of iron hydroxides were observed, which helps in suppressing the Fe^{2+} species regeneration and thereby reducing efficiency of treatment process (Wang 2008). In this Fenton's process with similar optimum conditions (5.44mM (H_2O_2), 0.12mM (Fe^{2+}) and 3.5 (pH)), 40-50

% removal of sulfates and nitrates was observed with adsorption on to the sludge produced after Fenton reaction. Finally, to confirm the accuracy of the experimental results, the normal probability distribution plots versus residuals were performed in A-III-1(a) (b) (c) (d). These plots were linear in nature and all the points were distributed along the straight line and it was confirmed that obtained results were in good agreement with model values. To know the distribution pattern of the residuals, the graphs were plotted for all nine set of experiments in A-III-2 (a) (b) (c) (d). From these figures, it was concluded that the points were randomly distributed along both the sides of the center line (0-line) and it is a good trend for all four responses.

4.3 TREATMENT OF DICAMBA

Here, the effect of several factors (H_2O_2 /COD (A), H_2O_2/Fe^{2+}(B), pH(C), and reaction time(D)) was studied on responses (% COD and % dicamba removal efficiency) by applying central composite design (CCD). Initially, the preliminary experiments were conducted to select the optimum range of values for H_2O_2 /COD (0.5-4.5), H_2O_2/Fe^{2+} (5-15, 16-26, 27-37) and pH (1.5-9) (Figure. 4.5(a)(b)(c)). It was found that the maximum removal (>80%) was observed at a value of 21, 2.125 and 3.5 for H_2O_2/Fe^{2+}, H_2O_2 /COD and pH respectively. The range of parameters along with design matrix is shown in Table 4.12 and 4.13. The ANOVA results of two responses are presented in Table 4.14.
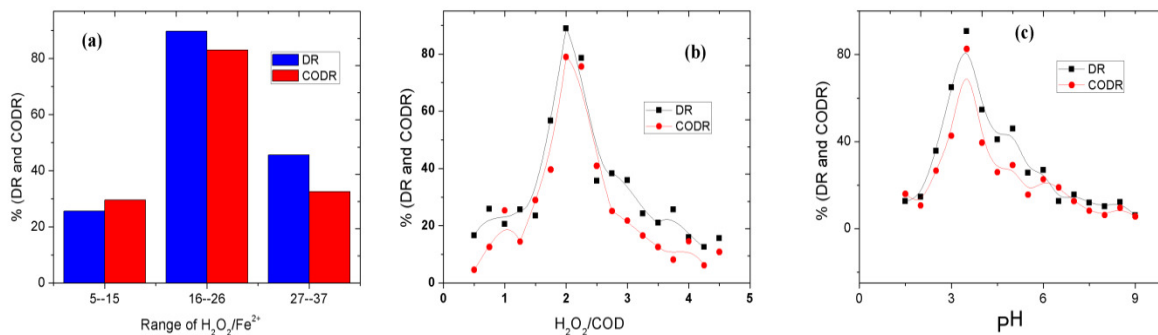
Figure.4.5 (a) Range of H_2O_2/Fe^{2+}vs. responses; dicamba$_0$=0.13mM, reaction time(min)=30-240, H_2O_2 /COD=1-3.25; pH=2-5 **b)** H_2O_2 /COD vs. responses; reaction

time(min)=240 , pH=3.5, H_2O_2/Fe^{2+}=21 **c)** pH vs responses; reaction time(min)=240, H_2O_2/Fe^{2+}=21, H_2O_2/COD=2.125.

4.3.1 Central composite design model and statistical analysis

The response functions along with interaction coefficients of independent variables are presented in Eqs. 4.10-4.11. These equations   involve one constant term, four linear terms (A, B, C, D), four quadratic terms (A*A, B*B, C*C, D*D) and six interaction terms (A*B, A*C, A*D, B*C, B*D, C*D).

Table 4.12. Levels of the parameters studied in the CCD

Factor	Name	Low(-1)	Middle(0)	High(+1)
A(X_1)	H_2O_2/COD	1	2.125	3.5
B(X_2)	H_2O_2/Fe^{2+}	5	21	37
C(X_3)	P^H	2	3.5	5
D(X_4)	Time (min)	30	135	240

% COD R (Y_1) = 65.64 - 0.44 A +1.52 B +0.98 C + 2.00 D - 23.95 A*A - 12.51 B*B -

19.11 C*C   + 16.49 D*D   + 0.44 A*B   – 0.11 A*C   +0.99 A*D

+ 2.09 B*C 0.55 B*D -2.2 B*D   (4.10)

% D R (Y_2) = 69.04 - 0.20 A + 0.87 B + 1.59 C + 2.11 D - 19.80 A*A - 16.45 B*B -

20.20 C*C+ 15.74 D*D   - 1.08 A*B   - 1.20 A*C+ 1.31 A*D

+ 2.52 B*C   – 0.07 B*D - 0.69 C*D   (4.11)

The intercept values are 65.64 and 69.04 for of COD (Y_1)   and dicamba removal (Y_2) respectively, implies that both the responses are showing a positive effect. Along with the intercept values, the coefficients of B, C, D, D^2, A*B, A*D, B*C are also having a positive effect on the % COD removal with the highest positive value of 16.49 (D^2). And, in case % dicamba removal efficiency (%DR) the coefficients of B, C, D, D^2, A*D, B*C have a positive effect, in which the reaction time (D^2) has the greatest positive value of 15.74. Hence, it can be concluded that the D^2 has a more positive influence on both responses. To find out the relation between the mean square (MS) and the residual error of the model, the F test (Fisher's test) analysis was performed. The experimentally calculated F values for both the responses are 9.93 and 7.57. These values are greater

50

than the tabular value of $F_{0.05 (14, 11)} = 2.74$, this implies that, the Fenton's treatment option was more significant towards the removal of dicamba from aqueous medium. The coefficient of determination (R^2) was calculated, which is the variation between the actual responses and fits (Ahmadi et al. 2005). The R^2 and R^2_{adj} depend on the sample size and the number of terms in the model. Usually, if the number of terms in the model is more with less sample size, then $R^2_{adj} < R^2$ (Zhang et al. 2012). These values (R^2 and R^2_{adj}) were found to be 92.67%, 90.34% and 90.59%, 88.62 for % dicamba and %COD removal efficiency respectively (The detail ANOVA results are shown in A-II-1.)

Table 4.13. CCD design matrix(D_0=0.39 mM)

Run	Independent variables (uncoded and coded)				Fenton's Reagent		Actual Responses(%)		Predicted Responses(%)	
	A (H$_2$O$_2$/COD)	B (H$_2$O$_2$/Fe^{2+})	C (P^H)	D (Time) min	H$_2$O$_2$ (mM)	Fe^{2+} (mM)	D R	COD R	D R	COD R
1	2.125(0)	21(0)	3.5(0)	30(-1)	11.38	0.33	74.46	70.10	82.68	80.13
2	2.125(0)	37(1)	3.5(0)	135(0)	11.38	0.19	45.31	47.25	53.47	54.65
3	3.25(1)	5(-1)	5(1)	30(-1)	17.4	2.13	24.30	22.63	23.42	21.61
4	2.125(0)	21(0)	3.5(0)	135(0)	11.38	0.33	83.43	82.41	79.04	75.64
5	3.25(1)	37(1)	2(-1)	30(-1)	17.4	0.29	22.30	23.51	20.10	20.48
6	2.125(0)	21(0)	2(-1)	135(0)	11.38	0.33	42.10	38.46	47.26	45.56
7	3.25(1)	37(1)	5(1)	240(1)	17.4	0.29	32.30	33.18	33.49	31.28
8	3.25(1)	5(-1)	5(1)	240(1)	17.4	2.13	29.60	24.39	29.00	24.29
9	2.125(0)	21(0)	3.5(0)	135(0)	11.38	0.33	84.01	81.53	79.04	75.64
10	1(-1)	37(1)	2(-1)	240(1)	5.35	0.09	27.30	29.67	26.60	27.57
11	1(-1)	21(0)	3.5(0)	135(0)	5.35	0.16	43.50	38.46	49.44	42.13
12	1(-1)	5(-1)	5(1)	30(-1)	5.35	0.66	25.60	25.27	26.67	25.57
13	2.125(0)	21(0)	3.5(0)	240(1)	11.38	0.33	85.33	83.29	86.89	84.14
14	1(-1)	37(1)	5(1)	30(-1)	5.35	0.09	38.42	36.70	35.75	32.99
15	2.125(0)	21(0)	5(1)	135(0)	11.38	0.33	45.80	43.73	50.43	47.51
16	3.25(1)	5(-1)	2(-1)	240(1)	17.4	2.13	33.56	30.54	34.65	31.13
17	3.25(1)	5(-1)	2(-1)	30(-1)	17.4	2.13	26.20	21.75	26.30	19.65
18	3.25(1)	37(1)	2(-1)	240(1)	17.4	0.29	31.00	29.67	29.06	29.77
19	1(-1)	5(-1)	2(-1)	240(1)	5.35	0.66	27.25	30.54	27.88	30.69
20	1(-1)	5(-1)	5(1)	240(1)	5.35	0.66	27.30	24.39	27.03	24.30
21	1(-1)	37(1)	5(1)	240(1)	5.35	0.09	36.78	27.03	35.82	29.53
22	1(-1)	5(-1)	2(-1)	30(-1)	5.35	0.66	27.52	24.39	24.75	23.17
23	2.125(0)	5(-1)	3.5(0)	135(0)	11.38	1.39	50.10	48.13	51.72	51.62
24	1(-1)	37(1)	2(-1)	30(-1)	5.35	0.09	24.03	21.75	23.76	22.25
25	3.25(1)	37(1)	5(1)	30(-1)	17.4	0.29	29.70	30.54	28.20	30.79
26	3.25(1)	21(0)	3.5(0)	135(0)	17.4	0.51	45.20	34.04	49.05	41.25

Here, it is seen that the variation between R^2 and R^2_{adj} is less than 2.5% for both responses and $R^2_{adj} < R^2$, which means that the obtained results are best fit with modeled values and the same trend was reported in other literatures also(Santos and Boaventura 2008, Zhang et al. 2012). According to the Joglekar and May (1987), the minimum R^2 value should be at least 80% and from the Table 4.13 and A-III-4, it was observed that R^2 values are > 80%. The pure error (difference between lack of fit and residual error) values are 0.17 and 0.39 for % dicamba (Y_2) and % COD removal (Y_1) respectively. It means that, less error was observed between the actual responses and fits. The noise in the responses (variation between experimental and predicted values) was measured with the lack of fit P values and the values were 3.8% and 5.2 % for Y_2 and Y_1 respectively, which were less than observed values (<14.4%) (Im et al. 2012).

Table 4. 14 . Analysis of Variance for % DR and %CODR

Parameter	% CODR	% DR
R^2 (coefficient of determination)	90.59	92.67
Standard deviation (S.D)	2.06	1.83
Coefficient of variation(CV) %	6.91	5.85
Adequate precision(AP)	61.7	37.5
Pure error	0.39	0.17
F-value	7.57	9.93

Note : Recommended values: C.V <10%(Beg et al., 2003) , F>2.74 ; A.P<4 (Zinatizadeh et al. 2006); R^2 >80% (Joglekar and May 1987); CODR=COD removal, DR=dicamba removal,

The standard deviation (S.D) tells about the how many values in responses are differing from the mean value and these values are 1.83, 2.06 for Y_2 and Y_1 respectively. The coefficient of variation (C.V) is the percentage ratio of standard error to the mean value of the response and values are 5.85% (Y_2) and 6.91% (Y_1). According to Beg et al. 2003 the C.V values should be less than 10% and the obtained values were less than 10%. The adequate precision (A.P) is the ratio of predicted values of the response to its error and the values are 37.5 (Y_2) and 61.7(Y_1) for both responses and the standard value is 4 or > 4 (Zinatizadeh et al. 2006). With all these observations, it is clear that the experimentally obtained results are more reliable. To know the exact pattern of all 26 runs, the graphs are plotted against the all the observations in A-III-3(a)(b) and the points are randomly

distributed along both positive and negative sides of the straight line and the maximum residual was observed in positive side. Hence, it is a good trend in the treatment process.

4.3.2 Effects of independent variables on the responses

The ratio of H_2O_2/COD is very important, which acts as the basis for considering a range of H_2O_2 dosages and the values were varied as 1, 2.125 and 3.25. It is seen that, as the ratio is decreased to 1 or increased to 3.25 from a center value of 2.125, less removal was observed. This implies that, the more number of $^\bullet$OH radicals are produced in the ratio of 2.125 (Kim et al. 1997) and thereby increasing the removal efficiency (Eq. 4.1). Hence, the H_2O_2/COD ratio of 2.125 was finally considered.

The suitable values H_2O_2/Fe^{2+} (B) ratios (5, 21, 37) were considered to enhance the OH radical production and based on these ratios the   dosage of iron (0.09-2.13 mM) and hydrogen peroxide(5.35-17.4 mM) were varied (Table 4.12 and4.13). Usually, it is seen that, the increase in the H_2O_2, increases the degradation of pollutants by generating more hydroxyl radicals (Pignatello 1992). When the hydrogen peroxide dosage was increased from 5.35-11.38 mM, the dicamba and COD removal was increased up to 84%. Further increase in H_2O_2 from 11.38-17.4mM, the removal efficiency was decreased, which is shown in Figure.4.6 (a). This was because, by adding the excess amount of H_2O_2 the treatment process was inhibited by decreasing the $^\bullet$OH radical production (scavenging effect) (Masomboon et al. 2009, Zhang et al. 2006).

Here, the iron   acts as a catalyst, which exploits the rate of reaction and hence the optimization of Fe^{2+} is as important as H_2O_2 (Mijangos et al. 2006). To understand the effect of Fe^{2+}on dicamba removal, the dosage of iron was varied from 0.09-2.13 mM shown in Figure. 4.6(b**).** At   high iron dosage of   0.66mM (run 12, 19, 20, 22), 1.39 (run 23) and 2.13 mM (run 3, 8, 16, 17) less dicamba removal (<34%) was achieved and this may be due to the fact that, more number of Fe^{2+} ions scavenged the already produced $^\bullet$OH radicals (Eq. 4.4) (Pignatello 1992). Furthermore, when iron>0.66mM, sludge formation was observed by forming iron hydroxide complexes and it requires pH control throughout the reaction to avoid precipitation. Suppose, if Fe^{2+}dosage was decreased to
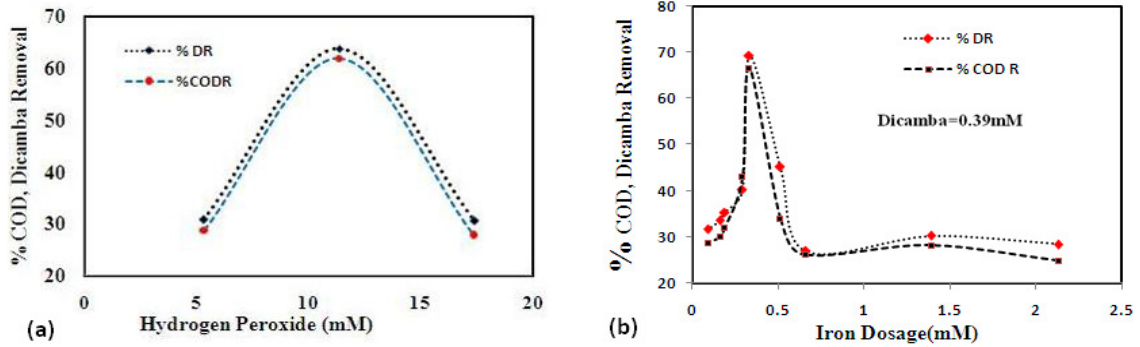
Figure. 4.6. a) Effect of H_2O_2 on % COD and dicamba removal efficiency b) Effect of Fe^{2+} on % COD and dicamba removal efficiency
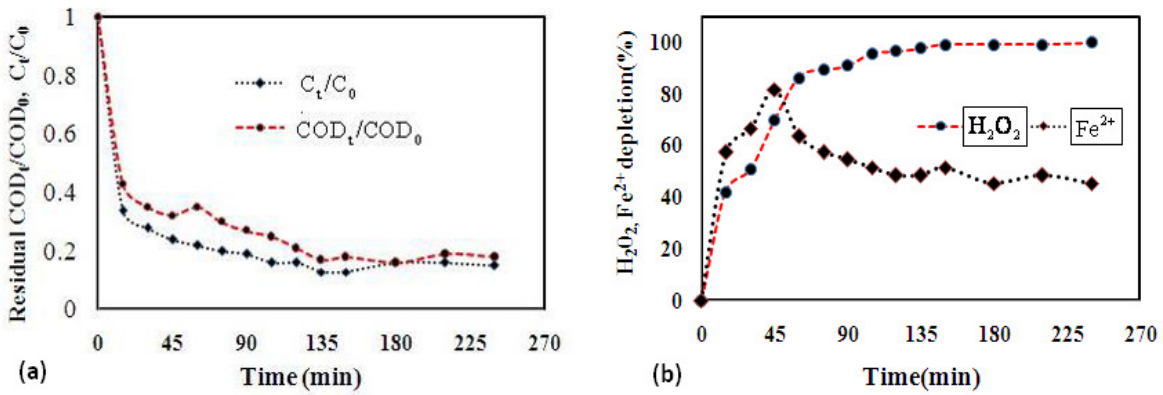
Figure. 4.7. a) Residual COD_t/COD_0 and C_t/C_0 vs time b)% H_2O_2 and Fe^{2+} depletion with time. H_2O_2=11.38mM; Fe^{2+}=0.25 mM;COD_0=182mg/L, C_0=0.39mM, pH =3.5
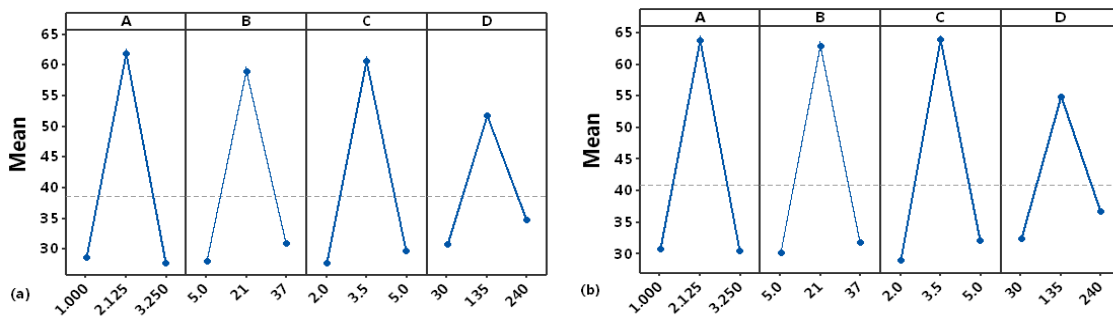
Figure. 4.8 Main effects plots a) % COD Removal b)% Dicamba Removal

0.09-0.29 mM, only 22-45 % removal was observed. At a low iron dosage, there is less Fe^{2+} ions are available to react with oxidant and then the H_2O_2 is going to react with already produced $^{\bullet}OH$ radicals to form a $^{\bullet}OOH$ radical (Eq. 4.8) and these radicals were having less oxidation capacity than $^{\bullet}OH$ radicals (Masomboon et al. 2009). Hence the, removal efficiency of dicamba was automatically reduced. Furthermore, in case of run 1, 4, 9 and 13 with Fe^{2+} dosage of 0.33 mM, the significant increase in the dicamba removal of 70-86% was observed for both responses. Therefore, the optimum iron dosage was considered as 0.33mM.

In case of run 6 and 15 with pH 2 and 5, the less dicamba removal was achieved even though Fe^{2+} dosage was 0.33 mM, this implies that the pH is also influencing on the removal efficiency. Therefore conclusively, when H_2O_2/Fe^{2+} ratio was 5 and 37, with a pH 5 and 2, the less removal was achieved and with H_2O_2/Fe^{2+} ratio of 21 and pH 3.5 the significant increase in removal was observed. The Fenton's process is largely influenced by the pH of a solution and literature says that, it works in the acidic range from 2- 4 (Masomboon et al. 2009). Hence, in this work, the pH varied from 2-5 with 3.5 as a center value. From the Table 4.13, it is seen that, when the pH is at 2 and 5, the slow degradation of 22-46% was achieved. Moreover, in case of runs 1, 4, 9 and 13 the higher removal was observed at pH 3.5. At pH >3.5, the deactivation of Fe^{2+} ions by forming ferric hydroxide complexes was observed and thereby suppressing generation of $^{\bullet}OH$ radicals (Lucas and Peres 2006). At lower pH (<3.5), may be the scavenging $^{\bullet}OH$ radicals by H^+ ions was observed, which leads to the lesser degradation (Eq 4.5) (Martins et al. 2010). It was also said from the literature (Oliveira et al. 2006), at pH<3, production of Oxonium ions was observed, which makes the oxidant less reactive. Hence, the optimum pH of 3.5 was maintained in the treatment system.

The reaction time (D) is also an important factor and was varied from 30-240 min and it has a significant influence in generating •OH radicals. In case of run 1 at 30 min, the reaction was faster and 70-74% of degradation was achieved. Furthermore, in case of runs 4, 9 and 13 with same experimental conditions (pH =3.5, Fe^{2+}=0.25 mM, H_2O_2 =11.38 mM), the reaction rate was slowly increased from 70-85%. This implies that at

30 min, more $^{\bullet}$OH radicals are generated (Eq.4.1) and accordingly the degradation rate was also faster and after 30 min, the hydroperoxyl radicals ($HO_2^{\bullet}$) were produced. However, in case of the runs (3, 5, 12, 14, 17, 22, 24, and 25) at 30 min, the less removal (20-36%) was achieved. This implies that the factors A, B and C are also influencing on removal efficiency.

To know the degradation rate at every 15 min, the kinetic studies were carried at optimum Fenton's dosage (Fe^{2+}=0.25mM, H_2O_2 =11.38mM and pH =3.5) that is shown in Figure.4.7 (a) and it was observed that after 135 min, removal rate was constant. Hence, finally optimum reaction time of 135 min was considered. The H_2O_2 and Fe^{2+} depletion was also monitored through the treatment process shown in Figure.4.7 (b), it is seen that 100% decomposition of H_2O_2 was observed within 240 min (run 13) and 98% consumption at H_2O_2 at run 9. However, from 0-45 min 81% of Fe^{2+} was converted to Fe^{3+}, then after that slowly the Fe^{2+} regeneration was observed and thereby achieving the maximum degradation rate in the treatment process. The similar results were reported in other research also (Colombo et al. 2013). Finally, from the Figure.4.8 (a) (b) the optimum values are confirmed as 2.125, 21, 3.5, and 135 for A, B, C and D respectively. From the Table 4.13 and A-III-4 (a) (b), it was concluded that the actual experimental and predicted values are similar in nature and the data points are distributed along the straight line, it implies that better results are achieved.

4.3.3 Degradation products (HPLC-MS analysis)

The decay of dicamba was analyzed after Fenton's treatment process and the release of chloride with time was monitored (Figure.4.9). Before and after treatment, the dicamba was eluted at same retention time (1.4 min), however, a relatively small peak was observed at the end of the reaction time (240 min). It clearly says that, after treatment a small portion of dicamba was retained in the treatment process. The 82% of the dicamba was degraded and finally it was mineralized to oxalic acid, chloride, CO_2 and H_2O. The % dicamba removal was calculated with the help of the calibration curve (A-I-3). This was confirmed with LCMS mass table (A-I-15) having a highest m/z value of 90 (oxalic acid), in comparison with NIST library and the peak at a m/z value of 223 (M+2)

corresponds to residual dicamba in the reactor. In addition, this mineralization process was confirmed with COD removal. The release of chloride ion was faster (31 mg/L) at the initial stage (0-15 min), then it slowly increased up to 64.7 mg/L till 135 min and after that no increase in the chloride concentration was observed. The similar kind of results were observed in the other literature (Brillas et al. 2003) and the possible mineralization process was written with the following Eq.4.12

$$C_8H_6Cl_2O_3 + OH^{\bullet} \rightarrow Oxalic\,acid + Cl^- + H_2O + CO_2 \qquad (4.12)$$
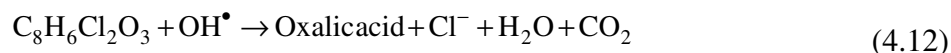
4.3.4 Contour overlay plot for validation

To find out the optimum region or working feasible region for Fenton's process, the contour plots were overlaid graphically, where all the variables meet simultaneously in a particular area (Ahmad et al. 2005). In this optimization process the desired goal was to maximize both the responses and therefore, the boundary values were defined as Y_1 (21.75, 81.53) and Y_2 (22.3, 84.01) with H_2O_2/Fe^{2+} (B) ratio of 21. The reaction time was considered as 135 min instead of 240 min, where the less difference in the removal efficiency (<2%) was observed. The overlay plot (Figure.4.10) is divided into 3 regions, which are separated by circular dotted lines. The shaded portion consists of two regions, in which the middle area is not feasible for both COD and dicamba removal efficiencies (NFRCD) and other region is feasible for only COD removal efficiency (Y_1). The remaining unshaded area is suitable for both responses and it was considered as an optimum region.To verify the results obtained in Table 4.13, four sets of additional laboratory experiments (runs 27, 28, 29 and 30) were performed, which is suggested by overlay plot from unshaded region. The experimental conditions are tagged in Figure. 4.10 and the results along with statistical analysis were shown in Table 4.15. The standard deviation, coefficient of variation and adequate precision were <4%, <8 and >12 respectively. These values are within the prescribed standard limits (Beg et al. 2003, Zinatizadeh et al. 2006). This implies that, the additional experiments confirm the all 26 experiments results and hence the RSM was successfully applied for the design of experiments.

4.3.5 3D surface plots and contour plots

From the above discussions, it is clear that all the four factors are interacting with each other. Hence, to confirm these interactive effects on the responses, the 3D surface plots were shown in A-III-5 and A-III-6. These plots are also used to optimize the independent variables involved in the treatment process. The A-III-5 (c), (e), (f) and A-III-6 (c), (e), (f) represents the surface plots for % COD and dicamba removal efficiency versus B and C, A and C, A and B respectively. These surface plots are showing the sharp convex surface and this implies that, the maximum removal of dicamba was occurred at exactly the center value of H_2O_2/COD (A), H_2O_2/Fe^{2+} (B) and pH (C). Hence, finally 2.125(A), 21 (B) and 3.5(C) were considered.

The A-III-5 (a) (b) (d) and A-III-6 (a) (b) (d) are showing surface plots with significant mutual interaction between both the responses versus C and D, B and D, A and D respectively, in which the D (reaction time) is common factor. These curves are of saddle type and the higher dicamba removal was achieved in 240 min. However, in case of run 4 and 13, with similar A, B and C values, no significant removal was observed. Hence, 135 min of reaction time was finally considered. In the similar way the effects of different concentration (0.13, 0.26) of dicamba on the responses were studied (other than 0.39mM) and a similar trend was observed with optimum values 1.25, 21, 3.5 and 135 for A, B, C and D respectively. However, the removal efficiency was decreased with increasing the initial concentration of dicamba. The design matrix along with removal efficiencies was shown in Tables 4.16, and 4.17.

Table 4.15. Optimization of additional experiments

Run	Independent Factors				% CODR[a]		% AR[b]		Error		S. D[c]		C.V[d]		A.P[e]	
	A	B	C	D	Ac[f]	Pr[g]	Ac	Pr	% CODR	% DR	% CODR	% DR	% CODR	% DR	% CODR	% DR
27	1.08	21	4.85	135	43.7	46.5	50.3	54.5	2.76	4.21	1.95	2.98	6.12	8.03	16.85	12.95
28	2.21	21	4.85	135	62.2	67.3	68.1	71.1	5.16	3.02	3.65	2.14	7.97	4.34	13.05	23.55
29	1.41	21	3.02	135	70.9	72.4	73.1	75.5	1.47	2.37	1.04	1.68	2.05	3.19	49.29	31.87
30	2.77	21	2.14	135	58.6	61.97	62.13	64.15	3.29	2.02	2.33	1.43	5.45	3.2	18.84	31.76

Note :[a] % CODR=% COD removal; [b] % DR= % dicamba removal; [c] S.D=Standard deviation ; [d] C.V= Coefficient of Variation ; [e] A.P= Adequate Precision ; [f] Ac=actual values; [g] Pr=predicted values
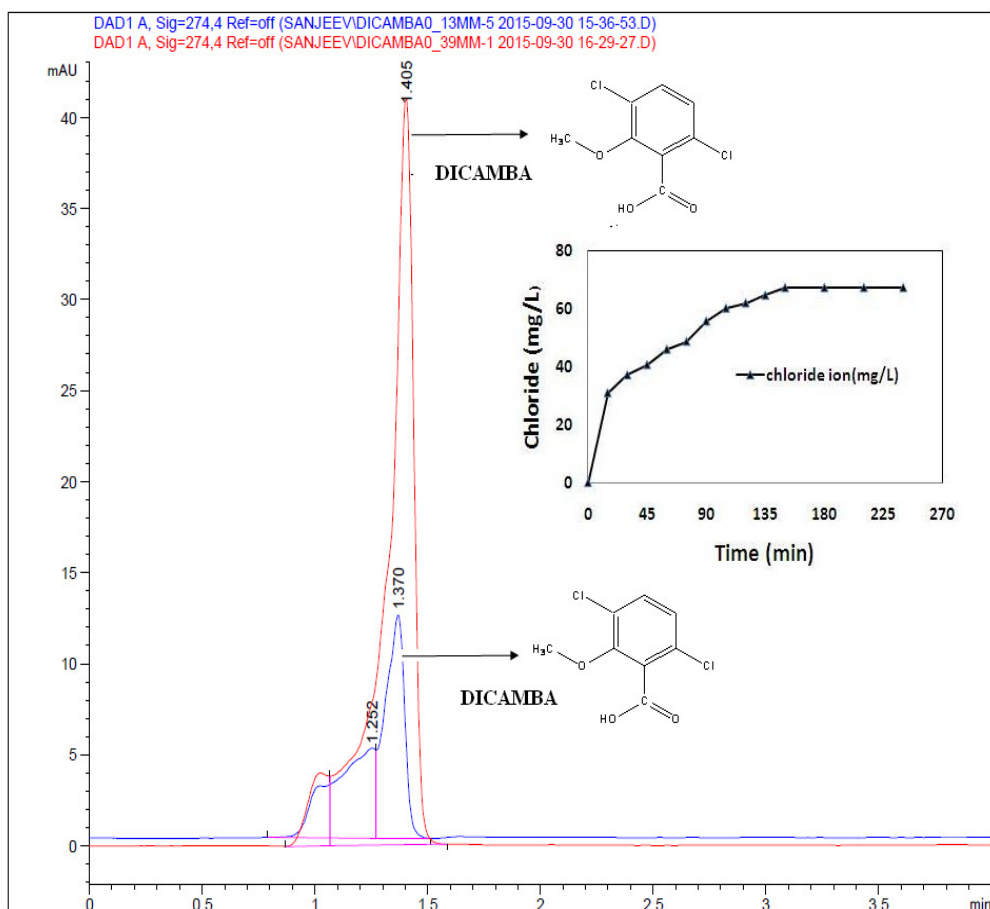
Figure. 4.9. HPLC along with LCMS analysis
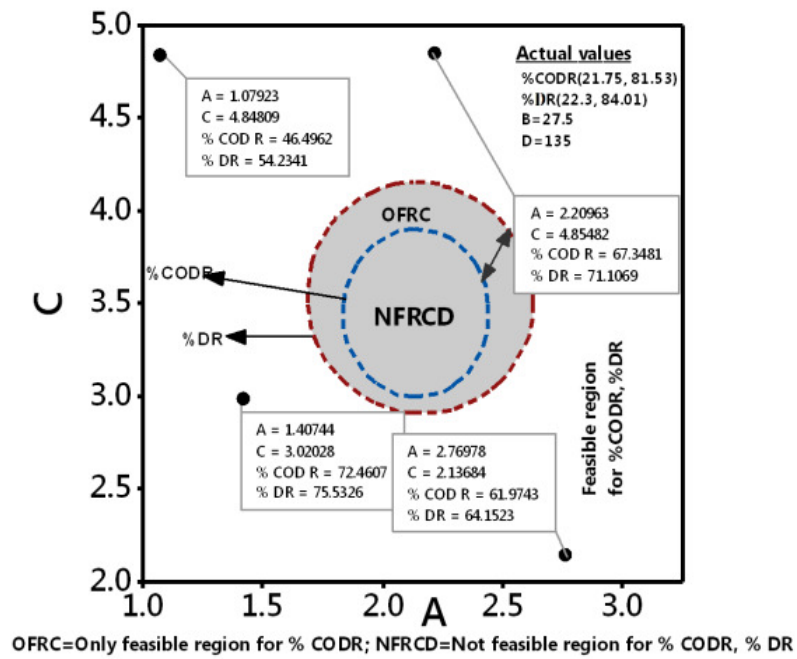
Figure.4.10. Contour overlay plot

Table 4.16. CCD Design Matrix (D_0=0.13mM)

Run	Independent variables (uncoded and coded)				Fenton's Reagent		Actual Responses(%)		Predicted Responses(%)	
	A (H_2O_2/COD)	B (H_2O_2/Fe^{2+})	C (P^H)	D (Time min)	H_2O_2 (mM)	Fe^{2+} (mM)	D R	COD R	% D R	COD R
1	2.125(0)	21(0)	3.5(0)	30(-1)	4.08	0.12	79.87	76.46	86.69	81.53
2	2.125(0)	37(1)	3.5(0)	135(0)	4.08	0.07	63.82	43.55	66.18	52.93
3	3.25(1)	5(-1)	5(1)	30(-1)	6.23	0.76	30.6	28.83	27.77	26.21
4	2.125(0)	21(0)	3.5(0)	135(0)	4.08	0.12	87.9	84.24	73.32	67.95
5	3.25(1)	37(1)	2(-1)	30(-1)	6.23	0.1	28.6	23.92	23.8	20.14
6	2.125(0)	21(0)	2(-1)	135(0)	4.08	0.12	47.09	44.55	49.51	48.3
7	3.25(1)	37(1)	5(1)	240(1)	6.23	0.1	38.5	36.19	41.05	37.4
8	3.25(1)	5(-1)	5(1)	240(1)	6.23	0.76	36.2	33.74	31.12	28.77
9	2.125(0)	21(0)	3.5(0)	135(0)	4.08	0.12	82.04	**82.91**	73.32	67.95
10	1(-1)	37(1)	2(-1)	240(1)	1.92	0.03	35.7	31.28	33.52	30.94
11	1(-1)	21(0)	3.5(0)	135(0)	1.92	0.06	45.0	43.55	49.44	50.05
12	1(-1)	5(-1)	5(1)	30(-1)	1.92	0.23	26.6	23.92	31.27	29.45
13	2.125(0)	21(0)	3.5(0)	240(1)	4.08	0.12	89.9	**80.27**	90.85	85.61
14	1(-1)	37(1)	5(1)	30(-1)	1.92	0.03	52.13	50.92	43.18	41.05
15	2.125(0)	21(0)	5(1)	135(0)	4.08	0.12	48.61	46.01	53.96	52.67
16	3.25(1)	5(-1)	2(-1)	240(1)	6.23	0.76	32.9	28.83	36.85	35.74
17	3.25(1)	5(-1)	2(-1)	30(-1)	6.23	0.76	21.26	19.01	22.79	19.82
18	3.25(1)	37(1)	2(-1)	240(1)	6.23	0.1	35.6	36.19	33.99	31.01
19	1(-1)	5(-1)	2(-1)	240(1)	1.92	0.23	38.19	41.1	38.28	37.76
20	1(-1)	5(-1)	5(1)	240(1)	1.92	0.23	29.6	25.92	29.4	26.74
21	1(-1)	37(1)	5(1)	240(1)	1.92	0.03	35.91	33.74	37.44	33.29
22	1(-1)	5(-1)	2(-1)	30(-1)	1.92	0.23	36.98	31.28	29.43	27.11
23	2.125(0)	5(-1)	3.5(0)	135(0)	4.08	0.5	56.25	48.46	61.66	49.5
24	1(-1)	37(1)	2(-1)	30(-1)	1.92	0.03	20.4	20.01	28.54	25.34
25	3.25(1)	37(1)	5(1)	30(-1)	6.23	0.1	38.6	36.19	41.57	39.89
26	3.25(1)	21(0)	3.5(0)	135(0)	6.23	0.18	44.6	44.55	47.92	48.46

Note:CODR=COD removal, DR=dicamba removal

Table 4.17. CCD Design Matrix(D_0=0.26mM)

Run	Independent variables (uncoded and coded)				Fenton's Reagent		Actual Responses(%)		Predicted Responses(%)	
	A (H$_2$O$_2$/COD)	B (H$_2$O$_2$/Fe^{2+})	C (P^H)	D (Time min)	H$_2$O$_2$ (mM)	Fe^{2+} (mM)	D R	COD R	% D R	COD R
1	2.125(0)	21(0)	3.5(0)	30(-1)	8.19	0.24	76.66	**73.9**	83.79	82.62
2	2.125(0)	37(1)	3.5(0)	135(0)	8.19	0.14	58.6	57.25	62.56	59.34
3	3.25(1)	5(-1)	5(1)	30(-1)	12.52	1.53	25.6	23.05	26.91	23.62
4	2.125(0)	21(0)	3.5(0)	135(0)	8.19	0.24	86.63	78.61	71.78	67.84
5	3.25(1)	37(1)	2(-1)	30(-1)	12.52	0.21	26.2	29.16	23.87	25.72
6	2.125(0)	21(0)	2(-1)	135(0)	8.19	0.24	41.77	40.15	49.35	47.03
7	3.25(1)	37(1)	5(1)	240(1)	12.52	0.21	34.2	33.25	37.68	36.34
8	3.25(1)	5(-1)	5(1)	240(1)	12.52	1.53	32.6	30.38	29.06	28.01
9	2.125(0)	21(0)	3.5(0)	135(0)	8.19	0.24	84.77	80.12	71.78	67.84
10	1(-1)	37(1)	2(-1)	240(1)	3.85	0.06	35.1	34.04	28.18	27.97
11	1(-1)	21(0)	3.5(0)	135(0)	3.85	0.11	42.75	41.37	49.05	45.94
12	1(-1)	5(-1)	5(1)	30(-1)	3.85	0.47	24	26.71	28.32	29.28
13	2.125(0)	21(0)	3.5(0)	240(1)	8.19	0.24	82.74	84.12	84.89	83.08
14	1(-1)	37(1)	5(1)	30(-1)	3.85	0.06	48.5	46.25	42.04	41.58
15	2.125(0)	21(0)	5(1)	135(0)	8.19	0.24	53.66	49.92	55.36	50.72
16	3.25(1)	5(-1)	2(-1)	240(1)	12.52	1.53	30.1	31.6	30.95	30.77
17	3.25(1)	5(-1)	2(-1)	30(-1)	12.52	1.53	25.4	24.26	24.95	24.46
18	3.25(1)	37(1)	2(-1)	240(1)	12.52	0.21	30.5	30.26	29.47	31.26
19	1(-1)	5(-1)	2(-1)	240(1)	3.85	0.47	20.43	19.38	24.98	24.28
20	1(-1)	5(-1)	5(1)	240(1)	3.85	0.47	28.2	26.71	24.92	24.66
21	1(-1)	37(1)	5(1)	240(1)	3.85	0.06	34.5	32.82	38.24	36.19
22	1(-1)	5(-1)	2(-1)	30(-1)	3.85	0.47	33.6	35.56	24.52	26.98
23	2.125(0)	5(-1)	3.5(0)	135(0)	8.19	1	51.13	47.36	56.45	52.95
24	1(-1)	37(1)	2(-1)	30(-1)	3.85	0.06	21.3	25.49	28.13	31.44
25	3.25(1)	37(1)	5(1)	30(-1)	12.52	0.21	37.2	34.04	35.94	32.72
26	3.25(1)	21(0)	3.5(0)	135(0)	12.52	0.36	46.01	41.65	48.99	44.76

4.4 TREATMENT OF AMETRYN

Here, also initial preliminary experiments were conducted to optimize   H$_2$O$_2$/COD (0.5-4.5), H$_2$O$_2$/Fe^{2+}(5-15,16-26, 27-37, 38-50) and   pH(1.5-9) for the highest   removal efficiency and the results are shown Figure.4.11(a)(b)(c). It was found that,   more than 95% removal was observed at a value of 27, 2.125 and 3.5 for H$_2$O$_2$/Fe^{2+}, H$_2$O$_2$ /COD and pH respectively and range of values are given in Table 4.18 and 4.19.
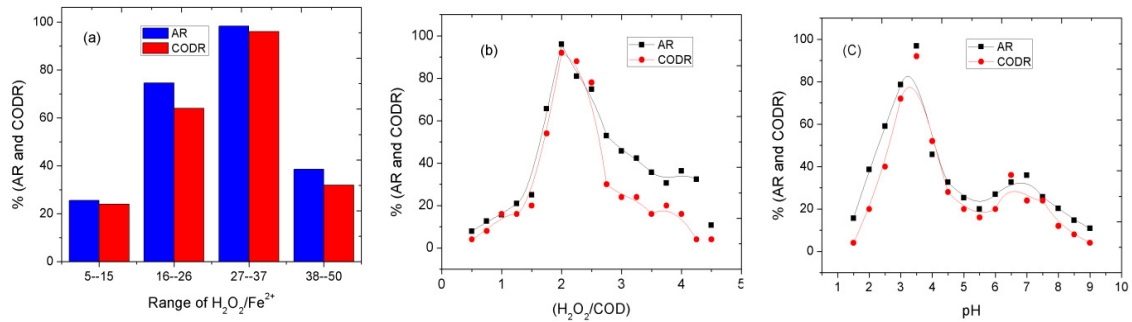
Figure.4.11 (a) Range of H_2O_2/Fe^{2+} vs. responses; Ametryn$_0$=0.02mM, reaction time (min)=30-240, H_2O_2/COD=1-3.25; pH=2-5 **b)** H_2O_2 /COD vs. responses; reaction time(min)=240 , pH=3.5, H_2O_2/Fe^{2+}=27 **c)** pH vs responses; reaction time(min)=240, H_2O_2/Fe^{2+}=27, H_2O_2 /COD=2.125.

Table 4.18. Levels of the parameters studied in the CCD

Factor	Name	Low(-1)	Middle(0)	High(+1)
A(X_1)	H_2O_2/COD	1	2.125	3.5
B(X_2)	H_2O_2/Fe^{2+}	5	27.5	50
C(X_3)	P^H	2	3.5	5
D(X_4)	Time (min)	30	135	240

4.4.1 ANOVA of Results

The second order quadratic equations for % CODR and % ametryn removal efficiency (%AR) are given in Eqs. 4.13 and 4.14. And the ANOVA results are shown in Table 4.20 and A-II-2.

Regression Equations

% COD R (Y_1) = 77.43 + 0.44 A - 0.44 B - 0.89 C + 3.33 D - 34.57 A*A - 14.57 B*B - 10.57 C*C + 11.43 D*D + 1.75 A*B + 1.25 A*C - 0.25 A*D + 1.75 B*C + 1.25 B*D + 0.75 B*D   (4.13)

% A R (Y_2) = 84.45 + 0.46 A + 1.10 B - 2.71 C + 2.81 D - 33.62 A*A - 13.58 B*B - 13.41 C*C + 8.89 D*D + 1.06 A*B + 1.28 A*C - 1.19 A*D + 0.77 B*C + 2.36 B*D - 0.03 C*D   (4.14)

Both Eqs.4.13 and 4.14 are having, the intercept values are 77.43, 84.45 and the coefficients of %AR (D^2, A*B, A*C, B*C, B*D, B*D), %CODR (A, B, D, D*D, A*B, A*C, B*C, B*D) are showing a positive effect. The reaction time (D^2) and (A*A) has the greatest positive and negative value respectively. The best significant factors were considered, if the P values < 0.05 and the factors are A^2, B^2, C^2, D^2 in and D, A^2, B^2, C^2, D^2 in %AR and CODR respectively. The F values were found to be (standard value: $F_{0.05 (14, 11)}$=value of 2.74) 18.54 and 35.64 for %AR and % CODR respectively.

Table 4.19. Design matrix (A_0=0.02mM)

Run	Independent variables (uncoded and coded)				Fenton's Reagent		Actual Responses(%)		Predicted Responses(%)	
	A (H$_2$O$_2$/COD)	B (H$_2$O$_2$/Fe^{2+})	C (P^H)	D (Time min)	H$_2$O$_2$ (mM)	Fe^{2+} (mM)	A R	COD R	A R	COD R
1	2.125(0)	27.5(0)	3.5(0)	30(-1)	0.5	0.011	81.01	76	80.53	77.14
2	2.125(0)	50(1)	3.5(0)	135(0)	0.5	0.006	76.71	64	71.97	61.8
3	3.25(1)	5(-1)	5(1)	30(-1)	0.765	0.094	33.26	28	29.59	24.61
4	2.125(0)	27.5(0)	3.5(0)	135(0)	0.5	0.011	92.87	80	94.45	82.26
5	3.25(1)	50(1)	2(-1)	30(-1)	0.765	0.009	34.5	28	32	25.5
6	2.125(0)	27.5(0)	2(-1)	135(0)	0.5	0.011	65.57	64	73.76	67.14
7	3.25(1)	50(1)	5(1)	240(1)	0.765	0.009	34.6	36	38.61	37.94
8	3.25(1)	5(-1)	5(1)	240(1)	0.765	0.094	28	28	28.06	29.33
9	2.125(0)	27.5(0)	3.5(0)	135(0)	0.5	0.011	93.05	80	94.45	82.26
10	1(-1)	50(1)	2(-1)	240(1)	0.235	0.003	40.3	28	41.92	30.83
11	1(-1)	27.5(0)	3.5(0)	135(0)	0.235	0.005	48.2	44	50.37	41.8
12	1(-1)	5(-1)	5(1)	30(-1)	0.235	0.029	25.21	24	25.84	24.22
13	2.125(0)	27.5(0)	3.5(0)	240(1)	0.5	0.011	100	100	96.15	93.36
14	1(-1)	50(1)	5(1)	30(-1)	0.235	0.003	22.32	20	22.75	20.83
15	2.125(0)	27.5(0)	5(1)	135(0)	0.5	0.011	70.84	68	68.33	65.36
16	3.25(1)	5(-1)	2(-1)	240(1)	0.765	0.094	35.01	32	32.53	30.61
17	3.25(1)	5(-1)	2(-1)	30(-1)	0.765	0.094	33.4	28	33.95	28.89
18	3.25(1)	50(1)	2(-1)	240(1)	0.765	0.009	40	32	40	32.22
19	1(-1)	5(-1)	2(-1)	240(1)	0.235	0.029	38.56	36	38.67	36.22
20	1(-1)	5(-1)	5(1)	240(1)	0.235	0.029	28.63	28	29.08	29.94
21	1(-1)	50(1)	5(1)	240(1)	0.235	0.003	35.33	32	35.41	31.55
22	1(-1)	5(-1)	2(-1)	30(-1)	0.235	0.029	41.36	36	35.3	33.5
23	2.125(0)	5(-1)	3.5(0)	135(0)	0.5	0.061	59.36	60	69.77	62.69
24	1(-1)	50(1)	2(-1)	30(-1)	0.235	0.003	28.56	24	29.13	23.11
25	3.25(1)	50(1)	5(1)	30(-1)	0.765	0.009	30.2	28	30.73	28.22
26	3.25(1)	27.5(0)	3.5(0)	135(0)	0.765	0.017	47.8	40	51.3	42.69

Note:CODR=COD removal, AR=ametryn removal.

Table 4. 20 . Analysis of Variance for % AR and %CODR

Parameter	% CODR	% AR
R^2 (coefficient of determination)	97.84	95.94
Standard deviation (S.D)	1.35	1.7
Coefficient of variation(CV) %	4.53	4.86
Adequate precision(AP)	42.75	80.1
Pure error	0.0	0.02
F-value	35.64	18.54

Note:CODR=COD removal, AR=ametryn removal

Furthermore, these values are supported by the coefficient of determination (R^2). The R^2 and R^2_{adj} values are found to be 95.94%, 90.76% and 97.84%, 95.10% for %AR and CODR respectively, in which R^2 and R^2_{adj} are close to each other. The $R^2_{adj} < R^2$, $R^2 > 80\%$ and F>2.74, confirms that the better experimental results were obtained (Santos and Boaventura 2008). The lack of fit and the residual error are showing the similar values 554.3 and 263 for both Y_2 and Y_1 responses respectively with pure error zero.

The lack of fit F values <2.5%, S.D<3, C.V<10 and A.P>4 confirms that, the obtained results are reliable (Im et al. 2012, Beg et al. 2003, Zinatizadeh et al. 2006). The fluctuation in all observations is plotted in A-III-7(a) (b) and it showed that values are randomly distributed along the space and it is a good trend for both responses.

4.4.2 Effects of H_2O_2/COD, H_2O_2/Fe^{2+} and pH on the responses

From the Table 4.19., it is seen that, as the H_2O_2/COD ratio decreased to 1 or increased to 3.25 from a center value of 2.125, less removal was achieved. This implies that the more number of hydroxyl radicals are produced in the ratio of 2.125 (Kim et al. 1997) and thereby increasing the removal efficiency (Eq. 4.1).

Based on the range of values selected (A and B), the dosage of H_2O_2 which is varied from 0.235 -0.765 mM and Fe^{2+} varied as 0.003-0.094 mM (Table 4.20 and Figure.4.12(a)(b)). Usually, it is seen that increase in the H_2O_2 increases removal efficiency (Pignatello 1992) and however, when the hydrogen peroxide was increased to 0.765mM less removal (25-48%) was achieved. This may be due to, the decreasing •OH radical production (scavenging effect) and increasing the O_2 production

(Masomboon et al. 2009). Furthermore, the dosage of H_2O_2 was decreased to 0.235mM and no significant removal was achieved.
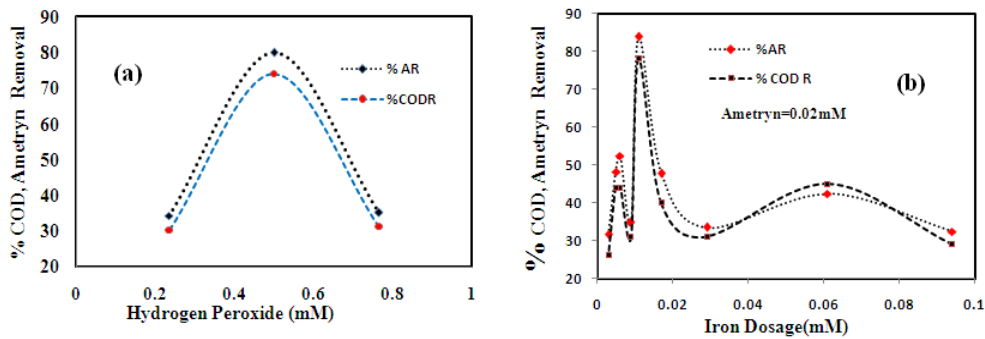
Figure. 4.12 a) Effect of H_2O_2 on % COD and ametryn removal efficiency b) Effect of Fe^{2+} on % COD and ametryn removal efficiency
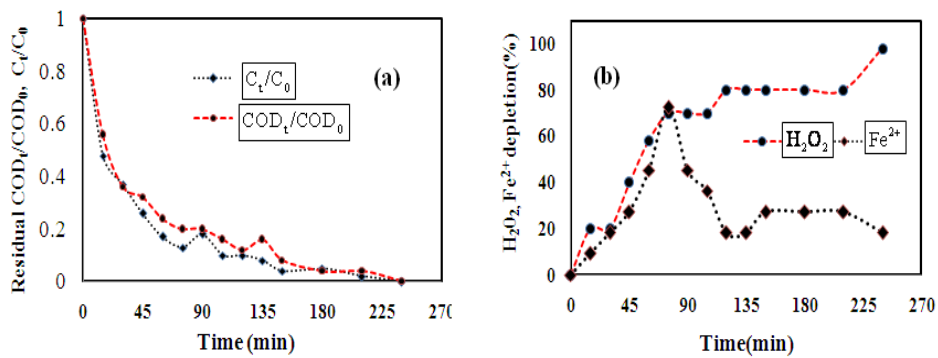
Figure. 4.13 a) Residual COD_t/COD_0 and C_t/C_0 vs time b)% H_2O_2 and Fe^{2+} depletion with time. H_2O_2=0.5mM; Fe^{2+}=0.011 mM;COD_0=8mg/L, C_0=0.02mM, pH =3.5
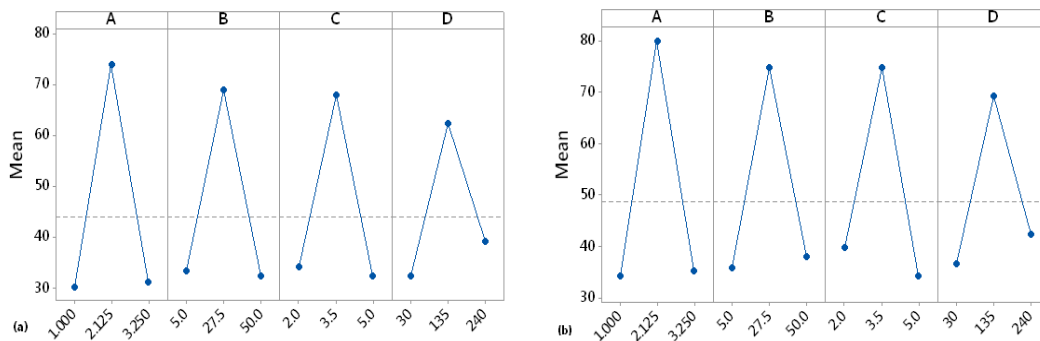
Figure.4. 14. Main affects plots for both responses a)% COD R b) % AR

66

When the iron concentration was increased from 0.011 -0.094 mM, less removal (28-60%) was achieved. This is due to, more amount of iron reacts with already produced $^\bullet$OH radicals and stops further production of radicals (Eq. 4.4) (Hameed and Lee 2009). And also here, the ratio of H_2O_2/Fe^{2+} plays an important role, when this ratio was 5 and 50, the less removal was observed (pH 5, 2) and if the ratio was 27.5 (run11), the degradation was maximum(100%) with 0.5 mM of H_2O_2. Moreover, if Fe^{2+} dosage was decreased from 0.011-0.003mM, only 34-40 % removal was achieved. At a low iron dosage, there are not enough Fe^{2+} ions available to react with oxidant and further, the available H_2O_2 is going to react with $^\bullet$OH radical to form a $^\bullet$OOH radical (Eq.4.8) (Masomboon et al. 2009) and sometimes, there is a formation of iron complexes. It was also true that, the formed $^\bullet$OOH radical oxidation potential is less than the $^\bullet$OH radical. In case run 13 with Fe^{2+} dosage of 0.011 mM, significant improvement in the removal (100%) efficiency was observed. Therefore, optimum value Fe^{2+} was considered as 0.011mM.

As discussed earlier the Fenton's process works in acidic pH and it varied from 2-5 with 3.5 as center value (Table.4.19). It is seen that, at pH 2 the removal efficiency in both responses was decreased to 28-65% and in the case of pH 5, the removal was 25-70%. When the pH is >3.5, both % AR and %CODR were reduced due to the decomposition of hydrogen peroxide by losing its oxidizing potential. Further, the deactivation of a Fe^{2+} was observed by forming ferric hydroxide complexes (Lucas and Peres 2006). At lower pH (<3.5), the scavenging $^\bullet$OH radicals by H^+ ions was the major reaction, which leads to the lesser degradation (Martins et al. 2010). Therefore, the optimum pH of 3.5 was finally selected.

4.4.3 Effects of D (reaction time) on the responses

In the present study, the reaction time was varied from 30-240 min. In case of run 1 at 30 min, the reaction was faster (maximum OH radicals produced) and 81 % of ametryn and 76% of COD removal was observed with experimental conditions of H_2O_2/COD (2.125), H_2O_2/Fe^{2+} (27.5), pH (3.5), Fe^{2+} (0.011mM) and H_2O_2 (0.5mM). Further, the reaction was continued with the same experimental conditions (run 4 and 13) up to 240

min and the reaction was slowly reduced, as it passes from 30-240 min (HO_2 $^\bullet$ radicals produced). At 135 min (run 4 or 9) the removal efficiency was 80-93% and at 240 min 100% removal was observed. In case of the runs (3, 5, 12, 14, 17, 22, 24, and 25) at 30 min, less removal was obtained. This implies that the selection of the proper ratio of A, B and C is highly essential.

The kinetic studies were carried at optimum Fenton's dosage (Fe^{2+}=0.011mM, H_2O_2 =0.5mM and pH =3.5) shown in Figure.4.13 (a) and it was observed that after 135 min, removal rate was slowly decreased and 100% removal was observed at 240 min. The H_2O_2 and Fe^{2+} depletion was also monitored (Figure.4.13 (b)), in which 98% decomposition of H_2O_2 was observed at 240 min (run 13) (2% residual) and 72% of Fe^{2+} was converted in to Fe^{3+}(0-75 min), after that slowly Fe^{2+} regeneration was observed. On the other hand, the mean values of both responses are also calculated (Figure. 4.14 (a) (b)) and the maximum values observed to be at 2.125, 27.5, 3.5 and 135 min for A, B, C, D respectively. Moreover, the experimental values are showing good correlation with model values shown in A-III-8, in which the data points are distributed along the straight line. The interactive effects were studied through surface plots (A-III-9 and A-III- 10). The figures A-III-9 (a), (c), (d) and A-III- 10 (b) (d) (f) regions show the sharp convex surface and this implies that, the maximum COD removal (100%) has occurred at exactly the center value of H_2O_2/COD (2.125), H_2O_2/Fe^{2+} (27.5), pH (3.5). In A-III-9 (b) (e) (f), the curves are of saddle type, in which the D (reaction time) factor is common and it is showing the most significant role among A, B and C. The maximum COD removal of 100% was achieved at 240 min and 80% at 135 min. Similar trends were observed in A-III- 10 (a) (c) (e)), where 100 % ametryn removal was achieved at 240 min and 93% in 135 min.

4.4.4 LCMS analysis of degradation products and validation

The decay of ametryn was analyzed before and after Fenton's treatment process (Figure.4.15). Before treatment, the ametryn was eluted at retention time of 8.872 min and after treatment no such peak was observed at 240 min. This implies that, 100 %

ametryn disappeared with the formation of thiocynate ion (S-CN with m/z=58) (A-I-14), which was confirmed with LCMS mass table. It was also found that 100% COD removal was observed, confirming the mineralization of ametryn in water. The optimum region was determined graphically in an overlay plot (Figure.4.16) by superimposing the contours for all responses. Here the boundary values were defined as Y_1 (20, 100) and Y_2 (22.32, 100), which are actual experimental values. The overlay plot consists of 3 regions, which are separated by circular dotted lines. The shaded portion consists of two regions, in which the middle area is not feasible for both responses and other region is feasible for only Y_2. The remaining unshaded area is suitable for both responses (optimum region). To verify the results, four sets of additional experiments (tagged in Figure. 4.16) were conducted, suggested by overlay plot from unshaded area. The results showed that (Table 4.21), the S.D <5, C.V< 6%, and A.P>10, implies that, all 26 experiments were successfully validated.
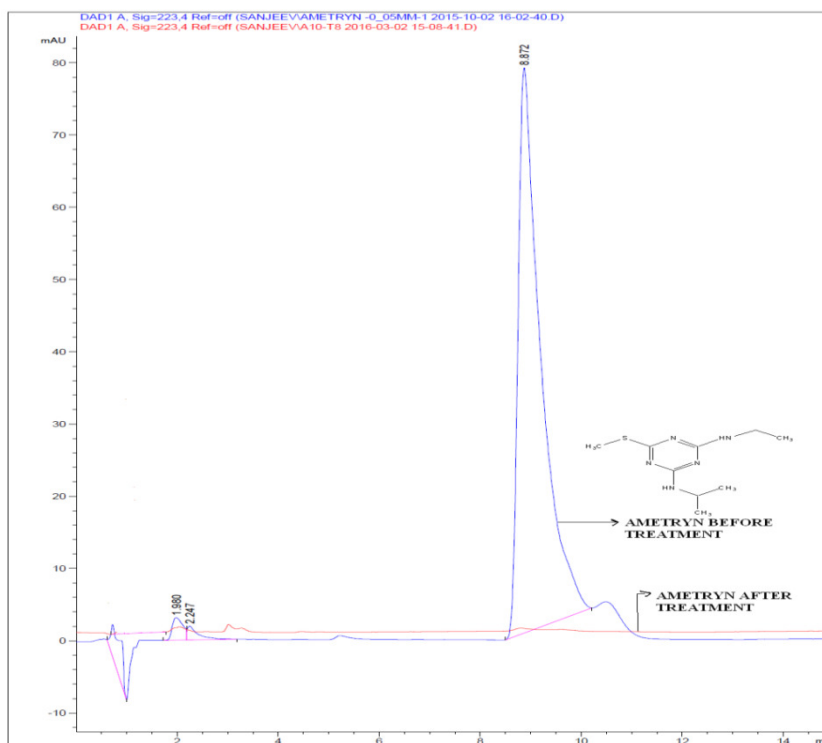
Figure.4.15 LCMS analysis of ametryn before and after treatment

Table 4.21. Optimization of additional experiments

Run	Independent Factors				% CODR[a]		% AR[b]		Error		S. D[c]		C.V[d]		A.P[e]	
	A	B	C	D	Ac[f]	Pr[g]	Ac	Pr	% CODR	% AR	% CODR	% AR	% CODR	% AR	% CODR	% AR
27	1.4	27.5	4.37	240	72	73.72	74.36	76.1	1.72	1.74	1.22	1.23	2.36	2.31	42.86	43.74
28	3.18	27.5	3.39	240	60	61.9	63.2	66	1.9	2.8	1.34	1.98	3.12	4.33	32.58	23.57
29	3.19	27.5	2.1	240	48	50.56	48.32	54.4	2.56	6.08	1.81	2.86	5.19	7.71	19.75	13.47
30	1.4	27.5	2.73	240	72	75.3	76.3	80.8	3.3	4.5	2.33	3.18	4.48	5.73	22.82	17.96

Note :[a] % CODR=% COD removal; [b] % AR= % ametryn removal; [c] S.D=Standard deviation ; [d]C.V= Coffcient of Variation ; [e] A.P= Adequate Precision ; [f] Ac=Actual values; [g] Pr=Pridicted values

Further, to understand the effect of initial concentration of ametryn on the responses, the experiments were conducted with different concentration of ametryn such as 0.04 and 0.06mM. The similar trend in the results was observed and the removal efficiency was decreased by increasing the initial concentration of the compound. The results of all the three concentrations (0.04 and 0.06 mM) are given in Tables. 4.22 and 4.23.
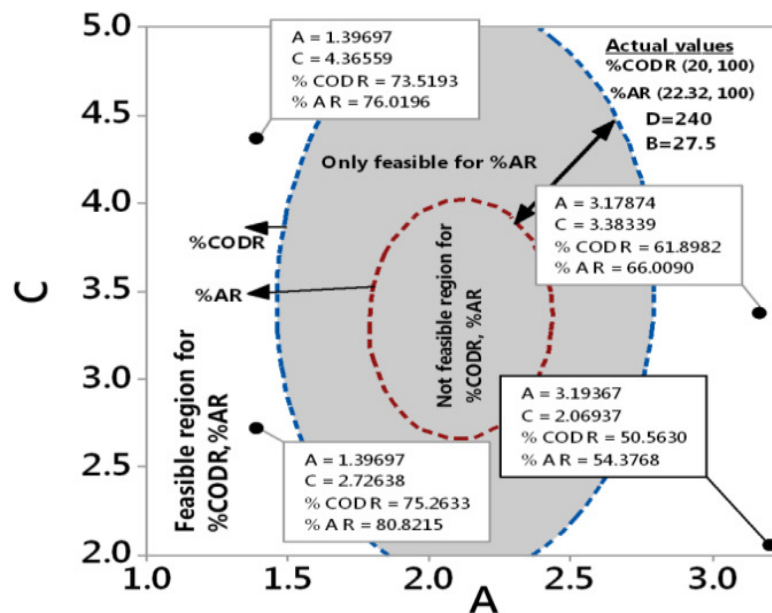
Figure.4.16. Contour overlay plot

Table 4.22. CCD Design Matrix(A_0=0.04mM)

Run	Independent variables (uncoded and coded)				Fenton's Reagent		Actual Responses(%)		Predicted Responses(%)	
	A (H$_2$O$_2$/COD)	B (H$_2$O$_2$/Fe^{2+})	C (P^H)	D (Time min)	H$_2$O$_2$ (mM)	Fe^{2+} (mM)	A R	COD R	A R	COD R
1	2.125(0)	27.5(0)	3.5(0)	30(-1)	0.963	0.021	60.84	58.44	67.97	67.49
2	2.125(0)	50(1)	3.5(0)	135(0)	0.963	0.012	52.78	48.05	51.63	45.16
3	3.25(1)	5(-1)	5(1)	30(-1)	1.472	0.18	30.62	37.66	25.33	26.62
4	2.125(0)	27.5(0)	3.5(0)	135(0)	0.963	0.021	82.88	79.22	73.11	68.83
5	3.25(1)	50(1)	2(-1)	30(-1)	1.472	0.018	30.66	32.46	26.6	25.75
6	2.125(0)	27.5(0)	2(-1)	135(0)	0.963	0.021	62.32	58.44	71.64	66.52
7	3.25(1)	50(1)	5(1)	240(1)	1.472	0.018	29.25	27.27	33.84	34.7
8	3.25(1)	5(-1)	5(1)	240(1)	1.472	0.18	24.32	28.65	26	27.92
9	2.125(0)	27.5(0)	3.5(0)	135(0)	0.963	0.021	81.61	79.22	73.11	68.83
10	1(-1)	50(1)	2(-1)	240(1)	0.453	0.006	35.78	22.07	38.71	28.35
11	1(-1)	27.5(0)	3.5(0)	135(0)	0.453	0.01	47.82	42.85	46.56	41.12
12	1(-1)	5(-1)	5(1)	30(-1)	0.453	0.055	22.31	16.88	23.74	22.72
13	2.125(0)	27.5(0)	3.5(0)	240(1)	0.963	0.021	97.8	94.8	86.76	82.68
14	1(-1)	50(1)	5(1)	30(-1)	0.453	0.006	20.12	23.56	20.07	19.11
15	2.125(0)	27.5(0)	5(1)	135(0)	0.963	0.021	68.35	63.63	65.12	62.48
16	3.25(1)	5(-1)	2(-1)	240(1)	1.472	0.18	39.63	37.66	37.32	35.86
17	3.25(1)	5(-1)	2(-1)	30(-1)	1.472	0.18	35.21	32.46	35.36	37.15
18	3.25(1)	50(1)	2(-1)	240(1)	1.472	0.018	38.52	37.66	37.93	34.85
19	1(-1)	5(-1)	2(-1)	240(1)	0.453	0.055	37.88	28.88	40.23	29.36
20	1(-1)	5(-1)	5(1)	240(1)	0.453	0.055	28.29	29.91	29.99	24.02
21	1(-1)	50(1)	5(1)	240(1)	0.453	0.006	35.0	32.46	35.69	30.8
22	1(-1)	5(-1)	2(-1)	30(-1)	0.453	0.055	39.63	42.85	32.68	30.66
23	2.125(0)	5(-1)	3.5(0)	135(0)	0.963	0.118	45.92	40.65	53.16	47.47
24	1(-1)	50(1)	2(-1)	30(-1)	0.453	0.006	22.63	16.88	21.79	19.26
25	3.25(1)	50(1)	5(1)	30(-1)	1.472	0.018	25.32	26.67	23.8	23.01
26	3.25(1)	27.5(0)	3.5(0)	135(0)	1.472	0.033	39.63	37.66	46.97	46.32

Note:CODR=COD removal, AR=ametryn removal

Table 4.23 CCD Design Matrix (A_0=0.06mM)

Run	Independent variables (uncoded and coded)				Fenton's Reagent		Actual Responses(%)		Predicted Responses(%)	
	A (H$_2$O$_2$/COD)	B (H$_2$O$_2$/Fe^{2+})	C (P^H)	D (Time min)	H$_2$O$_2$ (mM)	Fe^{2+} (mM)	A R	COD R	A R	COD R
1	2.125(0)	27.5(0)	3.5(0)	30(-1)	1.531	0.034	63.19	60.81	66.5	65.26
2	2.125(0)	50(1)	3.5(0)	135(0)	1.531	0.019	54.93	51.02	49.98	46.6
3	3.25(1)	5(-1)	5(1)	30(-1)	2.342	0.287	28.26	37.95	19.91	25.08
4	2.125(0)	27.5(0)	3.5(0)	135(0)	1.531	0.034	75.65	**73.87**	70.04	65.89
5	3.25(1)	50(1)	2(-1)	30(-1)	2.342	0.029	28.53	24.89	19.68	15.1
6	2.125(0)	27.5(0)	2(-1)	135(0)	1.531	0.034	61.08	57.55	65.88	61.48
7	3.25(1)	50(1)	5(1)	240(1)	2.342	0.029	28.52	28.16	30.03	26.54
8	3.25(1)	5(-1)	5(1)	240(1)	2.342	0.287	22.32	21.63	26.18	26.4
9	2.125(0)	27.5(0)	3.5(0)	135(0)	1.531	0.034	74.73	73.87	70.04	65.89
10	1(-1)	50(1)	2(-1)	240(1)	0.721	0.009	28.62	25.69	31.48	30.16
11	1(-1)	27.5(0)	3.5(0)	135(0)	0.721	0.016	42.32	37.95	41.7	34.62
12	1(-1)	5(-1)	5(1)	30(-1)	0.721	0.088	21.32	18.36	19.8	20.05
13	2.125(0)	27.5(0)	3.5(0)	240(1)	1.531	0.034	94.25	90.2	84.37	81.07
14	1(-1)	50(1)	5(1)	30(-1)	0.721	0.009	18.62	21.63	20.87	20.18
15	2.125(0)	27.5(0)	5(1)	135(0)	1.531	0.034	64.52	60.81	63.16	62.2
16	3.25(1)	5(-1)	2(-1)	240(1)	2.342	0.287	38.23	31.42	30.48	25.26
17	3.25(1)	5(-1)	2(-1)	30(-1)	2.342	0.287	14.98	11.83	21.86	18.23
18	3.25(1)	50(1)	2(-1)	240(1)	2.342	0.029	21.19	18.36	27.34	22.95
19	1(-1)	5(-1)	2(-1)	240(1)	0.721	0.088	36.23	31.42	38.37	31.66
20	1(-1)	5(-1)	5(1)	240(1)	0.721	0.088	24.52	21.63	27.88	23.81
21	1(-1)	50(1)	5(1)	240(1)	0.721	0.009	30.23	25.69	27.99	24.76
22	1(-1)	5(-1)	2(-1)	30(-1)	0.721	0.088	34.93	28.16	27.93	22.18
23	2.125(0)	5(-1)	3.5(0)	135(0)	1.531	0.187	42.63	37.95	51.02	47.69
24	1(-1)	50(1)	2(-1)	30(-1)	0.721	0.009	21.23	19.65	22.01	19.87
25	3.25(1)	50(1)	5(1)	30(-1)	2.342	0.029	22.23	21.25	24.73	24.4
26	3.25(1)	27.5(0)	3.5(0)	135(0)	2.342	0.052	35.62	24.89	39.68	33.53

Note:CODR=COD removal, AR=ametryn removal

4.5. TREATMENT OF 2, 4 –D

Preliminary experiments were conducted with different values of H$_2$O$_2$ /COD (0.5-4.5), H$_2$O$_2$/Fe^{2+}(5-15,16-26, 27-37,38-48,49-59) and pH(1.5-9) shown in Figure. 4.17(a)(b)(c) and it was found that the maximum removal (>75%) was observed at values of 32(H$_2$O$_2$/Fe^{2+}), 2.125(H$_2$O$_2$ /COD) and 3.5(pH). Based on this, later experiments were performed (Table 4.24 and 4.25) and the ANOVA results are presented in Table 4.26 and A-II-3.
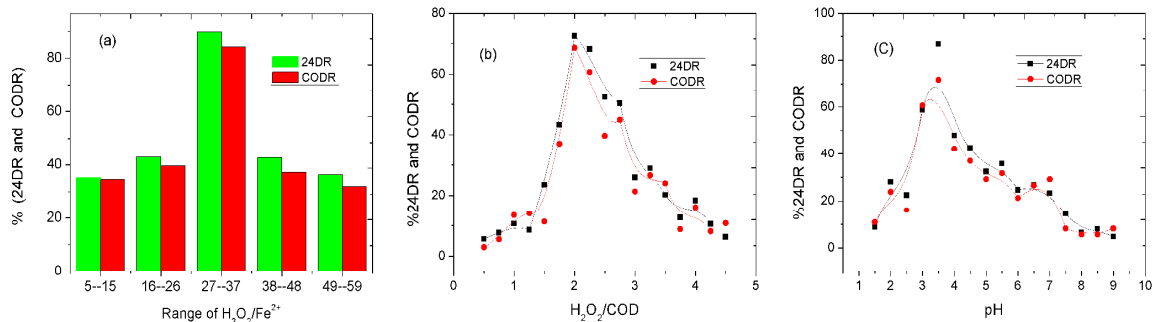
Figure.4.17 **(a)** Range of H_2O_2/Fe^{2+} vs. responses; $2,4-D_0=0.13mM$, reaction time(min)=30-240, $H_2O_2/COD=1-3.25$; pH=2-5 **b)** H_2O_2/COD vs. responses; reaction time(min)=240 , pH=3.5, $H_2O_2/Fe^{2+}=32$ **c)** pH vs responses; reaction time(min)=240, $H_2O_2/Fe^{2+}=32$, $H_2O_2/COD=2.125$.

4.5.1 Central composite design and ANOVA results

The relation between the responses and the variables are explained in model equations (Eqs.4.15 and 4.16). The intercept values ($68.59(Y_1)$, $70.93(Y_2)$), the coefficients of B, C, D, D^2, A*B, A*C, B*C, and B*D are showing a positive effect (D^2=highest positive values of $20.02(Y_1)$ and $17.22(Y_2)$) and the remaining factors are showing a negative effect on both responses (B^2 has highest negative value).

Table 4.24. Levels of the parameters studied in the CCD

Factor	Name	Low(-1)	Middle(0)	High(+1)
A(X_1)	H_2O_2/COD	1	2.125	3.5
B(X_2)	H_2O_2/Fe^{2+}	5	32	59
C(X_3)	P^H	2	3.5	5
D(X_4)	Time (min)	30	135	240

$$\% \text{ COD R}(Y_1) = 68.59 - 0.29\text{ A} + 2.04\text{ B} + 0.29\text{ C} + 4.95\text{ D} - 21.97\text{ A*A} - 24.57\text{ B*B} -$$
$$8.84\text{ C*C} + 20.02\text{ D*D} + 0.49\text{ A*B} + 3.12\text{ A*C} - 4.42\text{ A*D} + 0.82\text{ B*C}$$
$$+ 1.81\text{ B*D} - 2.13\text{ C*D} \qquad (4.15)$$

$$\%2,4\text{-D R }(Y_2) = 70.93 - 0.94\text{ A} + 1.66\text{ B} + 0.01\text{ C} + 4.51\text{ D} - 18.80\text{ A*A} - 23.63\text{ B*B} -$$
$$9.75\text{ C*C} + 17.22\text{ D*D} + 0.74\text{ A*B} + 3.07\text{ A*C} - 3.91\text{ A*D} + 0.77\text{ B*C}$$
$$+ 1.34\text{ B*D} - 2.70\text{ C*D} \qquad (4.16)$$

73

The experimentally calculated F values for both the responses are 4.91 and 5.24 (>2.74). The R^2 and R^2_{adj} values are found to be 89.55%, 86.55% and 91.62%, 89.55 for Y_2 and Y_2 respectively ($R^2_{adj} < R^2$, $R^2 > 80\%$). The pure error value is less than 4, lack of fit P values <0.13, S.D(2.72 (Y_2), 2.61(Y_1))<3, C.V(8.66% (Y_2) ,8.6% (Y_1))<10 and A.P(32.04 (Y_2), 38.85 (Y_1))>4 (Beg et al. 2003, Zinatizadeh et al. 2006), confirms that the obtained results are more satisfactory. To residual plot (A-III-11) shows that, the points are randomly distributed along both positive and negative sides of the straight line and it is a good trend in the treatment process.

4.5.2 Effects of independent variables on the responses (%2,4-DR and % CODR)

The ratio of H_2O_2/COD varied from 1-3.25 and highest removal was observed in 2.125, where the more number of $^{\bullet}$OH radicals are produced. Hence, the H_2O_2/COD ratio of 2.125 was considered. Further, H_2O_2/Fe^{2+} (B) were varied as 5, 32 and 59 and based on these ratios the dosage of iron (0.02-0.71 mM) and hydrogen peroxide (1.79-5.81 mM) were applied (Figure.4.18 a). According to the Pignatello (1992), an increase in the H_2O_2, increases the degradation of pollutants by generating more hydroxyl radicals. When the H_2O_2 dosage was increased from 1.79-3.81 mM the removal efficiency was > 84% for both responses. Further increase in H_2O_2 from 3.81-5.83mM the removal efficiency was decreased.
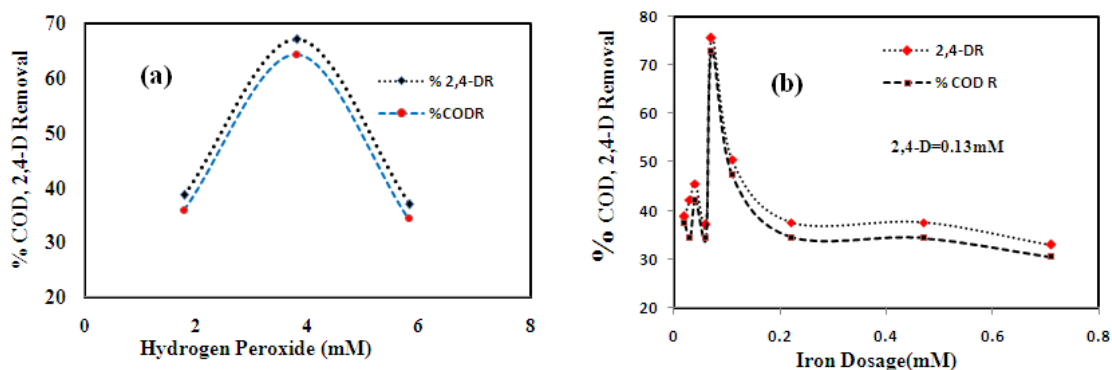
Figure. 4. 18 a) Effect of H_2O_2 on % COD and 2,4-D removal efficiency b) Effect of Fe^{2+} on % COD and 2,4-D removal efficiency
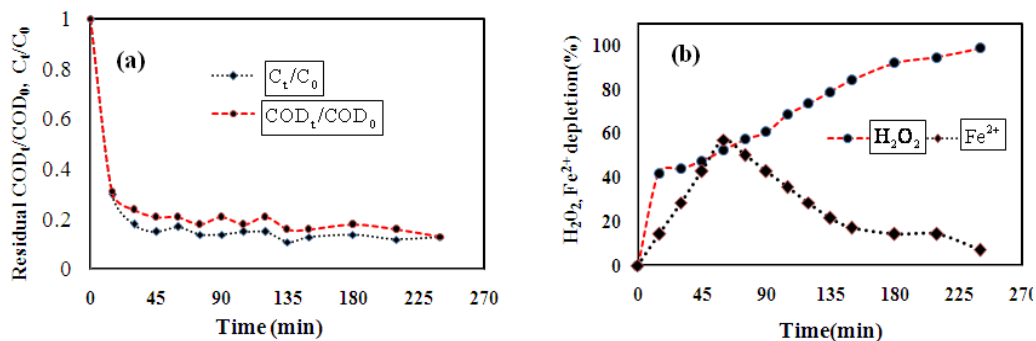
Figure. 4.19 a) Residual COD_t/COD_0 and C_t/C_0 vs reaction time b)% H_2O_2 and Fe^{2+} depletion vs time. H_2O_2=3.81mM; Fe^{2+}=0.07mM; COD_0=61mg/L, C_0=0.13mM, pH =3.5

Table 4.25. CCD Design Matrix

Run	Independent variables (uncoded and coded)				Fenton's Reagent		Actual Responses(%)		Predicted Responses(%)	
	A (H₂O₂/COD)	B (H₂O₂/Fe²⁺)	C (Pᴴ)	D (Time min)	H₂O₂ (mM)	Fe²⁺ (mM)	24D R	COD R	24D R	COD R
1	2.125(0)	32(0)	3.5(0)	30(-1)	3.81	0.07	81.81	76.39	84.43	80.53
2	2.125(0)	59(1)	3.5(0)	135(0)	3.81	0.04	45.6	42.29	48.91	46.29
3	3.25(1)	5(-1)	5(1)	30(-1)	5.83	0.71	30.5	29.18	38.47	36.54
4	2.125(0)	32(0)	3.5(0)	135(0)	3.81	0.07	89.28	86.88	81.1	87.61
5	3.25(1)	59(1)	2(-1)	30(-1)	5.83	0.06	28.4	26.55	29.06	26.47
6	2.125(0)	32(0)	2(-1)	135(0)	3.81	0.07	57.6	55.4	61.12	59.65
7	3.25(1)	59(1)	5(1)	240(1)	5.83	0.06	40	39.67	40.45	40.37
8	3.25(1)	5(-1)	5(1)	240(1)	5.83	0.71	35.3	31.8	31.42	28.79
9	2.125(0)	32(0)	3.5(0)	135(0)	3.81	0.07	86.65	84.26	81.1	87.61
10	1(-1)	59(1)	2(-1)	240(1)	1.79	0.02	62	60.65	62.53	60.11
11	1(-1)	32(0)	3.5(0)	135(0)	1.79	0.03	42.3	34.42	43.01	37.74
12	1(-1)	5(-1)	5(1)	30(-1)	1.79	0.22	34.8	29.18	27.86	23.08
13	2.125(0)	32(0)	3.5(0)	240(1)	3.81	0.07	84.65	81.63	93.28	89.46
14	1(-1)	59(1)	5(1)	30(-1)	1.79	0.02	26.1	23.93	28.57	24.98
15	2.125(0)	32(0)	5(1)	135(0)	3.81	0.07	53.4	52.78	61.12	60.5
16	3.25(1)	5(-1)	2(-1)	240(1)	5.83	0.71	36.2	31.8	32.22	27.57
17	3.25(1)	5(-1)	2(-1)	30(-1)	5.83	0.71	30	29.48	28.47	29.03
18	3.25(1)	59(1)	2(-1)	240(1)	5.83	0.06	32.52	27.18	38.16	33.47
19	1(-1)	5(-1)	2(-1)	240(1)	1.79	0.22	45	40.01	49.55	45.44
20	1(-1)	5(-1)	5(1)	240(1)	1.79	0.22	38.62	37.04	36.46	33.94
21	1(-1)	59(1)	5(1)	240(1)	1.79	0.02	42.3	43.67	42.53	44.3
22	1(-1)	5(-1)	2(-1)	30(-1)	1.79	0.22	32.11	32.16	30.15	28.28
23	2.125(0)	5(-1)	3.5(0)	135(0)	3.81	0.47	37.64	34.42	45.58	42.39
24	1(-1)	59(1)	2(-1)	30(-1)	1.79	0.02	25.2	21.31	27.78	24.5
25	3.25(1)	59(1)	5(1)	30(-1)	5.83	0.06	48	44.91	42.15	39.67
26	3.25(1)	32(0)	3.5(0)	135(0)	5.83	0.11	50.6	47.5	51.13	46.15

Table 4. 26 . Analysis of Variance for % 2,4-DR and %CODR

Parameter	% CODR	% 24DR
R^2 (coefficient of determination)	91.62	89.25
Standard deviation (S.D)	2.61	2.72
Coefficient of variation(C.V) %	8.60	8.66
Adequate precision(A.P)	38.85	32.04
Pure error	3.43	3.46
F-value	5.24	4.91

Note:CODR=COD removal, 2,4-DR=2,4-D removal
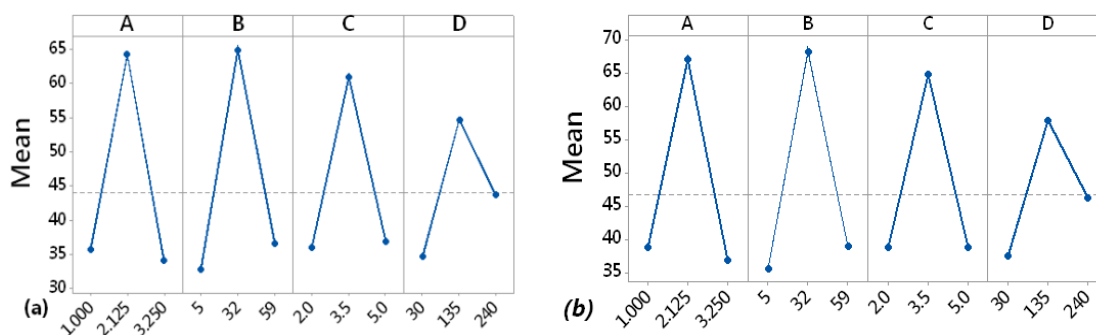
Figure. 4.20. Main effects plots for both responses a) % COD R b) % 2,4-DR

This was due to, excess amount of H_2O_2 inhibits •OH radical production (Masomboon et al. 2009; Zhang et al. 2006). The effect of Fe^{2+} on 2,4-D removal was studied (Figure.4.19(b)) and at   high iron dose of   0.22, 0.47 and 0.71 mM, less 2,4-D removal (<45%) was achieved. This may be due to the fact that, more number of Fe^{2+} ions are scavenged the already produced •OH radicals (Eq. 4.4) and also when iron dosage was at 0.71mM, sludge formation was observed by forming iron hydroxide complexes. Furthermore, if iron dosage decreased to 0.06-0.0.02 mM, only 26-48 % was observed. At a low iron dosage, there is less Fe^{2+} ions are available to react with oxidant and thereby forming •OOH radicals (oxidation potential>•OH radicals) (Masomboon et al. 2009). Hence the, removal efficiency of 2,4-D was gradually reduced. Furthermore, in case of run 1, 4, 9 and 13 with a Fe^{2+} dosage of 0.07mM, the significant increase of 75-90% was observed and hence it was finally considered. In case of run 6 and 15 with pH

2 and 5, the less 2,4-D removal was achieved even through Fe^{2+} dosage was 0.07 mM, this implies that the pH is contributing its influence on the removal efficiency.

Hence, to understand the effect of pH on the responses, it varied from 2-5 with 3.5 as a center value. It was observed that, when the pH is at 2 and 5, the lesser degradation of 26-48% was achieved (Table 4.25) and at pH 3.5 (runs 1, 4, 9 and 13) the higher removal was observed (>80%). At pH >3.5, may be the Fe^{2+} ions are deactivated by forming hydroxide complexes and thereby suppressing production of $^{\bullet}OH$ radicals (Lucas and Peres 2006). At lower pH (<3.5), may be the scavenging $^{\bullet}OH$ radicals by H^+ ions was observed (Martins et al. 2010). Hence, the optimum pH of 3.5 was maintained.

From the above two models (Eqs.4.15 and 4.16), the reaction time (D) is also influencing on responses and it was varied from 30-240 min. In case of run 1 at 30 min, the reaction was faster due to more $^{\bullet}OH$ radicals production and 76-81% of degradation was achieved. Furthermore, in case of runs 4, 9 and 13 with same experimental conditions (pH =3.5, Fe^{2+}=0.07mM, H_2O_2 =3.81mM), the reaction rate was slowly increased from 76-89%. This implies that, after 30 min the hydroperoxyl radicals were produced (Eqs. 4.6 and 4.7). However, in case of the runs (3, 5, 12, 14, 17, 22, 24, and 25) at 30 min, less removal of 26-47% was achieved. The kinetic studies were carried at optimum conditions (Fe^{2+} =0.07mM, H_2O_2 =3.81mM and pH =3.5) shown in Figure.4.19 (a) and it was observed that the removal rate was rapidly up to 45 min, then it slowly increased till 135 min and after that it was constant. The Figure.4.19(b) shows that, 98% decomposition of H_2O_2 was observed within 240 min (run 13) and 94% consumption of H_2O_2 at run 9. However, from 0-45 min 58% of Fe^{2+} was converted to Fe^{3+}, thereafter slowly the Fe^{2+} was regenerated. Finally, (Figure. 4.20(a) (b)) the optimum values are confirmed as 2.125, 32, 3.5, and 135 for A, B, C and D respectively. From the Table 4.25 and A-III-12(a) (b), it was concluded that the experimental and predicted values are distributed along the straight line, it implies that better results are achieved.

4.5.3 3D surface plots and contour plots

The surface plots were shown in A-III-13 and A-III-14. The Figures. A-III-13 (c), (e), (f) and A-III-14 (c), (e), (f) represents the sharp convex surface and   this implies that, the maximum removal of 2, 4-D was occurred   at exactly the center value of A, B and C. Hence, finally 2.125(A), 32 (B) and 3.5 (C) were considered. The A-III-13 (a) (b) (d) and A-III-14 (a) (b) (d) are showing saddle type and the highest removal was achieved at 240 min. However, in case of run 4 and 13, with similar A, B and C values, there is no significant difference in removal was observed and hence, 135 min was finally considered.

4.5.4. Degradation products (HPLC-MS analysis*)*

The degradation of 2,4-D was confirmed by LCMS analysis and it was found that slow release of chloride was observed with time shown in Figure.4.21. Before and after treatment 2,4-D was eluted at same retention time (1.58 min), however, a relatively small peak was observed at 240 min (after treatment). The 87% of 2,4-D was of mineralized to Maleic   acid, chloride, CO_2 and H_2O. This was confirmed with LCMS mass table (A-I-13) and   COD removal. The release of chloride ion was faster at initial stage of 20 mg/L (0-55 min), then it has increased up to 24.6 mg/L till 135 min and after that slowly reduced. The possible mineralization process was written as follows (Eq.4.17).

$$C_8H_6Cl_2O_3 + OH^\bullet \rightarrow Maleic\ acid + Cl^- + H_2O + CO_2 \qquad (4.17)$$
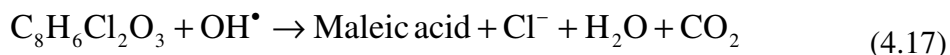
4.5.5 Contour overlay plot for validation

For validation contour plots were overlaid graphically in Figure.4.22**.** (Ahmad et al. 2005) and the boundary values were considered as Y_1 (21.75, 81.53) and Y_2 (22.3, 84.01) with H_2O_2/Fe^{2+} ratio of 32 and a reaction time of 135 min. The overlay plot is divided into 3 regions, which are separated by circular dotted lines**.** The shaded portion consists of two regions, in which the middle area is not feasible for both CODR and 2.4-DR

(NFRCD) and other region is feasible for only CODR(OFRC) (Y_1). The remaining unshaded area is the optimum region (suitable for both responses). The additional laboratory experiments (Run 27-30) that were conducted   suggested by overlay plot from the unshaded region (Table 4.27 and tagged in Figure. 4.22) and obtained results (S.D, C.V and A.P) are within prescribed standard limits.
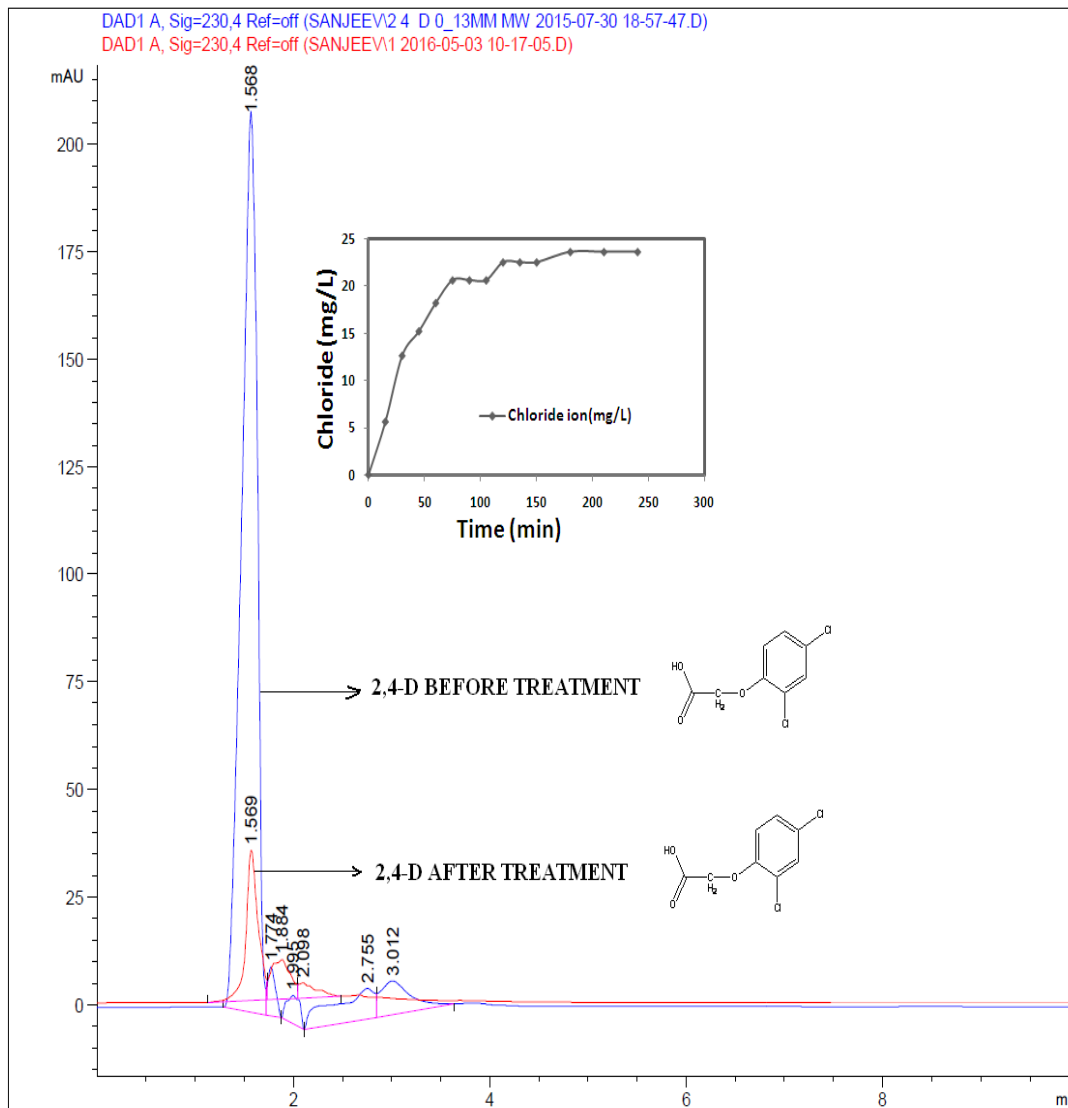
Figure.4.21 LCMS analysis of 2,4-D before and after treatment

Table 4.27. Optimization of additional experiments

Run	Independent Factors				% CODR[a]		% 24DR[b]		Error		S. D[c]		C.V [d]		A.P [e]	
	A	B	C	D	Ac[f]	Pr [g]	Ac[f]	Pr [g]	% CODR	% 24DR	% CODR	% 24DR	% CODR	% 24DR	% CODR	% 24DR
27	1.32	32	4.98	135	67.02	72.07	69.02	72.45	5.05	3.43	3.57	2.43	7.26	4.85	14.27	21.12
28	1.35	32	2.82	135	81.63	83.46	82.37	87.8	1.83	5.43	1.29	3.84	2.22	6.38	45.61	16.17
29	1.18	32	2.3	135	73.77	77.74	80.11	81.82	3.97	1.71	2.81	1.21	5.24	2.11	19.58	47.85
30	2.57	32	3.71	135	79.01	83.89	82.88	87.92	4.88	5.04	3.45	3.56	5.99	5.9	17.19	17.44

Note :[a] % CODR=% COD removal; [b] % 24DR= % 24D removal; [c] S.D=standard deviation ; [d]C.V= coefficient of variation ; [e] A.P= adequate precision ; [f] Ac=actual values; [g] Pr=predicted values

Similar way the effects of the different concentration (0.26 and 0.39 mM) of 2, 4-D on responses were studied(Table 4.28 and 4.29). The similar trend in the result was observed with optimum values 1.25, 21, 3.5 and 135 for A, B, C and D respectively.
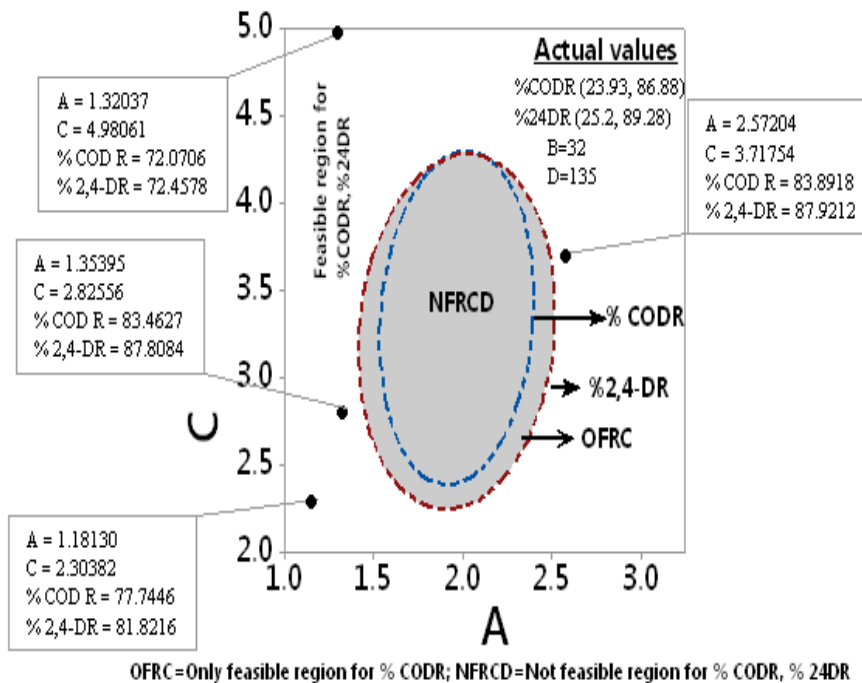
Figure.4.22. Contour overlay plot

Table 4.28. CCD Design Matrix (0.26mM)

Run	Independent variables (uncoded and coded)				Fenton's Reagent		Actual Responses(%)		Predicted Responses(%)	
	A (H$_2$O$_2$/COD)	B (H$_2$O$_2$/Fe^{2+})	C (P^H)	D (Time min)	H$_2$O$_2$ (mM)	Fe^{2+} (mM)	24D R	COD R	24D R	COD R
1	2.125(0)	32(0)	3.5(0)	30(-1)	8	0.15	77.29	73.75	81.03	77.08
2	2.125(0)	59(1)	3.5(0)	135(0)	8	0.08	63.71	57.5	56.81	53.05
3	3.25(1)	5(-1)	5(1)	30(-1)	12.24	1.5	29	31.25	36.02	38.56
4	2.125(0)	32(0)	3.5(0)	135(0)	8	0.15	88.22	82.5	78.16	74.18
5	3.25(1)	59(1)	2(-1)	30(-1)	12.24	0.13	27.6	23.75	28.37	25.5
6	2.125(0)	32(0)	2(-1)	135(0)	8	0.15	47.2	41.25	54.97	49.3
7	3.25(1)	59(1)	5(1)	240(1)	12.24	0.13	38.1	35	39.8	35.5
8	3.25(1)	5(-1)	5(1)	240(1)	12.24	1.5	32.5	30	27.65	26.41
9	2.125(0)	32(0)	3.5(0)	135(0)	8	0.15	84.24	80	78.16	74.18
10	1(-1)	59(1)	2(-1)	240(1)	3.76	0.04	64.31	58.75	55.43	50.64
11	1(-1)	32(0)	3.5(0)	135(0)	3.76	0.07	41	38.75	47.49	44.02
12	1(-1)	5(-1)	5(1)	30(-1)	3.76	0.46	30.6	28.75	22.45	20.85
13	2.125(0)	32(0)	3.5(0)	240(1)	8	0.15	82.65	77.5	90.96	85.55
14	1(-1)	59(1)	5(1)	30(-1)	3.76	0.04	30	25	35.91	31.2
15	2.125(0)	32(0)	5(1)	135(0)	8	0.15	50.3	47.5	54.58	50.83
16	3.25(1)	5(-1)	2(-1)	240(1)	12.24	1.5	44.9	40	37.14	33
17	3.25(1)	5(-1)	2(-1)	30(-1)	12.24	1.5	28	30	24.35	25.16
18	3.25(1)	59(1)	2(-1)	240(1)	12.24	0.13	32	26.25	38.99	32.1
19	1(-1)	5(-1)	2(-1)	240(1)	3.76	0.46	49.82	47.5	54.44	51.55
20	1(-1)	5(-1)	5(1)	240(1)	3.76	0.46	34.32	33.75	31.7	31.2
21	1(-1)	59(1)	5(1)	240(1)	3.76	0.04	40.5	37.5	42.99	40.3
22	1(-1)	5(-1)	2(-1)	30(-1)	3.76	0.46	27.6	22.5	24.04	21.2
23	2.125(0)	5(-1)	3.5(0)	135(0)	8	0.98	30.2	32.5	49.15	48.33
24	1(-1)	59(1)	2(-1)	30(-1)	3.76	0.04	23.5	20	27.2	21.55
25	3.25(1)	59(1)	5(1)	30(-1)	12.24	0.13	56.11	55	50.33	48.91
26	3.25(1)	32(0)	3.5(0)	135(0)	12.24	0.23	40.5	37.5	46.06	43.61

Note:CODR=COD removal, 2,4-DR=2,4-D removal

Table 4.29. CCD design matrix (0.39mM)

Run	Independent variables (uncoded and coded)				Fenton's Reagent		Actual Responses(%)		Predicted Responses(%)	
	A (H$_2$O$_2$/COD)	B (H$_2$O$_2$/Fe^{2+})	C (P^H)	D (Time min)	H$_2$O$_2$ (mM)	Fe^{2+} (mM)	24D R	COD R	24D R	COD R
1	2.125(0)	32(0)	3.5(0)	30(-1)	11.19	0.21	75.2	60.67	80.26	72.27
2	2.125(0)	59(1)	3.5(0)	135(0)	11.19	0.12	50.5	47.26	48.01	45.15
3	3.25(1)	5(-1)	5(1)	30(-1)	17.11	2.09	26.3	29.38	34.38	30.7
4	2.125(0)	32(0)	3.5(0)	135(0)	11.19	0.21	84.72	79.44	72.46	64.46
5	3.25(1)	59(1)	2(-1)	30(-1)	17.11	0.18	25.6	25.8	26.55	24.99
6	2.125(0)	32(0)	2(-1)	135(0)	11.19	0.21	45.6	44.58	52.34	45.66
7	3.25(1)	59(1)	5(1)	240(1)	17.11	0.18	38.6	31.17	38.92	32.78
8	3.25(1)	5(-1)	5(1)	240(1)	17.11	2.09	28.5	24.91	22.46	18.93
9	2.125(0)	32(0)	3.5(0)	135(0)	11.19	0.21	82.25	75.86	72.46	64.46
10	1(-1)	59(1)	2(-1)	240(1)	5.26	0.05	61.69	52.62	53.46	51.15
11	1(-1)	32(0)	3.5(0)	135(0)	5.26	0.1	38.5	31.17	42.4	34.63
12	1(-1)	5(-1)	5(1)	30(-1)	5.26	0.64	28.4	27.59	19.07	19.48
13	2.125(0)	32(0)	3.5(0)	240(1)	11.19	0.21	80.22	76.75	89.18	80.61
14	1(-1)	59(1)	5(1)	30(-1)	5.26	0.05	25.6	25.81	31.74	29.75
15	2.125(0)	32(0)	5(1)	135(0)	11.19	0.21	42.3	26.7	49.58	41.08
16	3.25(1)	5(-1)	2(-1)	240(1)	17.11	2.09	42.3	39.21	36.02	35.12
17	3.25(1)	5(-1)	2(-1)	30(-1)	17.11	2.09	30.2	24.02	24.64	21.85
18	3.25(1)	59(1)	2(-1)	240(1)	17.11	0.18	28	29.38	33.97	33.78
19	1(-1)	5(-1)	2(-1)	240(1)	5.26	0.64	59.06	57.98	63.26	60.54
20	1(-1)	5(-1)	5(1)	240(1)	5.26	0.64	30.6	26.7	29.5	27.36
21	1(-1)	59(1)	5(1)	240(1)	5.26	0.05	36	34.7	38.2	33.16
22	1(-1)	5(-1)	2(-1)	30(-1)	5.26	0.64	30	29.38	29.53	27.62
23	2.125(0)	5(-1)	3.5(0)	135(0)	11.19	1.37	26.2	23.12	42.7	40.69
24	1(-1)	59(1)	2(-1)	30(-1)	5.26	0.05	21.01	20.44	23.69	22.71
25	3.25(1)	59(1)	5(1)	30(-1)	17.11	0.18	62.36	55.3	54.8	49.02
26	3.25(1)	32(0)	3.5(0)	135(0)	17.11	0.33	30.2	19.55	40.31	31.55

Note:CODR=COD removal, 2,4-DR=2,4-D removal

4.6 DEGRADATION OF MIXTURE OF COMPOUNDS

The effect of a mixture of all the three compounds in Fenton's treatment process was studied. The initial concentration of three compounds (2,4-D=25mg/L, ametryn=3.5 mg/L and dicamba=94 mg/L) was considered, based on the characteristics of agriculture runoff water with similar levels of all four parameters(A, B, C and D) and responses(% ametryn(Y$_1$), COD(Y$_2$), dicamba(Y$_3$)and 2,4-D(Y$_4$) removal). The design matrix was shown in Table 4.30.

4.6.1 Central composite design and ANOVA results

The coefficient of determination, R^2 and R^2_{adj} values are found to be (84.62%, 82.66%)Y_1, (90.32%, 85.45%)Y_2, (88.31%, 82.62%)Y_3 and (94.26%, 88.11%)Y_4 respectively. Here, it is seen that the $R^2 \approx R^2_{adj}$, $R^2 > 80\%$, S.D (2.53 (Y_1), 2.23(Y_2), 2.55(Y_3), 1.96(Y_4))<3, C.V(6.45% (Y_1), 7.35%(Y_2), 7.21% (Y_3), 4.64% (Y_4))<10% and A.P(40.86 (Y_1), 106.78 (Y_2), 56.57 (Y_3), 47.23 (Y_4))>4, implies that obtained experimental results are better(Beg et al. 2003). To understand the variation in all 26 runs, residual plots were drawn against the all observations in A-III-15(a)(b)(c)(d) and it was observed that, points are randomly distributed along both positive and negative sides of the straight line.

4.6.2 Effects of independent variables on the responses (%AR, %2,4-DR, %DR and % CODR)

The ratio of H_2O_2/COD is varied as 1, 2.125 and 3.25 and it was found that maximum removal was observed at 2.125, by producing more number of $^\bullet$OH radicals. Further, H_2O_2/Fe^{2+} (B) were varied as 5, 25 and 50 and based on these ratios the dosage of iron (2.01-0.06 mM) and hydrogen peroxide(16.44-5.06 mM) were applied (Table 4.30). It is seen that, when the H_2O_2 dosage was increased from 10.75-16.44 mM or decreased from 10.75-5.06 mM, the removal efficiency decreased for all the four responses (Figure.4.23(a)). The excess amount of H_2O_2 inhibits •OH radical production (scavenging effect) (Zhang et al. 2006) and lower dose (5.06 mM) is not sufficient for the production of required •OH radicals.
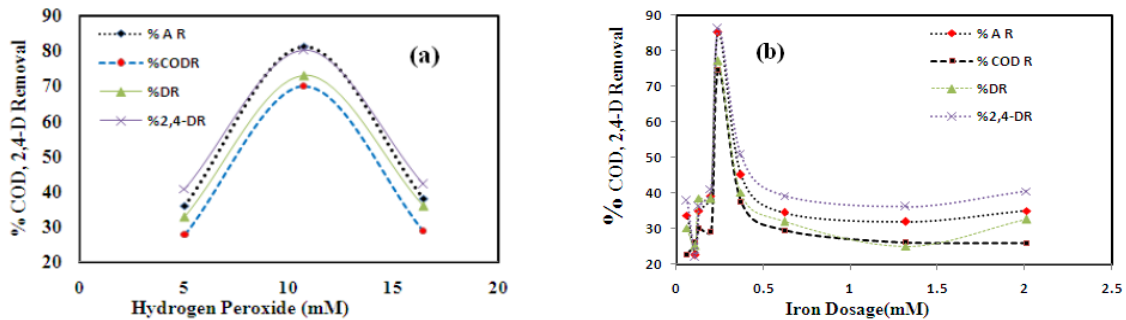
Figure. 4. 23 a) Effect of H_2O_2 on responses (Y_1, Y_2, Y_3, Y_4) b) Effect of Fe^{2+} on responses

Table 4.30: CCD design matrix for mixture of compounds (2,4-D_0=25mg/L, A_0=3.5 mg/L, D_0=94mg/L)

	Independent variables (uncoded and coded)				Fenton's Reagent		Actual Responses(%)				Predicted Responses(%)			
Run	A (H$_2$0$_2$/COD)	B (H$_2$0$_2$/Fe^{2+})	C (P^H)	D (Time min)	H$_2$O$_2$ (mM)	Fe^{2+} (mM)	A R	COD R	D R	24DR	A R	COD R	D R	24DR
1	2.125(0)	27.5(0)	3.5(0)	30(-1)	10.75	0.24	92.6	72.09	75.65	84.65	98.16	79.94	82.0	91.3
2	2.125(0)	50(1)	3.5(0)	135(0)	10.75	0.13	78.12	60	68.66	66.12	75.39	59.68	67.06	66.52
3	3.25(1)	5(-1)	5(1)	30(-1)	16.44	2.01	36.13	28.37	40.22	40.12	33.68	24.49	35.15	36.95
4	2.125(0)	27.5(0)	3.5(0)	135(0)	10.75	0.24	95.2	86.97	92.65	97.88	86.92	74.12	76.77	85.0
5	3.25(1)	50(1)	2(-1)	30(-1)	16.44	0.2	38.5	27.44	34.65	40.66	36.36	26.56	32.01	36.49
6	2.125(0)	27.5(0)	2(-1)	135(0)	10.75	0.24	60.2	55.34	55.2	68.65	72.63	65.26	64.75	77.98
7	3.25(1)	50(1)	5(1)	240(1)	16.44	0.2	40	25.58	42.45	45.6	42.44	30.03	43.29	44.6
8	3.25(1)	5(-1)	5(1)	240(1)	16.44	2.01	29.34	23.72	25.12	35.67	28.84	23.64	27.08	37.0
9	2.125(0)	27.5(0)	3.5(0)	135(0)	10.75	0.24	93.62	84.18	90.12	95.66	86.92	74.12	76.77	85.0
10	1(-1)	50(1)	2(-1)	240(1)	5.06	0.06	40.3	23.72	37.88	45.6	40.86	25.94	38.18	45.0
11	1(-1)	27.5(0)	3.5(0)	135(0)	5.06	0.11	50.2	40.46	45.66	58.54	50.95	42.42	46.14	57.94
12	1(-1)	5(-1)	5(1)	30(-1)	5.06	0.62	28.6	19.06	26.7	36.7	29.6	22.86	28.61	37.12
13	2.125(0)	27.5(0)	3.5(0)	240(1)	10.75	0.24	97.3	82.32	87.17	94.55	100.0	82.11	86.57	95.75
14	1(-1)	50(1)	5(1)	30(-1)	5.06	0.06	25.5	21.86	24.12	30.66	27.65	21.34	24.46	31.48
15	2.125(0)	27.5(0)	5(1)	135(0)	10.75	0.24	72.84	66.51	62.33	75.12	59.13	64.23	62.53	73.64
16	3.25(1)	5(-1)	2(-1)	240(1)	16.44	2.01	36.12	27.44	32.12	45.6	32.08	26.3	27.01	41.01
17	3.25(1)	5(-1)	2(-1)	30(-1)	16.44	2.01	38.5	24.65	33.15	40.67	37.95	24.83	33.51	41.11
18	3.25(1)	50(1)	2(-1)	240(1)	16.44	0.2	42.3	30.23	37.88	46.12	41.01	26.17	38.3	47.51
19	1(-1)	5(-1)	2(-1)	240(1)	5.06	0.62	37.8	35.81	32.12	40.12	36.95	35.84	34.47	40.62
20	1(-1)	5(-1)	5(1)	240(1)	5.06	0.62	29.3	28.37	25.6	34.6	29.56	27.59	23.47	35.0
21	1(-1)	50(1)	5(1)	240(1)	5.06	0.06	37.88	24.65	30.12	39.12	38.13	24.21	32.1	40.49
22	1(-1)	5(-1)	2(-1)	30(-1)	5.06	0.62	42.34	34.88	43.66	45.66	38.02	28.78	38.05	42.88
23	2.125(0)	5(-1)	3.5(0)	135(0)	10.75	1.32	60.45	52.55	52.15	58.65	51.9	50.51	53.49	56.09
24	1(-1)	50(1)	2(-1)	30(-1)	5.06	0.06	31.2	20.93	28.6	35.66	31.4	20.75	28.98	36.14
25	3.25(1)	50(1)	5(1)	30(-1)	16.44	0.2	36.2	33.02	38.6	32.12	36.76	32.74	38.58	33.43
26	3.25(1)	27.5(0)	3.5(0)	135(0)	16.44	0.37	45.11	37.67	40.2	50.66	53.07	43.35	49.47	49.11

Table 4. 31 . Analysis of Variance for all responses

Parameter	%AR	% CODR	%DR	% 24DR
R^2(oefficient of determination)	84.62	90.32	88.31	94.26
Standard deviation (S.D)	2.53	2.23	2.55	1.96
Coefficient of variation(CV) %	6.45	7.35	7.21	4.64
Adequate precision (AP)	40.86	106.7	56.57	47.23

Note:CODR=COD removal, AR=ametryn removal,DR=dicamba removal, 2,4-DR=2,4-D removal
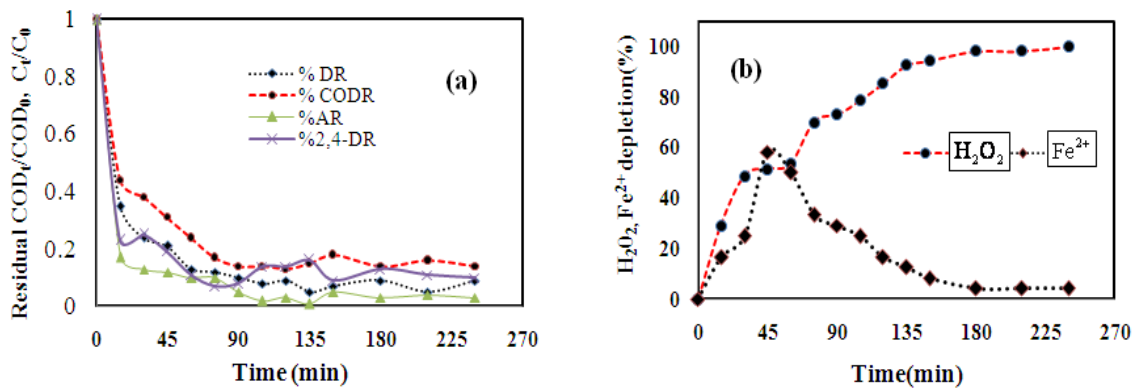
Figure. 4.24 a) Residual COD_t/COD_0 and C_t/C_0 (for 2,4-D, ametryn, and dicamba) with reaction time b)% H_2O_2 and Fe^{2+} depletion with time. H_2O_2=10.75mM; Fe^{2+}=0.24mM; COD_0=172mg/L, 2,4-D_0=25mg/L, A_0=3.5 mg/L, D_0=94mg/L, pH =3.5
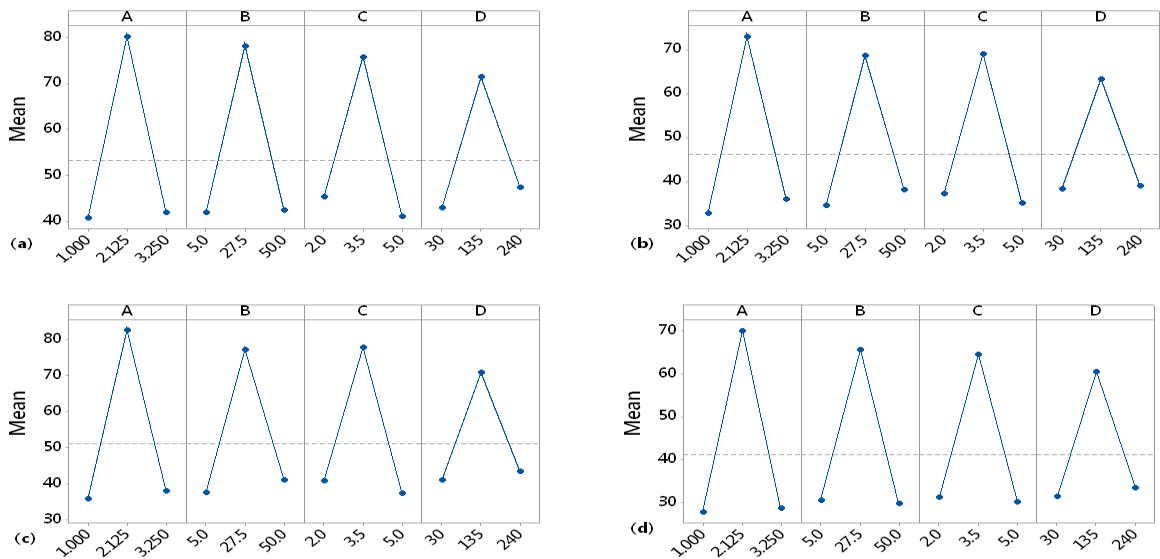
Figure. 4.25. Main effects plots a) % A R b)% CODR c)%DR d)%2,4-DR

To study the effect of Fe^{2+} on all responses, the dosage of iron was varied from 2.01-0.06 mM shown in Figure.4.23 (b). At   high iron dose (greater than 0.24mM), less removal was achieved and this may be due to excess iron scavenged the already produced $^{\bullet}OH$ radicals by producing excess sludge as iron hydroxide complexes. Furthermore, if iron dosage was <0.24mM,   the removal efficiency was decreased in all responses (<60%). At this stage there is formation of $^{\bullet}OOH$ radicals (oxidation potential<$^{\bullet}OH$ radicals). Hence, 0.24mM of iron was finally considered (Run 1, 4, 9 and 13). The effect of pH was also studied (2-5) and it was observed that, when the pH is at < or > 3.5, lesser degradation was observed. At pH >3.5, may be the formation of ferric hydroxide complexes (Lucas and Peres 2006) and at lower pH (<3.5), may be the scavenging $^{\bullet}OH$ radicals by H^{+} ions was observed (Eq. 4.5). Hence, the optimum pH of 3.5 was maintained.

The effect of reaction time (D) on responses was studied (30-240 min). In case of runs 1, 4, 9 and 13, it was observed that the degradation was fast at the initial 30 min and thereafter slowly progressed. In case of the runs (3, 5, 12, 14, 17, 22, 24, and 25) at 30 min, relatively lesser removal was observed and it clearly indicates that the factors A, B and C are also influencing on the responses. The kinetic studies were carried at optimum Fenton's dosage (Figure.4.24 (a)) and it was observed that the removal rate was rapid upto 90 min and after that, it is decreased. The H_2O_2 and Fe^{2+} depletion were also monitored (Figure.4.24(b)) and it was observed that 100 decomposition of H_2O_2 was achieved in 240 min and 60% of Fe^{2+} (0-60 min) was converted to Fe^{3+}, thereafter it is vice-versa. Finally, from the Figure 4.25(a) (b) (c), (d) the optimum values are confirmed (A=2.125, B=27.5, C=3.5 and D= 135). From the A-III-16 (a), (b), (c), (d), it was concluded that the experimental and predicted values are similar to each other.

CHAPTER 5

ADVANCE FENTON PROCESS

5.1 GENERAL

This chapter deals with advance Fenton's process (AFP) for the treatment of herbicides (ametryn, 2,4-D and dicamba) in aqueous medium . The laterite is used as a source of iron (precursor) rather than iron sulfate for the synthesis of FeNPs by using sustainable leaf extracts such as TG (Tactona Grandis) and EG (Eucalyptus Globulus). The synthesized FeNPs were applied as a Fenton catalyst and operating variables were optimized by using response surface methodology. The results are interpreted with ANOVA (analysis of variance), coefficient of determination (R^2), Fisher's test (F-test) along with the 2nd order polynomial equation.

5.2 TREATMENT OF AMETRYN

5.2.1 Total phenolic content and antioxidant property (AP) of EG leaves

The antioxidant property and the total phenollic content of the EG leaves were determined by FRAP (Ferric reducing antioxidant power) (Pulido et al., 2000) and standard methods (ISO, 2005) respectively. To optimize the antioxidant power on the different quantity of leaves (15-80g/L), the experiments were conducted in an Erlenmeyer flask (at 80 ^{0}C) and at every 15 min, the samples AP was determined (Figure.5.1a). The more quantity of leaves (80 g/L) possessed higher antioxidant property and also no significant difference between 60 and 80 g/L was observed and hence 60 g/L was finally selected. After 80 min, the antioxidant power was slowly reduced and it signifies that the better results were obtained at 80 min. Total phenolic content was also calculated for different quantities of leaves with the contact time of 80 min, which is shown in Figure.5.1b. It was found that highest phenolic content of 5 mM of gallic acid was extracted at 60g/L of EG leaves and this may be due to the wider dispersion of polyphenols.
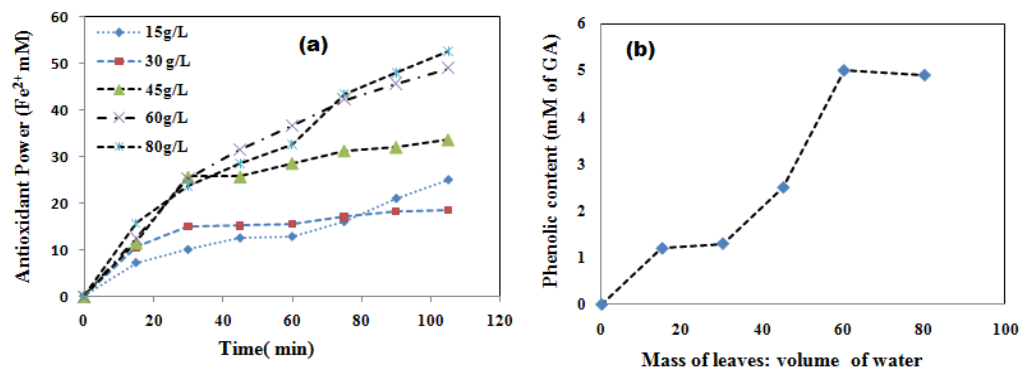
Figure.5.1 a) Antioxidant Power of different quantity (15-80g/L) of leaves b)Phenolic content vs mass of leaves :volume of water

5.2.2. Characterization of FeNPs

According to the BET analysis, it is seen that surface area and pore volume of   RLPs (Raw laterite particles) are 23.18 m^2/g, 0.0091 cm^3/g and for LGFeNPs (Laterite green iron nanopartilces) 36.62 m^2/g, 0.0394cm^3/g respectively. With these results, it can be concluded that LGFeNPs shows higher surface area and pore volume than RLPs. This may be due to the polyphenols that are present in the eucalyptus leaves, which acts as both reducing agent and capping agent**.** Figure.5.2 (a)(b) shows the FESEM images RLPs and LGFeNPs respectively and it is observed that, there is a formation of spherical iron nanoparticles of size 20-70 nm (Figure.5.2(b)).

The EDX analysis of RLPs (Figure. 5.3a) shows the peaks of C(19.38%), O(45.33%), Si (11.16%), Al(6.54%), Fe(16.47%) and along with a   small trace of Ti (1.12%). This proves that, there is existence of major portions of Fe$_2$O$_3$, Al$_2$O$_3$ and SiO$_2$. The Figure 5.3(b) shows the EDX spectrum of LGFeNPs with peaks of C (29.31%), O (22.3%) and Fe (48.39%). The C element is mainly from the polyphenol content in the leaves and there is no Si, Al and Ti present in LGFeNPs and this implies   that, 100% iron was extracted from laterite. Figure.5.4 (a) shows the XRD pattern of RLPs, where the peaks at 2θ=19.23 , 62.34 corresponds to the SiO$_2,$ and peaks at 2θ=25.29, 67.82 represents Fe$_2$O$_3.$ The other peaks at 36.35, 64.21, 72.85 are due to the Al$_2$O$_3$ and the peak at 34.66 is FeO (ICDD database).
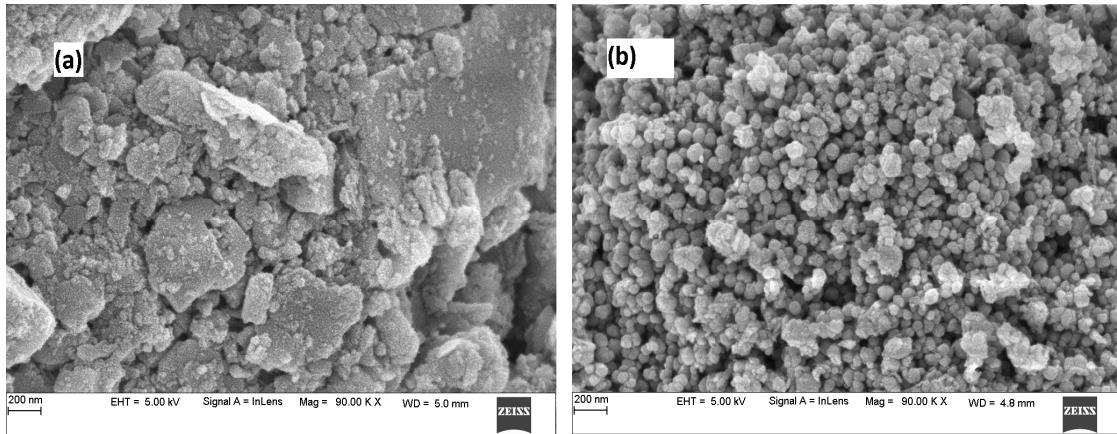
Figure.5.2 FESEM images of   a) Raw laterite particles b) Laterite green iron NPs
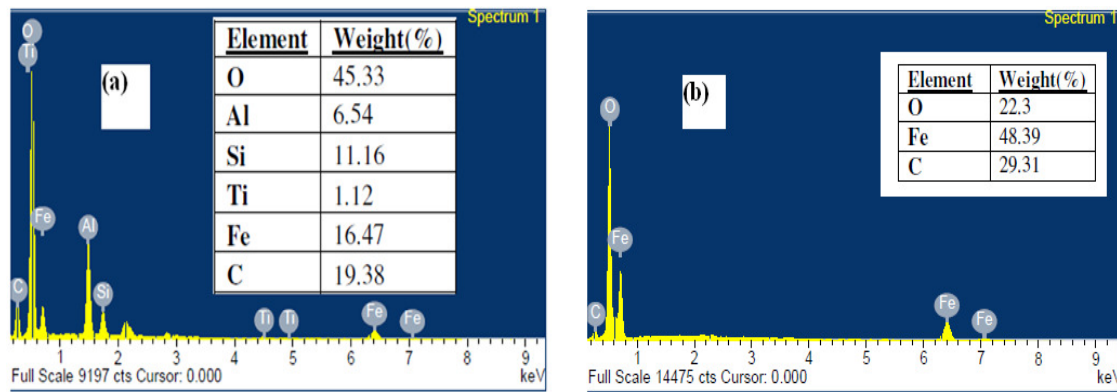
Figure. 5.3. EDS spectra of a) Raw laterite particles b) Laterite green iron NPs
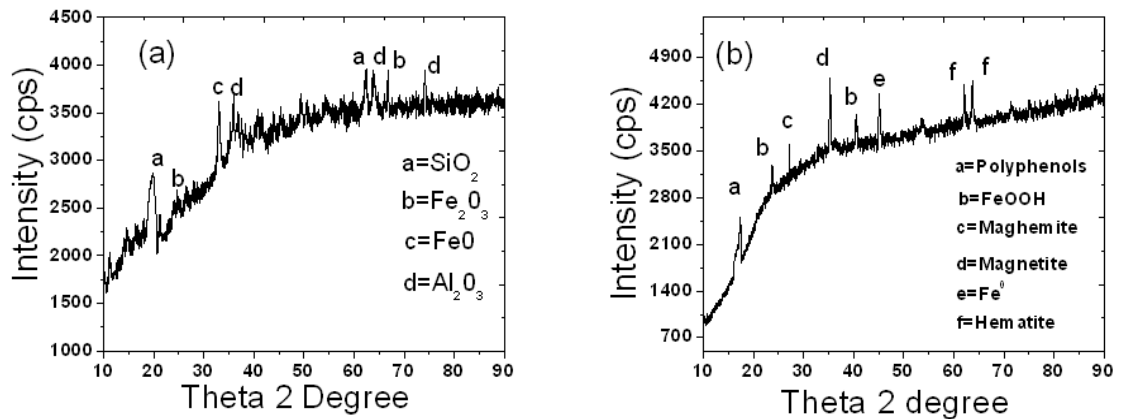
Figure.5.4. XRD patterns a) Raw laterite particles b) Laterite green iron NPs
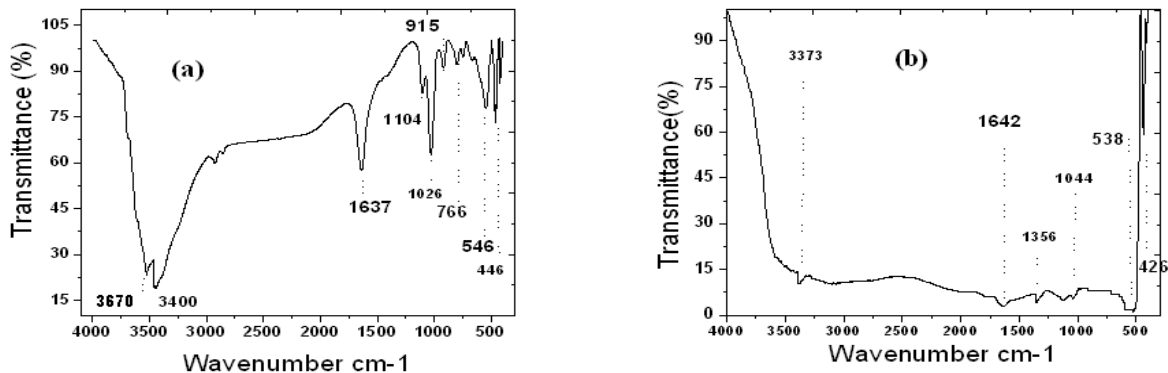
Figure.5.5 FTIR spectra of a) Raw laterite particles b) Laterite green iron NPs

Whereas the Figure. 5.4 (b) shows the XRD pattern of LGFeNPs in which, the peaks at 17.88, 27.21, 34 and 45.25 corresponds to the polyphenols (Njagi et al., 2011), meghemite (γ-Fe_2O_3), magnetite (Fe_3O_4) and zero valent iron (Fe^0) respectively. The peaks at 24.21, 38.53 represent the iron hydroxides and the peaks at 62.81, 63.59 represent the hematite (Fe_2O_3) respectively(Shahwan et al. 2011, Hoag et al. 2009, Khataee and Pakdehi 2014).

In FTIR analysis (Figure.5.5 (a)), the existence of Al-O-H is near to 3670 cm^{-1} and transmittance band between 3680 -3400 cm^{-1} were the OH group of Si, Al and Fe. The presence of H-O-H on the surface of laterite is near to 1637 cm^{-1} and strong stretching at 1026 cm^{-1} represents the Si-O. The 915, 766, 546 and 446 cm^{-1} indicate the presence of Al-OH, cristobalite, Fe_2O_3 and Fe-O respectively (Maiti et al. 2010). Figure. 5.5 (b) represents the FTIR spectra of LGFeNPs, in which the wave numbers 3373, 1642, 1356,1044, 538 and 426 cm^{-1} represents the presence of OH, C=C (polyphenols), C-N(aromatic amines), C-N (aliphatic amines), Fe-O(Fe_3O_4) and Fe-O (Fe_2O_3) (Kumar et al. 2013) respectively. The bands at 538 and 426 cm^{-1} confirms the formation of LGFeNPs and later these particles were oxidized to form iron oxides.

5.2.3. Preliminary experiments

Preliminary experiments were conducted to know the suitable range of variables (H_2O_2 /COD=1-3.25, H_2O_2/Fe=0-10, pH=1.5-9) and for the maximum removal efficiency of

90

>90% (both responses) was observed (Figure. 5.6(a)(b)(c)) at a value of 6, 2.125 and 3.5 respectively.
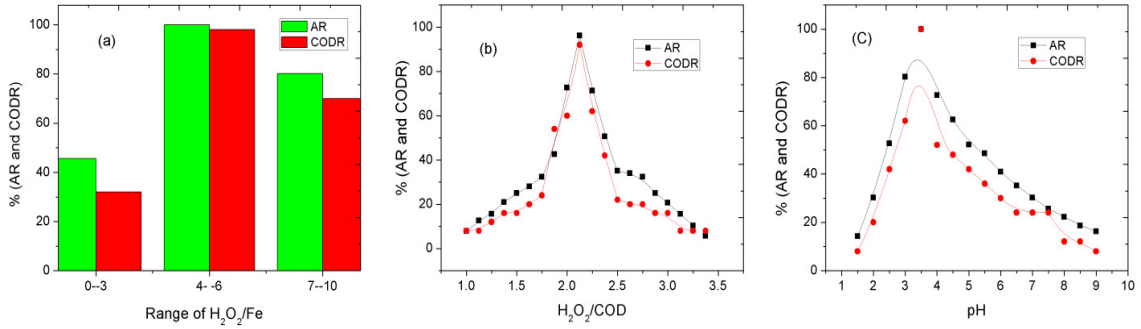
Figure.5.6 (a) Range of H_2O_2/Fe vs. responses; ametryn$_0$=0.02mM, reaction time (min)=30-240, H_2O_2 /COD=1-3.25; pH=2-5 **b)** H_2O_2 /COD vs. responses; reaction time(min)=135 , pH=3.5, H_2O_2/Fe=6 **c)** pH vs responses; reaction time(min)=135, H_2O_2/Fe=6, H_2O_2 /COD=2.125.

5.2.4 Degradation studies and statistical analysis

The degradation studies were performed according to the design matrix with four levels (Table. 5.1 and 5.2) and second order quadratic equations for both the responses % COD removal efficiency (% CODR) and % ametryn removal efficiency (%AR) were obtained (Eqs. 5.1 and 5.2).

% CODR (Y_1) = 70.34 - 0.67 A + 8.44 B +2.44 C + 0.44 D – 40.5 A*A – 10.5 B*B – 28.5 C*C+ 29.5 D*D - 1.25 A*B + 0.25 A*C -0.75 A*D - 0.75 B*C – 0.75 B*D+ 0.75 C*D   (5.1)

% AR (Y_2) = 73.75 + 0.36 A +11.82 B +2.47 C + 0.23 D – 40.23 A*A - 11.34 B*B – 24.36 C*C + 26.18 D*D – 0.4 A*B + 1.12 A*C - 0.76 A*D + 0.64 B*C + 0.51 B*D + 0.53 C*D   (5.2)

In equations, the intercept values and coefficients of B, C, D, D*D, A*C, C*D are showing a positive effect. Also in Eq 5.2 B*C and B*D are having a positive effect on the response. The coefficient of D^2 has the highest positive values of 29.5 and 26.18, it implies that the reaction time is the influencing parameter on both the responses. According to the ANOVA results (Table 5.3 and A-II-4), the most significant factors

are B, A^2, C^2, D^2 and A^2, C^2, D^2 for Y_2 and Y_1 respectively, with the P value< 0.05. The F values were observed to be 5.34 and 4.34 for Y_2 and Y_1 respectively and values are greater than tabular $F_{0.05\,(14,\,11)}$ value (2.74). The R^2 and R^2_{adj} values were found to be 92.34%, 95.46% and 91.36%, 92.3% for Y_2 and Y_1 respectively and are close to each other($R^2 > 80\%$ and $R^2_{adj} < R^2$). The lack of fit and the residual error are showing the similar values 2576.3 and 3099.7 with pure error zero for both ametryn and COD removal respectively. The S.D values are very less and are 2.21 and 2.26 for Y_2 and Y_1 respectively. The C.V values are 9.66 (Y_2), 8.62 (Y_1), which are less than 10% (Beg et al. 2003) and A.P values are 18.03 (Y_2), 17.17 (Y_1) and the desired value is 4 or > 4 (Zinatizadeh et al. 2006). All these results confirm the good agreement between the predicted and experimental values. The normal probability distribution of data points is plotted against the residuals in A-III-17 and the points are distributed near the straight line.

5.2.5. Effect of H_2O_2 and Fe on the responses

The effect of H_2O_2 on the removal efficiency was studied based on the H_2O_2/COD ratio (1, 2.125 and 3.25). It was observed that, as the ratio is decreased to 1 or increased to 3.25 from a center value of 2.125, less removal was observed. It indicates that, the more number of hydroxyl radicals are produced in the ratio of 2.125. Based on this, the dosage of H_2O_2 was varied from 8-26mg/L (Table 5.2). According to Pignatello (1992) increase in H_2O_2, increases the degradation of pollutants. However, when H_2O_2 dosage was 26mg/L, the removal efficiency (both Y_2 and Y_1) was <45% by decreasing •OH radical production (Eq.5.3). In addition, when the dosage of H_2O_2 was 8mg/L, the removal efficiency was <43%, because of insufficient H_2O_2 for •OH radical production. Hence, 17 mg/L of H_2O_2 with H_2O_2/COD ratio of 2.125 was finally considered, in which 100% removal was observed (Figure.5.7 (a)).

$$H_2O_2 + {}^\bullet OH \rightarrow H_2O + OOH^\bullet \qquad\qquad (5.3)$$

Table 5.1. Levels of the parameters studied in the CCD

Factor	Name	Low(-1)	Middle(0)	High(+1)
A(X_1)	H_2O_2/COD	1	2.125	3.25
B(X_2)	H_2O_2/Fe	2	6	10
C(X_3)	P^H	2	3.5	5
D(X_4)	Time (min)	30	135	240

The selection of iron dosage depends on the suitable values of H_2O_2/Fe ratio (2, 6 and 10). Based on this, the effect of iron (0.8-13 mg/L) was studied in the degradation process. At high iron doses of 13, 8.5 4.33 and 4 mg/L the less ametryn removal (<45%) was achieved and this may be due to the agglomeration of LGFeNPs (Garrido-Ramírez et al. 2010) and more number of Fe^{2+} ions scavenged the already produced $^•OH$ radicals shown in Eq 5.4 (Pignatello, 1992). Furthermore, when iron dose was <2.83 mg/L, there is a less production of Fe^{2+} ions (a reaction between Fe^0 and oxidant). After that, the H_2O_2 was going to react with already produced $^•OH$ radicals to form a $^•OOH$ radical (Eq. 5.5 and 5.6) and the formed $^•OOH$ radicals were having less oxidation capacity than $^•OH$ radicals (Masomboon et al. 2009). Hence, the optimum iron dose of 2.83mg/L (H_2O_2/Fe=6) was adopted in AFP (Figure. 5.7(b)).

$$Fe^{2+} + {}^•OH \rightarrow Fe^{3+} + OH^- \tag{5.4}$$

$$H_2O_2 + Fe^0 \rightarrow 2OH^- + Fe^{2+} \tag{5.5}$$

$$H_2O_2 + {}^•OH \rightarrow H_2O + OOH^• \tag{5.6}$$

5.2.6. Effect of pH on the responses

The heterogeneous (laterite) and homogeneous ($FeSO_4.7H_2O$, $FeCl_3$) Fenton processes were influenced by the pH and in the present study the pH varied from 2-5. In case of run 6 (pH 2, %AR and %CODR<36) and run 15 (pH 5, %AR and %CODR<46), the less ametryn removal was achieved even with optimum iron (2.83 mg/L) and H_2O_2 (17 mg/L).

Table 5.2. CCD Design Matrix

Run	Independent variables (uncoded and coded)				Fenton's Reagent		Actual Responses (%)		Predicted Responses(%)	
	A (H_2O_2/COD)	B (H_2O_2/Fe)	C (P^H)	D (Time min)	H_2O_2 (mg/L)	Fe (mg/L)	A R	COD R	A R	COD R
1	2.125(0)	6(0)	3.5(0)	30(-1)	17	2.83	82.35	80	79.639	77.82
2	2.125(0)	10(1)	3.5(0)	135(0)	17	1.7	65	56	64.22	68.33
3	3.25(1)	2(-1)	5(1)	30(-1)	26	13	25.6	24	20.37	20.12
4	2.125(0)	6(0)	3.5(0)	135(0)	17	2.83	100	100	97.21	96.21
5	3.25(1)	10(1)	2(-1)	30(-1)	26	2.6	42.23	36	40.21	26.9
6	2.125(0)	6(0)	2(-1)	135(0)	17	2.83	35.62	28	36.86	28.24
7	3.25(1)	10(1)	5(1)	240(1)	26	2.6	46.23	32	40.5	28.68
8	3.25(1)	2(-1)	5(1)	240(1)	26	13	12.31	16	15.34	17.29
9	2.125(0)	6(0)	3.5(0)	135(0)	17	2.83	100	100	97.21	96.21
10	1(-1)	10(1)	2(-1)	240(1)	8	0.8	35.21	28	34.8	29.12
11	1(-1)	6(0)	3.5(0)	135(0)	8	1.33	28.32	24	33.15	30.55
12	1(-1)	2(-1)	5(1)	30(-1)	8	4	8.31	8	11.09	11.73
13	2.125(0)	6(0)	3.5(0)	240(1)	17	2.83	100	100	100	100
14	1(-1)	10(1)	5(1)	30(-1)	8	0.8	43.62	40	35.8	38.21
15	2.125(0)	6(0)	5(1)	135(0)	17	2.83	45.62	36	48.12	40.12
16	3.25(1)	2(-1)	2(-1)	240(1)	26	13	10.21	8	8.39	8.9
17	3.25(1)	2(-1)	2(-1)	30(-1)	26	13	9.61	8	11.52	9.51
18	3.25(1)	10(1)	2(-1)	240(1)	26	2.6	28.52	24	30.98	23.29
19	1(-1)	2(-1)	2(-1)	240(1)	8	4	12.21	12	10.61	9.73
20	1(-1)	2(-1)	5(1)	240(1)	8	4	12.56	16	13.09	17.12
21	1(-1)	10(1)	5(1)	240(1)	8	0.8	36.52	32	39.86	33.51
22	1(-1)	2(-1)	2(-1)	30(-1)	8	4	14.62	12	10.71	7.34
23	2.125(0)	2(-1)	3.5(0)	135(0)	17	8.5	42.31	44	50.58	46.12
24	1(-1)	10(1)	2(-1)	30(-1)	8	0.8	30.62	28	32.84	29.73
25	3.25(1)	10(1)	5(1)	30(-1)	26	2.6	32.62	24	39.47	29.29
26	3.25(1)	6(0)	3.5(0)	135(0)	26	4.33	21.21	16	25.12	20.12

Note:CODR=COD removal, AR=ametryn removal.

Table 5.3 Analysis of Variance for % AR and %CODR

Parameter	% CODR	% AR
R^2 (coefficient of determination)	95.4%	92.34
Standard deviation (S.D)	2.26	2.21
Coefficient of variation(CV) %	8.62	9.66
Adequate precision(AP)	17.17	18.03
Pure error	0.8	1.6
F-value	4.34	5.34

Note:CODR=COD removal, AR=ametryn removal.
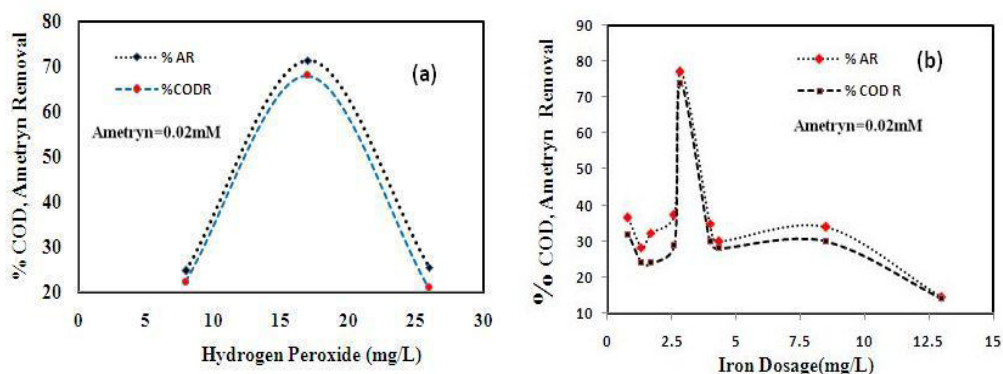
Figure. 5.7 . Removal efficiency vs a) dosage of H_2O_2 b) dosage of iron

It signifies that, relative increase (10%) in the ametryn removal was achieved at pH 5 than pH 2. Similar kind of results were observed in the literatures related to the heterogeneous Fenton process, for removal of many of the contaminants such as 17β-estradiol (α-FeOOH coated resin vs H_2O_2) with the removal efficiencies of 98.2% at pH 3.07 and 86.4% at pH 7.47 (Yaping and Jiangyong 2008), salicylic acid (H_2O_2 vs. goethite) with the removal efficiency from 95%-45% (pH 6- 11). In addition, few homogeneous Fenton degradation studies were reported that, the removal efficiency was maximum at pH 3 and negligible (<5%) at pH 7 (Zhou et al. 2004; Neppolian et al. 2004). This clearly indicates that, the heterogeneous Fenton process has relatively more advantage towards alkaline pH than acidic pH and this mainly depends on the surface characteristics and leaching potential of LGFeNPs. The heterogeneous Fenton process proceeds with adsorption of ametryn on to the surface of the iron oxides, iron

hydroxides and Fe^0 (XRD analysis of LGFeNPs) followed by production of the $^\bullet OH$ radicals and these radicals reacts with ametryn to form mineralization products. As discussed earlier, at pH 2 less ametryn removal was observed and this may be due to the leaching of iron from iron oxide and hydroxide surfaces. This dissolved iron forms oxyhydroxides, which are more stable with lesser catalytic activity. Similar kind of reaction mechanism was observed, when the heterogeneous process (dissolved iron, 86.4% removal E2 at pH 7.47) and homogeneous Fenton processes (Fe^{3+}, 46.3% removal E2 at pH 7.47) were compared (Yaping and Jiangyong 2008). Chou et al., 2001 also reported that, at pH <4 more leaching of iron was observed from the FeOOH. On the other hand, at pH 5, maybe it favors the adsorption of ametryn onto the surface of iron particles and after that, deactivation of Fe^{2+} ions by forming ferric hydroxide complexes, which reduces the generation of $^\bullet OH$ radicals(Lucas and Peres 2006) and stops further reactions. Finally from the Table 5.2, it was observed that at pH 3.5 (4, 9 and 13), 100 % removal (both responses) was achieved and may be at this stage (pH=3.5), no leaching of iron was observed and fully recycling of iron occurred directly on to the catalyst surface. Hence, the optimum pH of 3.5 was maintained in the treatment process.

The reaction time (D) was varied from 30-240 min and in case of run 1 at 30 min (pH =3.5, Fe=2.83mg/l, H_2O_2 =17mg/L), the reaction was faster and 83% of removal was achieved. With similar experimental conditions, the reaction process was continued (runs 4, 9 and 13) and it was observed that, 100% removal was achieved in 135 min. The possible degradation pathway consists of adsorption, generation of OH radicals and mineralization processes.

5.2.7 Effect of reaction time on the responses

The XRD analysis report shows that, there is existence of Fe_2O_3, Fe_3O_4 and Fe^0. At the initial stages (30 min), the ametryn adsorbs on the surface of the LGFeNPs and later the oxidant (H_2O_2) reacts with Fe^0 and converts to Fe^{2+} and also in parallel, the conversion of Fe^{2+}/ Fe^{3+} from Fe_2O_3/ Fe_3O_4 was observed by reacting with H^+ ions (optimum pH of the solution is 3.5). After that, the hydroxyl radicals were produced (the reaction between

oxidant and Fe^{2+}) (Eqs.5.7-5.10) (Xue et al. 2009; Garrido-Ramírez et al. 2010; Kuang et al. 2013). These OH radicals attack ametryn on the LGFeNPs surface and mineralize the process (CO_2, H_2O and mineral acids) (Eqs. 5.11-5.12). This was confirmed with an overlaid chromatograph (Figure.5.8), which indicates that, there are no peaks observed after the Fenton treatment process. After 30 min, the reaction was slowly reduced and this may be due to the production of hydroperoxyl radicals ($HO_2{}^{\bullet}$) (Eqs. 5.13-5.14) (Rusevova et al. 2012). However, in case of the runs (3, 5, 12, 14, 17, 22, 24, and 25) at 30 min, less removal (8-46%) was achieved, which indicates that the efficiency also depends on the dosage of iron, oxidant and pH.

$$\text{Ametryn} + \text{GLFeNPs} \rightarrow \text{Ametryn/GL FeNPs} \tag{5.7}$$

$$H_2O_2 + Fe^0 \rightarrow 2OH^- + Fe^{2+} \tag{5.8}$$

$$Fe_2O_3/Fe_3O_4 + H^+ \rightarrow Fe^{2+}/Fe^{3+} + H_2O \tag{5.9}$$

$$H_2O_2 + Fe^{2+} \rightarrow {}^{\bullet}OH + OH^- + Fe^{3+} \tag{5.10}$$

$$\text{Ametryn/GL FeNPs} + OH^{\bullet} \rightarrow \text{Intermedia tes/GL FeNPs} \tag{5.11}$$

$$\text{Intermedia tes/GLFeNP s} + OH^{\bullet} \rightarrow CO_2 + H_2O + \text{mineral acids} \tag{5.12}$$

$$H_2O_2 + Fe^{3+} \rightarrow H^+ + FeOOH^{2+} \tag{5.13}$$

$$FeOOH^{2+} \rightarrow HO_2{}^{\bullet} + Fe^{2+} \tag{5.14}$$
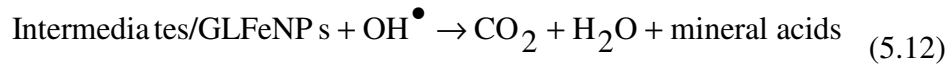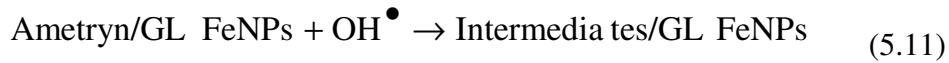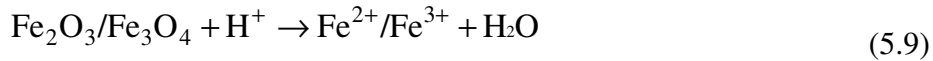
To understand the reaction kinetics involved in the whole treatment process, the experiments were conducted in optimal conditions (Fe=2. 83 mg/L, H_2O_2 =17 mg/L and pH =3.5) and obtained results were plotted in Figure.5.9 (a)(b) (ln C_t/C_0 and $1/C_t$ vs time as 1st order and 2nd order kinetics). It was clear that, the linear relationship was established with R^2 (correlation coefficient) value of >0.9 for 1st order kinetics and hence, the experimental data was best fit with the pseudo-first order kinetic model (Eqs.5.15-5.16).

$$\ln C_t/C_0 = -K_1 t \tag{5.15}$$

$$1/C_t = 1/C_0 + K_2 t \tag{5.16}$$

where C_t and C_0 concentration at time t and 0 min. The K_1 and K_2 are considered to be 1st order and 2nd order rate constants in min^{-1}. From the Figure.5.9 (a), it was clear that

the rate of reaction of % COD removal efficiency (0.024 min^{-1}) was less than the % ametryn removal efficiency (0.033 min^{-1}). This may be due to the fact that, the conversion from ametryn to the intermediates is faster than the intermediates to the mineralization (CO_2, H_2O and mineral acids).
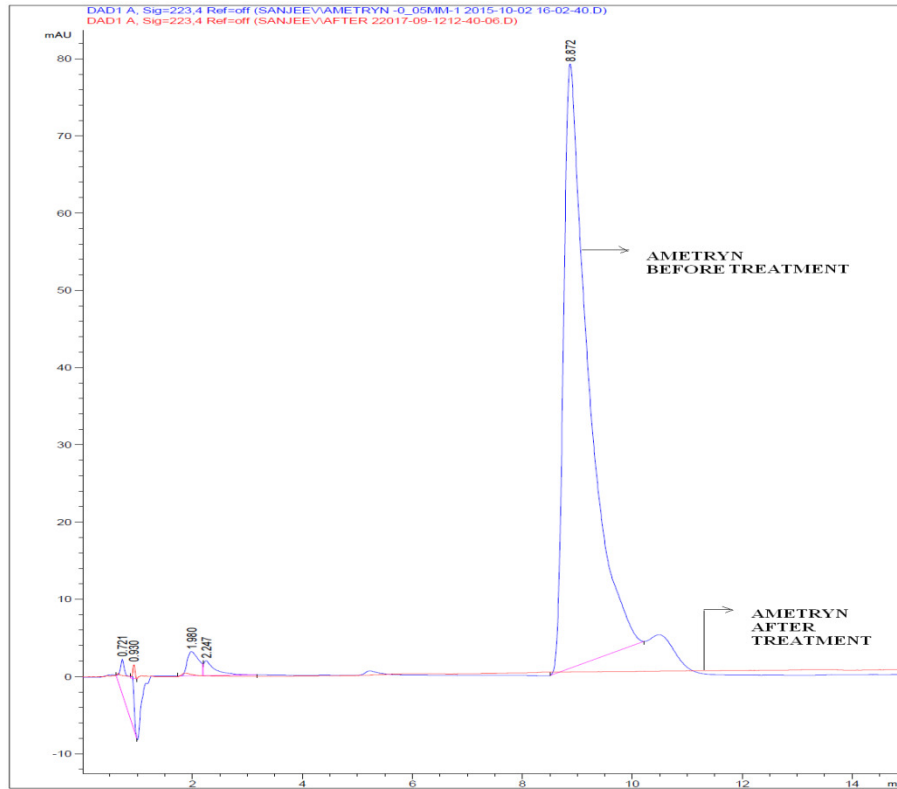

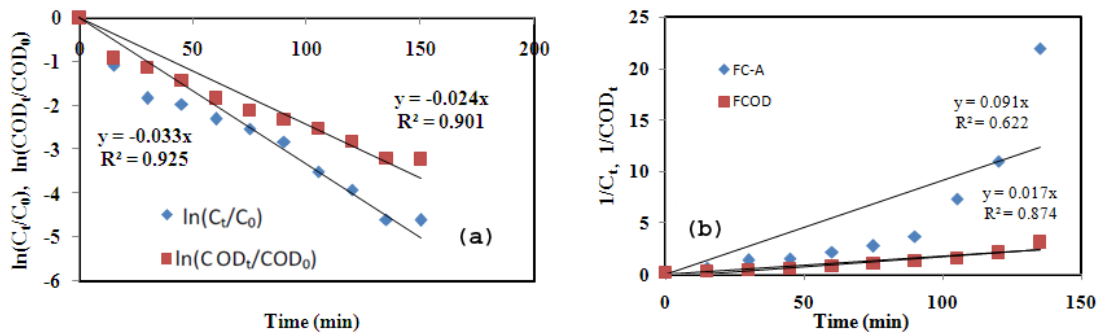**Figure. 5.8**. Overlaid chromatograph of ametryn before and after treatment process

Figure.5.9. a) 1st order kinetics **b)** 2nd order kinetics

A similar kind of pseudo-first order kinetic models were obtained in other studies also (Swaminathan et al. 2003(R^2=0.89-0.99, K=0.01-0.07 min^{-1}); Kong and Lemley, 2006(R^2=0.71-0.97, K=0.04-0.32 min^{-1}); Zhang et al. 2016 (R^2=0.99-1, K=0.0022-0.0046 min^{-1});Ma et al. 2000 (R^2=0.91-0.99, K=0.004-0.06 min^{-1})). Further, the oxidant decomposition was also monitored and 100% depletion was observed within 90 min. This implies that, more number of hydroxyl radicals was produced in the initial stages itself. Finally, from the A-III-18 (a) (b) the optimum values were confirmed as 2.125, 6, 3.5 and 135 for A, B, C and D respectively.

5.2.8. Optimization and validation

To determine the optimum region or working feasible region the contours are graphically overlaid for both responses (Ahmad et al., 2005) and in this process the desired goal was to maximize the responses Y_1 (%CODR) and Y_2 (%AR). Hence, the boundary values were defined as Y_1 (8, 100) and Y_2 (8.31, 100) with a reaction time of 135 min. The overlay plot consists of 3 regions, which are separated by circular dotted lines shown in Figure. 5.10. The shaded portion consists of 2 regions, the middle area is not a feasible region for both % AR and % CODR (NFRAC), and the other region is feasible for only % CODR (FRC). The remaining unshaded area (optimum region) is feasible for both responses and is considered for additional experiments (Table 5.4). The standard deviation (<5), coefficient of variation (<9%) and adequate precision (A.P) were greater than 12 and these values are within the prescribed limits (S.D<4, C.V<10% and A. P>4).

Table 5.4. Optimization of additional experiments

Run	Independent Factors				% CODR[a]		% AR[b]		Error		S. D[c]		C.V[d]		A.P[e]	
	A	B	C	D	Ac[f]	Pr[g]	Ac	Pr	CODR	AR	CODR	AR	CODR	AR	CODR	AR
27	1.87	6	4.2	135	92	94.98	92.31	97.62	2.98	5.31	2.11	3.75	3.19	5.59	31.87	18.38
28	2.44	6	4.21	135	88	92.63	93.3	96.97	4.63	3.67	3.27	2.6	5.13	3.86	20.01	26.42
29	1.56	6	2.22	135	64	69.69	71.58	73.82	5.69	2.24	4.02	1.58	8.51	3.08	12.25	32.96
30	2.71	6	2.67	135	76	79.23	78.62	82.6	3.23	3.98	2.28	2.81	4.16	4.94	24.53	20.75

Note :[a] % CODR=% COD removal; [b] % AR= % ametryn removal; [c] S.D=Standard deviation ; [d]C.V= Coefficient of Variation ; [e] A.P= Adequate Precision ; [f] Ac=Actual values; [g] Pr=Predicted values

Note: FRC=Feasible region for % CODR; NFRAC=Not feasible reagion for %AR,%CODR
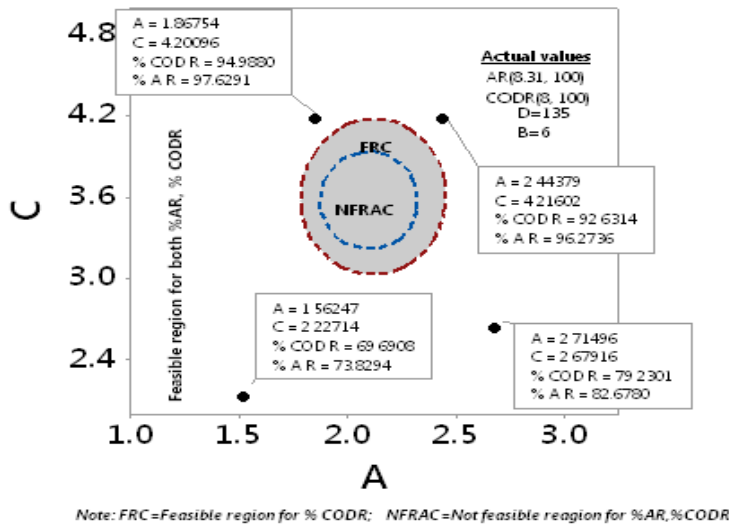
Figure.5.10. Contour overlay plot

5.3 DEGRADATION OF DICAMBA

Preliminary experiments were conducted by varying H_2O_2 /COD (1-3.375), H_2O_2/Fe^{2+}(2-6,7-11,12-16,17-21,22-26, 27-32) and pH(1.5-9) (Figure. 5.11(a)(b)(c) and complete degradation was observed at value of 17, 2.5 and 5 for H_2O_2/Fe^{2+}, H_2O_2 /COD and pH respectively. The design matrix and ANOVA results are shown in Table 5.5, 5.6, 5.7 and A-II-5.
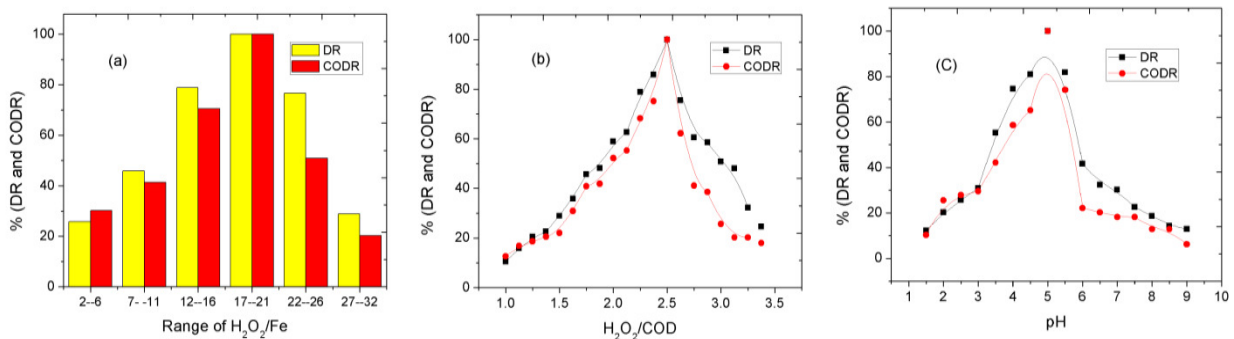
Figure.5.11 **(a)** Range of H_2O_2/Fe vs. responses; dicamba$_0$=0.39mM, reaction time(min)=30-240, H_2O_2 /COD=1-3.375; pH=1.5-9 **b)** H_2O_2 /COD vs. responses; reaction time(min)=135 , pH=5, H_2O_2/Fe=21 **c)** pH vs responses; reaction time(min)=135, H_2O_2/Fe=17, H_2O_2 /COD=2.5.

5.3.1 CCD matrix

The response equations along with interaction coefficients of variables are presented in Eqs. 5.17-5.1. The intercept values are showing positive effects (76.11, 81.81) along with some coefficients A, B, C, D, D^2, A*B, A*D, B*C (%CODR) and B, C, D, D^2, A*D, B*C (%DR).

Table 5.5. Levels of the parameters studied in the CCD

Factor	Name	Low(-1)	Middle(0)	High(+1)
A(X_1)	H_2O_2/COD	1	2.5	4
B(X_2)	H_2O_2/Fe	2	17	32
C(X_3)	P^H	3	5	7
D(X_4)	Time (min)	30	135	240

% COD R(Y_1)= 76.11 + 0.35 A + 1.43 B + 1.62 C + 3.85 D - 21.78 A*A - 18.65 B*B - 26.77 C*C+ 19.57 D*D+ 0.42 A*B - 0.71 A*C + 1.61 A*D + 1.57 B*C + 1.78 B*D + 0.40 C*D   (5.17)

%DR(Y_2) = 81.81 - 1.09 A + 0.84 B + 1.76 C + 3.06 D - 20.42 A*A - 20.47 B*B - 22.7 + 14.57 D*D- 0.68 A*B - 2.42 A*C + 1.71 A*D + 1.85 B*C - 0.47 B*D - 0.10 C*D   (5.18)

The experimentally calculated F values for both responses (7.31 and 4.99) are > 2.74 (Ahmadi et al. 2005). From ANOVA results, it is clear that the R^2 and R^2_{adj} values are >80% and $R^2 \approx R^2_{adj}$. The S.D(<4), C.V (<10) and A.P(>4) values are within standard limits. The distribution of all 26 runs is plotted in A-III-19 and are showing a better trend in the treatment system.

Figure. 5.12. a) Effect of H_2O_2 on % COD and dicamba removal efficiency b) Effect of Fe^{2+} on % COD and dicamba removal efficiency

Table 5.6. CCD design matrix (D_0=0.39 mM)

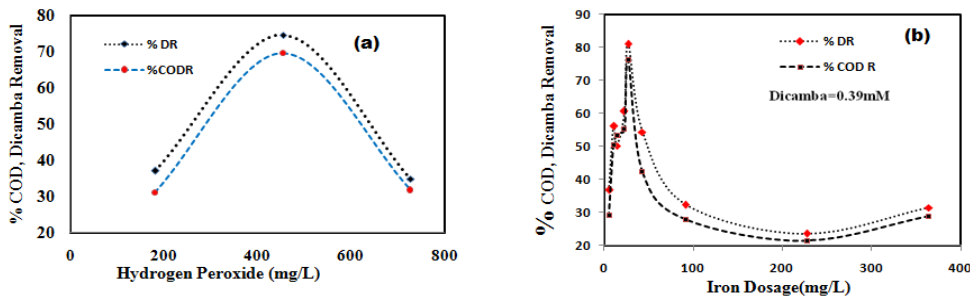|	Independent variables (uncoded and coded)				Fenton's Reagent		Actual Responses		Predicted Responses	
Run	A (H$_2$O$_2$/COD)	B (H$_2$O$_2$/Fe)	C (P^H)	D (Time)	H$_2$O$_2$ (mg/L)	Fe (mg/L)	% DR	% CODR	% DR	% CODR
1	2.5(0)	17(0)	5(0)	30(-1)	455	26.8	80.61	75.43	83.31	81.82
2	2.5(0)	32(1)	5(0)	135(0)	455	14.2	50.21	53.44	62.18	58.89
3	4(1)	2(-1)	7(1)	30(-1)	728	364	21	25.67	23.86	22.23
4	2.5(0)	17(0)	5(0)	135(0)	455	26.8	100	100	91.81	86.11
5	4(1)	32(1)	3(-1)	30(-1)	728	22.8	32.32	27.88	26.25	21.35
6	2.5(0)	17(0)	3(-1)	135(0)	455	26.8	48.21	40.22	57.32	47.72
7	4(1)	32(1)	7(1)	240(1)	728	22.8	35.33	42.78	37.21	40.8
8	4(1)	2(-1)	7(1)	240(1)	728	364	38.77	32.3	34.12	30.42
9	2.5(0)	17(0)	5(0)	135(0)	455	26.8	100	100	91.81	86.11
10	1(-1)	32(1)	3(-1)	240(1)	182	5.7	34.44	28.88	30.34	28.86
11	1(-1)	17(0)	5(0)	135(0)	182	10.7	56.21	50.52	62.48	53.98
12	1(-1)	2(-1)	7(1)	30(-1)	182	91	34.54	30.21	32.94	26.99
13	2.5(0)	17(0)	5(0)	240(1)	455	26.8	100	100	99.43	99.53
14	1(-1)	32(1)	7(1)	30(-1)	182	5.7	45.21	31.21	40.62	28.6
15	2.5(0)	17(0)	7(1)	135(0)	455	26.8	57.82	42.54	60.84	50.96
16	4(1)	2(-1)	3(-1)	240(1)	728	364	36	31.78	39.34	30.92
17	4(1)	2(-1)	3(-1)	30(-1)	728	364	30.21	25.67	28.67	24.36
18	4(1)	32(1)	3(-1)	240(1)	728	22.8	35.22	32.33	35.03	35.03
19	1(-1)	2(-1)	3(-1)	240(1)	182	91	32.22	27.77	31.93	26.42
20	1(-1)	2(-1)	7(1)	240(1)	182	91	31.54	25.66	36.37	28.73
21	1(-1)	32(1)	7(1)	240(1)	182	5.7	42.43	36.66	42.18	37.45
22	1(-1)	2(-1)	3(-1)	30(-1)	182	91	31.21	27.78	28.09	26.3
23	2.5(0)	2(-1)	5(0)	135(0)	455	227.5	60.33	45.56	60.49	56.03
24	1(-1)	32(1)	3(-1)	30(-1)	182	5.7	25.52	20.26	28.38	21.62
25	4(1)	32(1)	7(1)	30(-1)	728	22.8	30.33	24.67	28.83	25.5
26	4(1)	17(0)	5(0)	135(0)	728	42.8	54.44	42.21	60.3	54.68

Note:CODR=COD removal, DR=dicamba removal

Table 5.7 Analysis of Variance for % DR and %CODR

Parameter	% CODR	% DR
R^2 (Coefficient of determination)	92.3	96.3
Standard deviation (S.D)	3.15	2.71
Coefficient of variation(CV) %	7.71	9.41
Adequate precision(AP)	68.05	48.32
Pure error	0.6	0.6
F-value	4.99	7.31

Note:CODR=COD removal, DR=dicamba removal
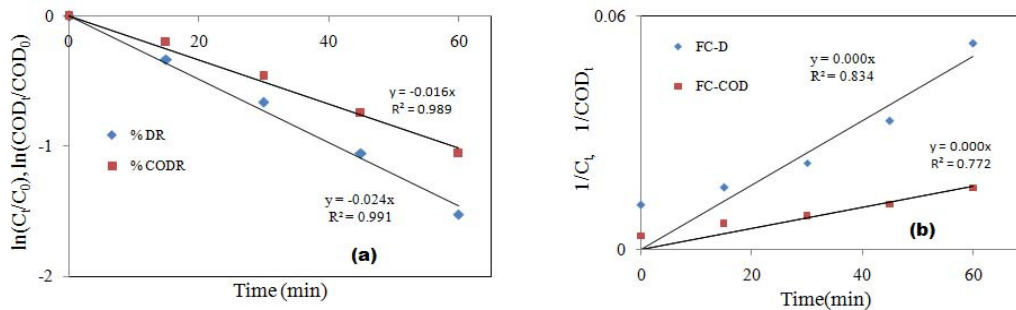
Figure.5.13. Kinetic studies a)1st order b)2nd order
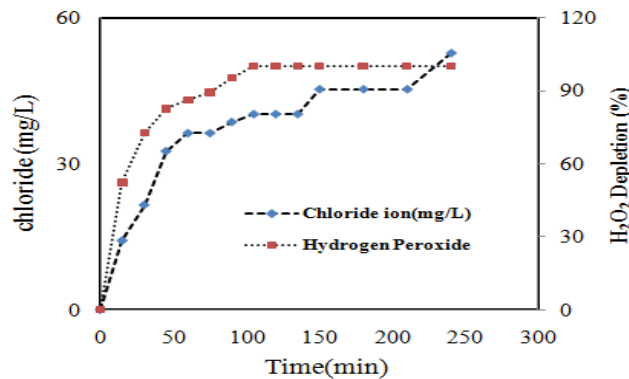
Figure.5.14. Depletion of hydrogen peroxide and release of chloride during AFPs

5.3.2 Effects of independent variables on the responses

The ratio of H_2O_2/COD is varied from 1-4 and it is seen that, the highest removal was at 2. 5 (near to 2.125). To find out the optimum iron and oxidant the suitable H_2O_2/Fe (B) values (2, 17, 32) were considered. Based on that, the dosage of iron (5.7-364 mg/L) and hydrogen peroxide (182-728 mg/L) were varied (Table 5.5 and 5. 6). When the H_2O_2 dosage was increased from 728 or decreased to 182 mg/L the less dicamba removal was

103

observed (Figure.5.12(a). This is mainly due to the scavenging effect of $^{\bullet}$OH radical (Zhang et al. 2006) and less H_2O_2 is not sufficient to produce required number of radicals. At high iron doses of 91, 227 and 364 mg/L (Figure.5.12(b)) less dicamba removal was achieved and this may be due to, more quantity of FeNPs suppresses $^{\bullet}$OH radical production (Pignatello 1992) by agglomerating the particles and it requires pH control throughout the reaction. If iron NPs were decreased to 5.7 and 22.2mg/L less removal (<45%) was observed. It is due to the less surface area available to promote adsorption followed by oxidation. Furthermore, in case of run 1, 4, 9 and 13, 100% removal was observed and hence, optimum value of 26.8mg/L was finally considered. Also, it was observed that, at run 6 and 15 (pH 3, 7), with iron dose 26.8mg/L the less removal was achieved and it clearly signifies that the pH is also influencing on both responses. Therefore, the effect of pH on degradation of ametryn was studied by varying it from 3-7 with a center value of 5. It is seen that, when the pH is at 3 and 7, less degradation was achieved and 100% removal was achieved at pH 5. However, the literature on conventional Fenton process said that, it works in acid range from 2-4 (Masomboon et al. 2009) and in the present study, the AFP is slightly towards the alkaline range. The lower pH helps in promoting scavenging effect on already produced OH radicals (Martins et al. 2010) and higher pH deactivate the reaction system with agglomeration of FeNPs by forming ferric hydroxide complexes(Lucas and Peres 2006). Hence, the optimum values (pH of 3.5, Fe=26.8mg/L, H_2O_2=455mg/L, H_2O_2/Fe=17, H_2O_2/COD=2.5) were maintained.

The reaction time (D) is also an important factor and was varied from 30-240 min. Here also, both 1st order and 2nd order models were studied at optimal conditions (Eqs. (5.19-5.20)).

$$\ln C_t/C_0 = -K_1 t \qquad (5.19)$$

$$1/C_t = 1/C_0 + K_2 t \qquad (5.20)$$

Where C_t, and $C_0$is the concentration of dicamba at time t and 0 min , K_1 and K_2 are the first and second order decay rate constants(min^{-1}).
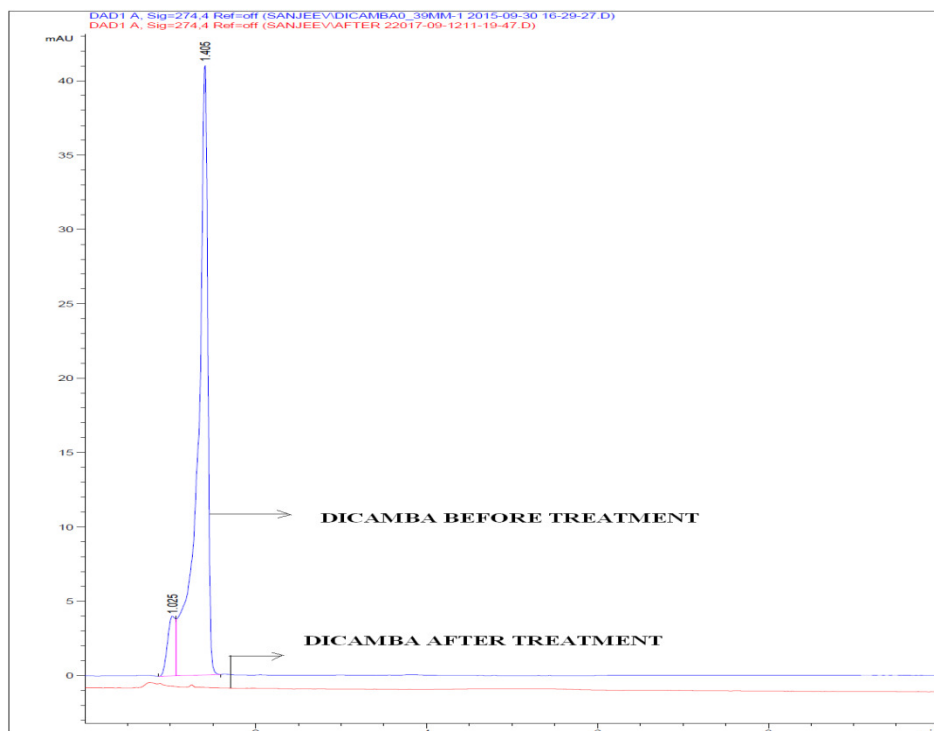
Figure. 5.15 Overlaid chromatograph of dicamba before and after treatment

In case of run 1 at 30 min, the removal efficiency was 75-80% and at 60 min it is 94-97%. The 100% removal was observed at 75 min and it is continued till 240 min (Figure.5.13(a)(b)). The R^2 (correlation coefficient) is >0.98 for both responses for the 1st order and <0.83 for 2nd order. Hence, it clearly indicates that 1st order reaction favors the treatment process than 2nd order. The rate constant for %DR (0.024) is more than %CODR (0.016) and it clearly indicates that degradation is faster than mineralization in first 60 min. The same trend was observed in other literatures, where the pseudo-first model was well fitted and the R^2 values are from 0.71-0.99 (Swaminathan et al. 2003, Wu et al. 2015, Kong and Lemley 2006, Khataee and Pakdehi 2014, Kakavandi et al. 2016, Zhang et al. 2016, shahwan et al. 2011). At first 60 min, it starts with adsorption onto the surface of iron oxides (LFeNPs) and zero valent iron and later ends with degradation followed by mineralization (Garrido-Ramírez et al. 2010, Kuang et al. 2013). Later, the oxidation process was decreased due to the formation of OOH radicals (Rusevova et al. 2012) (Eqs.4.7-4.15). To confirm the mineralization process, the release of chloride ion along with H_2O_2 decomposition was monitored in Figure. (5.14. (b)) and

105

it is seen that full decomposition of oxidant was observed with residual chloride of 57.2 mg/L. This was confirmed with an overlaid chromatograph (Figure.5.15), where no peaks were observed after treatment process. From the Table 5.6, it was concluded that the actual experimental and predicted values are similar in nature. To verify the results obtained in Table 5.6, four sets of additional experiments (runs 27, 28, 29 and 30) were conducted   suggested by overlay plot (Figure.5.16) from unshaded region and ANOVA results are shown in Table 5.8. The S.D, C.V, and A.P values were <4%, <10 and >4 respectively (Beg et al. 2003; Zinatizadeh et al. 2006) and hence the results are reliable.

Table 5.8. Validation

Run	Independent Factors				% CODR[a]		% AR[b]		Error		S. D[c]		C.V[d]		A.P[e]	
	A	B	C	D	Ac[f]	Pr[g]	Ac	Pr	% CODR	% DR	% CODR	% DR	% CODR	% DR	% CODR	% DR
27	3.0	17	5.8	135	65.85	69	70	75	3.15	5	2.23	3.54	4.67	6.9	21.9	15
28	1.65	17	5.6	135	62.15	67	71.21	74	4.85	2.79	3.43	1.97	7.51	3.84	13.81	26.52
29	3.0	17	3.9	135	60	66	68.52	72	6	3.48	4.24	2.46	9.52	4.95	11	20.69
30	1.25	17	3.5	135	41	45	49	54	4	5	2.82	3.53	9.3	9.7	11.25	10.8

Note :[a] % CODR=% COD removal; [b] % DAR= % Dicamba removal; [c] S.D=Standard deviation ; [d]C.V= Coffcient of Variation ; [e] A.P= Adequate Precision ; [f] Ac=Actual values; [g] Pr=Predicted values
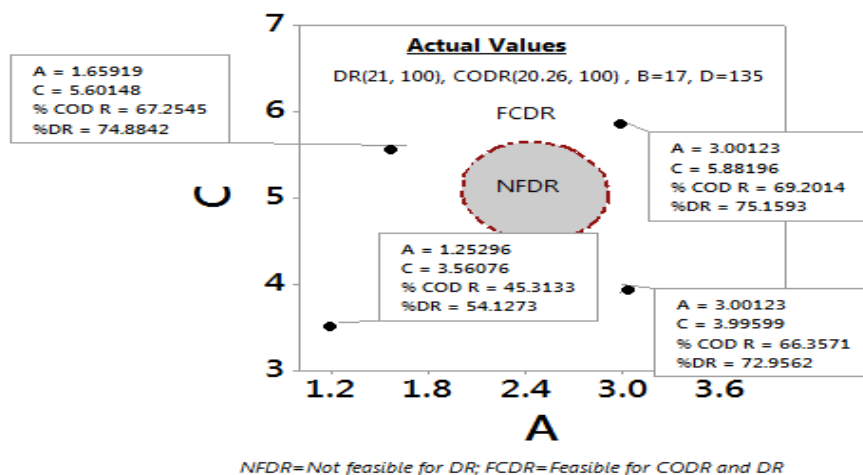
Figure.5.16. Contour overlay plot

5.4. TREATMENT OF 2, 4 –D

The preliminary experiments were conducted to fix the optimum range of values for H_2O_2 /COD (1-3.375), H_2O_2/Fe(2-22) and pH(1.5-9) shown Figure. 5.17(a)(b)(c) and the highest removal (>95%) was observed at values of 12, 2 and 4.5 respectively.
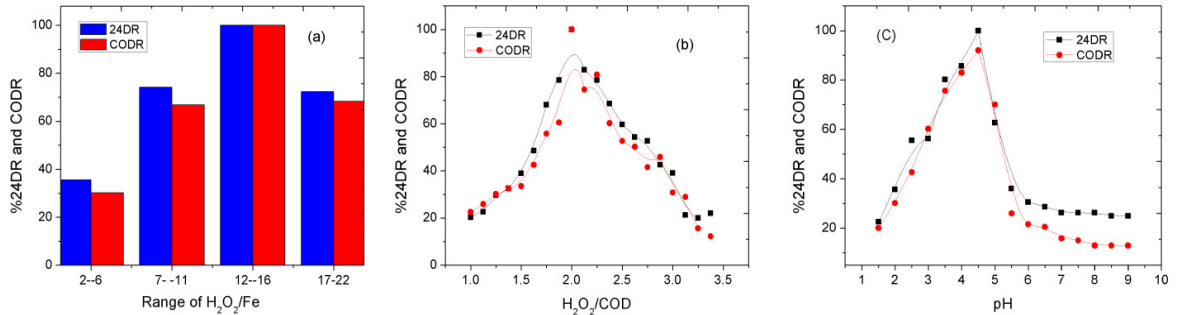
Figure. 5.17 (a) Range of H_2O_2/Fevs. responses; 2,4-D_0=0.13mM, reaction time(min)=30-240, H_2O_2 /COD=1-3.375; pH=1.5-9 **b)** H_2O_2 /COD vs. responses; reaction time(min)=135 , pH=4.5, H_2O_2/Fe=12 **c)** pH vs responses; reaction time(min)=135, H_2O_2/Fe=12, H_2O_2 /COD=2

5.4.1 CCD

The design details are shown in Table 5.9- 5.10 and ANOVA results in Table 5.11 and A-II-6. The model equations (Eqs. 5.21 and 5.22) show that the intercept values are >73, the coefficient of D^2 and A^2 are highest positive and negative values respectively.

Table 5.9. Levels of the parameters studied in CCD

Factor	Name	Low(-1)	Middle(0)	High(+1)
A(X_1)	H_2O_2/COD	1	2	3
B(X_2)	H_2O_2/Fe	2	12	22
C(X_3)	P^H	3	4.5	6
D(X_4)	Time (min)	30	135	240

% COD R(Y_1)= 73.48 + 0.57 A + 2.49 B + 1.26 C + 5.44 D - 27.82 A*A - 23.27 B*B - 20.60 C*C+ 27.51 D*D + 0.05 A*B + 2.81 A*C - 4.54 A*D + 0.67 B*C + 1.89 B*D - 0.88 C*D   (5.21)

$\%24DR(Y_2)$ $= 79.56 - 1.27\ A + 1.76\ B + 1.06\ C + 3.67\ D - 21.52\ A*A - 25.70\ B*B - 13.03\ C*C + 20.37\ D*D - 0.12\ A*B + 2.12\ A*C - 2.82\ A*D + 0.73\ B*C + 1.07\ B*D - 1.68\ C*D$ (5.22)

The experimentally calculated F values for both the responses are 3.8 and 4.25, which are > tabular F value (2.74). The coefficient of determination, R^2 and R^2_{adj} values are found to be similar for both responses and these values are > 90% (Joglekar and May 1987). The pure error value (0), lack of fit P values (0.7 and 0.2), S.D(<5), C.V(<10%), A.P (>4), which are below the recommended values (Beg et al. 2003). It means that, the obtained results are better. To residual plot (A-III-20) shows that all 26 runs are distributed on both sides of zero line with less residual (<15) and it is a good trend in the design matrix.

5.4.2 Effects of independent variables on the responses

The ratio of H_2O_2/COD varied from 1-3 with a center value as 2. When the ratio is decreased to 1 or increased to 3, less removal was observed. Further, H_2O_2/Fe (B) was varied from 2-122 with center value 12 (corresponding H_2O_2=61-183 mg/L; Fe=5.5-91.5 mg/L) (Table 5.9 and 5.10). Here also, increase (183mg/L) or decrease (61 mg/L) in H_2O_2 dosage, less removal was observed (Figure. 5.18 (a). More amount of oxidant acts like OH scavengers and less amount is not sufficient to produce more OH radicals (Masomboon et al. 20090). When the FeNPs dosage was more (91.5 mg/L) or less (5.5 mg/L) the less degradation was observed (Figure.5.18(b)). May be at this stage, the more FeNPs helps in the formation of iron hydroxides (surface area of catalyst reduced). Hence optimum dose of H_2O_2=122mg/L and FeNPs=10.7 mg/L was finally considered. Also in case of run 6 and 15 with an iron dosage of 10.7 mg/L (pH 3and 6), the less removal was observed. The pH of solution varied from 3-6 with a center value of 4.5 and maximum removal efficiency was observed at pH 4.5. May be at higher pH formation of hydroxide complex and lower pH scavenging effect of H^+ ions was observed (Martins et al. 2010). The reaction kinetics results (1st and 2nd order) showed that, the 1st order kinetic model was best fitted (R^2>0.94) than 2nd order model (R^2<0.8) shown in Figure.5.19 (a) (b). In parallel oxidant depletion and release of chloride ion was monitored (Figure.5.20),

18.2mg/L of Cl⁻ was observed with 100% decomposition of H_2O_2. From the table 4.12, 100% degradation was observed within 30 min of reaction time. And 100% mineralization (%CODR=100) was confirmed with HPLC overlaid chromatograph (Figure.5.21), where no such peaks were observed after AFPs. Finally, the CCD is validated by conducting additional experiments suggested contour overlay plot (Figure.5.22 and Table 5.12).
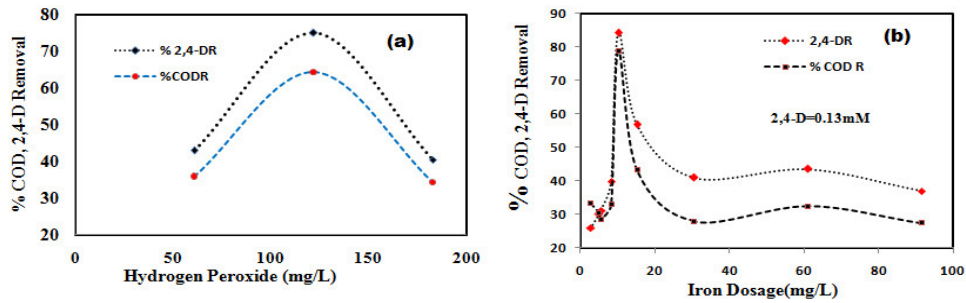

Figure. 5. 18 a) Effect of H_2O_2 on % COD and 2,4-D removal efficiency b) Effect of Fe on % COD and 2,4-D removal efficiency.
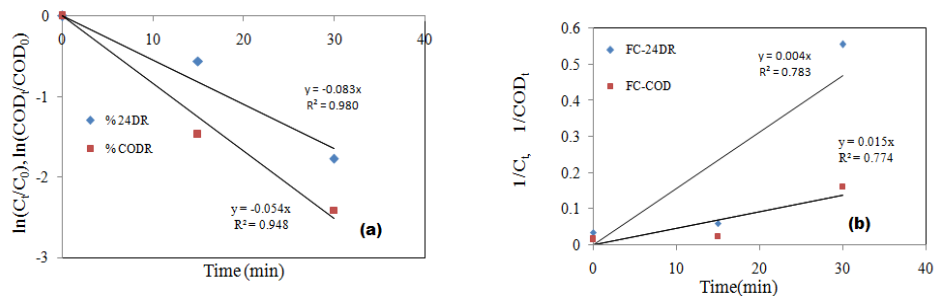

Figure. 5.19 a) 1ˢᵗ order reaction kinetics b) 2ⁿᵈ order kinetics H_2O_2=122mg/L; Fe=10.7mg/L; COD_0=61mg/L, C_0=0.13mM, pH =4.5.
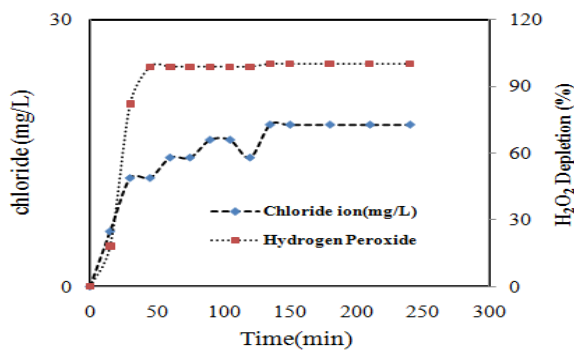

Figure.5.20 Depletion of hydrogen peroxide and release of chloride during AFP.

Table 5.10. CCD design matrix

	Independent variables (uncoded and coded)				Fenton's Reagent(mg/L)		Actual Responses (%)		Predicted Responses (%)	
Run	A	B	C	D	H_2O_2	Fe	24DR	CODR	24DR	CODR
1	2(0)	12(0)	4.5(0)	30(-1)	122	10.17	100	100	95.27	95.56
2	2(0)	22(1)	4.5(0)	135(0)	122	5.55	50.54	42.32	55.62	52.7
3	3(1)	2(-1)	6(1)	30(-1)	183	91.5	32.33	30.31	41.13	32.63
4	2(0)	12(0)	4.5(0)	135(0)	122	10.17	100	100	98.56	93.44
5	3(1)	22(1)	3(-1)	30(-1)	183	8.32	34.56	30.32	32.55	24.02
6	2(0)	12(0)	3(-1)	135(0)	122	10.17	60.56	42.45	65.48	51.63
7	3(1)	22(1)	6(1)	240(1)	183	8.32	45.65	42.41	44.2	39.08
8	3(1)	2(-1)	6(1)	240(1)	183	91.5	38.88	28.65	37.31	28.89
9	2(0)	12(0)	4.5(0)	135(0)	122	10.17	100	100	98.56	93.44
10	1(-1)	22(1)	3(-1)	240(1)	61	2.77	65.67	54.34	52.42	44.82
11	1(-1)	12(0)	4.5(0)	135(0)	61	5.08	45.67	30.34	59.31	45.1
12	1(-1)	2(-1)	6(1)	30(-1)	61	30.5	43.54	22	33.53	16.89
13	2(0)	12(0)	4.5(0)	240(1)	122	10.17	100	100	100	100
14	1(-1)	22(1)	6(1)	30(-1)	61	2.77	34.65	21.45	36.62	19.31
15	2(0)	12(0)	6(1)	135(0)	122	10.17	58.89	45.65	67.59	54.15
16	3(1)	2(-1)	3(-1)	240(1)	183	91.5	42.21	28.89	35.78	23.82
17	3(1)	2(-1)	3(-1)	30(-1)	183	91.5	34.54	22.23	32.88	24.06
18	3(1)	22(1)	3(-1)	240(1)	183	8.32	28.68	23.45	39.74	31.36
19	1(-1)	2(-1)	3(-1)	240(1)	61	30.5	40.21	34.19	47.97	37.49
20	1(-1)	2(-1)	6(1)	240(1)	61	30.5	43.45	32.21	41.01	31.3
21	1(-1)	22(1)	6(1)	240(1)	61	2.77	45.67	40.32	48.38	41.28
22	1(-1)	2(-1)	3(-1)	30(-1)	61	30.5	36.77	23.45	33.77	19.57
23	2(0)	2(-1)	4.5(0)	135(0)	122	61	43.56	40.43	52.1	47.73
24	1(-1)	22(1)	3(-1)	30(-1)	61	2.77	31.32	16.78	33.93	19.33
25	3(1)	22(1)	6(1)	30(-1)	183	8.32	50.45	35.76	43.73	35.25
26	3(1)	12(0)	4.5(0)	135(0)	183	15.25	56.79	43.32	55.77	46.24

Table 5.11. Analysis of Variance for % 24DR

Parameter	% CODR	% DR
R^2 (coefficient of determination)	94.9	92.3
Standard deviation (S.D)	3.43	3.6
Coefficient of variation(CV) %	9.43	9.07
Adequate precision(AP)	19.20	20.1
Pure error	0.2	0.7
F-value	4.25	3.8

Note:CODR=COD removal, DR=dicamba removal

Table 5.12. Optimization of additional experiments

Run	Independent Factors				% CODR[a]		% 24DR[b]		Error		S. D[c]		C.V [d]		A.P [e]	
	A	B	C	D	Ac[f]	Pr[g]	Ac	Pr	% CODR	% 24DR	% CODR	% 24DR	% CODR	% 24DR	% CODR	% 24DR
27	2.44	12	5.0	30	62.8	66.0	68.1	73.5	3.2	5.4	2.26	3.82	4.97	7.63	20.63	13.61
28	2.44	12	3.7	30	58.1	62.5	68.3	70.9	4.4	2.6	3.11	1.84	7.3	3.74	14.2	27.27
29	1.11	12	3.3	30	36.8	40.5	54.0	57.1	3.7	3.1	2.62	2.19	9.57	5.58	10.95	18.42
30	1.15	12	4.7	30	48.2	52	61.0	64.5	3.8	3.5	2.69	2.47	7.58	5.58	13.68	18.43

Note :[a] % CODR=% COD removal; [b] % 24DR= % 24D removal; [c] S.D=Standard deviation ; [d]C.V= Coffcient of Variation ; [e] A.P= Adequate Precision ; [f] Ac=Actual values; [g] Pr=Predicted values
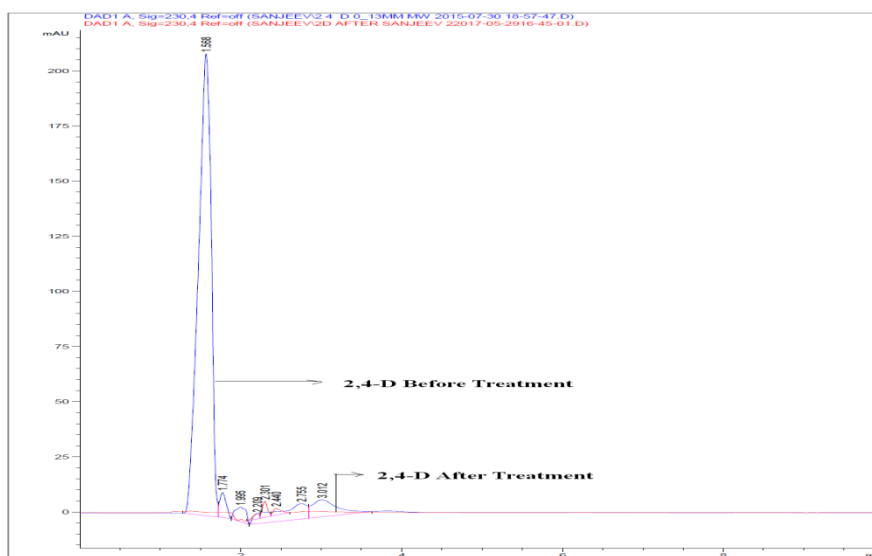

Figure.5.21 Overlaid chromatograph of   2,4-D before and after treatment

111
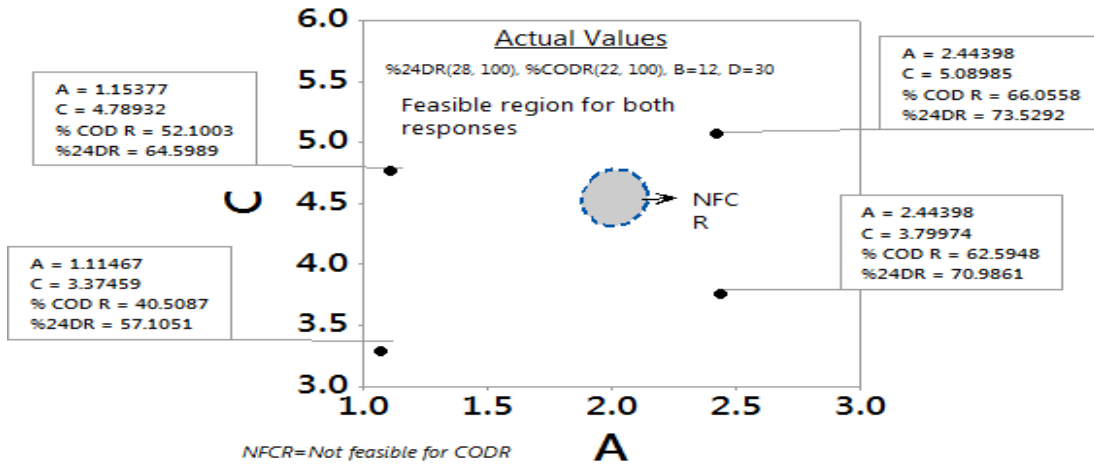
Figure.5.22. Contour overlay plot

5.5 DEGRADATION OF MIXTURE OF COMPOUNDS WITH EG EXTRACTS

The effect of the mixture of all the three compounds on the removal efficiencies (% ametryn(Y_1), COD(Y_2), dicamba(Y_3)and 2,4-D(Y_4) removal) having the initial concentration (2,4-D=25mg/L, ametryn=3.5 mg/L and dicamba=94 mg/L) was studied based on the characteristics of agriculture runoff water (Sangami and Manu, 2017). The design matrix is shown in Table 5.13 and here the optimized levels of dicamba were considered because the concentration of dicamba is more than 2,4-D and ametryn (Table 5.5). The ANOVA results are given in Table 5.14, A-II-7 and A-II-8 along with 2nd order polynomial equations **(5.23-5.26)**. The coefficient of C^2 is considered as more influencing parameter and S.D<5, C.V<10% and A.P>10 are within standard recommend values.

$$\%AR(Y_1) = 72.60 + 0.24\,A + 0.14\,B + 0.62\,C + 0.17\,D - 30.35\,A*A - 14.02\,B*B$$
$$+ 9.49\,C*C + 5.91\,D*D - 1.19\,A*B - 0.70\,A*C + 1.59\,A*D - 1.46\,B*C$$
$$+ 2.40\,B*D + 1.08\,C*D \qquad (5.23)$$

$$\%\ COD\ R(Y_2) = 76.63 + 0.79\,A - 0.10\,B + 1.99\,C + 1.01\,D - 29.73\,A*A - 17.25\,B*B$$
$$+ 14.87\,C*C + 2.87\,D*D - 1.11\,A*B + 0.30\,A*C + 1.41\,A*D - 2.45\,B*C$$
$$+ 0.74\,B*D + 1.47\,C*D \qquad (5.24)$$

112

$$\%DR(Y_3) = 73.72 \ -0.34\,A \ +0.15\,B \ +1.59\,C \ -1.06\,D \ -30.74\,A*A \ -14.57\,B*B$$
$$+13.77\,C*C+5.34\,D*D \ -0.54\,A*B \ -0.22\,A*C \ +3.76\,A*D \ +0.20\,B*C$$
$$+2.90\,B*D+0.41\,C*D \hspace{2cm} (5.25)$$

$$\%\ 2,4D\text{-}R\ (Y_4)= 76.00 \ -1.38\,A \ +1.00\,B \ +1.46\,C \ -0.78\,D \ -27.8\,A*A \ -12.6\,B*B$$
$$+10.9\,C*C \ \ \ \ +5.5\,D*D \ +1.63\,A*B \ +1.26\,A*C \ +2.37\,A*D \ +0.56\,B*C$$
$$+1.44\,B*D+1.67\,C*D \hspace{2cm} (5.26)$$

5.5.1 Effects of independent variables on the responses

The H_2O_2/COD, H_2O_2/Fe were varied as 1-4 and 2-32 and 100% removal was observed at 2.5 and 17 respectively. The corresponding H_2O_2 and Fe dosages were found to be 172-688 mg/L and 5.38-344 mg/L of FeNPs respectively. It is seen that, when the H_2O_2 (688mg/L) and FeNPs dosage (344 mg/L) were increased, the removal efficiency was decreased. The excess amount of H_2O_2 and iron inhibits •OH radical production by forming hydroxide complex (Zhang et al. 2006) and lower dose of iron is not sufficient to provide required surface area for adsorption. Hence, 25.29 of FeNPs and 430 mg/L of H_2O_2 was finally considered(Run 15). The effect of pH was also studied by varying from 3-7 and it was found that, pH 7 has the highest removal efficiency than 5 and 3. This implies that, the AFP is working at neutral pH than conventional Fenton process (acidic pH=3-4). The kinetic studies were conducted for both 1st and 2nd order model (Figure. 5.23(a) (b)). It was found that, 1st order kinetic model (R^2>0.87) was the best fitted than 2nd order (R^2<0.81). The chloride >150mg/L was released during Fenton's treatment with 100% depletion of H_2O_2 (Figure.5.24). The 100% mineralization was confirmed with the HPLC overlaid chromatograph (Figure.5.25), in which no peaks were observed after treatment process. However, when all these compounds were mixed, there is a formation of different compounds (retention time of each compound is shifted to 0.98 and 2.1 min). Finally, all 26 experiments were validated (A.P>4) with additional four experiments (Table 5.15) suggested by overlay plot (Figure.5.26).

Table 5.13: CCD design matrix for mixture of compounds (2,4-D_0=25 mg/L, A_0=3.5 mg/L, D_0=94 mg/L)

Run	H$_2$O$_2$/COD	H$_2$O$_2$/Fe	P^H	Time (min)	H$_2$O$_2$	Fe	A R	COD R	D R	24DR	A R	COD R	D R	24DR
							Actual Responses (%)				Predicted Responses (%)			
1	2.5(0)	17(0)	5(0)	30(-1)	430	25.29	61.52	48.62	52.63	55.41	62.27	60.12	68.33	58.49
2	2.5(0)	32(1)	5(0)	135(0)	430	13.44	42.56	31.63	31.89	34.96	44.42	39.3	48.72	39.28
3	4(1)	2(-1)	7(1)	30(-1)	688	344	28.52	26.96	22.52	18.8	28.36	28.53	35.85	30.97
4	2.5(0)	17(0)	5(0)	135(0)	430	25.29	65.2	67.99	56.74	60.89	56	53.72	62.6	56.63
5	4(1)	32(1)	3(-1)	30(-1)	688	21.5	35.62	31.63	25.74	34.1	28.64	20.02	31.26	25.44
6	2.5(0)	17(0)	3(-1)	135(0)	430	25.29	61.21	68.52	52.85	58.6	65.47	65.9	71.47	69.51
7	4(1)	32(1)	7(1)	240(1)	688	21.5	32.62	25.6	28.56	35.9	41.26	34.38	36.51	31.44
8	4(1)	2(-1)	7(1)	240(1)	688	344	32.89	34.55	26.63	31.9	31.99	28.97	36.73	37.28
9	2.5(0)	17(0)	5(0)	135(0)	430	25.29	68.89	58.69	61.32	66.9	56	53.72	62.6	56.63
10	1(-1)	32(1)	3(-1)	240(1)	172	5.38	42.99	32.96	32.32	38.1	28.64	24.21	34.76	27.23
11	1(-1)	17(0)	5(0)	135(0)	172	10.12	28.89	24.66	21.63	25.4	29.56	23.33	32.01	26.11
12	1(-1)	2(-1)	7(1)	30(-1)	172	86	36.21	24.66	30.5	32.6	36.6	36.1	37.57	29.41
13	2.5(0)	17(0)	5(0)	240(1)	430	25.29	72.52	65.9	61.96	62.3	60.71	58.01	68.68	60.5
14	1(-1)	32(1)	7(1)	30(-1)	172	5.38	29.63	24.66	32.33	35	33.57	32.06	32.52	25.05
15	2.5(0)	17(0)	7(1)	135(0)	430	25.29	100	100	98.6	100	88.39	89.09	92.71	93.49
16	4(1)	2(-1)	3(-1)	240(1)	688	344	35.62	26.96	27.62	22.8	24.33	25.79	31.83	24.85
17	4(1)	2(-1)	3(-1)	30(-1)	688	344	40.21	27.89	31.62	35.7	27.38	27	35.25	24.45
18	4(1)	32(1)	3(-1)	240(1)	688	21.5	38.63	32.96	34.8	36.8	31.38	30.41	37.43	28.81
19	1(-1)	2(-1)	3(-1)	240(1)	172	86	23.63	18.52	16.78	31.1	28.12	17.44	24.39	18.84
20	1(-1)	2(-1)	7(1)	240(1)	172	86	28.63	25.6	17.85	25.2	30.76	21.48	32.09	30.07
21	1(-1)	32(1)	7(1)	240(1)	172	5.38	31.52	24.63	23.21	26.6	33.5	29.04	36.64	28.67
22	1(-1)	2(-1)	3(-1)	30(-1)	172	86	38.96	31.63	41.62	45.9	40.64	33.7	34.17	24.07
23	2.5(0)	2(-1)	5(0)	135(0)	430	215	51.63	42.66	42.87	46.6	42.41	39	48.44	39.48
24	1(-1)	32(1)	3(-1)	30(-1)	172	5.38	38.63	31.63	30	36.9	35.39	28.87	34.95	29.5
25	4(1)	32(1)	7(1)	30(-1)	688	21.5	26.63	21.89	21.8	30.3	31.85	22.35	26.03	22.17
26	4(1)	17(0)	5(0)	135(0)	688	40.47	32.63	24.66	20.8	25.7	26.81	22.64	32.48	27.68

Note:CODR=COD removal, AR=ametryn removal,DR=dicamba removal, 2,4-DR=2,4-D removal

Table 5.14 . Analysis of Variance for % AR , %24DR, % CODR and %DR

Parameter	% AR	% 24DR	%CODR	%DR
R^2 (coefficient of determination)	87.21	85.12	90.25	87.88
Standard deviation (S.D)	3.51	3.6 9	3.79	3.36
Coefficient of variation(CV) %	8.31	9.34	9.77	9.65
Adequate precision(AP)	21.4	22.29	15.46	14.51
Pure error	0	0	5.61	3.87
F-value	3.1	3.13	4.11	3.74

Note:CODR=COD removal, AR=ametryn removal,DR=dicamba removal, 2,4-DR=2,4-D removal

Table 5.15. Optimization of additional experiments

Run	Independent Factors				% CODR[a]		% AR[b]		%DR[c]		%24DR[d]		A.P [e]		%DR	%24DR
	A	B	C	D	Ac[f]	Pr [g]	Ac[f]	Pr [g]	Ac[f]	Pr [g]	Ac[f]	Pr [g]	% CODR	% AR		
27	3.35	17	6.36	135	45.3	50.9	48.2	52.3	41.6	45.7	45.3	48	9.1	12.8	11.1	17.8
28	3.38	17	4.01	135	45.3	49.3	50.2	54.4	40.2	45.2	45.2	47.1	12.3	13	9	24.8
29	1.11	17	5.8	135	29.6	33.6	35.6	38.5	26.9	30.8	32.3	35.4	8.4	13.3	7.9	11.4
30	1.16	17	3.58	135	35.9	38.3	38.2	42	31.9	35	35.3	40.2	16	11.1	11.3	8.2

Note :[a] % CODR=% COD removal; [b] % AR= % ametryn removal; [c] DR=% Dicamba removal; [d]24DR=%
24D removal ; [e] A.P= Adequate Precision ; [f] Ac=Actual values; [g] Pr=Predicted values
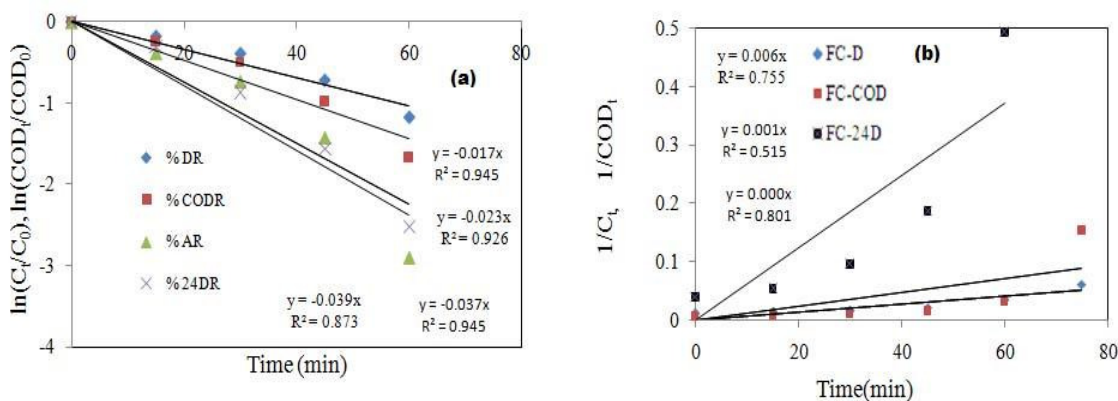

Figure. 5.23 a) 1st order reaction kinetics b) 2nd order kinetics, H_2O_2=430mg/L;
Fe=25.29 mg/L; COD_0=172 mg/L, 2,4-D_0=25 mg/L, A_0=3.5 mg/L, D_0=94 mg/L, pH =7
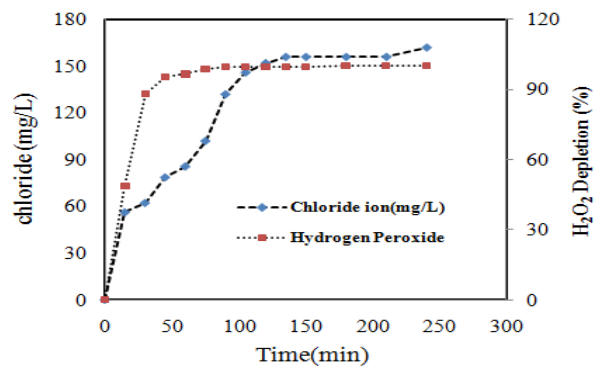
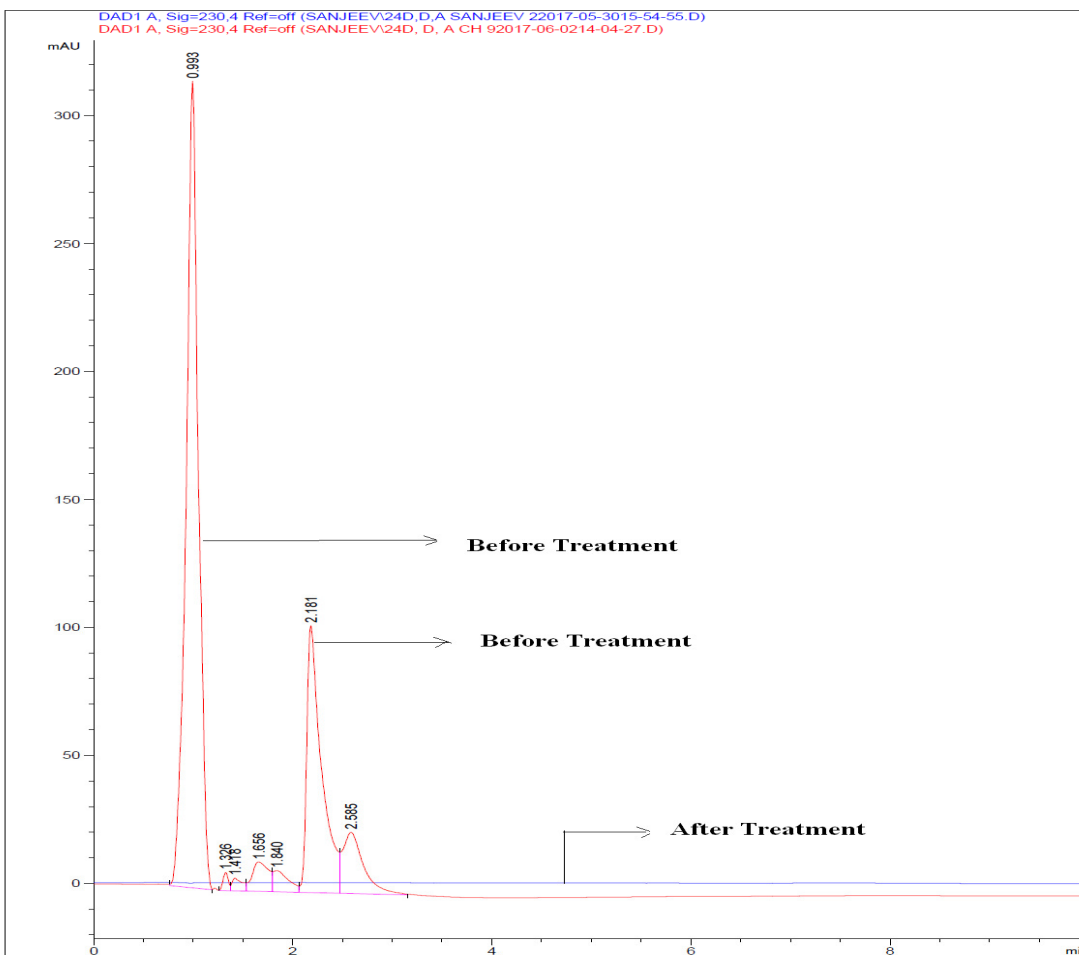**Figure.5.24** Depletion of hydrogen peroxide and release of chloride during AFP

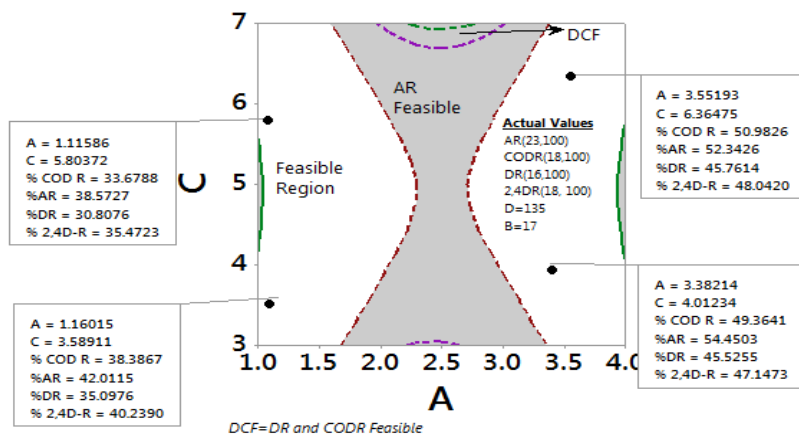**Figure.5.25** Overlaid chromatograph of mixture of compounds (before and after treatment)

116

A = 1.11586
C = 5.80372
% COD R = 33.6788
%AR = 38.5727
%DR = 30.8076
% 2,4D-R = 35.4723

A = 3.55193
C = 6.36475
% COD R = 50.9826
%AR = 52.3426
%DR = 45.7614
% 2,4D-R = 48.0420

Actual Values
AR(23,100)
CODR(18,100)
DR(16,100)
2,4DR(18, 100)
D=135
B=17

A = 1.16015
C = 3.58911
% COD R = 38.3867
%AR = 42.0115
%DR = 35.0976
% 2,4D-R = 40.2390

A = 3.38214
C = 4.01234
% COD R = 49.3641
%AR = 54.4503
%DR = 45.5255
% 2,4D-R = 47.1473

DCF=DR and CODR Feasible

Figure. 5.26 contour overlay plot

5.6 DEGRADATION OF MIXTURE OF COMPOUNDS WITH TG EXTRACT

5.6.1 Antioxidant property and polyphenols

To optimize the antioxidant power on the different quantity of leaves (15-80g/L), the experiments were conducted in an Erlenmeyer flask (at 80 ^{0}C) and at every 15 min the samples antioxidant property (AP) was measured using the FRAP method (Figure.5.27a). It was found that, more quantity of leaves (80 g/L) possessing higher antioxidant property. However, there is no such variation between 60 and 80 g/L was observed and hence, 60 g/L was finally selected. After 60 min, the antioxidant power was reduced and it indicates that, the better extraction   was observed. Total phenolic content was also calculated for different quantities of leaves at an optimized contact time (60 min) shown in Figure.5.27b and it was found that highest phenolic content of 3.5 mM of gallic acid was extracted.

5.6.2. Characterization

FESEM and EDX

The FESEM images before and after synthesis are shown in Figure. 5.28(a)(b) with resolution of 40KX and a lot of difference in the morphology was observed. After synthesis, the chain like spherical particles (50-100 nm) were observed and in some places the spherical particles are merged due to their magnetic properties.
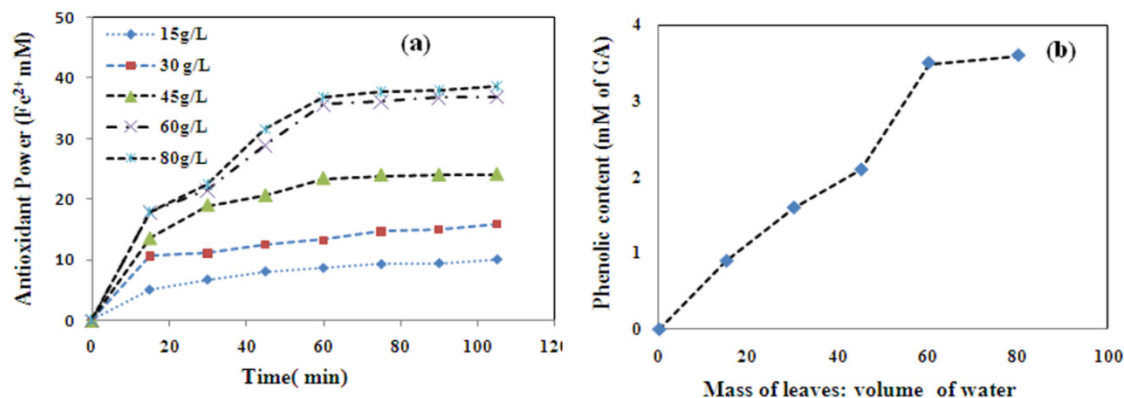
Figure.5.27. a)Antioxidant Power of different quantity(15-80g/L) of leaves b) Phenolic content vs mass of leaves :volume of water

The elemental composition of powdered laterite particles (PLPs) and laterite based iron nano particles (LFeNPs) are shown in Figure. 5.29(a)(b). The PLPs surface mainly consists of O(43.26), C(20.38), Fe(17.01), Si(12.23) and other trace elements(Al, Ti). The LFeNPs   consist of mainly iron as 57.9%, without having Si, Al and Ti, which is more than the PLPs. Hence, it can be concluded that maximum iron was extracted from laterite. And also O element was reduced from 43.26 - 24.62%, maybe this is due to the partial oxidation of iron. The C element in LFeNPs is mainly due to the polyphenols and is higher than the PLPs. This elemental composition was further confirmed by the XRD and FTIR analysis.

XRD, FTIR, and BET analysis

The mineralogical composition of PLPs was expressed as the characteristic peaks of 2θ values vs. intensity Figure.5.30(a). This is mainly composed of SiO_2, $(53.86^0, 62.8^0)$, $Fe_2O_3(21.8^0, 27.31^0)$, $Al_2O_3(.35.55^0, 49.52^0, 65.34^0, 71.2,^0)$ and $FeO(32.95^0)$ (ICDD database). Figure.5.30(b) shows the 2θ values of LFeNPs namely   polyphenols (18.89), meghemite γ-Fe_2O_3 (33.9), $Fe_3O_4(35.71)$ and Fe^0 (49.5, 54.19, 58.16) (Njagi et al. 2011). The other 2θ values represent the hydroxides of iron(24.45, 39.2) and $Fe_2O_3(62.4, 64.10)$ (Khataee and Pakdehi 2014, Shahwan et al. 2011). Figure.5.31(**a**)represent FTIR spectrum of PLPs, it is mainly composed of OH group Al, Si, Fe (3612-3426 cm^{-1}), H-O-H(1627 cm^{-1}), SiO(1104-1026 cm^{-1}), cristobalite (917, 743 cm^{-1}), Fe_2O_3 (543 cm^{-1}),

Fe-O (446 cm^{-1}) (Maiti et al. 2010). The FTIR spectra (Figure.5.31(b)) of LFeNPs   is having wave numbers 3194 cm^{-1} (OH), 1634(phenolic group), 1125(aromatic amines), 971(aliphatic amines) and 797(C-H). The other bands   538 cm^{-1} (Fe$_3$O$_4$) and 426 cm^{-1} (Fe$_2$O$_3$) represent the iron oxide particles (Kumar et al., 2013). To confirm the formation spherical particles in SEM images, BET method was applied and it was observed that surface area was increased from 24.12 -31.0 m^2/g and pore volume was also increased from 0.008 -0.035cm^3/g. Higher surface area and pore volume confirm the formation of nanoparticles.
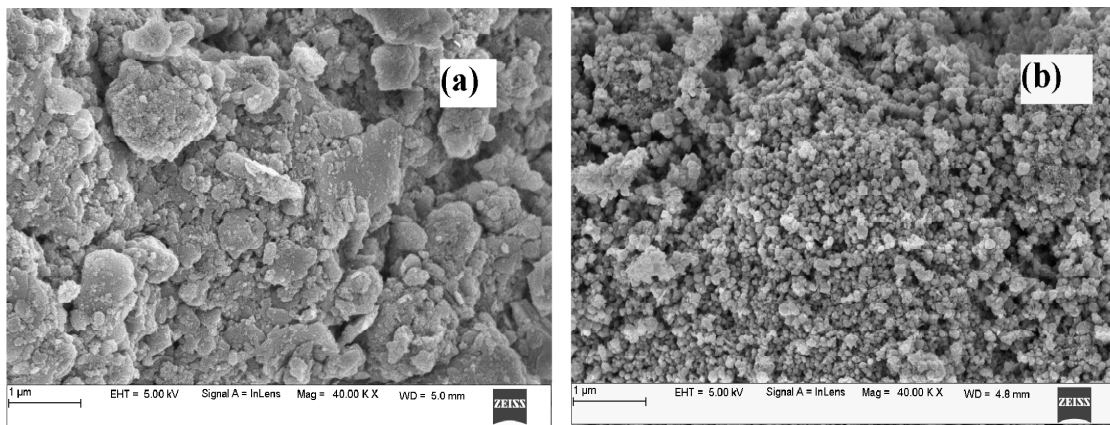

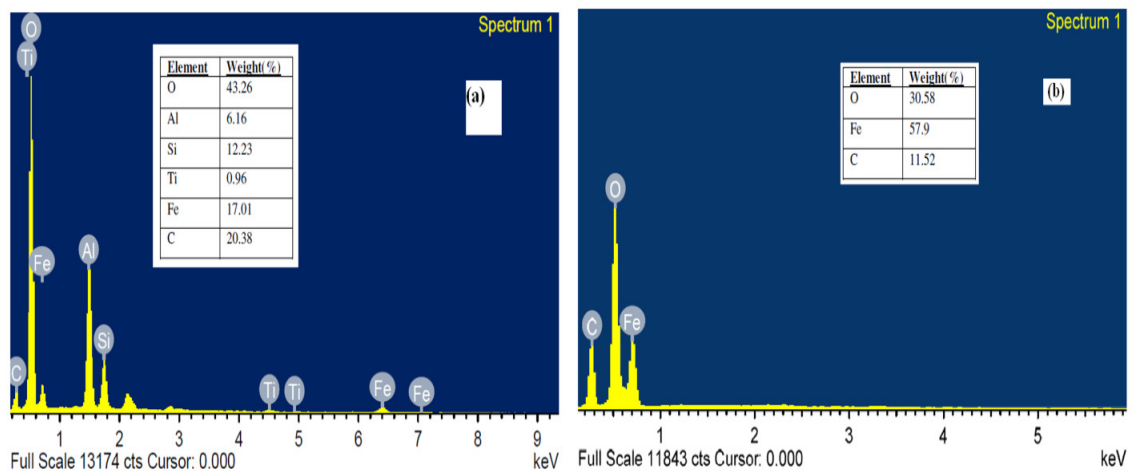**Figure.5.28.** FESEM images   a) Before synthesis of FeNP$_S$ b) After synthesis of FeNP$_S$

Figure. 5.29 EDS spectra of FeNPs a) Before synthesis b) After synthesis
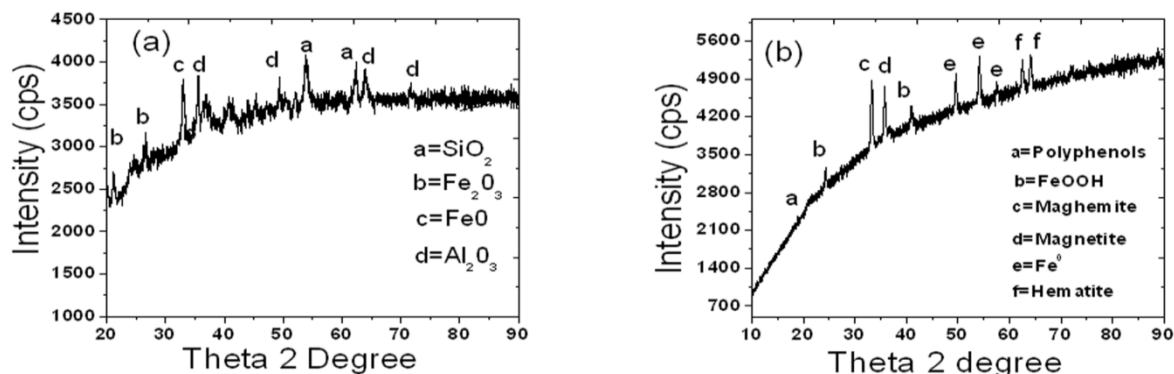
119

Figure 5.30 XRD patterns of FeNPs a) Before synthesis b) After synthesis
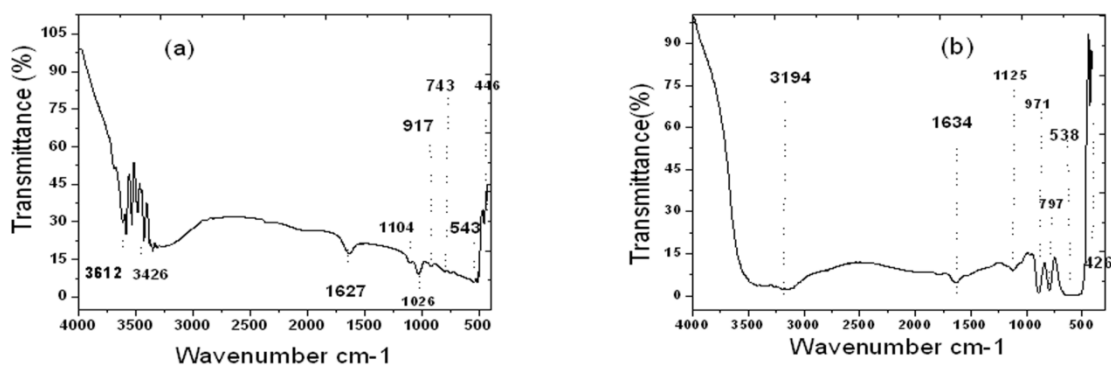
Figure. 5.31 FTIR patterns of FeNPs   a) Before synthesis   b) After synthesis

5.6.3 Central composite design

 To study the interactive effects between the independent factors (A, B, C and D) and responses (Y_1-Y_4), four 2nd order polynomial equations were obtained (Eqs. 5.27-5.30) from the design matrix (Table 5.16) and range of values (Independent variables) from the previous section were considered (dicamba or mixture of compounds with EG extracts).

%AR (Y_1)= 88.97 + 1.65 A + 1.14 B - 2.34 C - 0.34 D - 33.39 A*A - 13.15 B*B -

14.55 C*C+ 11.56 D*D   + 0.59 A*B   + 2.81 A*C   - 0.51 A*D   + 0.40 B*C

+ 2.06 B*D + 0.34 C*D   (5.27)

120

% 2,4D-R (Y$_2$) = 89.04 + 2.33 A + 1.85 B - 0.66 C + 3.76 D - 27.33 A*A - 23.85 B*B -

6.06 C*C + 10.77 D*D + 0.83 A*B + 1.55 A*C - 0.15 A*D + 1.64 B*C

+ 3.10 B*D + 0.60 C*D   (5.28)

% COD R(Y$_3$) = 82.39 + 0.35 A - 0.69 B - 1.01 C + 0.31 D - 37.99 A*A - 15.94 B*B -

12.71 C*C+ 14.58 D*D + 1.62 A*B + 0.67 A*C - 1.77 A*D + 0.62 B*C

0.83 B*D - 0.80 C*D   (5.29)

%DR (Y$_4$)= 79.54 + 4.15 A + 1.20 B - 0.85 C - 0.69 D - 25.49 A*A - 16.92 B*B -

13.14 C*C+ 14.74 D*D + 1.32 A*B + 1.60 A*C - 0.57 A*D + 1.34 B*C

+ 1.36 B*D + 0.47 C*D   (5.30)

In all four equations few term coefficients are showing positive effects on the responses ((%AR and %DR- A, B, D^2, AB, AC, BC, BD, CD), (2,4DR- A, B, D, D^2, AB, AC, BC, BD, CD), (%CODR- A, D, D^2, AB, AC, BC)) and D^2 has the highest positive value. To confirm this   ANOVA analysis was performed in Table 5.17, A-II-9 (%AR and 2,4-DR) and A-II-10 (% CODR and DR), where the F-values of all the four models are greater than 2.74 (F $_{0.05 (14, 11)}$) and pure error is less than 2.6, with lack of fit F value (<9%). Also, in all the four responses the lack of fit and the residual errors are almost close to each other. The accuracy of the model was evaluated with R^2 (A-III-21) and values are >88%. The R^2 $_{adj}$ was applied to correct the R^2 values and it was found that R^2 $_{adj}$ ≈R^2. The S. D<4, C.V<10% and A. P>4 confirms the best suitability of the model.

5.6.4. Effect of independent variables (A, B, C and D) on responses

In this heterogeneous Fenton's oxidation, the H$_2$O$_2$ dosage was varied from 172-688 mg/L (Figure.5.32(a)) and was   decided based on the   H$_2$O$_2$/COD ratio(1-4). When the H$_2$O$_2$ concentration was 430 mg/L (H$_2$O$_2$/COD=2.5), the removal efficiency was about 78-100%, where more OH radicals are produced.

Table 5.16 CCD design matrix for mixture of compounds (2,4-D_0=25 mg/L, A_0=3.5 mg/L, D_0=94 mg/L)

	Independent variables (uncoded and coded)				Fenton's Reagent		Actual Responses (%)				Predicted Responses (%)			
Run	A (H₂O₂/COD)	B (H₂O₂/Fe)	C (PH)	D (Time min)	H₂O₂ (mg/L)	Fe (mg/L)	A R	CODR	D R	24DR	A R	CODR	D R	24DR
1	2.5(0)	17(0)	5(0)	30(-1)	430	25.29	96.78	87.88	80.81	92.31	100	86.65	84.97	86.04
2	2.5(0)	32(1)	5(0)	135(0)	430	13.44	78.45	67.89	60.62	70.77	76.96	65.76	63.81	67.04
3	4(1)	2(-1)	7(1)	30(-1)	688	344	45.67	34.34	54.43	42.32	42.01	30.21	41.93	40.35
4	2.5(0)	17(0)	5(0)	135(0)	430	25.29	96.34	91.45	90	100	88.97	82.39	89.54	89.04
5	4(1)	32(1)	3(-1)	30(-1)	688	21.5	40	34.56	54.43	43.32	41.07	32.82	43.69	38.95
6	2.5(0)	17(0)	3(-1)	135(0)	430	25.29	65.66	65.43	60.61	70.77	76.75	70.69	67.25	83.65
7	4(1)	32(1)	7(1)	240(1)	688	21.5	45.67	22.34	50.32	56.67	45.22	28.8	48.06	57.43
8	4(1)	2(-1)	7(1)	240(1)	688	344	32.31	28.9	32.31	43.32	36.84	27.35	37.63	42.58
9	2.5(0)	17(0)	5(0)	135(0)	430	25.29	94.45	91.45	92.31	100	88.97	82.39	89.54	89.04
10	1(-1)	32(1)	3(-1)	240(1)	172	5.38	42.43	28.99	31.32	50.45	44.97	30.79	36.34	48.24
11	1(-1)	17(0)	5(0)	135(0)	172	10.12	57.89	42.32	56.9	60.45	53.93	44.05	49.9	59.38
12	1(-1)	2(-1)	7(1)	30(-1)	172	86	30.33	24.56	28.89	32.32	33.24	27.87	31.93	33.94
13	2.5(0)	17(0)	5(0)	240(1)	430	25.29	100	100	100	100	100.19	100	100	100
14	1(-1)	32(1)	7(1)	30(-1)	172	5.38	27.77	26.78	31.32	32.34	31.02	26.15	31.63	33.06
15	2.5(0)	17(0)	7(1)	135(0)	430	25.29	78.89	67.88	64.44	77.89	72.08	68.66	65.55	82.32
16	4(1)	2(-1)	3(-1)	240(1)	688	344	40.41	32.56	45.65	47.77	36.04	30.86	37.85	42.88
17	4(1)	2(-1)	3(-1)	30(-1)	688	344	44.98	27.89	36.78	43.33	42.54	30.54	44.05	43.06
18	4(1)	32(1)	3(-1)	240(1)	688	21.5	45.67	32.32	40.43	50.43	42.81	29.83	42.94	51.16
19	1(-1)	2(-1)	3(-1)	240(1)	172	86	40.43	35.67	34.44	43.32	40.55	38.3	36.53	43.29
20	1(-1)	2(-1)	7(1)	240(1)	172	86	32.32	32.69	26.66	36.6	30.13	32.1	29.91	36.79
21	1(-1)	32(1)	7(1)	240(1)	172	5.38	33.67	28.9	36.78	45.67	36.16	27.07	35.06	48.29
22	1(-1)	2(-1)	3(-1)	30(-1)	172	86	45.67	39.67	45.67	47.79	45	30.88	40.44	42.86
23	2.5(0)	2(-1)	5(0)	135(0)	430	215	68.9	58.96	56.87	52.31	74.68	67.13	61.42	63.34
24	1(-1)	32(1)	3(-1)	30(-1)	172	5.38	45.67	24.32	34.56	32.32	41.18	26.69	34.8	35.41
25	4(1)	32(1)	7(1)	30(-1)	688	21.5	42.21	36.78	43.45	40.43	42.14	34.97	46.91	42.81
26	4(1)	17(0)	5(0)	135(0)	688	40.47	48.98	40.43	43.45	55.67	57.23	44.74	58.2	64.05

Note:CODR=COD removal, AR=ametryn removal,DR=dicamba removal, 2,4-DR=2,4-D removal

Table 5.17. Analysis of Variance for % AR, %24DR, % CODR and %DR

Parameter	% AR	% 24DR	%CODR	%DR
R^2(coefficient of determination)	90.82	93.46	88.62	90.63
Standard deviation (S.D)	2.49	2.78	2.34	3.19
Coefficient of variation(CV) %	6.75	6.49	8.01	9.11
Adequate precision(AP)	75.83	89.2	20.76	29.75
Pure error	1.79	0	0	2.6
F-value	18.79	11.43	19.44	5.17

Note:CODR=COD removal, AR=ametryn removal,DR=dicamba removal, 2,4-DR=2,4-D removal

Table 5.18. Optimization of additional experiments

Run	Independent Factors				% CODR[a]		% AR[b]		%DR[c]		%24DR[d]		A.P [e]			
	A	B	C	D	Ac[f]	Pr[g]	Ac[f]	Pr[g]	Ac[f]	Pr[g]	Ac[f]	Pr[g]	CODR	AR	%DR	%24DR
27	1.59	17	6.5	135	60.02	63.71	64.49	66.28	58.91	61.3	72.99	78.12	17.3	37	25.6	15.2
28	3.35	17	6.42	135	63.31	65.22	71.2	72.59	66.97	68.52	78.56	80.89	34.1	52.2	44.2	34.7
29	1.18	17	3.59	135	47.58	51.12	57.91	60.85	51.29	56.21	64.31	66.62	14.4	20.7	11.4	28.8
30	3.41	17	3.89	135	64.8	65.8	73.36	78.81	68.44	72.88	78.21	82.96	65.8	14.5	16.4	17.5

Note :[a] % CODR=% COD removal; [b] % AR= % ametryn removal; [c] DR=% Dicamba removal; [d]24DR=% 24D removal ; [e] A.P= Adequate Precision ; [f] Ac=Actual values; [g] Pr=Predicted values

Many literatures say that, higher dosage of H_2O_2, increases the removal efficiency (Pignatello et al. 2006, Xu and Wang 2011), however, when concentration increased to 688 mg/L the degradation was reduced (scavenging effect). However, in case run 6 and 23, with optimum H_2O_2 dosage of 430 mg/L oxidation rate decreased. This clearly says that, the efficiency also depends on the other variables such as pH and H_2O_2/Fe.

The effect of iron nanoparticles was tested for all four responses (Figure. 5.32(b)) and accordingly dosage was varied from 5.38-344mg/L. The results show that, the removal rate was reduced, as the catalyst dosage was increased (40.47, 86, 215, 344 mg/L). This may be due to the formation of cluster of nanoparticles leads to the suppression of $^{\bullet}$OH radicals. When iron dose was decreased (21.5, 13.44, 10.12, 5.38 mg/L) the lesser degradation rate was observed and this may be due to the formation of $^{\bullet}$OOH radicals by reducing the re-generation of Fe^{2+} ions (Garrido-Ramírez et al. 2010, Masomboon et al. 2009). The XRD pattern clearly indicates that, LFeNPs consists of oxides of iron and Fe^0

and the regeneration of Fe^{2+}/Fe^{3+} was observed through the diffusion on oxide core surface. The diffusion rate was maximum at 25.29mg/L of FeNPs and also in situ generation of Fe^{2+}/Fe^{3+} was observed through Fe^0 NPs. Hence, finally of 25.29mg/L FeNPs was considered.

The pH varied from 3-7 and in runs (1, 4, 9 and 13) at pH 5, the highest removal efficiency was observed with optimum Fenton's dosage (H_2O_2=430mg/L, Fe=25.29mg/L, H_2O_2/COD=2.5, H_2O_2/Fe=17). In contrast, in case of run 6 and 15 with similar optimum conditions, comparatively less removal was observed (<79%) and also there is a significant increase in removal efficiency at pH 7 than pH 3. It clearly indicates that, an increase in pH from 6-8 has the positive effect on advanced Fenton process (AFP) than conventional Fenton process ($FeSO_4$. $7H_2O$, $FeCl_3$).

In comparison with pH 5 (Run 13) and 7(run 15), 100% removal was observed at pH 5 by producing more hydroxyl radicals. At pH 7, fast decomposition of oxidant to H_2O and O_2 and also a less electrostatic attraction with herbicides and LFeNPs was observed, which leads to less OH radical production. The similar kind of optimal pH was established in the other advanced Fenton process (86.4% degradation of 17β-estradiol at pH 7.47; 95% removal of salicylic acid at pH 6 (Yaping and Jiangyong 2008). It is totally reverse in conventional processes, where the optimum pH was at 3-3.5 (Manu and Mahmood 2011, Wang et al. 2016, Kuang et al. 2013, Zhou et al. 2004, Ambika et al. 2016, Neppolian et al. 2004, Zhang et al. 2017). This variation in pH depends on the morphological characteristics of the catalyst such as leaching and adsorption. At pH 5, the adsorption of herbicides on the LFeNPs (Fe_2O_3, Fe_3O_4, $Fe(OH)_x$, Fe^0) along with generation of $^\bullet$OH radicals, thereby 100% removal of these herbicides is achieved. At pH 3(<4), high amount of dissolved Fe was leached from the catalyst surface, which reduces the adsorption capacity and this dissolved iron has less stable towards the catalyst activity (Chou et al., 2001). At pH 7, maybe there is a formation of iron hydroxide complexes (Lucas and Peres 2006), which leads to lesser degradation than pH 5. Hence, it clearly indicates that, at pH 5 no leaching of iron was observed and favored the recycle of LFeNPs until the completion of mineralization.
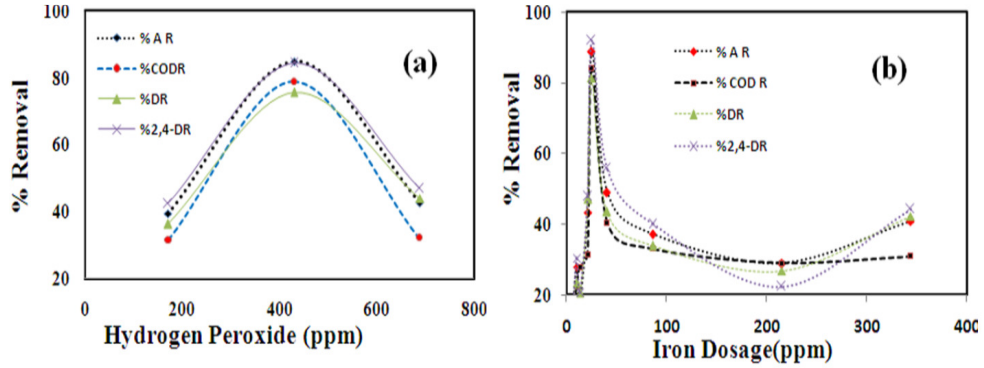
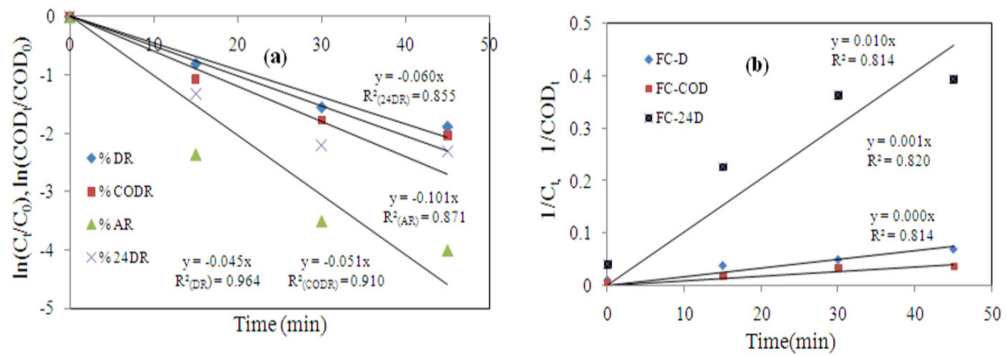**Figure. 5.32.** Removal efficiency vs a) dosage of H_2O_2 b) dosage of iron

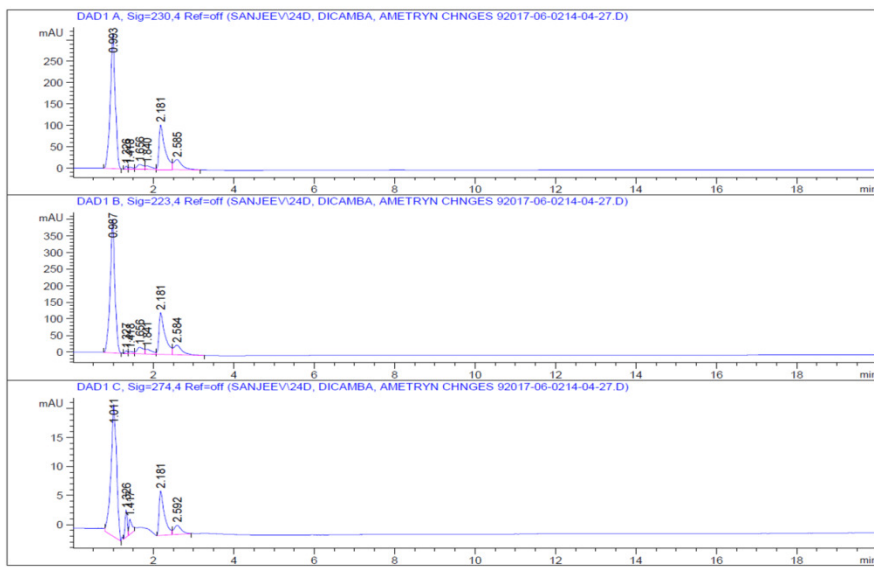**Figure. 5.33. a)** 1st order kinetics b) 2nd order kinetics

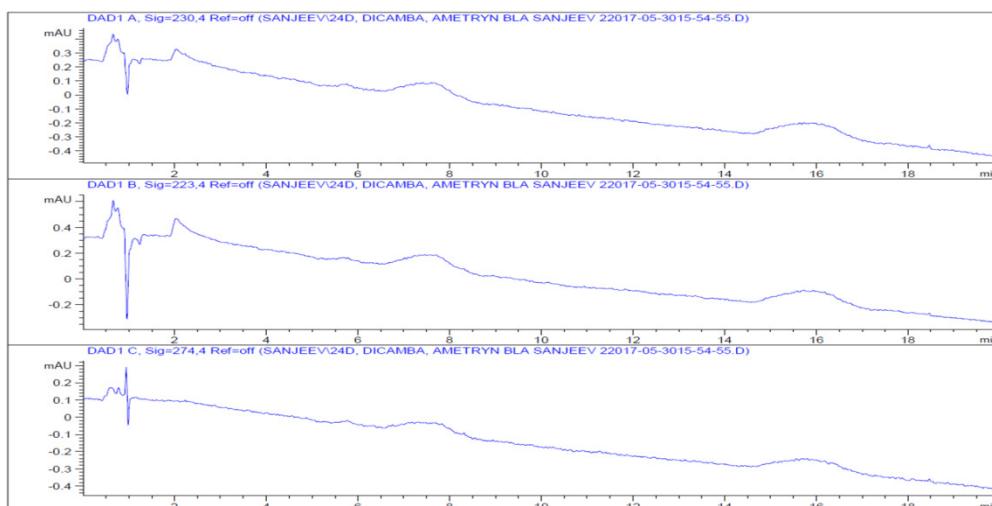**Figure. 5.34** HPLC chromatograph before mixing all three herbicides

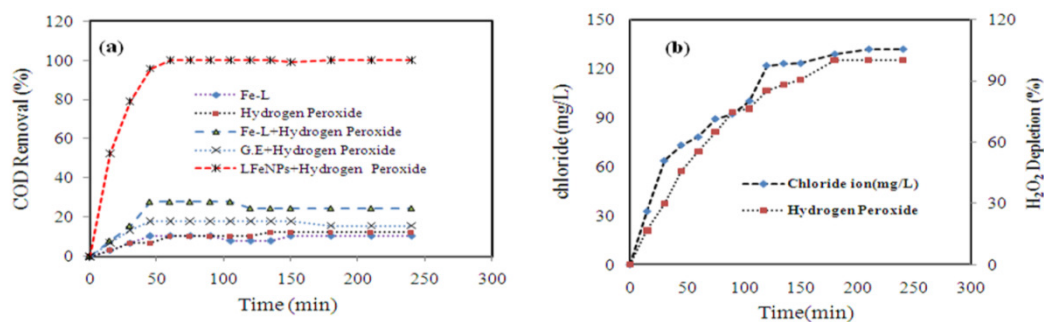**Figure. 5.35** HPLC chromatograph after mixing all three herbicides

Figure. 5.36. a) Effect of COD removal on different type of combinations vs time   b) release of chloride and hydrogen peroxide depletion vs time

5.6.5 Kinetic studies

From the Table 5.16, it was observed that   optimum conditions are 25.29 mg/L of iron, 430 mg/L of H_2O_2 with pH 5, and these conditions are maintained to study the kinetic aspects. It is seen that, the degradation was faster with   removal efficiency of 80-96% till 30 min, after that degradation efficiency was fully reduced, and   all herbicides are fully degraded in 135 min. Here also, both pseudo 1st and 2nd order kinetics were studied (Eqs(5.19-5.20)) and are   plotted in Figure.5.33(a)(b). From this figure, it is clear that, the R^2 values are >0.85 (R^2_{24DR} =0.855, R^2_{AR}=0.871, R^2_{CODR}=0.910, R^2_{DR}=0.964) for 1st

order model   and for the 2nd order model the values are <0.82(R^2_{24DR} $=0.814$, $R^2_{DR}=0.820$, R^2_{CODR} $=0.814$). It clearly indicates that, 1st order kinetics was best fitted than 2nd order. The rate constants are also significantly increased from 0.04-0.1 min^{-1} (K_{24DR} $=0.06$, $K_{AR}=0.10$, $K_{CODR}=0.05$, $K_{DR}=0.04$ min^{-1}) and ametryn has the highest rate constant of 0.1. It confirms that, the degradation of ametryn is more endothermic in nature than other herbicides and this may be due to the more number of electrons that are activated on the surface of the LFeNPs in aqueous phase and are quickly transferred to H_2O_2 for further oxidation (Chen et al. 2013). Also, the rate constant of %CODR is less than the %24DR and %AR and more than %DR.

It clearly signifies that, the degradation of 2, 4-D and ametryn was faster than the mineralization and in case of dicamba it is reverse. Many of the AFPs literatures are witnessed for the suitability pseudo-1st order model where the R^2 values are from 0.71-0.99 (Swaminathan et al. 2003, Wu et al. 2015, Kong and Lemley 2006, Khataee and Pakdehi 2014, Kakavandi et al. 2016, Zhang et al. 2016, Shahwan et al. 2011). This AFPs at the initial stages (45 min) starts with adsorption onto the surface of iron oxides (LFeNPs) and Fe^0 and later ends with degradation followed by mineralization. To confirm this, mixture of herbicides is analyzed through HPLC before (Figure.5.34) and after (Figure.5.35) Fenton process. When all the three herbicides are mixed, there is a formation of different type compounds at the starting stage itself (actual retention time of all three compounds (1.38, 8.82, 1.7 min) is different from combined one) and after treatment no such peaks were observed. The oxidation process includes the conversion of Fe^0- Fe^{2+} and in parallel, Fe^{2+}/ Fe^{3+} from Fe$_2$O$_3$/ Fe$_3$O$_4$ by generating OH radicals at pH 5 and these radicals react with herbicides to form mineralized products (Garrido-Ramírez et al. 2010, Kuang et al. 2013). After 45 min, the oxidation process was decreased due to the formation of OOH radicals. To confirm the optimized conditions, the different types of control experiments were performed (Figure. 5.36(a)) and combination of LFeNPs + H_2O_2 showed the   highest removal efficiency. The other combinations such as Fe-L(laterite extracted iron), H_2O_2, Fe-L+H_2O_2, G.E (Green Extract)+ H_2O_2 are yielding lesser COD   removal efficiency(<32%). To confirm the

mineralization process, the release of chloride ion along with H_2O_2 decomposition was monitored (Figure. 5.36.(b)) and full depletion of oxidant was observed with residual chloride of 123 mg/L, which is within the standard limits(IS10500-2012). The excess chloride is removed with reverse asmosis, ion exchange, electrochemical and adsorption methods followed by Fenton process. The Figure A-III-22 confirms the optimum operating conditions. Finally, the cost of production of FeNPs was evaluated and it was found that, Rs. 205/10 g of FeNPs (A-II-11).

This heterogeneous Fenton process was finally validated by superimposing the contours for all four responses in Figure.5.37 (Mason et al., 2003). Here, minimum and maximum constraints were selected based on the observed values(% 24DR(32, 100), % DR(26, 100), % AR(30 , 100), % CODR(22, 100)) with a reaction time of 135 min. To validate the optimum region, four sets of additional experiments were conducted (Table 5.18) and results are reliable.

In the present study, COD values considered instead of TOC, with the assumption that, complete oxidation of the organic components from the action of strong oxidizing agents. In a real situation, some aromatic compounds are not completely oxidized under acidic conditions and also Fe^{2+} (inorganic) contribute its COD to the total organic load, thus making the observed values an incorrect reflection of the actual oxygen requirements for oxidation. To establish the relation between TOC and COD removal, two sets of experiments (experimental conditions of run 27 and Run 29) were performed. In case of run 27 (COD=60mg/L) and run 29 (COD=47 mg/L), the TOC removal was found to be 66.2% and 50.6% respectively (Initial TOC concentration (TOC_0) =49.8 mg/L). With these results, it can be concluded that, 3-6% increase in the mineralization was observed.
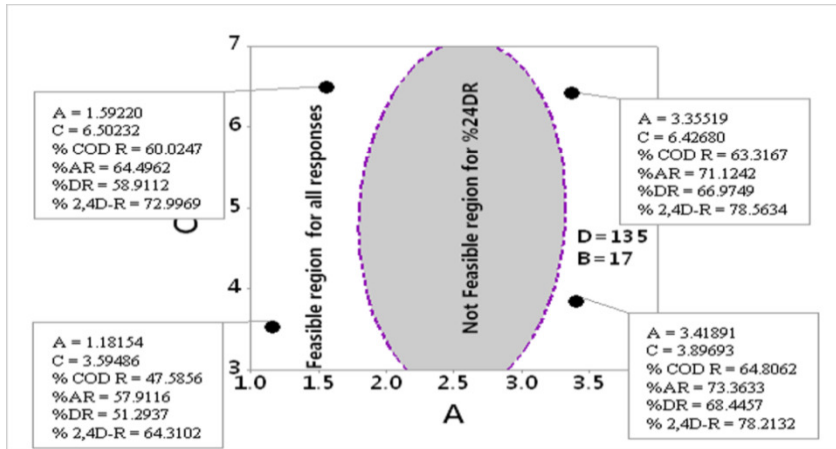
Figure.5.37. Contour overlay plot

CHAPTER 6

CONCLUSIONS

Agricultural runoff water and aqueous solution containing herbicides (ametryn, dicamba and 2,4-D) were successfully treated with conventional Fenton's process(CFP). Later, the advanced Fenton process (AFP) was adopted to increase the removal efficiency of herbicides. In AFP the iron nanoparticles were synthesized from a raw laterite using eucalyptus globules (EG) and Tactona Glandis(TG) leaf extracts. After that, these nanoparticles were used as a catalyst in Fenton –like process for the oxidation of ametryn, dicamba, 2,4-D and mixture of compounds in aqueous medium. Based on the results, the following conclusions were drawn.

6.1. Conventional Fenton's process (CFP)

6.1.1 Agriculture runoff water

- The conventional Fenton process has established the potential for the treatment of agriculture runoff water containing herbicides and maximum removal efficiencies were observed to be 100%, 95% and 88% for ametryn, dicamba and 2, 4-D respectively, with the reaction time of 135 min. Here, the H_2O_2/COD parameter is influencing more than the other variables (Percent contribution=67.57% and highest F-value).

- In addition, H_2O_2/Fe^{2+}, the reaction time and pH were ranked as 2 for all four responses. The optimum values were observed to be 2.125, 27.5, 3.5 and 135 min for A(H_2O_2/COD)=2.125, B=27.5($H_2O_2/Fe^{2+)}$, C= 3.5(pH) and D(reaction time)= 240 min respectively with H_2O_2 dosage of 5.44mM and Fe^{2+} dosage of 0.12mM.

6.1.2 Aqueous Solution

- The highest removal efficiency of 83-85% was achieved (H_2O_2 =11.38 mM, Fe^{2+}=0.33 mM, pH=3.5, reaction time=135 min) and LC/MS analysis confirmed that, 82% of dicamba was mineralized to oxalic acid, chloride ion, CO_2, and H_2O.

131

- The 100% ametryn was degraded with optimum values of H_2O_2= 0.5 mM, Fe^{2+}= 0.011 mM, pH=3.5 with the reaction time=240 min and LCMS analysis shows that there is a formation of thiocynate ion.

- In case of 2, 4-D, > 80% removal was observed with Fenton's dosage of H_2O_2=3.81mM, Fe^{2+}=0.07mM and LCMS analysis indicates that, there is a production of Maleic acid. Finally the mixture of compounds in aqueous medium was successfully treated (>75%).

- The ANOVA results of all three herbicides confirmed that S.D (<5), C.V(<10%) and A.P(>4) values were within the recommended values and treatment process was successfully validated with contour overlay plot.

- A mixture of compounds in aqueous medium was successfully treated with optimum Fenton's dosage of H_2O_2=10.75mM, Fe^{2+}=0.24mM

- In all treatment process, the 98-100% consumption of H_2O_2 in 240 min and 65-85% of herbicides removal was observed in less than 30 min.

6.2. Advance Fenton's process (AFP)

- With FESEM and BET analysis, it was found that 20-70nm(EG) and 50-100nm(TG) of spherical particles were formed with surface area of 31- 36.62 m^2/g, which are having a pore volume of 0.038-0.0394cm^3/g for TG and EG respectively. The XRD analysis shows that, LGFeNPs consists of mainly Fe^0, Fe_2O_3, Fe_3O_4 and polyphenols. The Functional groups were confirmed by FTIR analysis.

- The 100% removal of ametryn, dicamba, 2,4-D and mixture of compounds (both extracts) was achieved with optimum conditions{[2.125 (A), 6 (B), 3.5 (C) , 135 (D), H_2O_2=17 mg/L, Fe=2.83], [2.5 (A), 17 (B), 5 (C) , 135 (D), H_2O_2=455 mg/L, Fe=26.8 mg/L], [2 (A), 12 (B), 4.5 (C), 30 (D), H_2O_2=122 mg/L, Fe=10.17mg/L] ,[2.5 (A), 17 (B), 5 (C), 135 (D), H_2O_2=430mg/L, Fe=25.29 mg/L]} for ametryn, dicamba, 2,4-D and mixture of compounds (EG and TG extracts) respectively.

- The EG extract is showing higher polyphenols and antioxidant property (5 mM of GA, 50mM of Fe^{2+}) than TG extract(3.5mM of GA, 33mM of Fe^{2+}).

- The pseudo-1st order kinetic model was best fitted to the experimental data than the 2nd order model (R^2 >0.85 in both responses).

- The cost of production of FeNPs was found to be Rs. 205/10 g FeNPs, which is cheaper than the commercial grade nanoparticles and thereby making the treatment process cost effective.

- ANOVA results prove that, very good model equations were developed (A.P >4, C.V<10) and optimized conditions were successfully validated with the help of contour overlay plot.

Based on the above findings some general conclusions were drawn:

- The agriculture runoff water containing herbicides and aqueous solution can be easily treated with Fenton process even at higher concentration.

- The AFP is working near to the neutral pH, which can overcome the limitation of the conventional Fenton process.

- The advance Fenton process (AFP) is able to yield higher removal efficiency than the conventional Fenton process (CFP).

- The drawback of sludge formation in CFP can be overcome by the application of GLFeNPs as a Fenton catalyst.

- The sustainable plant extracts showed better results in synthesizing FeNPs.

- The synthesis of laterite based nanoparticles using sustainable extracts proved to be an alternative and novel catalyst for the Fenton's oxidation of herbicides.

- The cost of production of FeNPs is less compared to the commercially available Fe nanopowders.

All the results are satisfactory for degradation and mineralization of herbicides. Hence, AFP is recommended for oxidation studies.

6.3 Scope for the future work

The present research work can be extended:

- To study the reusability charecteristics of laterite based FeNPs.

- To synthesize laterite based nanopartciles for different kind of leaf extracts.

- To the continuous treatment process for the degradation of these herbicides.

REFERENCES

Aga, D. S., and Thurman, E. M. (2001). "Formation and transport of the sulfonic acid metabolites of alachlor and metolachlor in soil". *Environmental Science and Technology*, *35*(12), 2455-2460.

Ahmadi, M., Vahabzadeh, F., Bonakdarpour, B., Mofarrah, E., and Mehranian, M. (2005). "Application of the central composite design and response surface methodology to the advanced treatment of olive oil processing wastewater using Fenton's peroxidation". *Journal of Hazardous Materials*, *123*(1), 187-195.

Ahmad, A. L., Ismail, S., and Bhatia, S. (2005). "Optimization of coagulation–flocculation process for palm oil mill effluent using response surface methodology". *Environmental Science and Technology*, *39*(8), 2828-2834.

Aleksić, M., Kušić, H., Koprivanac, N., Leszczynska, D., and Božić, A. L. (2010). "Heterogeneous Fenton type processes for the degradation of organic dye pollutant in water—The application of zeolite assisted AOPs". *Desalination*, *257*(1), 22-29.

Ali, N., Neto, V. F., Mei, S., Cabral, G., Kousar, Y., Titus, E., ... and Gracio, J. (2004). "Optimisation of the new time-modulated CVD process using the Taguchi method". *Thin Solid Films*, *469*, 154-160.

Amritha, A. S., and Manu, B. (2016). "Low cost Fentons oxidative degradation of 4-nitroaniline using iron from laterite". *Water Science and Technology*, *74*(8), 1919-1925.

Ambika, S., Devasena, M., and Nambi, I. M. (2016). "Synthesis, characterization and performance of high energy ball milled meso-scale zero valent iron in Fenton reaction". *Journal of Environmental Management*, *181*, 847-855.

APHA, AWWA, WPCF (Eds.), 2005, 21st edition, "Standard methods for the examination of water and wastewater". Washington DC.

Arora, S., and Gopal, M. (2004). "Residues of pendimethalin after weed control in cabbage crop (Brassica oleracea var L. Capitata)".*Bulletin of Environmental Contamination and Toxicology*, *73*(1), 106-110.

Ayodele, O. B., and Togunwa, O. S. (2014). "Catalytic activity of copper modified bentonite supported ferrioxalate on the aqueous degradation and kinetics of mineralization of Direct Blue 71, Acid Green 25 and Reactive Blue 4 in photo-Fenton process". *Applied Catalysis A: General*, *470*, 285-293.

Aziz, A. A., and Daud, W. M. A. W. (2012). "Oxidative mineralisation of petroleum refinery effluent using Fenton-like process". *Chemical Engineering Research and Design*, *90*(2), 298-307.

Bach, A., Shemer, H., and Semiat, R. (2010). "Kinetics of phenol mineralization by Fenton-like oxidation". *Desalination*, *264*(3), 188-192.

Barbash, J. E., Thelin, G. P., Kolpin, D. W., and Gilliom, R. J. (2001). "Major herbicides in ground water". *Journal of Environmental Quality*, *30*(3), 831-845.

Beg, Q. K., Sahai, V., and Gupta, R. (2003). "Statistical media optimization and alkaline protease production from Bacillus mojavensis in a bioreactor". *Process Biochemistry*, *39*(2), 203-209.

Beltrán, F. J., & Rey, A. (2018). Free Radical and Direct Ozone Reaction Competition to Remove Priority and Pharmaceutical Water Contaminants with Single and Hydrogen Peroxide Ozonation Systems. *Ozone: Science & Engineering*, *40*(4), 251-265.

Bigda, R. J. (1995). "Consider Fentons chemistry for wastewater treatment". *Chemical Engineering Progress*, *91*(12).

Box, G. E., and Behnken, D. W. (1960). "Some new three level designs for the study of quantitative variables". *Technometrics*,*2*(4), 455-475.

Box, G. E. P. and Wilson, K. B. (1951). "On the experimental attainment of optimum conditions". *J. Roy. Statist. Soc. Ser. B.*, 13, 1–45.

Broholm, M. M., Rügge, K., Tuxen, N., Højberg, A. L., Mosbæk, H., and Bjerg, P. L. (2001). "Fate of herbicides in a shallow aerobic aquifer: a continuous field injection experiment (Vejen, Denmark) ".*Water Resources Research*, *37*(12), 3163-3176.

Brillas, E., Banos, M. A., Skoumal, M., Cabot, P. L., Garrido, J. A., and Rodríguez, R. M. (2007). "Degradation of the herbicide 2, 4-DP by anodic oxidation, electro-Fenton and photoelectro-Fenton using platinum and boron-doped diamond anodes". *Chemosphere*,*68*(2), 199-209.

Brillas, E., Boye, B., Sirés, I., Garrido, J. A., Rodríguez, R. M., Arias, C., and Comninellis, C. (2004). "Electrochemical destruction of chlorophenoxy herbicides by anodic oxidation and electro-Fenton using a boron-doped diamond electrode".*Electrochimica Acta*, *49*(25), 4487-4496.

Brillas, E., Banos, M. A., and Garrido, J. A. (2003). "Mineralization of herbicide 3, 6-dichloro-2-methoxybenzoic acid in aqueous medium by anodic oxidation", electro-Fenton and photoelectro-Fenton.*Electrochimica Acta*, *48*(12), 1697-1705.

Brillas, E., Calpe, J. C., and Casado, J. (2000). "Mineralization of 2, 4-D by advanced electrochemical oxidation processes". *Water Research*, *34*(8), 2253-2262.

Calabrese, E. J., and Kostecki, P. T. (1989). "Petroleum Contaminated Soil, Remedation Technologies, Environmental Fate, Risk Assessment, Analytical Methodologies". vol. 2.

Celis, E., Elefsiniotis, P., and Singhal, N. (2008). "Biodegradation of agricultural herbicides in sequencing batch reactors under aerobic or anaerobic conditions". *Water Research*, *42*(12), 3218-3224.

Chu, W., Kwan, C. Y., Chan, K. H., and Chong, C. (2004). "An unconventional approach to studying the reaction kinetics of the Fenton's oxidation of 2, 4-dichlorophenoxyacetic acid".*Chemosphere*, *57*(9), 1165-1171.

Chu, W., Gao, N., Li, C., and Cui, J. (2009). "Photochemical degradation of typical halogenated herbicide 2, 4-D in drinking water with UV/H 2 O 2/micro-aeration". *Science in China Series B: Chemistry*, *52*(12), 2351-2357.

Chen, H., Zhang, Z., Yang, Z., Yang, Q., Li, B., and Bai, Z. (2015). "Heterogeneous fenton-like catalytic degradation of 2, 4-dichlorophenoxyacetic acid in water with FeS". *Chemical Engineering Journal*, *273*, 481-489.

Chen, Z., Wang, T., Jin, X., Chen, Z., Megharaj, M., and Naidu, R. (2013). "Multifunctional kaolinite-supported nanoscale zero-valent iron used for the adsorption and degradation of crystal violet in aqueous solution". *Journal of Colloid and Interface Science*, *398*, 59-66.

Chen, Y., Wang, J., Ou, Y., Chen, H., Xiao, S., Liu, G., ... and Huang, Q. (2014). "Cellular antioxidant activities of polyphenols isolated from Eucalyptus leaves (Eucalyptus grandis× Eucalyptus urophylla GL9) ". *Journal of Functional Foods*, *7*, 737-745.

Chou, S., Huang, C., and Huang, Y. H. (2001). "Heterogeneous and homogeneous catalytic oxidation by supported γ-FeOOH in a fluidized-bed reactor: kinetic approach". *Environmental Science and Technology*, *35*(6), 1247-1251.

Chrysochoou, M., Johnston, C. P., and Dahal, G. (2012). "A comparative evaluation of hexavalent chromium treatment in contaminated soil by calcium polysulfide and green-tea nanoscale zero-valent iron". *Journal of Hazardous Materials*, *201*, 33-42.

Conte, L. O., Schenone, A. V., and Alfano, O. M. (2016). "Photo-Fenton degradation of the herbicide 2, 4-D in aqueous medium at pH conditions close to neutrality". *Journal of Environmental Management*, *170*, 60-69.

Conte, L. O., Farias, J., Albizzati, E. D., and Alfano, O. M. (2012). "Photo-Fenton degradation of the herbicide 2, 4-dichlorophenoxyacetic acid in laboratory and solar pilot-plant reactors". *Industrial and Engineering Chemistry Research*, *51*(11), 4181-4191.

Coupe, R. H., and Blomquist, J. D. (2004). "Water-soluble pesticides in finished water of community water supplies". *Journal (American Water Works Association)*, *96*(10), 56-68.

Colombo, R., Ferreira, T. C., Alves, S. A., Carneiro, R. L., and Lanza, M. R. (2013). "Application of the response surface and desirability design to the Lambda-cyhalothrin degradation using photo-Fenton reaction". *Journal of Environmental Management*, *118*, 32-39.

Cserhati, T., and Forgacs, E. (1998). "Phenoxyacetic acids: separation and quantitative determination". *Journal of Chromatography B: Biomedical Sciences and Applications*, *717*(1), 157-178.

Davis, A. P. (2007). "Field performance of bioretention: Water quality". *Environmental Engineering Science*, *24*(8), 1048-1064.

Derylo-Marczewska, A., Blachnio, M., Marczewski, A. W., Swiatkowski, A., and Tarasiuk, B. (2010). "Adsorption of selected herbicides from aqueous solutions on activated carbon". *Journal of Thermal Analysis and Calorimetry*, *101*(2), 785-794.

De la Plata, G. B. O., Alfano, O. M., and Cassano, A. E. (2010). "Decomposition of 2-chlorophenol employing goethite as Fenton catalyst. I. Proposal of a feasible, combined reaction scheme of heterogeneous and homogeneous reactions". *Applied Catalysis B: Environmental*, *95*(1), 1-13.

Dehghani, M., Nasseri, S., and Karamimanesh, M. (2014). "Removal of 2, 4-Dichlorophenolylxacetic acid (2, 4-D) herbicide in the aqueous phase using modified granular activated carbon". *Journal of Environmental Health Science and Engineering*, *12*(1), 28.

Ding, L., Lu, X., Deng, H., and Zhang, X. (2012). "Adsorptive removal of 2, 4-dichlorophenoxyacetic acid (2, 4-D) from aqueous solutions using MIEX resin". *Industrial and Engineering Chemistry Research*, *51*(34), 11226-11235.

Drzewicz, P., Gehringer, P., Bojanowska-Czajka, A., Zona, R., Solar, S., Nałcz-Jawecki, G., ... and Trojanowicz, M. (2005). "Radiolytic degradation of the herbicide dicamba for environmental protection". *Archives of Environmental Contamination and Toxicology*, *48*(3), 311-322.

Duesterberg, C. K., and Waite, T. D. (2006). "Process optimization of Fenton oxidation using kinetic modeling". *Environmental Science and Technology*, *40*(13), 4189-4195.

FAO. (2011), "Food and Agricultural Organization". Main Report.

Fabbri, D., Prevot, A. B., and Pramauro, E. (2007). "Analytical monitoring of the photo-induced degradation of 3, 6-dichloro-2-methoxybenzoic acid in homogeneous and heterogeneous systems". *Research on Chemical Intermediates*, *33*(3), 393-405.

Farré, M., Fernandez, J., Paez, M., Granada, L., Barba, L., Gutierrez, H., ... and Barcelo, D. (2002). "Analysis and toxicity of methomyl and ametryn after biodegradation". *Analytical and Bioanalytical Chemistry*, *373*(8), 704-709.

Farran, A., and Ruiz, S. (2004). "Application of solid-phase extraction and micellar electrokinetic capillary chromatography to the study of hydrolytic and photolytic degradation of phenoxy acid and phenylurea herbicides". *Journal of Chromatography A*, *1024*(1), 267-274.

García, O., Isarain-Chávez, E., Garcia-Segura, S., Brillas, E., and Peralta-Hernández, J. M. (2013). "Degradation of 2, 4-dichlorophenoxyacetic acid by electro-oxidation and electro-Fenton/BDD processes using a pre-pilot plant". *Electrocatalysis*,*4*(4), 224-234.

Garrido-Ramírez, E. G., Theng, B. K. G., and Mora, M. L. (2010). "Clays and oxide minerals as catalysts and nanocatalysts in Fenton-like reactions—a review". *Applied Clay Science*, *47*(3), 182-192.

Gao, N. Y., Deng, Y., and Zhao, D. (2009). "Ametryn degradation in the ultraviolet (UV) irradiation/hydrogen peroxide (H 2 O 2) treatment". *Journal of Hazardous Materials*, *164*(2), 640-645.

García-Gómez, C., Vidales-Contreras, J. A., Nápoles-Armenta, J., and Gortáres-Moroyoqui, P. (2016). "Optimization of phenol removal using Ti/PbO 2 anode with response surface methodology". *Journal of Environmental Engineering*, *142*(4), 04016004.

Ghoshdastidar, A. J., and Tong, A. Z. (2013). "Treatment of 2, 4-D, mecoprop, and dicamba using membrane bioreactor technology". *Environmental Science and Pollution Research*, *20*(8), 5188-5197.

Gualtieri, M. L., Romagnoli, M., Pollastri, S., and Gualtieri, A. F. (2015). "Inorganic polymers from laterite using activation with phosphoric acid and alkaline sodium silicate solution: mechanical and microstructural properties". *Cement and Concrete Research*,*67*, 259-270.

Hallberg, G. R. (1989). "Pesticides pollution of groundwater in the humid United States. *Agriculture, Ecosystems and Environment*,*26*(3-4), 299-367.

Han, D., Jia, W., and Liang, H. (2010). "Selective removal of 2, 4-dichlorophenoxyacetic acid from water by molecularly-imprinted amino-functionalized silica gel sorbent". *Journal of Environmental Sciences*, *22*(2), 237-241.

Hameed, B. H., and Lee, T. W. (2009). "Degradation of malachite green in aqueous solution by Fenton process". *Journal of Hazardous Materials*, *164*(2), 468-472.

Hassan, H., and Hameed, B. H. (2011). "Fe–clay as effective heterogeneous Fenton catalyst for the decolorization of Reactive Blue 4". *Chemical Engineering Journal*, *171*(3), 912-918.

Hamilton, D. J., Ambrus, A., Dieterle, R. M., Felsot, A. S., Harris, C. A., Holland, P. T., ... and Wong, S. S. (2003). "Regulatory limits for pesticide residues in water (IUPAC Technical Report) ". *Pure and applied Chemistry*, *75*(8), 1123-1155.

Hermosilla, D., Merayo, N., Ordóñez, R., and Blanco, Á. (2012). "Optimization of conventional Fenton and ultraviolet-assisted oxidation processes for the treatment of reverse osmosis retentate from a paper mill". *Waste Management*, *32*(6), 1236-1243.

Heppell, C. M., and Chapman, A. S. (2006). "Analysis of a two-component hydrograph separation model to predict herbicide runoff in drained soils". *Agricultural Water Management*, *79*(2), 177-207.

Hoag, G. E., Collins, J. B., Holcomb, J. L., Hoag, J. R., Nadagouda, M. N., and Varma, R. S. (2009). "Degradation of bromothymol blue by 'greener'nano-scale zero-valent iron synthesized using tea polyphenols". *Journal of Materials Chemistry*, *19*(45), 8671-8677.

Hoigné, J., and Bader, H. (1983). "Rate constants of reactions of ozone with organic and inorganic compounds in water—I: non-dissociating organic compounds". *Water Research*, *17*(2), 173-183.

Huang, L., Weng, X., Chen, Z., Megharaj, M., and Naidu, R. (2014). "Synthesis of iron-based nanoparticles using oolong tea extract for the degradation of malachite green". *Spectrochimica Acta Part A: Molecular and Biomolecular Spectroscopy*, *117*, 801-804.

Ignat, I., Volf, I., and Popa, V. I. (2011). "A critical review of methods for characterisation of polyphenolic compounds in fruits and vegetables". *Food Chemistry*, *126*(4), 1821-1835.

Im, J. K., Cho, I. H., Kim, S. K., and Zoh, K. D. (2012). "Optimization of carbamazepine removal in O 3/UV/H 2 O 2 system using a response surface methodology with central composite design". *Desalination*, *285*, 306-314.

ISO (2005). "Determination of substances characteristic of green and black tea – Part 1: Content of total polyphenols in tea – Colorimetric method using Folin-Ciocalteu reagent". ISO 14502-1.

Jacomini, A. E., Camargo, P. B. D., Avelar, W. E., and Bonato, P. S. (2009). "Determination of ametryn in river water, river sediment and bivalve mussels by liquid chromatography-tandem mass spectrometry". *Journal of the Brazilian Chemical Society*, *20*(1), 107-116.

Jiang, L., Huang, J., Liang, L., Zheng, P. Y., and Yang, H. (2008). "Mobility of prometryne in soil as affected by dissolved organic matter". *Journal of Agricultural and Food Chemistry*, *56*(24), 11933-11940.

Jones, R. J., and Kerswell, A. P. (2003). "Phytotoxicity of photosystem II (PSII) herbicides to coral". *Marine Ecology Progress Series*, *261*, 149-159.

Joglekar, A. M., and May, A. T. (1987). "Product excellence through design of experiments". *Cereal Foods World*, *32*(12), 857.

Kamble, S. P., Deosarkar, S. P., Sawant, S. B., Moulijn, J. A., and Pangarkar, V. G. (2004). "Photocatalytic degradation of 2, 4-dichlorophenoxyacetic acid using concentrated solar radiation: batch and continuous operation". *Industrial and Engineering Chemistry Research*, *43*(26), 8178-8187.

Kavitha, V., and Palanivelu, K. (2004). "The role of ferrous ion in Fenton and photo-Fenton processes for the degradation of phenol". *Chemosphere*, *55*(9), 1235-1243.

Kasozi, G. N., Nkedi-Kizza, P., Li, Y., and Zimmerman, A. R. (2012). "Sorption of atrazine and ametryn by carbonatic and non-carbonatic soils of varied origin". *Environmental Pollution*, *169*, 12-19.

Kakavandi, B., Takdastan, A., Jaafarzadeh, N., Azizi, M., Mirzaei, A., and Azari, A. (2016). "Application of Fe 3 O 4@ C catalyzing heterogeneous UV-Fenton system for tetracycline removal with a focus on optimization by a response surface method". *Journal of Photochemistry and Photobiology A: Chemistry*, *314*, 178-188.

Kasiri, M. B., and Khataee, A. R. (2011). "Photooxidative decolorization of two organic dyes with different chemical structures by UV/H 2 O 2 process: experimental design".*Desalination*, *270*(1), 151-159.

Karale, R., Manu, B., and Shrihari, S. (2013). "Catalytic use of laterite iron for degradation of 2-aminopyridine using advanced oxidation processes". *Int. J. Sci. Eng. Res.*, 4, 207–10.

Khataee, A., Salahpour, F., Fathinia, M., Seyyedi, B., and Vahid, B. (2015). "Iron rich laterite soil with mesoporous structure for heterogeneous Fenton-like degradation of an azo dye under visible light". *Journal of Industrial and Engineering Chemistry*, *26*, 129-135.

Khataee, A. R., and Pakdehi, S. G. (2014). "Removal of sodium azide from aqueous solution by Fenton-like process using natural laterite as a heterogeneous catalyst: Kinetic modeling based on nonlinear regression analysis". *Journal of the Taiwan Institute of Chemical Engineers*, *45*(5), 2664-2672.

Khataee, A., Gholami, P., Sheydaei, M., Khorram, S., and Joo, S. W. (2016). "Preparation of nanostructured pyrite with N 2 glow discharge plasma and the study of its catalytic performance in the heterogeneous Fenton process". *New Journal of Chemistry*, *40*(6), 5221-5230.

King, P., Srinivas, P., Kumar, Y. P., and Prasad, V. S. R. K. (2006). "Sorption of copper (II) ion from aqueous solution by Tectona grandis lf (teak leaves powder) ". *Journal of Hazardous Materials*,*136*(3), 560-566.

Kim, S. M., Geissen, S. U., and Vogelpohl, A. (1997). "Landfill leachate treatment by a photoassisted Fenton reaction". *Water Science and Technology*, *35*(4), 239-248.

Kolpin, D. W., Thurman, E. M., and Linhart, S. M. (1998). "The environmental occurrence of herbicides: the importance of degradates in ground water". *Archives of Environmental Contamination and Toxicology*, *35*(3), 385-390.

Kong, S. H., Watts, R. J., and Choi, J. H. (1998). "Treatment of petroleum-contaminated soils using iron mineral catalyzed hydrogen peroxide". *Chemosphere*, *37*(8), 1473-1482.

Kore, K. J., Pradip, Jadhav, J., Shete, R. V., Shetty, S. C.: "Diuretic property of *Tectona grandis* leaves aqueous extract in Wistar rats". Inter. J. Pharm. Res. Dev. 3, 141–146 (2011).

Koffi, E. N., Cissé, I., Kassi, A. B., Lozano, P. R., Adima, A. A., Assidjo, E. N., and Bekro, Y. A. (2015). "Optimization of ultrasound-assisted extraction of phenolic antioxidants from Tectona grandis leaves, using experimental design". *European Journal of Medicinal Plants*, *10*(3), 1-10.

Kong, L., and Lemley, A. T. (2006). "Kinetic modeling of 2, 4-dichlorophenoxyacetic acid (2, 4-D) degradation in soil slurry by anodic Fenton treatment". *Journal of Agricultural and Food Chemistry*, *54*(11), 3941-3950.

Kuang, Y., Wang, Q., Chen, Z., Megharaj, M., and Naidu, R. (2013). "Heterogeneous Fenton-like oxidation of monochlorobenzene using green synthesis of iron nanoparticles". *Journal of Colloid and Interface Science*, *410*, 67-73.

Kumar, K. M., Mandal, B. K., Kumar, K. S., Reddy, P. S., and Sreedhar, B. (2013). "Biobased green method to synthesise palladium and iron nanoparticles using Terminalia chebula aqueous extract". *Spectrochimica Acta Part A: Molecular and Biomolecular Spectroscopy*, *102*, 128-133.

Kwan, C. Y., and Chu, W. (2003). "Photodegradation of 2, 4-dichlorophenoxyacetic acid in various iron-mediated oxidation systems". *Water Research*, *37*(18), 4405-4412.

Laabs, V., Amelung, W., Pinto, A. A., Wantzen, M., da Silva, C. J., and Zech, W. (2002). "Pesticides in surface water, sediment, and rainfall of the northeastern Pantanal basin, Brazil". *Journal of Environmental Quality*, *31*(5), 1636-1648.

Li, H., Zhou, S., Sun, Y., and Lv, J. (2010). "Application of response surface methodology to the advanced treatment of biologically stabilized landfill leachate using Fenton's reagent". *Waste Management*, *30*(11), 2122-2129.

Li, H., Li, Y., Xiang, L., Huang, Q., Qiu, J., Zhang, H., ... and Valange, S. (2015). "Heterogeneous photo-Fenton decolorization of Orange II over Al-pillared Fe-smectite: response surface approach, degradation pathway, and toxicity evaluation". *Journal of Hazardous Materials*, *287*, 32-41.

Li, X. Q., Elliott, D. W., and Zhang, W. X. (2006). "Zero-valent iron nanoparticles for abatement of environmental pollutants: materials and engineering aspects". *Critical Reviews in Solid state and Materials Sciences*, *31*(4), 111-122.

Lopez, A., Mascolo, G., Tiravanti, G., and Passino, R. (1997). "Degradation of herbicides (ametryn and isoproturon) during water disinfection by means of two oxidants (hypochlorite and chlorine dioxide) ". *Water Science and Technology*, *35*(4), 129132-130136.

Lucas, M. S., Dias, A. A., Sampaio, A., Amaral, C., and Peres, J. A. (2007). "Degradation of a textile reactive Azo dye by a combined chemical–biological process: Fenton's reagent-yeast". *Water Research*, *41*(5), 1103-1109.

Lucas, M. S., and Peres, J. A. (2006). "Decolorization of the azo dye Reactive Black 5 by Fenton and photo-Fenton oxidation". *Dyes and Pigments*, *71*(3), 236-244.

Malato, S., Blanco, J., Richter, C., Curco, D., and Gimenez, J. (1997). "Low-concentrating CPC collectors for photocatalytic water detoxification: comparison with a medium concentrating solar collector". *Water Science and Technology*, *35*(4), 157-164.

Machado, S., Pinto, S. L., Grosso, J. P., Nouws, H. P. A., Albergaria, J. T., and Delerue-Matos, C. (2013). "Green production of zero-valent iron nanoparticles using tree leaf extracts". *Science of the Total Environment*, *445*, 1-8.

Mantilla, A., Tzompantzi, F., Fernandez, J. L., Góngora, J. D., Mendoza, G., and Gomez, R. (2009). "Photodegradation of 2, 4-dichlorophenoxyacetic acid using ZnAlFe layered double hydroxides as photocatalysts". *Catalysis Today*, *148*(1), 119-123.

Masomboon, N., Chen, C. W., Anotai, J., and Lu, M. C. (2010). "A statistical experimental design to determine o-toluidine degradation by the photo-Fenton process". *Chemical Engineering Journal*, *159*(1), 116-122.

Ma, Y. S., Huang, S. T., and Lin, J. G. (2000). "Degradation of 4-nitrophenol using the Fenton process". *Water Science and Technology*, *42*(3-4), 155-160.

Masomboon, N., Ratanatamskul, C., and Lu, M. C. (2009). "Chemical oxidation of 2, 6-dimethylaniline in the Fenton process". *Environmental Science and Technology*, *43*(22), 8629-8634.

Madhavi, V., Prasad, T. N. V. K. V., Reddy, A. V. B., Reddy, B. R., and Madhavi, G. (2013). "Application of phytogenic zerovalent iron nanoparticles in the adsorption of hexavalent chromium". *Spectrochimica Acta Part A: Molecular and Biomolecular Spectroscopy*, *116*, 17-25.

Martins, R. C., Rossi, A. F., and Quinta-Ferreira, R. M. (2010). "Fenton's oxidation process for phenolic wastewater remediation and biodegradability enhancement". *Journal of Hazardous Materials*, *180*(1), 716-721.

Mater, L., Rosa, E. V. C., Berto, J., Correa, A. X. R., Schwingel, P. R., and Radetski, C. M. (2007). "A simple methodology to evaluate influence of H 2 O 2 and Fe 2+ concentrations on the mineralization and biodegradability of organic compounds in water and soil contaminated with crude petroleum". *Journal of Hazardous Materials*, *149*(2), 379-386.

Manu, B., and Mahamood, S. (2011). "Enhanced degradation of paracetamol by UV-C supported photo-Fenton process over Fenton oxidation". *Water Science and Technology*, *64*(12), 2433-2438.

Manu, B., Mahamood, S., Vittal, H., and Shrihari, S. (2011). "A novel catalytic route to degrade paracetamol by Fenton process". *IJRCE*,*1*.

Mason, R. L., Gunst, R. F., and Hess, J. L. (2003). "*Statistical design and analysis of experiments: with applications to engineering and science*". (Vol. 474). John Wiley and Sons

Maiti, A., Basu, J. K., and De, S. (2010). "Development of a treated laterite for arsenic adsorption: effects of treatment parameters". *Industrial and Engineering Chemistry Research*, *49*(10), 4873-4886.

Mendoza-Marín, C., Osorio, P., and Benítez, N. (2010). "Decontamination of industrial wastewater from sugarcane crops by combining solar photo-Fenton and biological treatments". *Journal of Hazardous Materials*, *177*(1), 851-855.

Mijangos, F., Varona, F., and Villota, N. (2006). "Changes in solution color during phenol oxidation by Fenton reagent". *Environmental Science and Technology*, *40*(17), 5538-5543.

Mills, P. C., Kolpin, D. W., Scribner, E. A., and Thurman, E. M. (2005). "Herbicides and degradates in shallow aquifers of Illinois: Spatial and temporal trends". *Journal of the American Water Resources Association(JAWRA)*, *41*(3), 537-547.

Myers, R., and Montgomery, D. (2002). "*Response surface methodology: Process and product optimization using designed experiments*", 2nd Ed., Wiley, New York.

Myers, R. H., Khuri, Andre. I.   and Carter, W. H. Jr. (1989), " Response surface methodology.". *Technometrics,* 31 (2), 137-153.

Navaratna, D., Elliman, J., Cooper, A., Shu, L., Baskaran, K., and Jegatheesan, V. (2012). "Impact of herbicide Ametryn on microbial communities in mixed liquor of a membrane bioreactor (MBR) ".*Bioresource Technology*, *113*, 181-190.

Nadagouda, M. N., Castle, A. B., Murdock, R. C., Hussain, S. M., and Varma, R. S. (2010). "In vitro biocompatibility of nanoscale zerovalent iron particles (NZVI) synthesized using tea polyphenols". *Green Chemistry*, *12*(1), 114-122.

Navalon, S., Alvaro, M., and Garcia, H. (2010). "Heterogeneous Fenton catalysts based on clays, silicas and zeolites". *Applied Catalysis B: Environmental*, *99*(1), 1-26.

Nalvothula, R., Nagati, V. B., Koyyati, R., Merugu, R., and Padigya, P. R. M. (2014). "Biogenic synthesis of silver nanoparticles using tectona grandis leaf extract and evaluation of their antibacterial potential". *Int J ChemTech Res*, *6*(1), 293-298.

Neppolian, B., Park, J. S., and Choi, H. (2004). "Effect of Fenton-like oxidation on enhanced oxidative degradation of para-chlorobenzoic acid by ultrasonic irradiation". *Ultrasonics Sonochemistry*, *11*(5), 273-279.

Njagi, E. C., Huang, H., Stafford, L., Genuino, H., Galindo, H. M., Collins, J. B., ... and Suib, S. L. (2010). "Biosynthesis of iron and silver nanoparticles at room temperature using aqueous sorghum bran extracts". *Langmuir*, *27*(1), 264-271.

Oliveira, R., Almeida, M. F., Santos, L., and Madeira, L. M. (2006). "Experimental design of 2, 4-dichlorophenol oxidation by Fenton's reaction". *Industrial and Engineering Chemistry Research*, *45*(4), 1266-1276.

Pignatello, J. J. (1992). "Dark and photoassisted iron (3+)-catalyzed degradation of chlorophenoxy herbicides by hydrogen peroxide". *Environmental Science and Technology*, *26*(5), 944-951.

Pignatello, J. J., Oliveros, E., and MacKay, A. (2006). "Advanced oxidation processes for organic contaminant destruction based on the Fenton reaction and related chemistry". *Critical Reviews in Environmental Science and Technology*, *36*(1), 1-84.

Poyatos, J. M., Muñio, M. M., Almecija, M. C., Torres, J. C., Hontoria, E., and Osorio, F. (2010). "Advanced oxidation processes for wastewater treatment: state of the art". *Water, Air, and Soil Pollution*, *205*(1-4), 187.

Pulido, R., Bravo, L., and Saura-Calixto, F. (2000). "Antioxidant activity of dietary polyphenols as determined by a modified ferric reducing/antioxidant power assay". *Journal of Agricultural and Food Chemistry*, *48*(8), 3396-3402.

Rajkumar, D., and Palanivelu, K. (2004). "Electrochemical treatment of industrial wastewater". *Journal of Hazardous Materials*, *113*(1), 123-129.

Rao, A. N., Wani, S. P., Ramesha, M., & Ladha, J. K. (2015). Weeds and weed management of rice in Karnataka state, India. *Weed technology*, *29*(1), 1-17.

Rivière, J., Bergeron, F., Tremblay, S., Gasparutto, D., Cadet, J., and Wagner, J. R. (2004). "Oxidation of 5-hydroxy-2 '-deoxyuridine into isodialuric acid, dialuric acid, and hydantoin products". *Journal of the American Chemical Society*, *126*(21), 6548-6549.

Rice-Evans, C., Miller, N., & Paganga, G. (1997). Antioxidant properties of phenolic compounds. *Trends in plant science*, *2*(4), 152-159.

Roberts, T., and Hutson, D. (1999). " Metabolic pathways of agrochemicals-part one herbicides and plant growth regulation". *The Royal Soc. Chem., London*, 188-215.

Rusevova, K., Kopinke, F. D., and Georgi, A. (2012). "Nano-sized magnetic iron oxides as catalysts for heterogeneous Fenton-like reactions—Influence of Fe (II)/Fe (III) ratio on catalytic performance". *Journal of Hazardous Materials*, *241*, 433-440.

Saeed, M. O., Azizli, K., Isa, M. H., and Bashir, M. J. (2015). "Application of CCD in RSM to obtain optimize treatment of POME using Fenton oxidation process". *Journal of Water Process Engineering*, *8*, e7-e16.

Sandoval-Carrasco, C. A., Ahuatzi-Chacón, D., Galíndez-Mayer, J., Ruiz-Ordaz, N., Juárez-Ramírez, C., and Martínez-Jerónimo, F. (2013). "Biodegradation of a mixture of the herbicides ametryn, and 2, 4-dichlorophenoxyacetic acid (2, 4-D) in a compartmentalized biofilm reactor". *Bioresource Technology*, *145*, 33-36.

Santos, S. C., and Boaventura, R. A. (2008). "Adsorption modelling of textile dyes by sepiolite". *Applied Clay Science*, *42*(1), 137-145.

Sangami, S., and Manu, B. (2017). "Fenton's treatment of actual agriculture runoff water containing herbicides". *Water Science and Technology*, *75*(2), 451-461.

Schenone, A. V., Conte, L. O., Botta, M. A., and Alfano, O. M. (2015). "Modeling and optimization of photo-Fenton degradation of 2, 4-D using ferrioxalate complex and response surface methodology (RSM) ". *Journal of Environmental Management*, *155*, 177-183.

Setiawan, C., Purnomo, H., and Kusnadi, J. (2013). "Antioxidant extraction of teak (Tectona grandis) leaves using microwave-assisted extraction". *International Journal of Pharm Tech Research*, *5*(3), 1410-1415.

Shin, E. H., Choi, J. H., Abd El-Aty, A. M., Khay, S., Kim, S. J., Im, M. H., ... and Shim, J. H. (2011). "Simultaneous determination of three acidic herbicide residues in food crops using HPLC and confirmation via LC-MS/MS". *Biomedical Chromatography*, *25*(1-2), 124-135.

Shahwan, T., Sirriah, S. A., Nairat, M., Boyacı, E., Eroğlu, A. E., Scott, T. B., and Hallam, K. R. (2011). "Green synthesis of iron nanoparticles and their application as a Fenton-like catalyst for the degradation of aqueous cationic and anionic dyes". *Chemical Engineering Journal*, *172*(1), 258-266.

Shurvell, T., Keir, G., Jegatheesan, V., Shu, L., and Farago, L. (2014). "Removal of ametryn through nanofiltration and reverse osmosis". *Desalination and Water Treatment*, *52*(4-6), 643-649.

Sun, Y., and Pignatello, J. J. (1993). "Organic intermediates in the degradation of 2, 4-dichlorophenoxyacetic acid by iron (3+)/hydrogen peroxide and iron (3+)/hydrogen peroxide/UV". *Journal of Agricultural and Food Chemistry*, *41*(7), 1139-1142.

Swaminathan, K., Sandhya, S., Sophia, A. C., Pachhade, K., and Subrahmanyam, Y. V. (2003). "Decolorization and degradation of H-acid and other dyes using ferrous–hydrogen peroxide system". *Chemosphere*, *50*(5), 619-625.

Tawabini, B. S. (2014). Simultaneous removal of MTBE and benzene from contaminated groundwater using ultraviolet-based ozone and hydrogen peroxide. *International Journal of Photoenergy*, *2014*.

Tiwari, B. K., Muthukumarappan, K., O'Donnell, C. P., and Cullen, P. J. (2008). "Modelling colour degradation of orange juice by ozone treatment using response surface methodology". *Journal of Food Engineering*, *88*(4), 553-560.

Torrades, F., Saiz, S., and García-Hortal, J. A. (2011). "Using central composite experimental design to optimize the degradation of black liquor by Fenton reagent". *Desalination*, *268*(1), 97-102.

USEPA)., (2005). "Prevention, Pesticides and Toxic Substances (7508C). Registration Eligibility Decision for 2,4-D". Available on: http://archive.epa.gov/pesticides/reregistration/web/pdf/24d_red.pdf (Acessed on 25-2-2016).

USEPA., (2010). "Reregistration Eligibility Decision (RED) for Ametrn" https://archive.epa.gov/pesticides/reregistration/web/pdf/ametryn_red.pdf (accessed on 07-5-2017).

U.S EPA., (1999). "Integrated Risk Information System (IRIS) on 2,4-Dicholophenoxyacetic Acid." National Center for Environmental Assessment, Office of Research and Development, Washington, D.C

Valle-Orta, M., Diaz, D., Santiago-Jacinto, P., Vázquez-Olmos, A., and Reguera, E. (2008). "Instantaneous synthesis of stable zerovalent metal nanoparticles under standard reaction conditions". *The Journal of Physical Chemistry B*, *112*(46), 14427-14434.

Wang, Q., and Lemley, A. T. (2001). "Kinetic model and optimization of 2, 4-D degradation by anodic Fenton treatment". *Environmental Science and Technology*, *35*(22), 4509-4514.

Wang, T., Lin, J., Chen, Z., Megharaj, M., and Naidu, R. (2014a). "Green synthesized iron nanoparticles by green tea and eucalyptus leaves extracts used for removal of nitrate in aqueous solution". *Journal of Cleaner Production*, *83*, 413-419.

Wang, T., Jin, X., Chen, Z., Megharaj, M., and Naidu, R. (2014b). "Green synthesis of Fe nanoparticles using eucalyptus leaf extracts for treatment of eutrophic wastewater". *Science of the Total Environment*, *466*, 210-213.

Wang, S. (2008). "A comparative study of Fenton and Fenton-like reaction kinetics in decolourisation of wastewater". *Dyes and Pigments*, *76*(3), 714-720.

Wang, L., Yang, J., Li, Y., Lv, J., and Zou, J. (2016). "Removal of chlorpheniramine in a nanoscale zero-valent iron induced heterogeneous Fenton system: influencing factors and degradation intermediates". *Chemical Engineering Journal*, *284*, 1058-1067.

Wang, C. B., and Zhang, W. X. (1997). "Synthesizing nanoscale iron particles for rapid and complete dechlorination of TCE and PCBs". *Environmental Science and Technology*, *31*(7), 2154-2156.

Wang, T., Qu, G., Sun, Q., Liang, D., & Hu, S. (2015). Formation and roles of hydrogen peroxide during soil remediation by direct multi-channel pulsed corona discharge in soil. *Separation and Purification Technology*, *147*, 17-23.

World Health Organization (WHO) (2003). "2,4-D in Drinking-water: Background Document for Development of WHO Guidelines for Drinking-water Quality". Available on: http://www.who.int/water_sanitation_health/dwq/chemicals/ 24D.pdf (Accessed on 25-2-2016).

World Health Organization, (1993). "Guidelines for Drinking- Water Quality Recommendations." Volume 1, 2nd Edition, Geneva.

Wu, T., and Englehardt, J. D. (2012). "A new method for removal of hydrogen peroxide interference in the analysis of chemical oxygen demand". *Environmental Science and Technology*, *46*(4), 2291-2298.

Wu, H., Jiang, F., Lu, S., Guan, Y., Deng, D., and Chen, X. (2015). "Using Goethite as a Heterogeneous Fenton Catalyst for the Removal of Tetracycline Hydrochloride: Effects of Its Adsorptive and Reductive Activities". In *Proceedings of the 11th International Congress for Applied Mineralogy (ICAM)* (pp. 405-423). Springer, Cham.

Venkatadri, R., and Peters, R. W. (1993). "Chemical oxidation technologies: ultraviolet light/hydrogen peroxide, Fenton's reagent, and titanium dioxide-assisted photocatalysis". *Hazardous Waste and Hazardous Materials*, *10*(2), 107-149.

Xu, B., Gao, N. Y., Cheng, H., Hu, C. Y., Xia, S. J., Sun, X. F., ... and Yang, S. (2009). "Ametryn degradation by aqueous chlorine: kinetics and reaction influences". *Journal of Hazardous Materials*,*169*(1), 586-592.

Xu, L., and Wang, J. (2011). "A heterogeneous Fenton-like system with nanoparticulate zero-valent iron for removal of 4-chloro-3-methyl phenol". *Journal of Hazardous Materials*, *186*(1), 256-264.

Xu, L., and Wang, J. (2012). "Fenton-like degradation of 2, 4-dichlorophenol using Fe 3 O 4 magnetic nanoparticles". *Applied Catalysis B: Environmental*, *123*, 117-126.

Xue, X., Hanna, K., and Deng, N. (2009). "Fenton-like oxidation of Rhodamine B in the presence of two types of iron (II, III) oxide". *Journal of Hazardous Materials*, *166*(1), 407-414.

Xu, X. R., Li, H. B., Wang, W. H., and Gu, J. D. (2004). "Degradation of dyes in aqueous solutions by the Fenton process".*Chemosphere*, *57*(7), 595-600.

Yaping, Z., and Jiangyong, H. (2008). "Photo-Fenton degradation of 17β-estradiol in presence of α-FeOOHR and H 2 O 2". *Applied Catalysis B: Environmental*, *78*(3), 250-258.

Yirsaw, B. D., Megharaj, M., Chen, Z., and Naidu, R. (2016). "Reduction of hexavalent chromium by green synthesized nano zero valent iron and process optimization using response surface methodology". *Environmental Technology and Innovation*, *5*, 136-147.

Yoon, J., Lee, Y., and Kim, S. (2001). "Investigation of the reaction pathway of OH radicals produced by Fenton oxidation in the conditions of wastewater treatment". *Water science and technology: a journal of the Inter. Association on Water Pollution Research*, *44*(5), 15-21.

Zhang, H., Zhang, D., and Zhou, J. (2006). "Removal of COD from landfill leachate by electro-Fenton method". *Journal of Hazardous Materials*, *135*(1), 106-111

Zhang, H., Li, Y., and Wu, X. (2011). "Statistical experiment design approach for the treatment of landfill leachate by photoelectro-Fenton process". *Journal of Environmental Engineering*, *138*(3), 278-285.

Zhang, H., Li, Y., Wu, X., Zhang, Y., and Zhang, D. (2010). "Application of response surface methodology to the treatment landfill leachate in a three-dimensional electrochemical reactor". *Waste Management*, *30*(11), 2096-2102.

Zhang, S., Zhao, X., Niu, H., Shi, Y., Cai, Y., and Jiang, G. (2009). "Superparamagnetic Fe 3 O 4 nanoparticles as catalysts for the catalytic oxidation of phenolic and aniline compounds". *Journal of Hazardous Materials*, *167*(1), 560-566.

Zhang, S., Shen, X., Zheng, Z., Ma, Y., and Qu, Y. (2015). "3D graphene/nylon rope as a skeleton for noble metal nanocatalysts for highly efficient heterogeneous continuous-flow reactions". *Journal of Materials Chemistry A*, *3*(19), 10504-10511.

Zhang, W., Gao, H., He, J., Yang, P., Wang, D., Ma, T., ... and Xu, X. (2017). "Removal of norfloxacin using coupled synthesized nanoscale zero-valent iron (nZVI) with H 2 O 2 system: Optimization of operating conditions and degradation pathway". *Separation and Purification Technology*, *172*, 158-167.

Zhang, Y., Klamerth, N., Messele, S. A., Chelme-Ayala, P., and El-Din, M. G. (2016). "Kinetics study on the degradation of a model naphthenic acid by ethylenediamine-N, N'-disuccinic acid-modified Fenton process". *Journal of Hazardous Materials*, *318*, 371-378.

Zhou, D., Wu, F., Deng, N., and Xiang, W. (2004). "Photooxidation of bisphenol A (BPA) in water in the presence of ferric and carboxylate salts". *Water Research*, *38*(19), 4107-4116.

Zinatizadeh, A. A. L., Mohamed, A. R., Abdullah, A. Z., Mashitah, M. D., Isa, M. H., and Najafpour, G. D. (2006). "Process modeling and analysis of palm oil mill effluent treatment in an up-flow anaerobic sludge fixed film bioreactor using response surface methodology (RSM) ". *Water Research*, *40*(17), 3193-3208.

Zolgharnein, J., Shahmoradi, A., and Ghasemi, J. B. (2013). "Comparative study of Box–Behnken, central composite, and Doehlert matrix for multivariate optimization of Pb (II) adsorption onto Robinia tree leaves". *Journal of Chemometrics*, *27*(1-2), 12-20.

Zuin, V. G., Schellin, M., Montero, L., Yariwake, J. H., Augusto, F., and Popp, P. (2006). "Comparison of stir bar sorptive extraction and membrane-assisted solvent extraction as enrichment techniques for the determination of pesticide and benzo [a] pyrene residues in Brazilian sugarcane juice". *Journal of Chromatography A*, *1114*(2), 180-187.

IS:2720 "Indian Standard methods of test for soils (IS:2720(Part XXV)-1982 (https://law.resource.org/pub/in/bis/S03/is.2720.25.1982.pdf .

Bureau of Indian Standards (BIS) IS: 10500:2012, Drinking Water Specifications, (http://cgwb.gov.in/documents/wq-standards.pdf).

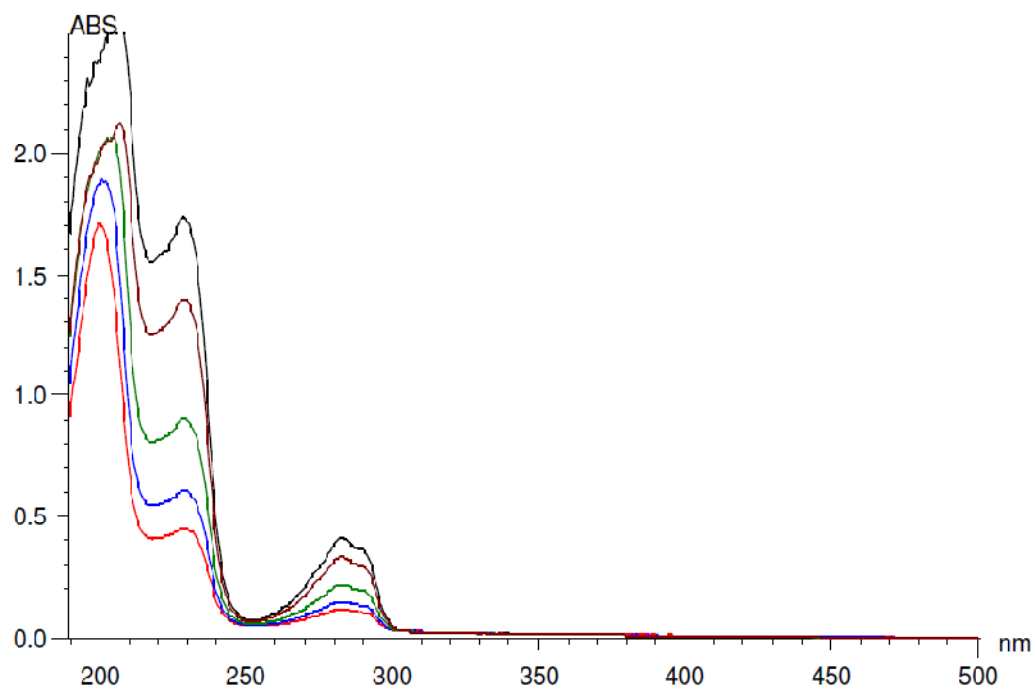http://www.ecifm.rdg.ac.uk/pesticides.html (accessed on 10-10-2014)
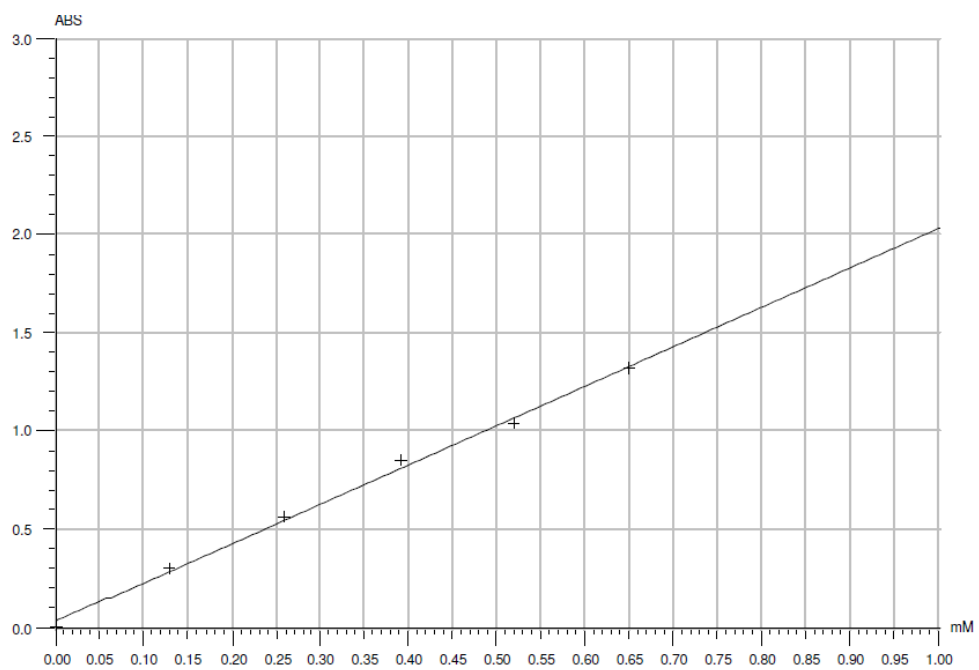
APPENDIX-I [A-I]
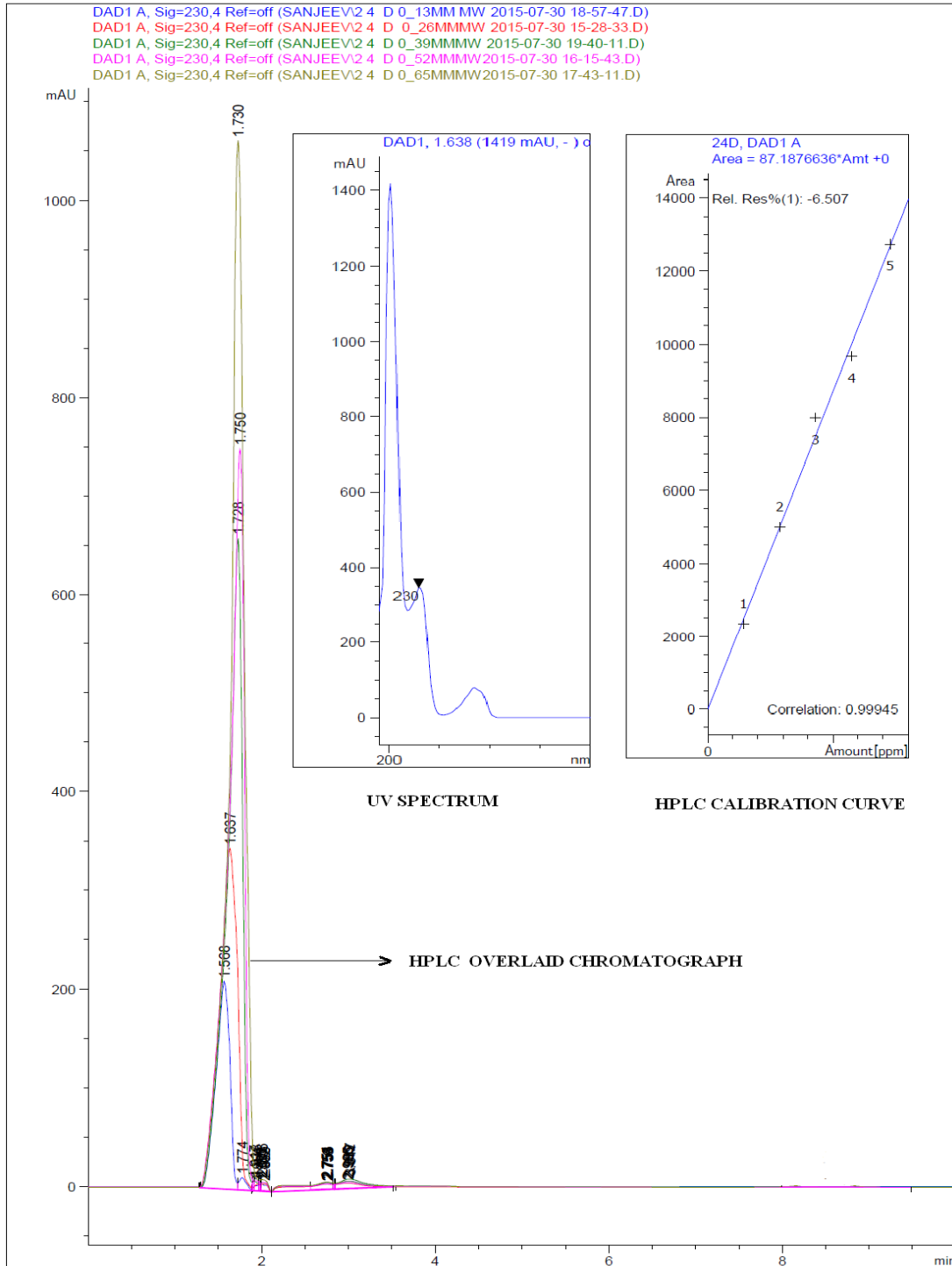
1. HPLC chromatograph 2,4-D along with UV-spectrum and HPLC calibration curve

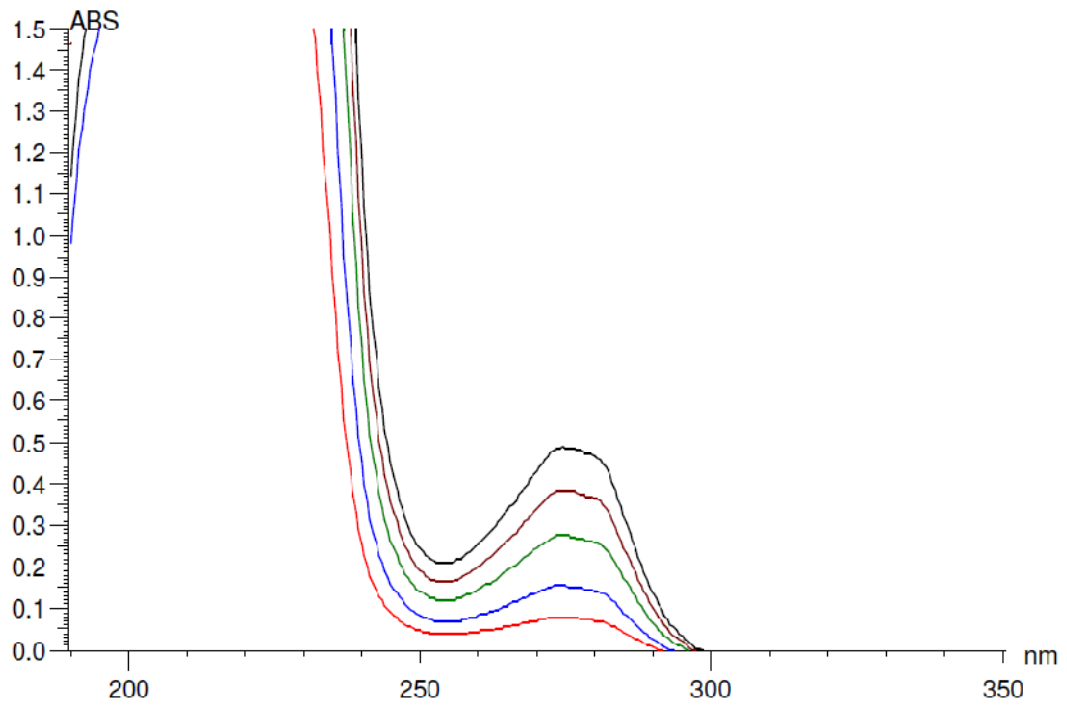2. HPLC chromatograph ametryn along with UV-spectrum and HPLC calibration curve
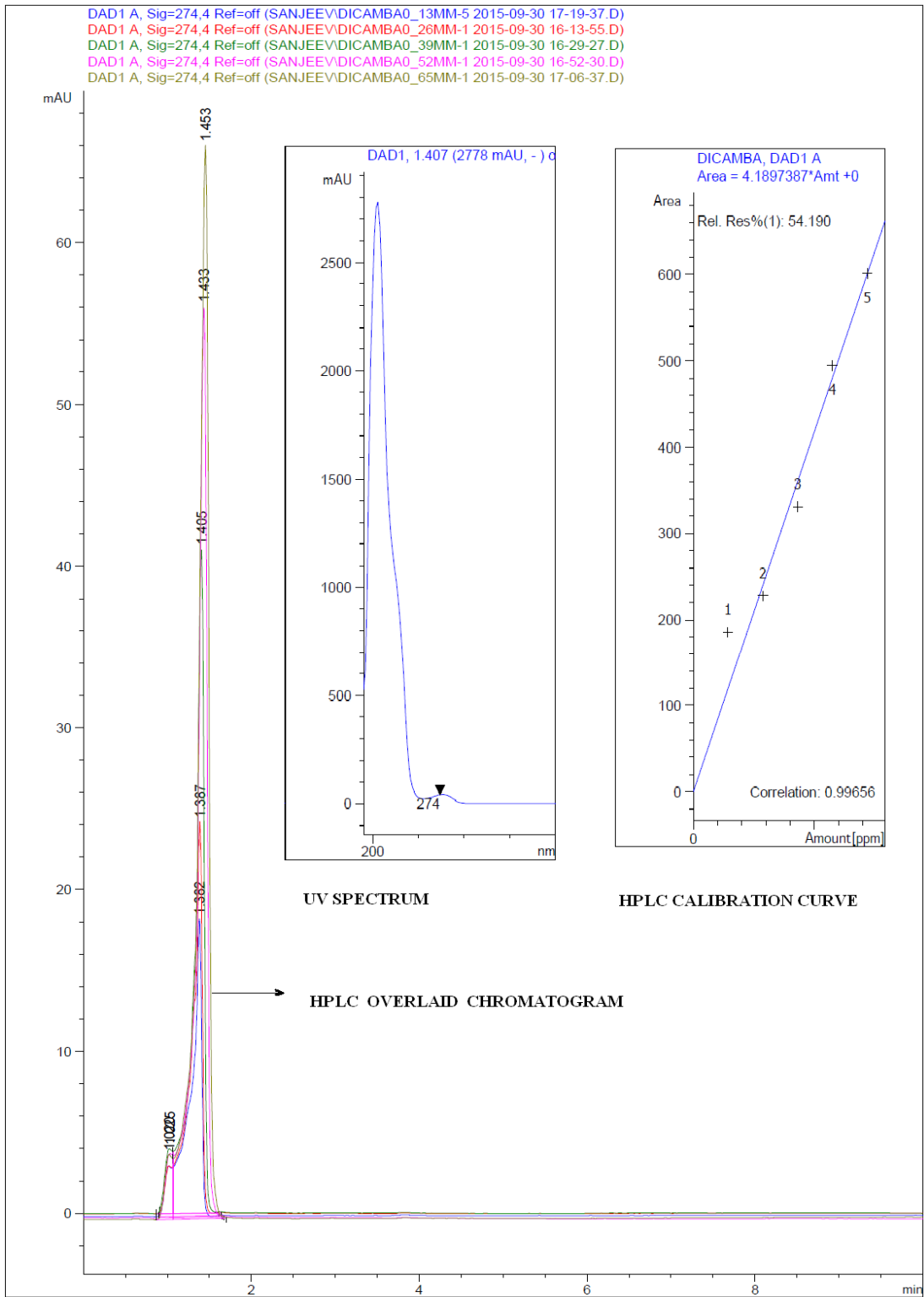
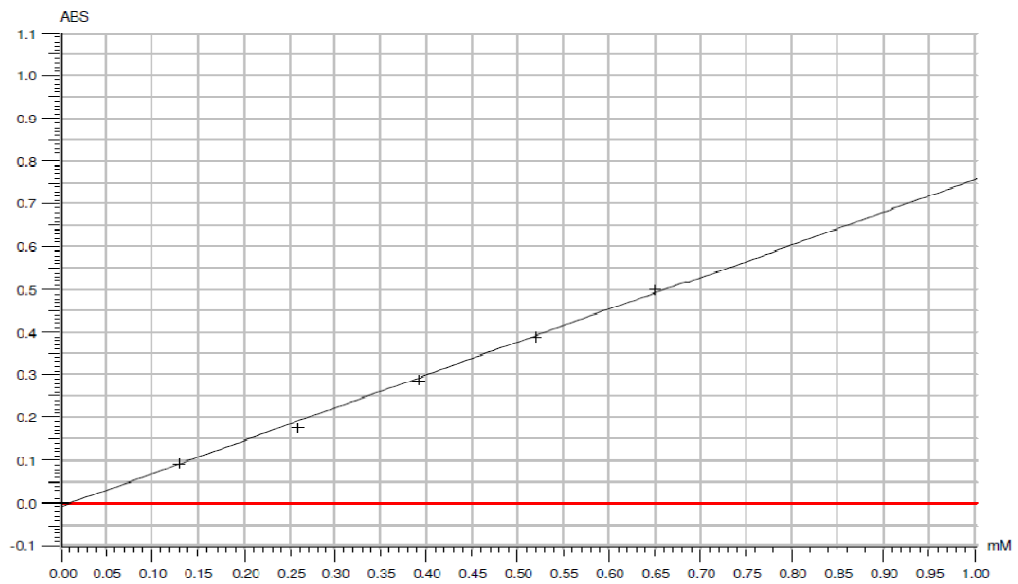3. HPLC chromatograph dicamba along with UV-spectrum and HPLC calibration curve
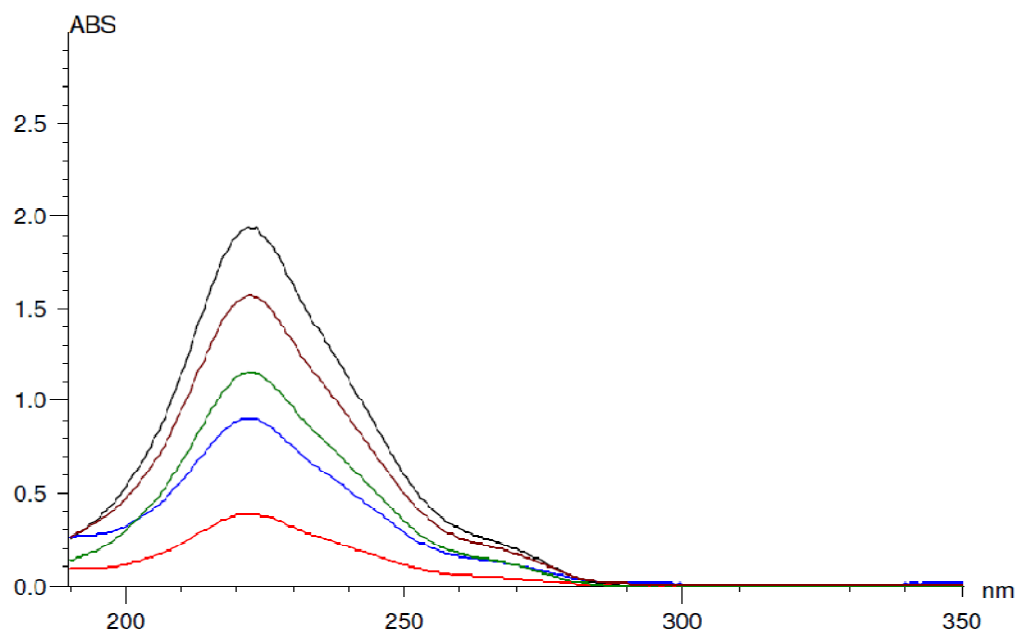
159

4. Overlaid UV-spectrum of 2,4-D
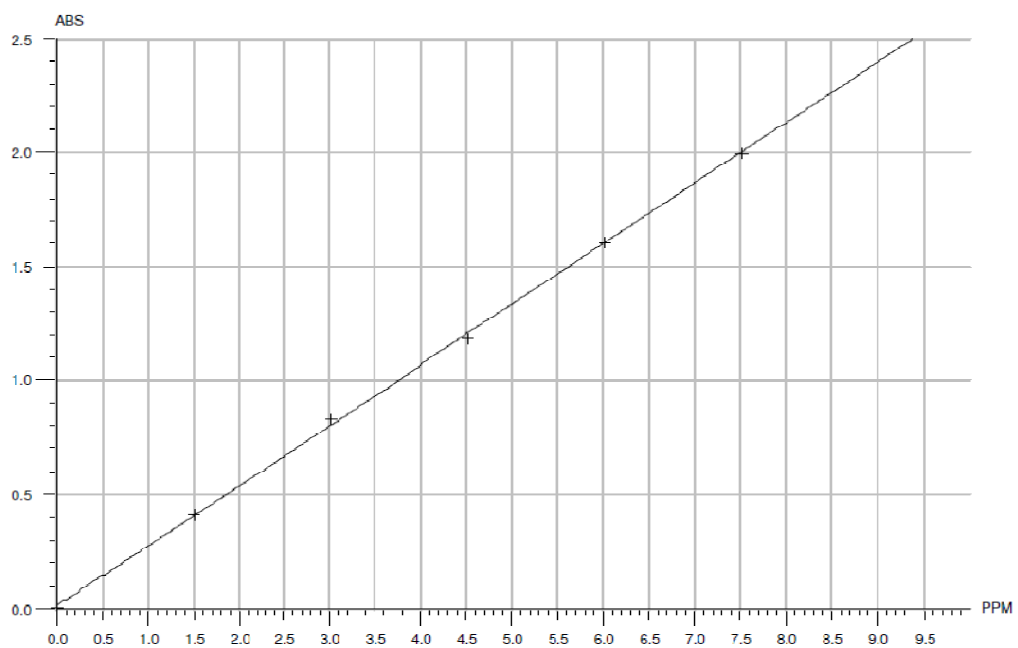

5. UV-calibration curve of 2,4-D

160

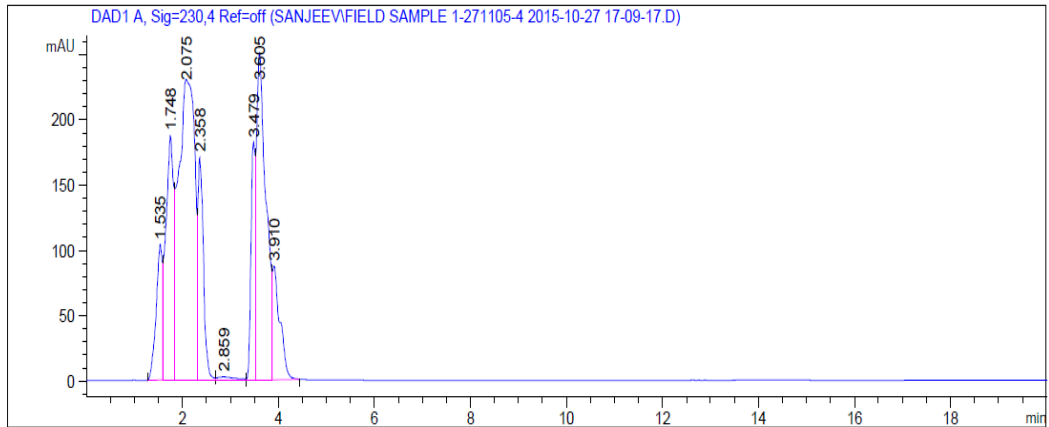6. Overlaid UV-spectrum of dicamba
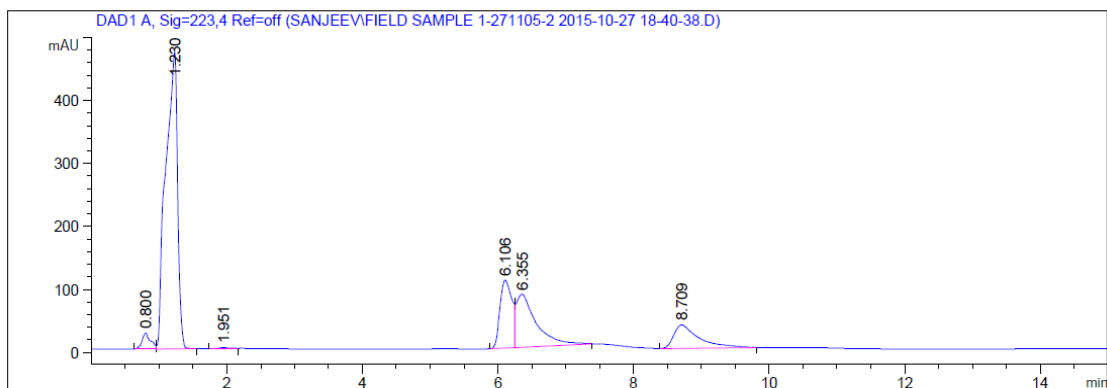

7. UV-calibration curve of dicamba

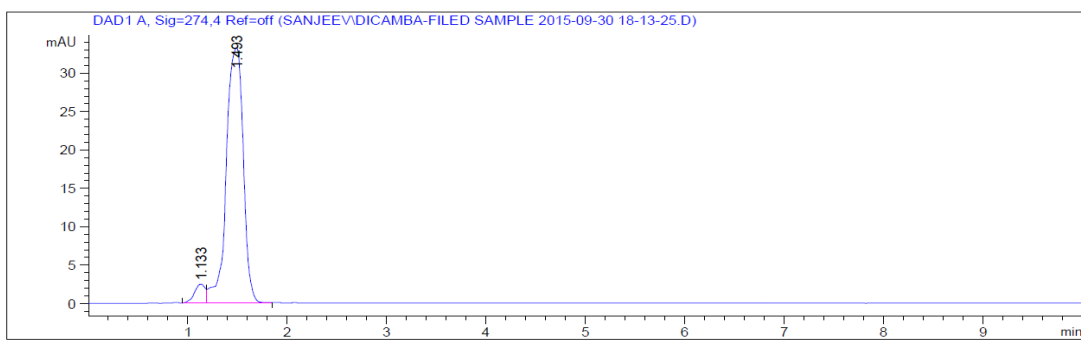8. Overlaid UV-spectrum of ametryn

9. UV-calibration curve of ametryn

10. HPLC analysis of 2,4 -D=25 mg/L, retention Time =1.748 min (actual sample)

11. HPLC analysis of Ametryn =2.7 mg/L, Retention Time =8.709min (actual sample)

12. HPLC analysis of Dicamba=90 mg/L, Retention Time =1.493min (actual sample)
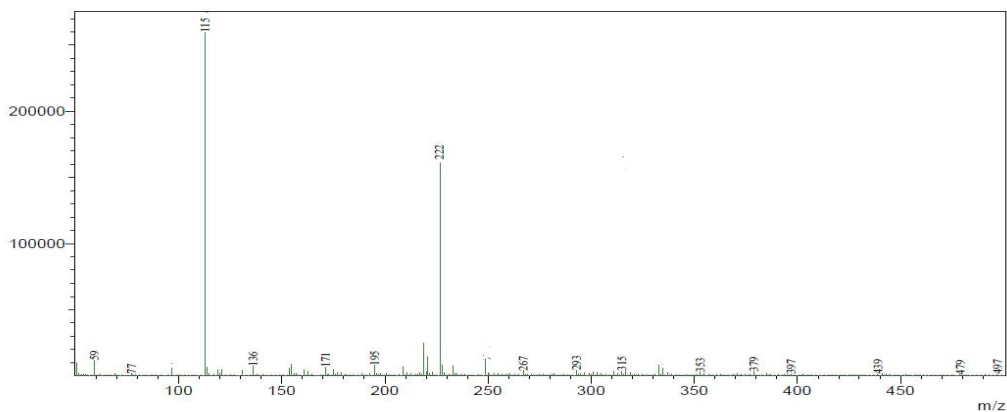
13. Mass table for 2,4-D after treatment and formation of maleic acid
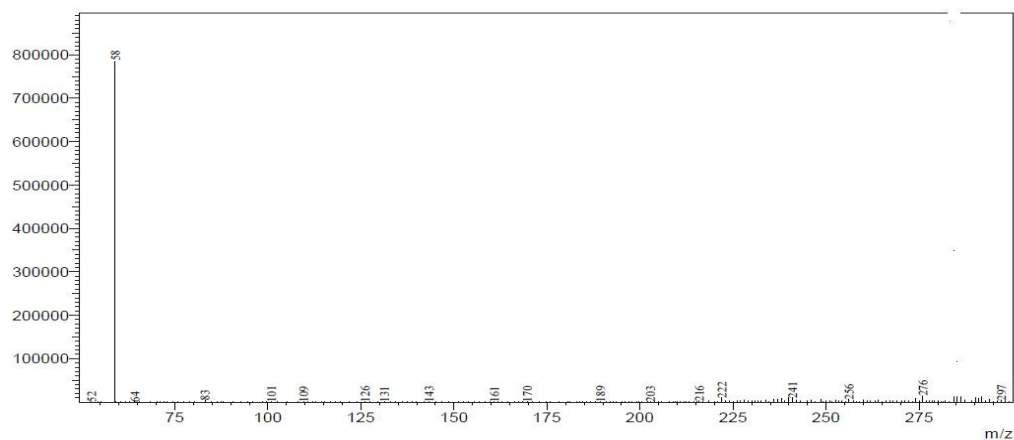
14. Mass table for ametryn after treatment and formation of Thiocynate ion

15. Mass table for dicamba after treatment and formation of oxalic acid

164

16. UV calibration curve for FRAP method

17. UV calibration curve for determination of total polyphenols

APPENDIX-II [A-II]

1. Analysis of Variance for % DR and CODR

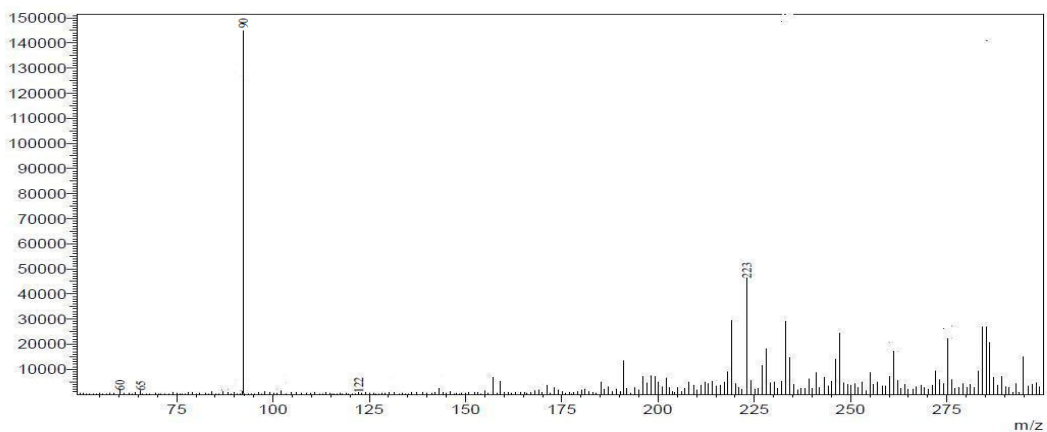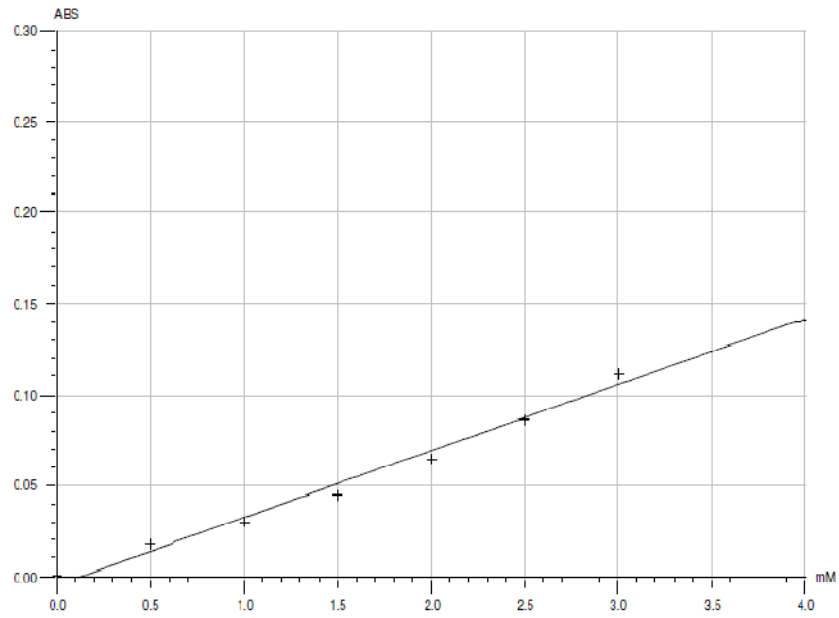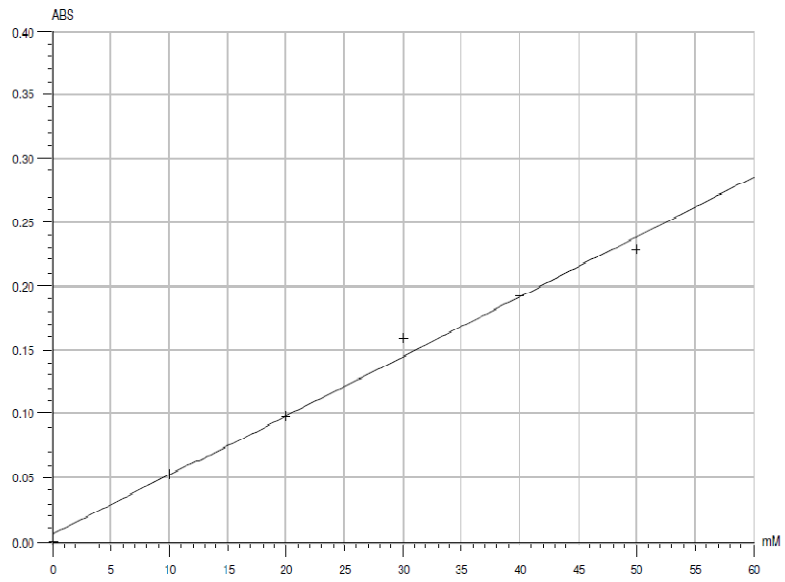| Response		%DR				%CODR			
Source	DF	Adj SS	Adj MS	F-Value	P-Value>F	Adj SS	Adj MS	F-Value	P value>F
Model	14	8818.39	629.88	9.93	0.000	8442.98	603.07	7.57	0 001
Linear	4	139.42	34.85	0.55	0.703	134.24	33.56	0.42	0.790
A	1	0.70	0.70	0.01	0.918	3.51	3.51	0.04	0.838
B	1	13.71	13.71	0.22	0.651	41.31	41.31	0.52	0.487
C	1	45.25	45.25	0.71	0.416	17.17	17.17	0.22	0.652
D	1	79.76	79.76	1.26	0.286	72.24	72.24	0.91	0.362
Square	4	8500.90	2125.23	33.51	0.000	8138.00	2034.50	25.52	0.000
A*A	1	1004.21	1004.21	15.83	0.002	1469.20	1469.20	18.43	0.001
B*B	1	692.75	692.75	10.92	0.007	400.91	400.91	5.03	0.046
C*C	1	1045.19	1045.19	16.48	0.002	934.94	934.94	11.73	0.006
D*D	1	634.72	634.72	10.01	0.009	696.65	696.65	8.74	0.013
2-Way Interaction	6	178.07	29.68	0.47	0.818	170.74	28.46	0.36	0.891
A*B	1	18.53	18.53	0.29	0.600	3.09	3.09	0.04	0.848
A*C	1	22.94	22.94	0.36	0.560	0.20	0.20	0.00	0.961
A*D	1	27.30	27.30	0.43	0.525	15.66	15.66	0.20	0.666
B*C	1	101.51	101.51	1.60	0.232	69.68	69.68	0.87	0.370
B*D	1	0.08	0.08	0.00	0.972	4.81	4.81	0.06	0.811
C*D	1	7.70	7.70	0.12	0.734	77.31	77.31	0.97	0.346
Residual	11	697.60	63.42			876.85	79.71		
Lack-of-Fit	10	697.43	69.74	414.64	0.038	876.46	87.65	226.36	0.052
Pure Error	1	0.17	0.17			0.39	0.39		
Total	25	9515.99				9319.82			

Note: DR R^2=92.67%;R^2_{adj}=90.34%; Standard deviation (SD)=1.83; Coefficient of variation(CV)=5.85% ;Adequate precision(AP)=37.5.

Note: CODR R^2=90.59%;R^2_{adj}=88.62%; Standard deviation (S.D)=2.06;Coefficient of variation(CV)=6.91%;Adequate precision(AP)=61.7

2. Analysis of Variance for % AR and CODR

Response		%AR				%CODR			
Source	DF	Adj SS	Adj MS	F-Value	P-Value >F	Adj SS	Adj MS	F-Value	P-Value> F
Model	14	13082.1	934.44	18.54	0.000	11929.0	852.07	35.64	0.000
Linear	4	300.4	75.11	1.49	0.271	221.3	55.33	2.31	0.122
A	1	3.8	3.83	0.08	0.788	3.6	3.56	0.15	0.707
B	1	21.6	21.63	0.43	0.526	3.6	3.56	0.15	0.707
C	1	132.7	132.68	2.63	0.133	14.2	14.22	0.59	0.457
D	1	142.3	142.30	2.82	0.121	200.0	200.00	8.37	0.015
Square	4	12616.7	3154.17	62.60	0.000	11549.7	2887.43	120.79	0.000
A*A	1	2894.5	2894.52	57.44	0.000	3060.8	3060.84	128.04	0.000
B*B	1	472.6	472.57	9.38	0.011	543.8	543.76	22.75	0.001
C*C	1	460.8	460.81	9.15	0.012	286.2	286.20	11.97	0.005
D*D	1	202.2	202.22	4.01	0.030	334.5	334.49	13.99	0.003
2-Way	6	165.0	27.50	0.55	0.764	158.0	26.33	1.10	0.420
A*B	1	17.8	17.81	0.35	0.564	49.0	49.00	2.05	0.180
A*C	1	26.1	26.11	0.52	0.487	25.0	25.00	1.05	0.328
A*D	1	22.8	22.85	0.45	0.515	1.0	1.00	0.04	0.842
B*C	1	9.5	9.49	0.19	0.673	49.0	49.00	2.05	0.180
B*D	1	88.7	88.74	1.76	0.211	25.0	25.00	1.05	0.328
C*D	1	0.0	0.01	0.00	0.987	9.0	9.00	0.38	0.552
Residual	11	554.3	50.39			263.0	23.90		
Lack-of-Fit	10	554.3	55.43	3421.3	0.013	263.0	26.30	1521.32	0.021
Pure Error	1	0	0.02			0	0.00		
Total	25	13636.4				12192.0			

Note: AR R^2=95.94%;R^2_{adj}=90.76%;Standard deviation (SD)=1.70;Coefficient of variation(CV)=4.86% ;Adequate precision(AP)=80.1.

Note: CODR R^2=97.84%;R^2_{adj}=95.10%; Standard deviation (S.D)=1.35;Coefficient of variation(CV)=4.53%;Adequate precision(AP)=42.75

3. Analysis of Variance for % 24DR and CODR

Response		%24DR				%CODR			
Source	DF	Adj SS	Adj MS	F-Value	P-Value >F	Adj SS	Adj MS	F-Value	P-Value>F
Model	14	7918.84	565.63	4.91	0.006	8683.80	620.27	5.24	0.004
Linear	4	431.93	107.98	0.94	0.478	519.68	129.92	1.10	0.405
A	1	15.89	15.89	0.14	0.717	1.55	1.55	0.01	0.911
B	1	49.83	49.83	0.43	0.524	74.87	74.87	0.63	0.443
C	1	0.00	0.00	0.00	1.000	1.53	1.53	0.01	0.912
D	1	366.21	366.21	3.18	0.102	441.74	441.74	3.73	0.079
Square	4	6927.39	1731.85	15.04	0.000	7556.15	1889.04	15.97	0.000
A*A	1	904.80	904.80	7.86	0.017	1236.01	1236.01	10.45	0.008
B*B	1	1429.55	1429.55	12.41	0.005	1546.51	1546.51	13.07	0.004
C*C	1	243.27	243.27	2.11	0.174	200.08	200.08	1.69	0.220
D*D	1	759.73	759.73	6.60	0.026	1026.04	1026.04	8.67	0.013
2-Way	6	559.53	93.25	0.81	0.584	607.97	101.33	0.86	0.554
A*B	1	8.78	8.78	0.08	0.788	3.86	3.86	0.03	0.860
A*C	1	151.11	151.11	1.31	0.276	155.25	155.25	1.31	0.276
A*D	1	244.84	244.84	2.13	0.173	313.29	313.29	2.65	0.132
B*C	1	9.56	9.56	0.08	0.779	10.76	10.76	0.09	0.769
B*D	1	28.65	28.65	0.25	0.628	52.13	52.13	0.44	0.520
C*D	1	116.59	116.59	1.01	0.336	72.68	72.68	0.61	0.450
Residual	11	1267.04	115.19			1301.33	118.30		
Lack-of-Fit	10	1263.58	126.36	36.54	0.128	1297.90	129.79	37.82	0.126
Pure Error	1	3.46	3.46			3.43	3.43		
Total	25	9185.88	565.63			9985.14			

Note: 24DR R^2=89.25%;R^2_{adj}=86.56%; standard deviation (SD)=2.72; coefficient of variation(CV)=8.66% ;adequate precision(AP)=32.04.

Note: CODR R^2=91.62%;R^2_{adj}=89.55%; standard deviation (S.D)=2.61; coefficient of variation(CV)=8.60%; adequate precision(AP)=38.85

4. Analysis of Variance for % AR and CODR(AFP)

Response		%24DR				%CODR			
Source	DF	Adj SS	Adj MS	F-Value	P-Value >F	Adj SS	Adj MS	F-Value	P-Value>F
Model	14	17499.5	1249.96	5.34	0.004	17107.7	1221.98	4.34	0.010
Linear	4	2630.0	657.51	2.81	0.079	1402.7	350.67	1.24	0.348
A	1	2.4	2.38	0.01	0.921	8.0	8.00	0.03	0.869
B	1	2516.5	2516.48	10.74	0.007	1283.6	1283.56	4.56	0.056
C	1	110.2	110.21	0.47	0.507	107.6	107.56	0.38	0.549
D	1	1.0	0.98	0.00	0.950	3.6	3.56	0.01	0.913
Square	4	14822.6	3705.64	15.82	0.000	15643.0	3910.76	13.88	0.000
A*A	1	4145.6	4145.61	17.70	0.001	4191.8	4191.75	14.88	0.003
B*B	1	329.6	329.55	1.41	0.261	280.0	280.05	0.99	0.340
C*C	1	1522.1	1522.06	6.50	0.027	2073.9	2073.90	7.36	0.020
D*D	1	1754.8	1754.76	7.49	0.019	2235.2	2235.17	7.93	0.017
2-Way	6	46.9	7.82	0.03	1.000	62.0	10.33	0.04	1.000
A*B	1	2.6	2.56	0.01	0.919	25.0	25.00	0.09	0.771
A*C	1	19.9	19.89	0.08	0.776	1.0	1.00	0.00	0.954
A*D	1	9.2	9.18	0.04	0.847	9.0	9.00	0.03	0.861
B*C	1	6.6	6.60	0.03	0.870	9.0	9.00	0.03	0.861
B*D	1	4.2	4.24	0.02	0.895	9.0	9.00	0.03	0.861
C*D	1	4.4	4.41	0.02	0.893	9.0	9.00	0.03	0.861
Residual	11	2576.3	234.21			3099.7	281.79		
Lack-of-Fit	10	2576.3	257.63	1.6		3099.7	309.97	**0.8**	
Pure Error	1	0.0	0.00			0.0	0.00		
Total	25	20075.8				20207.4			

Note: %AR R^2=92.34%;R^2_{adj}=91.36%;Standard deviation (SD)=2.21;Coefficient of variation(CV)=9.66% ;Adequate precision(AP)=18.03.

Note: CODR R^2=95.4%;R^2_{adj}=92.30%; Standard deviation (S.D)=2.26;Coefficient of variation(CV)=8.62%;Adequate precision(AP)=17.17

5. Analysis of Variance for % DR and CODR (AFP)

Response		%DR				%CODR			
Source	DF	Adj SS	Adj MS	F-Value	P-Value>F	Adj SS	Adj MS	F-Value	P-Value
Model	14	12104.0	864.57	7.31	0.001	12372.2	883.73	4.99	0.006
Linear	4	258.0	64.50	0.55	0.706	353.5	88.38	0.50	0.738
A	1	21.6	21.56	0.18	0.678	2.2	2.23	0.01	0.913
B	1	12.8	12.82	0.11	0.748	36.7	36.72	0.21	0.658
C	1	55.5	55.55	0.47	0.507	47.1	47.14	0.27	0.616
D	1	168.1	168.06	1.42	0.258	267.4	267.42	1.51	0.245
Square	4	11640.2	2910.04	24.61	0.000	11873.7	2968.43	16.75	0.000
A*A	1	1067.3	1067.34	9.03	0.012	1215.4	1215.35	6.86	0.024
B*B	1	1073.1	1073.10	9.07	0.012	890.7	890.72	5.03	0.047
C*C	1	1322.6	1322.55	11.18	0.007	1835.2	1835.21	10.35	0.008
D*D	1	543.3	543.28	4.59	0.055	980.4	980.36	5.53	0.038
2-Way Interaction	6	205.8	34.30	0.29	0.929	145.0	24.16	0.14	0.988
A*B	1	7.4	7.38	0.06	0.807	2.8	2.76	0.02	0.903
A*C	1	93.4	93.36	0.79	0.393	8.0	7.97	0.04	0.836
A*D	1	46.6	46.61	0.39	0.543	41.6	41.57	0.23	0.638
B*C	1	54.7	54.72	0.46	0.510	39.5	39.47	0.22	0.646
B*D	1	3.5	3.54	0.03	0.866	50.6	50.59	0.29	0.604
C*D	1	0.2	0.17	0.00	0.971	2.6	2.62	0.01	0.905
Residual	11	1300.8	118.26			1949.8	177.25		
Lack-of-Fit	10	1300.8	130.08	0.3		1949.8	194.98	**0.6**	
Pure Error	1	0.0	0.00			0.0	0.00		
Total	25	13404.8				14322.0			

Note: DR R^2=96.3%;R^2_{adj}=90.76%;Standard deviation (SD)=2.71;Coefficient of variation(CV)=9.41% ;Adequate precision(AP)=48.32

Note: CODR R^2=92.3%;R^2_{adj}=91.5%; Standard deviation (S.D)=3.15;Coefficient of variation(CV)=7.71%;Adequate precision(AP)=68.05

6. Analysis of Variance for % 24DR and CODR (AFP)

Response		%24DR				%CODR			
Source	DF	Adj SS	Adj MS	F-Value	P-Value>F	Adj SS	Adj MS	F-Value	P-Value e>
Model	14	9663.7	690.27	3.80	0.016	13105.6	936.11	4.25	0.010
Linear	4	347.0	86.74	0.48	0.752	677.6	169.41	0.77	0.567
A	1	29.0	29.03	0.16	0.697	5.8	5.85	0.03	0.873
B	1	55.8	55.83	0.31	0.591	111.5	111.45	0.51	0.492
C	1	20.0	20.03	0.11	0.746	28.5	28.53	0.13	0.726
D	1	242.1	242.07	1.33	0.273	531.8	531.81	2.42	0.148
Square	4	9044.6	2261.16	12.44	0.000	11895.2	2973.80	13.51	0.000
A*A	1	1186.3	1186.28	6.52	0.027	1981.4	1981.41	9.00	0.012
B*B	1	1691.8	1691.81	9.30	0.011	1386.8	1386.79	6.30	0.029
C*C	1	434.6	434.63	2.39	0.150	1086.3	1086.28	4.93	0.048
D*D	1	1062.9	1062.92	5.85	0.034	1938.8	1938.80	8.81	0.013
2-Way Interaction	6	272.1	45.35	0.25	0.949	532.7	88.79	0.40	0.862
A*B	1	0.2	0.24	0.00	0.972	0.0	0.04	0.00	0.989
A*C	1	72.2	72.17	0.40	0.542	126.7	126.68	0.58	0.464
A*D	1	127.6	127.58	0.70	0.420	329.4	329.42	1.50	0.247
B*C	1	8.6	8.58	0.05	0.832	7.1	7.08	0.03	0.861
B*D	1	18.3	18.32	0.10	0.757	57.2	57.23	0.26	0.620
C*D	1	45.2	45.23	0.25	0.628	12.3	12.29	0.06	0.818
Residual	11	2000.1	181.83			2421.4	220.13		
Lack-of-Fit	10	2000.1	200.01	0.7		2421.4	242.14	0.2	
Pure Error	1	0.0	0.00			0.0	0.00		
Total	25	11663.8		3.80		15527.0			

Note: 24DR R^2=92.3%;R^2_{adj}=95.6%;Standard deviation (SD)=3.61;Coefficient of variation(CV)=9.07% ;Adequate precision(AP)=20.10.

Note: CODR R^2=94.9%; R^2_{adj}=92.7%; Standard deviation (S.D)=3.43;Coefficient of variation(CV)=9.43%;Adequate precision(AP)=19.20

7 . Analysis of Variance for % AR and %24DR(AFP-EG)

Source	DF	Adj MS[a]	F-Value[a]	P-Value>F[a]	Adj MS[b]	F-Value[b]	P-Value>F[b]
Model	14	405.73	3.10	0.111	324.17	3.13	0.426
Linear	4	2.21	0.01	1.000	25.41	0.09	0.984
A	1	1.02	0.01	0.943	34.17	0.12	0.736
B	1	0.36	0.00	0.967	18.12	0.06	0.806
C	1	6.91	0.04	0.853	38.43	0.13	0.721
D	1	0.54	0.00	0.959	10.90	0.04	0.849
Square	4	1363.97	7.07	0.005	1049.09	3.66	0.039
A*A	1	2359.47	12.23	0.005	1981.16	6.91	0.023
B*B	1	503.26	2.61	0.135	405.52	1.41	0.259
C*C	1	230.73	1.20	0.298	306.31	1.07	0.324
D*D	1	89.35	0.46	0.510	77.23	0.27	0.614
2-Way Interaction	6	35.93	0.19	0.975	40.08	0.14	0.988
A*B	1	22.75	0.12	0.738	42.58	0.15	0.707
A*C	1	7.84	0.04	0.844	25.25	0.09	0.772
A*D	1	40.45	0.21	0.656	89.78	0.31	0.587
B*C	1	33.93	0.18	0.683	4.95	0.02	0.898
B*D	1	92.06	0.48	0.504	33.35	0.12	0.740
C*D	1	18.53	0.10	0.762	44.56	0.16	0.701
Residual	11	192.95			286.78		
Lack-of-Fit	10	198.56	31.08	0.139	290.65	17.37	0.185
Pure Error	1	5.61			3.87		
Total	25						

Note: $R^2 = 87.21\%^a$, $85.12\%^b$; $R^2_{adj} = 91.2\%^a$, $R^2_{adj} = 89.12\%^b$; $S.D^a = 3.51$, $S.D^b = 3.69$; $C.V^a = 8.31\%$, $C.V^b = 9.34$; $A.P^a = 21.4$, $A.P^b = 22.29$; a=%AR; b=%24DR

8. Analysis of Variance for % CODR and %DR (AFP-EG)

Source	DF	Adj MS^c	F-Value^c	P-Value>F^c	Adj MS^d	F-Value^d	P-Value>F^d
Model	14	438.52	4.11	0.109	401.28	3.74	0.181
Linear	4	25.23	0.12	0.972	17.05	0.07	0.989
A	1	11.12	0.05	0.821	2.10	0.01	0.926
B	1	0.19	0.00	0.977	0.39	0.00	0.968
C	1	71.40	0.34	0.570	45.60	0.20	0.665
D	1	18.22	0.09	0.773	20.12	0.09	0.773
Square	4	1461.49	7.03	0.005	1294.97	5.61	0.010
A*A	1	2263.65	10.89	0.007	2419.80	10.48	0.008
B*B	1	761.65	3.67	0.082	543.94	2.36	0.153
C*C	1	566.24	2.72	0.127	485.68	2.10	0.175
D*D	1	21.09	0.10	0.756	73.06	0.32	0.585
2-Way Interaction	6	32.06	0.15	0.984	61.65	0.27	0.941
A*B	1	19.69	0.09	0.764	4.62	0.02	0.890
A*C	1	1.41	0.01	0.936	0.74	0.00	0.956
A*D	1	31.84	0.15	0.703	226.65	0.98	0.343
B*C	1	95.89	0.46	0.511	0.63	0.00	0.959
B*D	1	8.78	0.04	0.841	134.56	0.58	0.461
C*D	1	34.78	0.17	0.690	2.69	0.01	0.916
Residual	11	207.80			230.86		
Lack-of-Fit	10	224.26	5.19	0.330	252.90	24.11	0.157
Pure Error	1	43.24			10.49		
Total	25						

Note: R^2=90.25%^{c}, 87.88%^{d}; R^2_{adj}=94.52%^{c}, R^2_{adj}=86.12%^{d}; S.D^c=3.79, S.D^d=3.36; C.V^c=9.77%, C.V^d=9.68%; A.P^c=15.46, A.P^d =14.51, c=%CODR; d=%DR

9. Analysis of Variance for % AR and %24DR (AFP-TG)

Source	DF	Adj MS[a]	F-Value[a]	P-Value>F[a]	Adj MS[b]	F-Value[b]	P-Value>F[b]
Model	14	880.80	18.79	0.000	803.87	11.43	0.000
Linear	4	43.24	0.92	0.485	105.65	1.50	0.268
A	1	49.07	1.05	0.328	98.00	1.39	0.263
B	1	23.39	0.50	0.495	61.68	0.88	0.369
C	1	98.37	2.10	0.175	7.92	0.11	0.744
D	1	2.11	0.05	0.836	255.00	3.63	0.083
Square	4	2987.53	63.73	0.000	2644.78	37.60	0.000
A*A	1	2855.72	60.92	0.000	1912.83	27.20	0.000
B*B	1	443.05	9.45	0.011	1456.71	20.71	0.001
C*C	1	542.38	11.57	0.006	94.04	1.34	0.272
D*D	1	342.35	7.30	0.021	296.79	4.22	0.065
2-Way Interaction	6	34.68	0.74	0.629	42.08	0.60	0.727
A*B	1	5.51	0.12	0.738	11.16	0.16	0.698
A*C	1	126.06	2.69	0.129	38.56	0.55	0.475
A*D	1	4.21	0.09	0.770	0.38	0.01	0.942
B*C	1	2.57	0.05	0.819	43.03	0.61	0.451
B*D	1	67.94	1.45	0.254	153.51	2.18	0.168
C*D	1	1.80	0.04	0.848	5.81	0.08	0.779
Residual	11	46.88			70.33		
Lack-of-Fit	10	51.39	04.77	0.144	77.37	6.1	0.042
Pure Error	1	1.79			0.00		
Total	25						

Note: R^2=90.82%; R^2_{adj}=93.46%; S.D[a]=2.49, S.D[b]=2.78; C.V[a]=6.75%, C.V[b]=6.47; A.P[a]=75.83, A.P[b]=89.2; a=%AR; b=%24DR

10 Analysis of Variance for % CODR and %DR (AFP-TG)

Source	DF	Adj MS^c	F-$Value^c$	P-$Value> F^c$	Adj MS^d	F- $Value^d$	P-$Value> F^d$
Model	14	992.09	19.44	0.000	645.50	5.17	0.005
Linear	4	7.71	0.15	0.959	89.35	0.72	0.599
A	1	2.15	0.04	0.841	310.09	2.48	0.143
B	1	8.49	0.17	0.691	25.75	0.21	0.659
C	1	18.48	0.36	0.560	12.99	0.10	0.753
D	1	1.74	0.03	0.857	8.58	0.07	0.79
Square	4	3432.93	67.25	0.000	2135.92	17.10	0.000
A*A	1	3695.78	72.40	0.000	1663.83	13.32	0.004
B*B	1	650.57	12.75	0.004	733.08	5.87	0.034
C*C	1	413.60	8.10	0.016	442.11	3.54	0.087
D*D	1	544.15	10.66	0.008	556.50	4.46	0.038
2-Way Interaction	6	21.12	0.41	0.855	22.64	0.18	0.976
A*B	1	41.96	0.82	0.384	27.93	0.22	0.646
A*C	1	7.22	0.14	0.714	40.83	0.33	0.579
A*D	1	50.30	0.99	0.342	5.22	0.04	0.84
B*C	1	6.14	0.12	0.735	28.57	0.23	0.642
B*D	1	10.97	0.21	0.652	29.7	0.24	0.635
C*D	1	10.13	0.20	0.665	3.59	0.0	0.86
Residual	11	51.04			124.89		
Lack-of-Fit	10	56.15	8.21	0.12	137.11	05.39	0.108
Pure Error	1	0.00			2.6		
Total	25						

Note: R^2=88.62%;R^2_{adj}=91.62%; $S.D^c$=2.34, $S.D^d$=3.19; $C.V^c$=8.01%, $C.V^d$=9.01%; $A.P^c$=20.76, $A.P^d$ =29.75, c=%CODR; d=%DR

11. Cost of Production Laterite based FeNPs

Stage I:Saperation of Silica from Laterite			
Items	**Equipment**	**Details of Power and Required Time**	**Total Power Consumption (W)**
Laterite Crushing	Ball mill	750 W, 2 min	25
Heating	Hotplate	1000W, 1hr	1000
Drying	Oven	1000W, 1hr and 10 samples	100
Vaccum Filtration	Vaccum Filter	50W, 5min	4.1
Silica separation	Muffle Furnace	2000W, 10min	333
Stage II:Saperation of Iron from Laterite			
Boiling	Hot plate	1000W, 10 min	166
Vaccum Filtration	Vaccum Filter	50W, 5min	4.1
Heating	Hot Plate	1000W, 10 min	166
Iron separation	Muffle Furnace	2000W, 10min	333
Stage III: Synthesis Process			
Preparation of leaf extract	Mixer	750 W, 2 min	25
Vaccum Filtration	Vaccum Filter	50W, 5min	4.1
Drying	Oven	1000W, 10 hr and 10 samples	1000
		Total=3160.3W=3.16 units*10 rupees=31.6 rupees	
Reagents for the extraction of Iron From Laterite			
Name of Chemical	Quantity	Total Amount in Rs	
HCl	30 ml	8.34	
NaOH	4N, 20 ml	2.0	
NH_4Cl	4 gm	2.44	
Ammonia Solution	5ml	1.6	
Whatman 42 Filter paper	1	10	
		Total=24.38 rupees	
Total=31.6+24.38=55.98=Rs 56 per 1.5g of extracted iron			
For 5.5g=205 rupees			
Mixing of 5.5g/L and 60g/L of extract =9.82 g of FeNPs≈10g			
Conclusion: For the production of 10 g FeNPs Rs 205 is required			
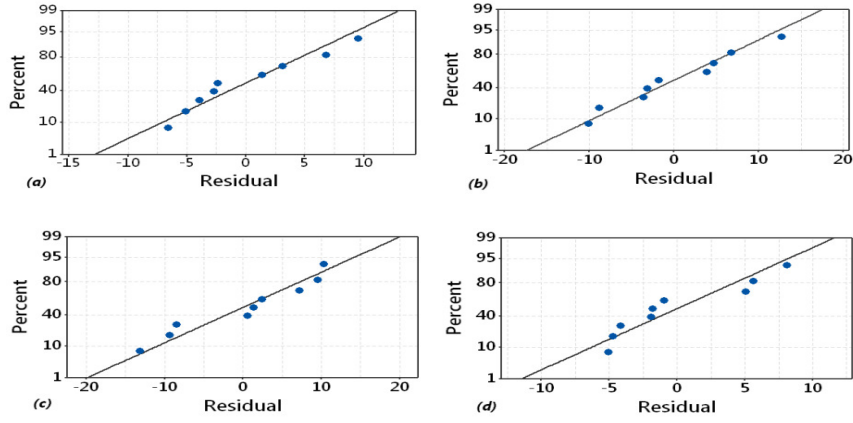
1. (a) (b) (c) (d) Normal plot of residuals a) % COD R b) % AR c) % D R d) %2,4-D R
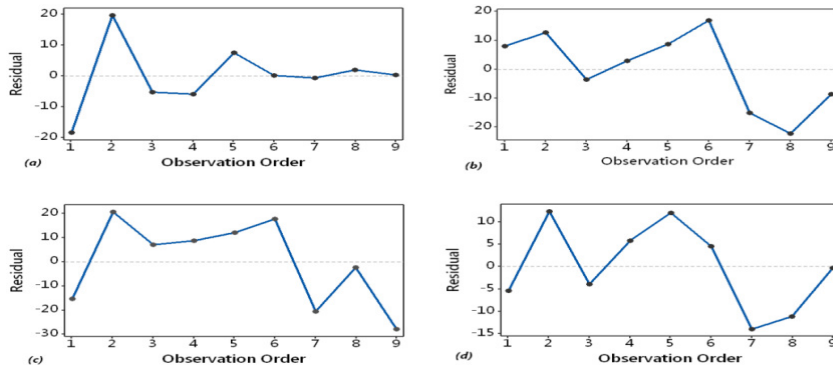
2. (a) (b) (c) (d) Residuals vs. observation order a) % COD R b) % AR c) % D R d) %2,4-D R
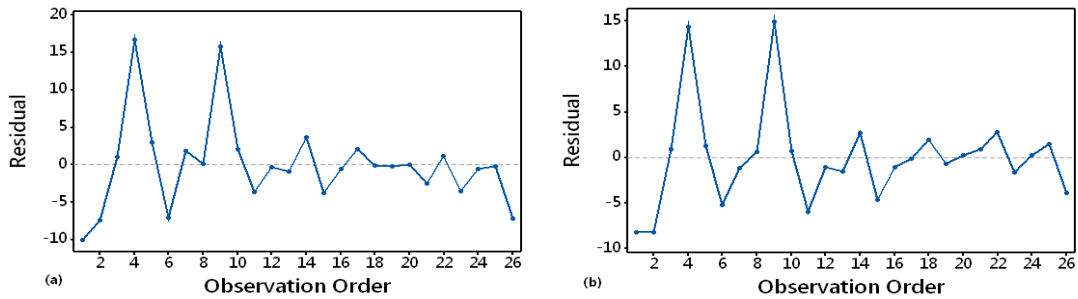
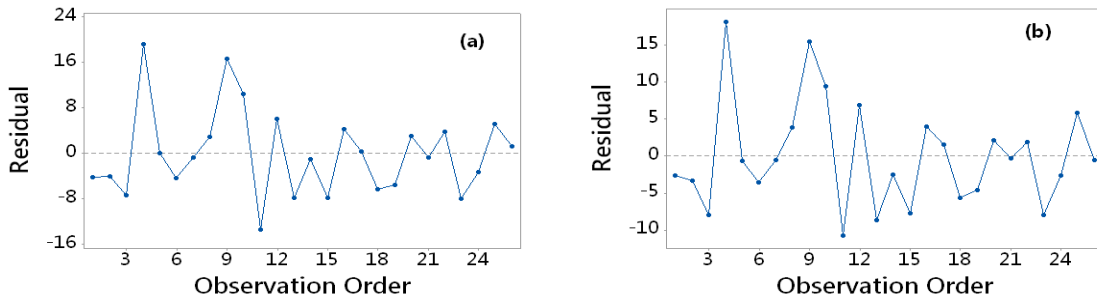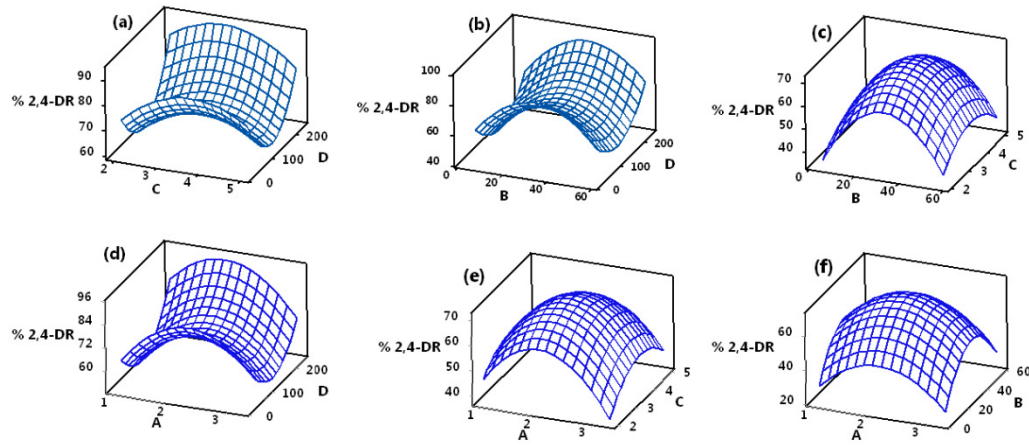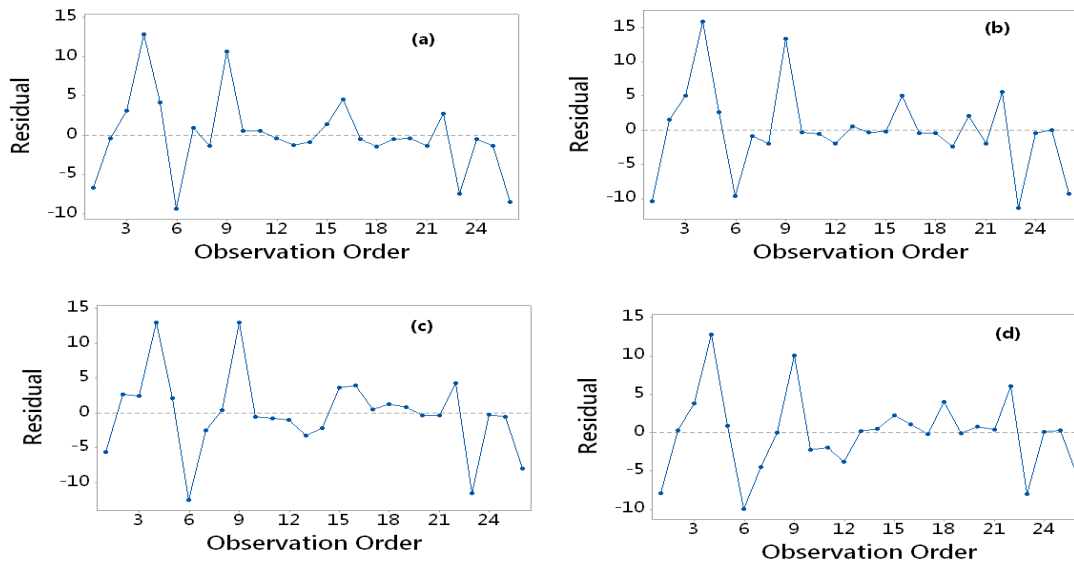**3.** Residual plots vs. total number of runs a)% COD R b)% DR
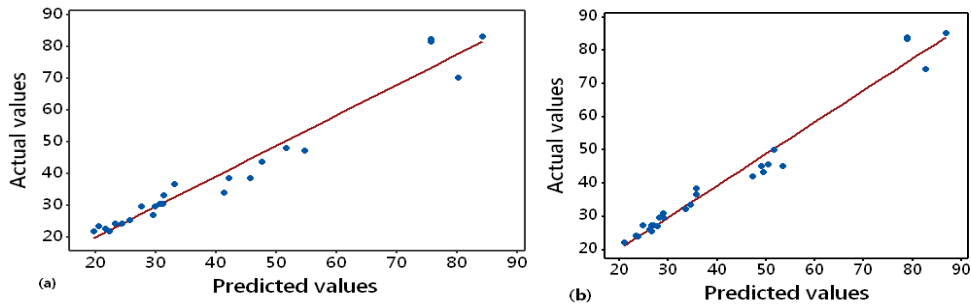
4. Plot of predicted versus actual values for both responses a a)% COD R b)% DR
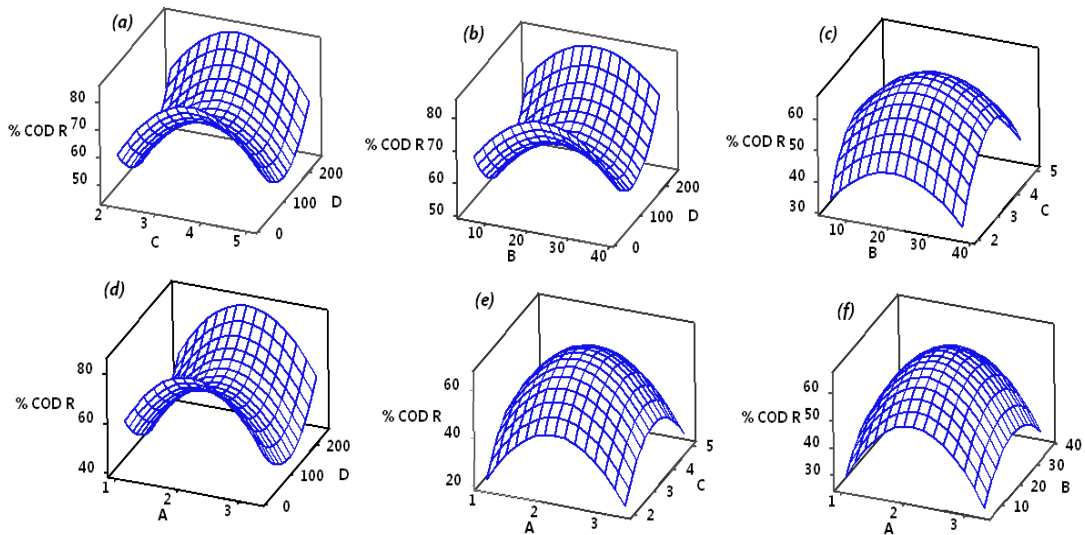

5. Surface response plots of % COD removal efficiency as a function of a) pH(C) and D(reaction time)   b) H_2O_2/Fe^{2+}(B) and reaction time (D) c) H_2O_2/Fe^{2+}(B) and pH(C) d) H_2O_2/COD(A) and D(reaction time) e) H_2O_2/COD (A) and pH(C)   f) H_2O_2/COD (A)andH_2O_2/Fe^{2+}(B)
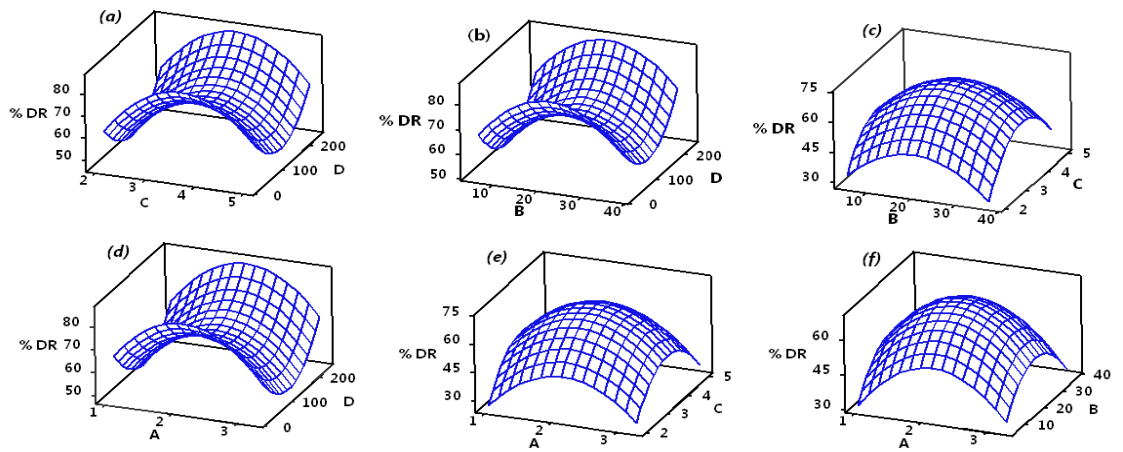
6. Surface response plots for % DR efficiency as a function of a) pH(C) and D(reaction time)   b) H_2O_2/Fe^{2+}(B)   and   reaction time (D) c) H_2O_2/Fe^{2+}(B) and pH(C)   d) H_2O_2/COD(A) and D(reaction time) e) H_2O_2/COD (A) and pH(C)   f) H_2O_2/COD (A) and H_2O_2/Fe^{2+}(B)
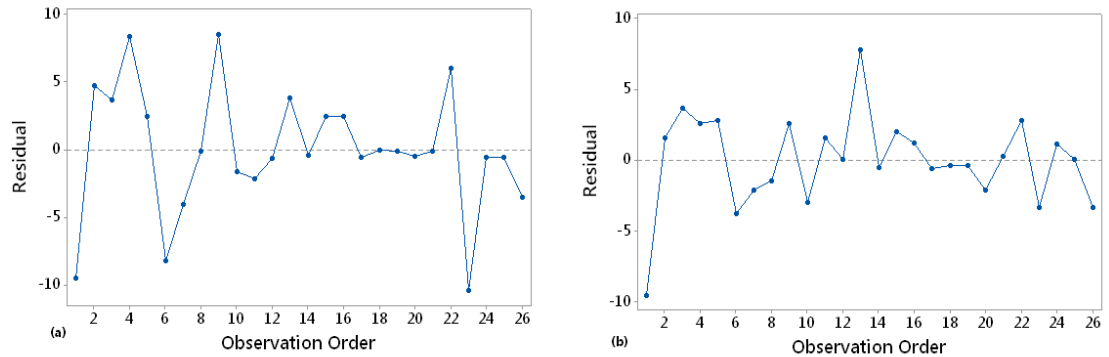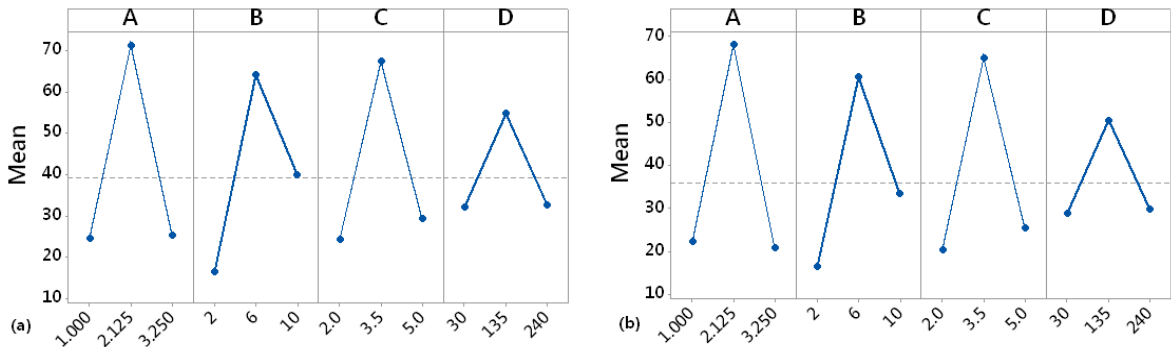

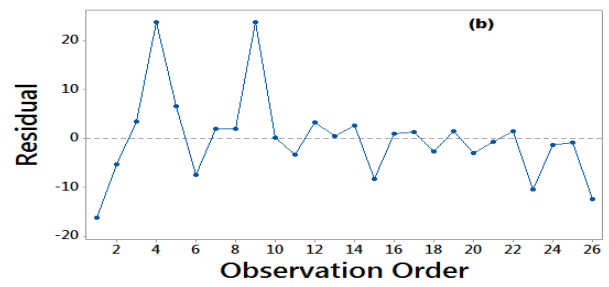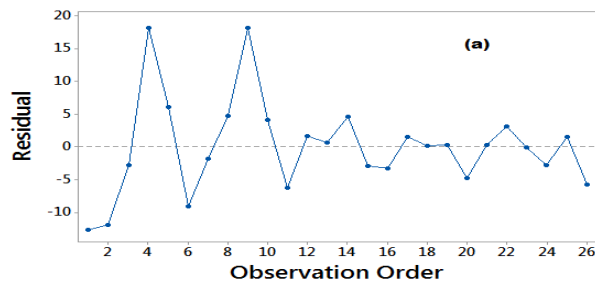**7.** Residual plots vs. Total number of runs a) % AR b) % COD R
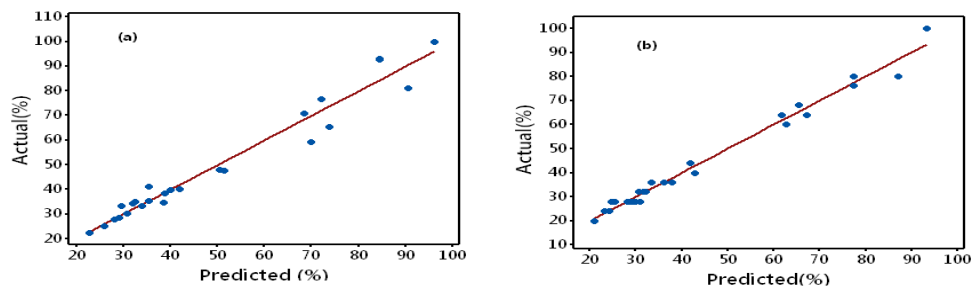
8. Plot of predicted versus actual values for both responses a)% AR b) % COD R

181
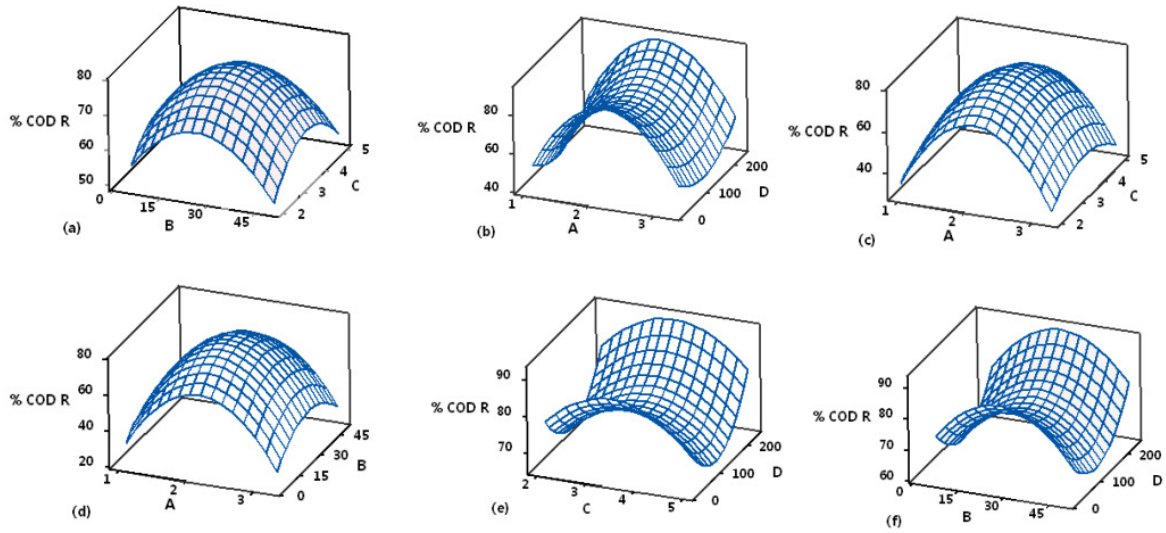
9. Surface response plots of % COD removal efficiency as a function of **a)** H_2O_2/Fe^{2+}(B) and pH(C) **b)** H_2O_2/COD(A) and D(Reaction time) **c)** H_2O_2/COD (A) and pH(C) **d)** H_2O_2/COD (A) and H_2O_2/Fe^{2+}(B) **e)** pH(C) and D(Reaction time) **f)** H_2O_2/Fe^{2+}(B) and Reaction time (D)
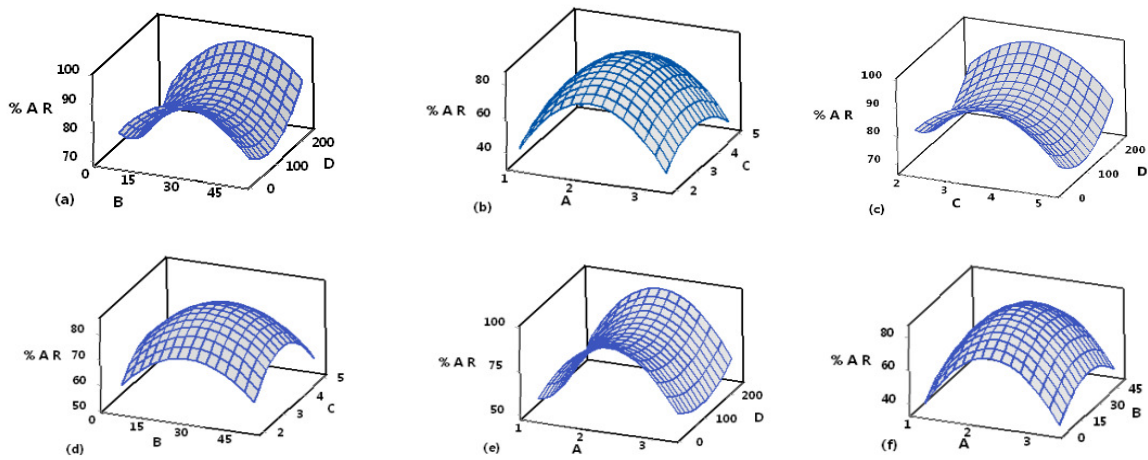
10. Surface response plots for % AR removal efficiency as a function of **a)** H_2O_2/Fe^{2+}(B)   and Reaction time (D) **b)** H_2O_2/COD (A) and pH(C)   **c)** pH(C)   and Reaction time (D)   **d)** H_2O_2/Fe^{2+}(B)   and pH(C)   **e)** H_2O_2/COD (A) and Reaction time (D)   **f)** H_2O_2/COD (A) and H_2O_2/Fe^{2+}(B)

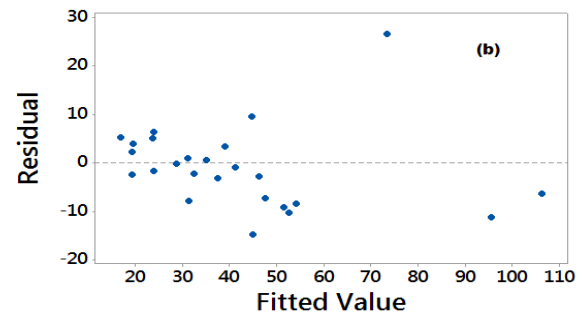**Fig. 11.** Residual plots vs. Total number of runs a) % COD R b)% 2,4DR
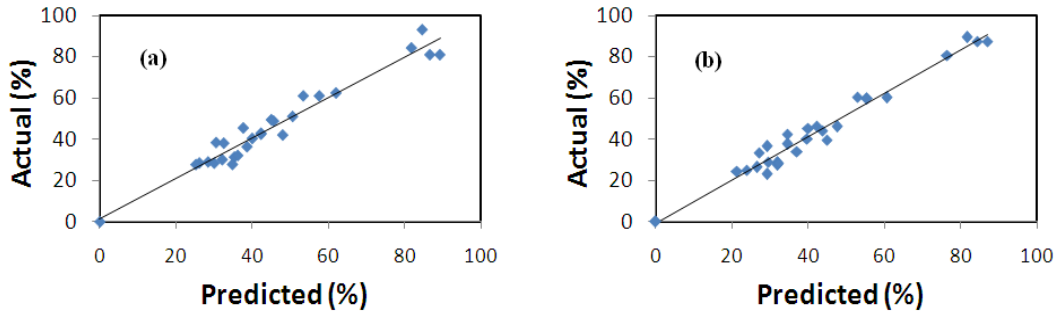
**12.** Plot of predicted versus actual values for both responses a) % 2,4-DR b) % COD R
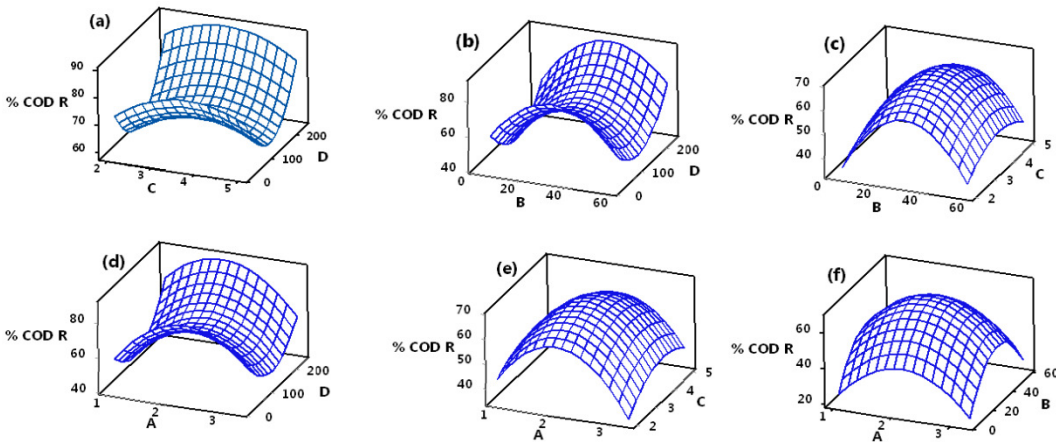
13. Surface response plots of % COD removal efficiency as a function of a) pH(C) and D(reaction time) b) H_2O_2/Fe^{2+}(B) and reaction time (D) c) H_2O_2/Fe^{2+}(B) and pH(C) d) $H_2O_2/COD(A)$ and D (reaction time) e) H_2O_2/COD (A) and pH(C) f) H_2O_2/COD (A) and H_2O_2/Fe^{2+}(B)

14. Surface response plots for % 2,4-DR efficiency as a function of a) pH(C) and D(reaction time) b) H_2O_2/Fe^{2+}(B) and reaction time (D) c) H_2O_2/Fe^{2+}(B) and pH(C) d) H_2O_2/COD(A) and D(reaction time) e) H_2O_2/COD (A) and pH(C) f) H_2O_2/COD (A) and H_2O_2/Fe^{2+}(B)

15. Residual plots vs. Total number of runs a) % A R b)% CODR c)%DR d)%2,4-DR

184
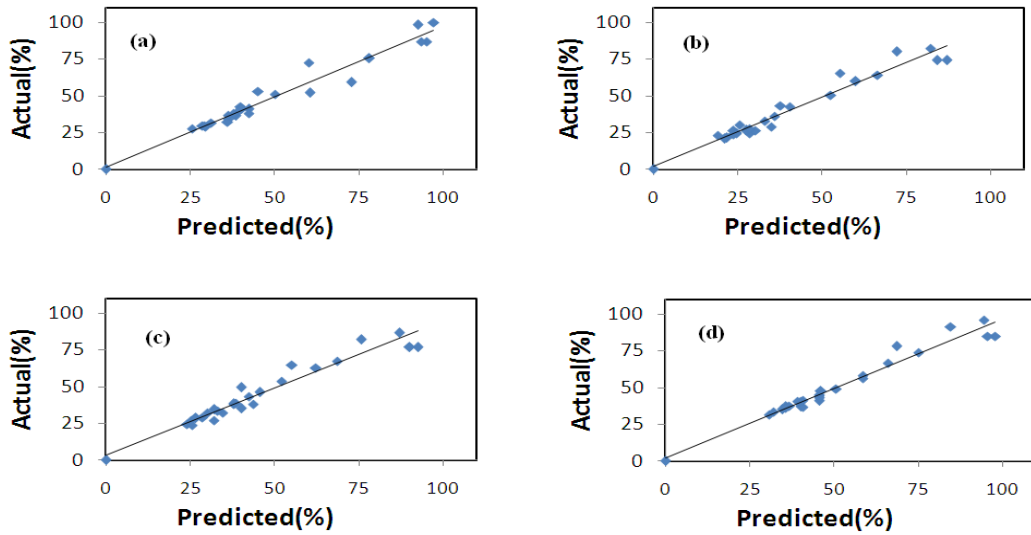
16. Plot of predicted versus actual values for both responses a) % A R b)% CODR c)%DR d)%2,4-DR
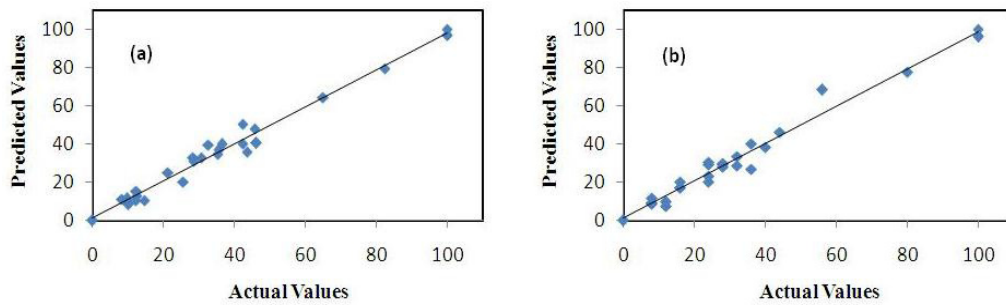
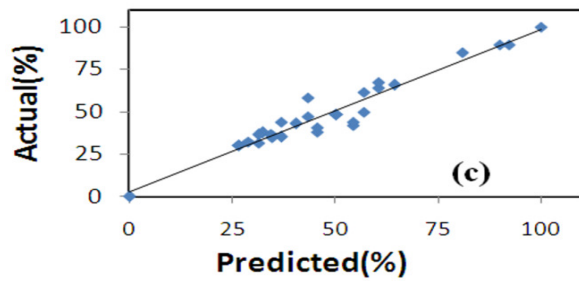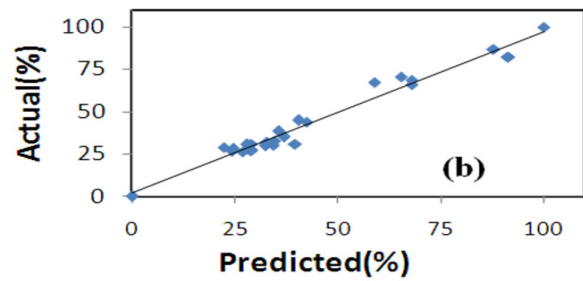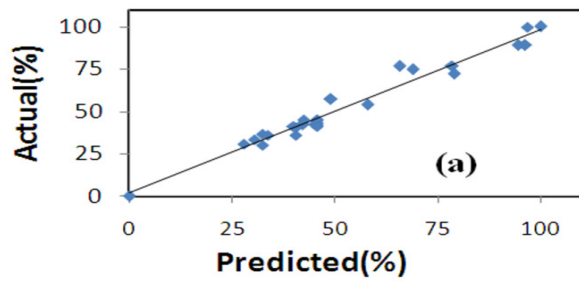**17.** Plot of predicted versus actual values for both responses a) % COD R b) % AR

18. Main affects plots for both responses a) % COD R b) % AR(A-III-18)
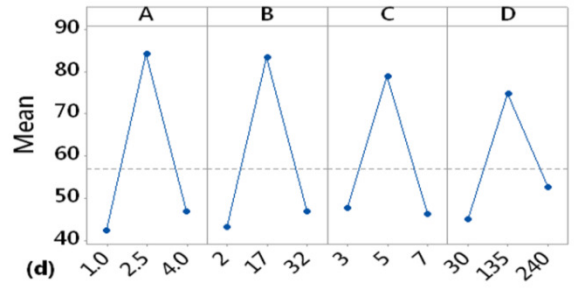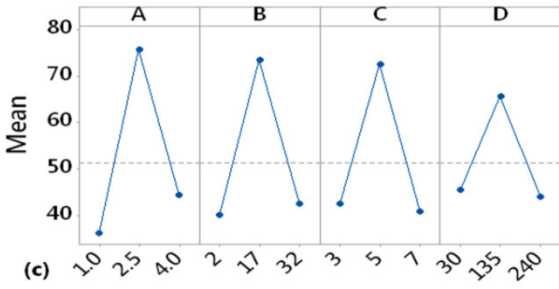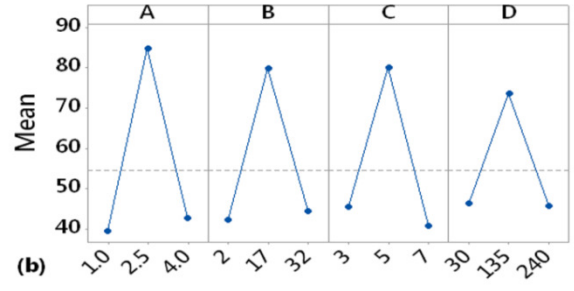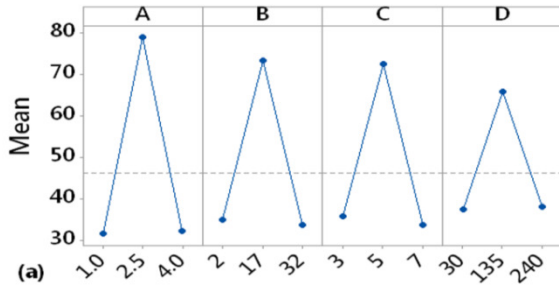
19. Residual plots vs. total number of runs a)% COD R b)% DR
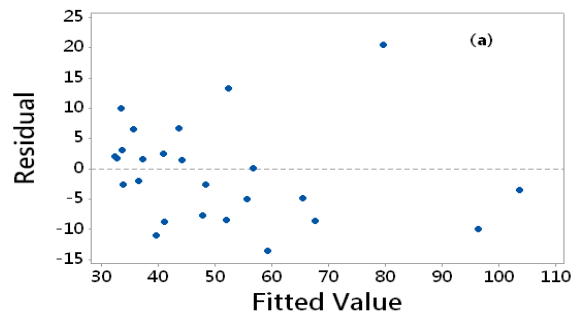
20. Residual plots vs. Total number of runs a) % COD R b)% 2,4DR
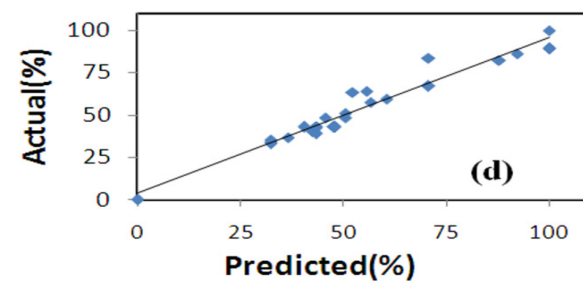
21 a)% DR b) % AR c) % 2,4R d) % COD R

22. Main effects plots a))% DR b) % AR c) % 2,4R d) % COD R

PUBLICATIONS BASED ON PRESENT WORK

International Journals Published

1. Sangami, S., & Manu, B. (2018). Catalytic efficiency of laterite-based FeNPs for the mineralization of mixture of herbicides in water. *Environmental Technology*, 1-13 *(Tailor and Francies).*

2. Sangami, S., and Manu. B., (2016). "Fenton's treatment of actual agriculture runoff water containing herbicides". ***Water Science and Technology, (75.2), 451-46. (IWA)***

3. Sangami, S., and Manu. B., (2017). "Optimization of Fenton's oxidation of herbicide dicamba in water using response surface methodology". ***Applied Water Science, 7(8),4269-4280. (Springer Nature)***

4. Sangami, S., and Manu. B., (2017). "Synthesis of Green Iron Nanoparticles using Laterite and their application as a Fenton-like catalyst for the degradation of herbicide Ametryn in water". ***Environmental Technology & Innovation** (8). 150–163.(Elsevier)*

International Conference

4. Sangami, S., and Manu, B. (2017) "Application of central composite design in Fenton's oxidation of Herbicide 2,4-D in aqueous medium", *Proc. of International conference* on ICGCSC 2017, 17-18th march, Moodabidri *(**Best Paper Award**)* ISBN:978-93-5267-355-1.

International Journals- Under review-

5. Sangami, S., and Manu, B. "Fenton's Oxidation of Herbicide Ametryn in aqueous medium: Optimization using Response Surface Methodology**".** ***J. of Env. Engineering (ASCE).***

RESUME

Name	:	Mr. Sanjeev Sangami
Date of Birth	:	30-07-1985
Permanent Address	:	At: Gadikop Po: Parishwad,
		Po: Parishwad Ta: Khanapur
		Dist: Belgaum State: Karnataka
		India
Contact Number	:	+91-9945754311
Email	:	sanjeevenv08@gmail.com

ACADEMIC QUALIFICATION:

Degree	Specialization	Institute	Duration	Percentage/CPI
Ph. D	Environmental Engineering	NITK, Surathkal	2014-2018	9.25
M. Tech	Environmental Engineering	NITK, Surathkal	2008-2010	8.31
B E	Environmental Engineering	SJCE, Mysore	2004-2008	71.98%

PUBLICATIONS:

A. International Journals

1. Sangami, S., and Manu. B., (2016). "Fenton's treatment of actual agriculture runoff water containing herbicides". *Water Science and Technology, (75.2), 451-46.* **(IWA)**

2. Sangami, S., and Manu. B., (2017). "Optimization of Fenton's oxidation of herbicide dicamba in water using response surface methodology". *Applied Water Science,* **7(8),4269-4280.** **(SPRINGER NATURE)**

3. Sangami, S., and Manu. B., (2017). "Synthesis of Green Iron Nanoparticles using Laterite and their application as a Fenton-like catalyst for the degradation of herbicide Ametryn in water". *Environmental Technology & Innovation* *(*8). 150–163. *(ELSEVIER*)

4. Sangami, S., & Manu, B. (2018). Catalytic efficiency of laterite-based FeNPs for the mineralization of mixture of herbicides in water *Environmental Technology*, 1-13 *(TAILOR AND FRANCIES).*

5. **Sanjeev S**, Arunkumar H, Ramu S, Chandrashekar.A, Anand A , Abhiram.K.A, Abdul Latheef, Thomas J (2012) "Treatment of Rice mill Effluent using Aerobic Reactor " *Int.Journal of Envi. Engg andMgt* . Volume 3(4), page no 264-267 ISSN**:2231-1349.**

6. **Sanjeev. S** , Rahasya K R, Ramya, Shruthi , Shashiram   (2013), Electrocoagulation For The Removal of Iron From Ground Water. *Int. Journal of Civil Engg and Applications* Vol 3, Number 7- 2013 ISSN 2249-426X.

7. **Sanjeev. S** , Prithviraj.H. K , Mithun.B M, Mahesh. A. M , Ganesh.K. S , Sharath.M R , Adarsh (2013). Effect Of Different Kind Of Food Waste In Biogas Production : A Case Study. *Int. Journal of Environmental Research and Development*   Vol 3, Number 5-2013 ,ISSN 2249-3131.

8. Anand S A , Nagarajappa D P , **Sanjeev S** , Ramu S (2014).   Removal of Hexavalent Chromium From Simulated Waste Water Using Rice Husk Ash as Carbon Adsorbent. *International Journal of Innovative Research in Science, Engineering and Technology ISSN: 2319-8753.* Vol. 3, Issue 7, July 2014.

9. Gagana Kattimani , Nethravathi H M , Priyanka O , Anand S Amaravati, **Sanjeev S**. (2015) Modern Soil Stabilization using Biomass and Chemicals. *International Journal of Innovative Research in Science, Engineering and Technology ISSN: 2319-8753.* Vol. 4, Issue 6, June 2015.

B. International Conferences

10. **Sanjeev Sangami** and Basavaraju Manu "(2017) " Application of central composite design in Fenton's oxidation of Herbicide 2,4-D in aqueous medium ,*Proc. of International conference* on ICGCSC 2017, 17-18th march, Moodabidri *(Best Paper Award)* ISBN:978-93-5267-355-1.

11. Sanjeev. S, Rohini. J, Naveeen .S. M, Mahesh. S. (2008)"Electrocoagulation Using DC current for Removal of Fluoride from Ground Water" .Proceedings of the World

Academy of Science, Engineering and Technology, page no 219-223,ISSN: 2070-3740. (B. E Project work).

12.**Sanjeev. S** and Basavarju Manu (2010)"Treatment of 2-Fluorophenol containing aqueous solutions using Fenton' s reagent": Proceedings of the International conference on sustainable development . page no 13-18 (M Tech project work).

13.**Sanjeev S**. Arunkumar H, Ramu S, Chandrashekar.A, Anand A , Abhiram.K.A, Abdul Latheef, Thomas J (2012). "Treatment of Rice mill Effluent using Aerobic Reactor". Presented in International Conference "AFSET – 2012" Organized by "Krishi Sanskriti"On 28th & 29th Oct. 2012.

14. **Sanjeev. S** , Rahasya K R , Ramya, Shruthi , Shashiram (2013), "Electrocoagulation for The Removal of Iron From Ground Water. International Conference On "Sustainable Innovative Techniques in Civil and Environmental Engineering *(SITCEE – 2013)*5th and 6th June, 2013.

15. **Sanjeev. S** , Prithviraj.H.K , Mithun.B M, Mahesh. A. M , Ganesh.K. S , Sharath.M R , Adarsh (2013). "Effect Of Different Kind of Food Waste In Biogas Production : A Case Study ."International Conference On "Sustainable Innovative Techniques in Civil and Environmental Engineering *(SITCEE – 2013)*5th and 6th June, 2013.

C. National Conferences

16. **Sanjeev . S,** and Basavarju Manu.(2009)" Treatment of 4-Fluorophenol containing aqueous solutions using Fenton' s reagent". Proceedings of the National Conference ON SWORM.(2009). page no:1- 9. (M Tech project work).

17. Suresh .G, **Sanjeev. S**, Rajmohan. B. .(2009) "Bio remediation of contaminated soil. A Review on technological status". Proceedings of the National Conference page no:276-283.

18. **Sanjeev S** , Soumya N.J, Chandrasheker A, Gaurav.E, Prasagowda.C , Devendra.B.P, Avinash.H.P. "Suitability of Eggshell Stabilized Lateritic Soil as Sub grade Material for Road Construction. National Conference on Developments and

Opportunities in Civil Engineering, Applied Sciences and Mechanical Engineering (DOCAM), May 18th -19th, 2012, East West Institute of Technology , , Bangalore.

19. **Sanjeev S** , Arunkumar .H, Deejan Ferrao, Karthik Navada, Pramod S. Water Quality Index of Payaswini River,Sullia,D.K National Conference on Engineering (DOCAM-2012), May 18th -19th, 2012, East West Institute of Technology , , Bangalore.

20. **Sanjeev. S**, Rakshith.H.S, Jithin Thambi, Mohammed Shaheer, Jolsna.K Grey water reuse towards water Conservation; A case study. National Conference on Engineering (DOCAM-2012), May 18th -19th, 2012, East West Institute of Technology. Bangalore.

D. Under Review

21. Sanjeev Sangami and Basavaraju Manu "Fenton's Oxidation of Herbicide Ametryn in aqueous medium: Optimization using Response Surface Methodology**"** *Journal Environmental Engineering* (ASCE*).*

22. Sanjeev Sangami, Viplav Gritlahre, Yash Malviya, Basavaraju Manu "Performance Evaluation of Copper and German silver electrodes during electrochemical oxidation of Ametry in water" *chemosphere* (**Elsevier).**